UNIVERSIDADE D
COIMBRA

Jorge Villarroel-Ortega

Characterisation of Stress-Strain Behaviour of a Chemically Stabilised Soft Soil Reinforced with Fibres Under Monotonic and Cyclic Loadings

Thesis in the context of the PhD in Civil Engineering, Geotechnics supervised by Professors António Alberto Santos Correia, Paulo José da Venda Oliveira, and Luís Joaquim Leal Lemos presented to the Civil Engineering Department of the Faculty of Sciences and Technology of the University of Coimbra.

April of 2022

There are men who struggle for a day and they are good.
There are men who struggle for a year and they are better.
There are men who struggle many years, and they are better still.
But there are those who struggle all their lives:
These are the indispensable ones.

BERTOL BRETCH

Faculty of Sciences and Technology of the University of Coimbra

CHARACTERISATION OF STRESS-STRAIN BEHAVIOUR OF A CHEMICALLY STABILISED SOFT SOIL REINFORCED WITH FIBRES UNDER MONOTONIC AND CYCLIC LOADINGS

Jorge Villarroel-Ortega

Thesis in the context of the PhD in Civil Engineering in Geotechnics and Foundations supervised by Professors António Alberto Santos Correia, Paulo José da Venda Oliveira, and Luís Joaquim Leal Lemos presented to the Civil Engineering Department of the Faculty of Sciences and Technology of the University of Coimbra.

April of 2022

1 2 9 0

UNIVERSIDADE D
COIMBRA

CONTENTS

AKNOWLEDGEMENTS

I have spent almost the last 5 years of my life in this country (Portugal) with the big goal of finishing my postgraduate studies and many people have been present in this period to whom I would like to dedicate a small space in a humble way in this section.

Those of us who move from our place of origin to another place to do a postgraduate, tend to globalise our perception of work/study by making it a work life, which moves us day by day to achieve our goals, and this sometimes exhausts us, resulting in weaker and unexpected results. That is why I would like to special thanks for the encourage, patience, energy, sacrifice, will and selfless sharing of knowledge to Professor Dr. António Alberto Santos Correia.

I would like to thank to my others supervisor Dr. Luís Leal Lemos and Dr. Paulo José da Venda Oliveira for their continuous support and enthusiasm in every each stage and steps of this project.

I also like to acknowledge the professors of the Geotechnics Department of UC, namely to professor Dr. Paulo Coelho and to professors Dr. Jorge Almeida e Sousa, Dr. Jose Grazina, Dr. Isabel Pinto, Dr. Paulo Pinto, for the teachings delivered in the class process and for their constant kindness and disposition to cooperate in any matter. Also, Dr. António Pedro, Nicole Santos, Ligia Abreu and Zé António for their constant cooperation in the development of the tests carried out and to all collaborators and students passing through this laboratory. My truly thanks also include all people around to DEC that I spent time talking and cheering up every single day from the last years who will be always in my heart, people from Canteen: Hermina Fonseca, Don Orlando, Sra. Minervina, Sra. Carla e os Gonçalos. Also people from DEC, Ricardo Oliveira, Nelson, Nuno Almeida, Gaby Pimentel, Sra. Maria Luis, Dra. Dulce and Hugo.

To my colleagues at the University of Magallanes, Raúl Gallardo, Dr. Manuel Manríquez, Dra. Yasna Segura, Berta Vivar, Claudio Villarreal, Jessica Perez, Homero Villegas and José Cárcamo for their constant concern and to replace my activities in UMAG during my study period.

My heartfelt thanks to my mother for always being the best person in the world, to my sister Jessica for always supporting me in every situation. To my two new loves, Josefa and Joaquin, whose first years I have unfortunately missed but that I will make up for when I return. To

the couple that includes my sister Javier. To my father (RIP), my nana (RIP) and my uncles/cousin (Cristina, Mario, Fabiola, Jacko, Javier, Rodrigo, and Richard) who are also always present in my life.

To my geotechnical friends, Dr. João Camões for the constant and interesting conversations and unselfish way of transmitting his knowledge, forever be very willing to deliver a friendship from the start. To my colleagues, friends, and all people give me support in this period to Francisco Cruz, Felipe Rodrigues, João Cajada, Andre Silva, João Baiao, Ruben Ventura, David Montes Gonzalez, Diogo Teles, João Moreno, Martim Matos, Mario Pastrana, Fabian Cabrera, Christian Miculas, Mateus Veloso and Ana, Bruno Pedrosa and Sara, Rohola and Pegah, Charles Cenci, Flavia Bellesia, David Torres, Melaku, Christian Rebata, Dorival Fijamo, João Nunes, Wellington Oliveira, Kleber Gonçalves, Luis Pereira, Ester Sousa, Frank Deba bon, Ana Ripke, Luca, Ricardo, Sandrita, Luiz Cancellier, Kaan, Denilson Ramos, Imene Abidi, Damjan and Eli. To my dear chilean friends, Ariel Maldonado, Adrian Bahamonde, Pedro Bahamondez, Gonzalo Quiñones, Leo Bahamonde, Estefani, Lorena, Jonathan Kamann, Sebastián Águila, Rodrigo Diaz, Franco Gonzalez, Daniel Navarro, Gonzalo Uribe, and Carlos Santorsola.

To Laura *"por nuestros tres siempre*s", and her family that adopted me (Raquel, João, João Luís, Matilde, Januário).

I would like to express thanks to CIMPOR and to Biu International for supplying the binders and the fibres. Special thanks to the University of Magallanes for the institutional permission and to the Ministry of Science, Technology, Knowledge and Innovation and their agency (ANID) via CONICYT, CONICYT PAI / INDUSTRY 79090016 for sponsoring the stay. Furthermore, mention to the Portuguese Foundation for Science and Technology (project PTDC/ECI-CON/28382/2017) and the R&D Unit Institute for Sustainability and Innovation in Structural Engineering (ISISE), under reference UIDB / 04029/2020, and the R&D Unit Chemical Processes and Forest Products Engineering (CIEPQPF) Project UIDB00102/2020, I appreciate it all.

ABSTRACT

Due to the development of cities and industrial areas, it is becoming increasingly necessary to build on soils with precarious mechanical characteristics, an example of such soils are soft soils, which exist everywhere in the world, and are characterised by low mechanical strength and high deformability. Chemical stabilisation of soils is a solution that has shown good results, allowing construction on soft soils.

To improve existing knowledge about the mechanical behaviour of these chemically stabilised soils, an experimental study was carried out on the Baixo Mondego soil. Samples of unreinforced and polypropylene fibre reinforced, chemically stabilised Baixo Mondego soil were studied under monotonic and cyclic loads. This study analyses their mechanical behaviour using the compression and tension, compressibility, and shear stress-strain responses. The effect of curing conditions, type, and amount of binder, as well as the influence of the type of failure mechanism imposed by the different types of tests, were studied. The effect of fibre addition was analysed as well as the parameters characterising the cyclic loading, i.e., number of cycles, frequency, stress level, and amplitude.

One of the main conclusions is that the introduction of fibres can reduce cementitious bonds, causing yielding to occur earlier. However, and simultaneously, the presence of fibres may improve the mechanical behaviour under cyclic loading since, due to the deformations occurring during the cyclic phase, they allow the mobilisation of the fibres and these, in turn, result in yielding occurring at higher stresses.

RESUMO

Devido ao desenvolvimento das cidades e áreas industriais, torna-se cada vez mais necessário construir sobre solos com fracas características mecânicas. Um exemplo deste tipo de solos são os solos moles, que existem em todo o mundo, e que se caracterizam por baixa resistência mecânica e elevada deformabilidade. A estabilização química dos solos é uma solução que tem mostrado bons resultados, permitindo a construção em solos moles.

Para melhorar os conhecimentos existentes sobre o comportamento mecânico destes solos moles quimicamente estabilizados, foi elaborado um estudo experimental sobre solo mole do Baixo Mondego. Foram estudadas amostras deste solo estabilizado quimicamente não reforçadas e reforçadas com fibras de polipropileno, sob cargas monotónicas e cíclicas. Analisa-se o efeito das condições de cura, tipo e quantidade de ligante, bem como a influência do tipo de mecanismo de rotura imposto por diferentes tipos de ensaios. Analisa-se o efeito da introdução de fibras, assim como os parâmetros que caracterizam a ação cíclica, isto é, o número de ciclos, a frequência, o nível de tensão e amplitude.

Uma das principais conclusões é que a introdução de fibras pode reduzir as ligações cimentícias, fazendo com que a cedência ocorra mais cedo. Contudo, e simultaneamente, a presença de fibras pode melhorar o comportamento mecânico sob cargas cíclicas uma vez que as deformações que ocorrem durante a fase cíclica permitem a mobilização das fibras e estas, por sua vez, fazem com que a cedência ocorra para tensões mais elevadas.

RESUMEN

Debido al desarrollo de las ciudades y las zonas industriales, cada vez se hace más necesario construir sobre suelos de pobres características mecánicas. Un ejemplo de este tipo de suelos son los suelos blandos, los cuales existen por todas partes en el mundo, y se caracterizan por tener baja resistencia mecánica y elevada deformabilidad. La estabilización química en los suelos es una solución que ha mostrado buenos resultados, permitiendo la construcción en suelos blandos.

De acuerdo con mejorar el conocimiento acerca del comportamiento mecánico de estos suelos químicamente estabilizados, fue elaborado un estudio experimental sobre el suelo de Baixo Mondego. Se estudió este suelo estabilizado químicamente no reforzado y reforzado con fibras de polipropileno sometida a cargas monotónicas y cargas cíclicas. Se estudió el efecto de las condiciones de curado, el tipo y la cantidad de aglutinante, así como la influencia del tipo de mecanismo de falla impuesto por los diferentes ensayos. Se analizó el efecto de la introducción de fibras, así como los parámetros que caracterizan la acción cíclica, es decir, el número de ciclos, la frecuencia, el nivel de tensión y la amplitud.

Algunas de las principales conclusiones es que la introducción de fibras puede ocasionar la reducción de ligaciones cementicias, haciendo con que la fluencia ocurra antes, sin embargo, al mismo tiempo la presencia de las fibras bajo cargas cíclicas puede originar una mejora en el comportamiento mecánico, pues, debido a las deformaciones ocurridas durante la fase cíclica permiten la movilización de las fibras y éstas a su vez, provocar que la fluencia ocurra para tensiones más elevadas.

LIST OF FIGURES

LIST OF TABLES

SYMBOLOGY

A: Skempton Parameter
B: Skempton Parameter
c' : Cohesion
C_c : Compressibility index,
C_r : Re-compressibility index,
c_v : consolidation coefficient
CIU: Consolidated Isotropically Undrained Test
E: Young's modulus
e_0: Initial void ratio
E_f : Tensile modulus
$E_{u\ tan}$:Undrained Tangent stiffness
E_u: Undrained Stiffness Modulus
E_{u50} : Undrained Stiffness Modulus at 50% of q_u max
$\varepsilon_{ax\text{-}perm:}$ Permanent axial strain
$f_{cd:}$ Tensile strength for DTS test
f_{cf}: Tensile strength for FS test
f_{ct}: Tensile strength for STS test
G: Shear modulus
G_s: Specific gravity
k: Permeability Coefficient
Load, F: Load
LOI: Loss on ignition
NC: Normally Consolidated
O.M : Organic Matter
OC: Over Consolidated
OCR: Overconsolidation ratio
p': Mean effective stress
p'_y: Mean effective yield stress
q/p': Stress ratio
q: Deviatoric stress
q_{max}: Maximum deviatoric stress
$q_{u\ max}$: Maximum unconfined strength
σ'_f : Tensile strength
S_u: Undrained Shear Strength

τ_{cyc} max : Maximum shear cyclic strength
V_p: Compression wave velocity
V_s: Shear wave velocity
$w_{f:}$ Final water content
$w_{L:}$ Liquid Limit
w_{nat} : Water content
$w_{P:}$ Plastic Limit
Δu: Back pressure
$\delta_{v:}$ Vertical displacement
$\delta_{v\text{-}perm:}$ Permanent axial displacement
$\delta\varepsilon_{vol}/\delta\varepsilon_s$: Dilatancy
ε_a: Axial strain
ε_r: Axial strain at rupture/failure
ε_{vol}: Volumetric strain
ν: Poisson's ratio
ρ: Density
$\sigma'_{v:}$ Effective vertical stress
ϕ' : Frictional strength angle
$\gamma_{sat:}$ Saturated density
ν: Poisson's ratio

ACRONYMS

ASTM: American Society for Testing and Materials
BMSS: Baixo Mondego Soft soils
BQ: Binder quantity
BS: British Standard
CRSP: Constant Rate Strain Pump
CSL: Critical State Line
CSS: Chemical Stabilisation of Soils
CSSRF: Chemical Stabilisation of Soil Reinforced with Fibres
DTS: Direct tensile strength
FS: Flexural strength
LMG: Last Maximum Glacier
LNEC: National Laboratory of Civil Engineering (Portugal)
MSS: Magallanes soft soils
NCh: Chilean Standard
NLC: Number of loading cycles
NP: Portuguese Standard
PA: Nylon/Polyamide
PE: Polyetilene
PET: Polyester
PP: Polypropylene
PVC: Polyvinyl chloride
STS: Splitting tensile strength
UCS: Unconfined compressive strength
XRD: X-ray diffraction

CHEMICAL NOTATIONS

CO_2 – Carbone dioxide
CaO – Calcium oxide
SiO_2 –silica
Al_2O_3 –aluminium
Fe_2O_3 – iron oxide
CaH_2O - calcium hydroxide
$CaO.SiO_2.H_2O$ - hydrated calcium silicates
$2CaO.SiO_2$ – bicalcium
$CaO.Al_2O_3.SiO_2.H_2O$ - hydrated calcium silico-aluminates-compound

CHAPTER 1 - INTRODUCTION

1.1 Construction on softs soils

When infrastructures such as bridge foundations or embankments are built on soft soil deposits, these soils tend to exhibit deformation over long periods due to consolidation and creep phenomena. Such behaviour of soft soils is a consequence of their weak geotechnical characteristics (low strength and excessive deformability) fundamentally due to the high-water content, high specific surface of the particles (clays, silts) and high organic matter (OM) content. Therefore, it is essential to ensure the stability and to control/minimise the deformations during the construction stage and structure life (Kitazume and Terashi, 2013). It is important to mention that in the past construction on soft soil deposits was avoided (Venda Oliveira et al., 2018) due to the above-mentioned stability and deformation problems. However, due to the population growth, development of societies and expansion of urban and industrial areas, the pressure to build on these soft soils has increased, which poses challenges in terms of geotechnical engineering.

Traditional geotechnical engineering techniques are often not a viable solution to allow construction on such soils, due to their high costs or environmental limitations. For example, the granular bases used for transportation infrastructures (e.g., roads) become unviable because of the costs associated with transport and environmental impact when these materials are very far from the worksite (Foppa, 2005).

There are two main geotechnical solutions to solve these types of problems: add reinforcement elements to the ground, or improve the soil's properties by mechanical, physical or chemical methods (Kitazume & Terashi, 2013). Venda Oliveira et al., (2018) have mentioned that the choice of the ground improvement technique for a specific geotechnical problem depends on many factors such as costs, logistics, environmental aspects, etc. Regarding the improvement through chemical methods, it can be achieved by adding stabilising materials (binders) which are sometimes combined with fibres, creating a composite material with better mechanical behaviour than the original soil (Correia et al., 2017).

Nowadays, sustainability is an increasingly important issue in geotechnical engineering and therefore, the ground improvement technique selected should use fewer raw materials and minimise energy consumption. The improvement using chemical additives (binders) reinforced with fibres is as a technique that mixes the binder-soil-fibres in situ, where binders can incorporate industrial by-products (such as fly-ash, blast furnace granulated slag, etc.) and the fibres may be natural fibres and / or obtained from re-used materials (screws, tyre wire, etc.), thus, contributing to reducing the need for raw materials. The binder-soil-fibres mixture will induce changes in the mechanical behaviour of the original soil, leading to an increase in strength and stiffness (Venda Oliveira et al., 2018). The presence of the fibres attenuates the brittle behaviour of the composite material, and improves its tensile strength (Sukontasukkul and Jamsawang, 2012; Correia et al., 2015). The field of application of this technique is vast, for example: embankments on soft soils, stabilisation of slopes, stabilisation of contaminated soils, mitigation of vibrations induced by high-speed trains, retaining walls, etc. (Correia, 2011; Kitazume and Terashi, 2013).

Some geotechnical structures are often subjected to cyclical loadings induced by different types of actions, such as wind, earthquakes, traffic loads, heavy machinery, sea waves on offshore structures and even vibrations due to explosives. It is very important to assess the repercussions of cyclical loadings on the mechanical behaviour of chemically stabilised, fibre-reinforced soft soils (Venda Oliveira et al., 2018).

1.2 Research Objectives

The aim of this research is to improve existing knowledge about the behaviour of stabilised soils reinforced with fibres (SSRF) under monotonic/static and cyclic loading, thereby contributing to an effective future application of such composite materials. This objective can be divided into two main goals: to improve knowledge concerning SSRF under monotonic and cyclic loadings and, in addition, to define the yield surface of these composite materials. This definition should contribute to the development of more realistic constitutive models that can predict the behaviour of cement-based stabilised soils, especially when reinforced with fibres and under cyclic loading conditions. To achieve such goals a comprehensive laboratory test programme was designed comprising the execution of monotonic and cyclic loading tests with unreinforced and fibre-reinforced stabilised soft soils.

The cyclic loading experimental tests were designed to evaluate the impact of cyclic loading parameters (number of cycles, frequency, level of stress and amplitude) on the mechanical behaviour of SSRF. As has already been shown, in some cases, the cyclic loading might promote

an enhancement of the mechanical behaviour of the composite material. As expected, the breakage of the cementitious bonds that occurs during the cyclic stage induces a degradation of the mechanical properties of the stabilised material; however, in some cases this effect seems to be largely compensated for by the mobilisation of the tensile strength of the fibres, resulting in the improvement of the mechanical behaviour of these materials. This behaviour, which is in apparent contradiction to the generalised belief stated within the scientific community, might be a breakthrough in terms of designing geotechnical structures with SSRF. Consequently, it is of paramount importance to perform a comprehensive study and an in-depth analysis that may confirm these potentialities.

The specific objectives of the present thesis are as follows:

- to analyse the influence of the introduction of fibres on the mechanical behaviour of this composite material;
- to study the compressive and tensile behaviour of stabilised soils that are unreinforced or reinforced with fibres;
- to improve the knowledge and scientific understanding of the cyclic loading parameters on the mechanical behaviour of chemically stabilised reinforced and unreinforced soft soils;
- to characterise the compressibility of chemically stabilised reinforced and unreinforced soft soils under static/monotonic and cyclic loading conditions;
- to improve knowledge about the yield surface of such composite materials, contributing to the future development of conceptual models that describe the behaviour of these composite materials more realistically;
- and, finally, to open up new research directions within the field of geotechnics.

1.3 Motivation

One of the most important limitations of the chemical soil stabilisation technique is related to the poor tensile strength and brittle behaviour exhibited by the stabilised soil (Sukontasukkul & Jamsawang, 2012; Correia et al., 2015), which prevents its application in situations where the material is subjected to horizontal displacements induced by lateral earth pressures, earthquakes, etc. To overcome this problem, two methodologies are generally used, reinforcement with steel H-beams or the inclusion of short fibres into the stabilised soil mixture (SSRF). The latter methodology has been widely studied using monotonic tests and making use of synthetic fibres, while only a few authors have presented any results based on cyclic loading tests. The aim of the

present research work is to contribute to improving knowledge about the mechanical behaviour of these stabilised materials, both unreinforced or fibre-reinforced, under monotonic/static and cyclic loadings.

Moreover, the knowledge and skills acquired during the preparation of the present PhD thesis will be beneficial for the scientific career of the author and will make a positive contribution to improving the scientific knowledge in Chile when returning to the University of Magallanes (UMAG).

1.4 Outline

This thesis is has nine chapters, including the present introductory chapter with the purpose of briefly describing its structure. The remaining chapters are:

Chapter 2: This chapter compares Portuguese and Chilean soft soils, focusing on the soft soils from the Baixo Mondego area (Coimbra region, Portugal) and Magallanes area (Chile), respectively. The former has a fluvio-marine sedimentation environment, while the latter has a marine and lacustrine depositional environment. Besides the apparent differences, they share similar geological and geotechnical properties, as presented in the chapter.

Chapter 3: This chapter presents a comprehensive literature review on the mechanical behaviour of chemically stabilised soils that are unreinforced and reinforced with fibres, under monotonic and cyclic loadings The chapter ends by presenting some studies on the definition of the yield surface of natural and cemented clays, highlighting the different yield criteria described in the literature.

Chapter 4: This chapter characterises all the materials used in the study, namely the soft soil collected from the Baixo Mondego area in the central region of Portugal, the binders selected for the chemical stabilisation and the fibres used for reinforcement. The laboratory procedure adopted in the preparation of the chemically stabilised samples, reinforced or not with fibres is also presented. Furthermore, all the testing equipment used to perform the testing programme is described.

Chapter 5: The aim of this chapter is to define the base testing conditions for the experimental study on the chemically stabilised soft soil, with and without reinforced fibres. The effect of the curing conditions, especially the immersed versus emersed cure, and a vertical stress applied on samples during the curing period, are studied. The influence of the binder type (Portland cement) and the partial substitution of Portland cement by other more sustainable binders (blast furnace

slag, fly ash and eggshell powder), are also studied. The curing time and the binder quantity are parameters that also influence the mechanical behaviour of the stabilised soil and, therefore, are analysed too. Once the base conditions of the experimental study are defined, the study proceeds by carrying out the reference tests under static/monotonic loading conditions for chemically stabilised samples unreinforced or reinforced with polypropylene fibres. The objective of these tests is to define and characterise the behaviour under compression and tension to be used as a reference for the following chapters.

Chapter 6: This chapter studies the mechanical behaviour of the chemically stabilised soft soil, which is unreinforced and fibre-reinforced, under cyclic loading. For such, a laboratory test programme is developed to focus on studying the influence of several parameters of the cyclic loading (number of load cycles, frequency, amplitude, and stress level of cyclic loading) on the mechanical behaviour of the composite material.

Chapter 7: This chapter contributes to the characterisation of the chemically stabilised Baixo Mondego soft soil (unreinforced and reinforced with polypropylene fibres) under static and cyclic loading, focusing on aspects related to compressibility. A new base test condition is required because it must be guaranteed that the pore pressure is almost null for the oedometer tests, i.e., the effective stress is equal to the total stress applied. For this, the oedometer samples must be in a submerged condition. The results of the oedometer tests, with and without a prior cyclic loading stage are presented and followed by a detailed discussion. The oedometer results are compared with the compressive strength tests carried out in confined conditions.

Chapter 8: This chapter is focused on the stress-strain-shear strength behaviour and the yield surface of the chemically stabilised Baixo Mondego soft soil (unreinforced and reinforced with polypropylene fibres) under static/monotonic and cyclic loading. The characterisation of the yield surface is important since it allows the researchers to distinguish between elastic and plastic behaviour, i.e., it defines where destructuration of the stabilised material begins. This knowledge is essential to develop more realistic constitutive models that can predict the behaviour of cement-based stabilised soils, especially when reinforced with fibres and under cyclic loading conditions.

Chapter 9: This chapter summarises the main conclusions of this research work, pointing out some suggestions for future research.

CHAPTER 2: GEOLOGICAL – GEOTECHNICAL FRAMEWORK OF SOFT SOILS

2.1 Introduction

One of the main purposes of this research work is to evaluate the mechanical behaviour of soft soils chemically stabilised and reinforced with fibres, subjected to monotonic and cyclic loads, based on laboratory tests. The term soft soils refers to soils with a grain size composition predominantly made of silt and/or clay, most of the time, with organic matter, exhibiting a poor mechanical behaviour characterised by low strength and high deformability (Coelho, 2000). Brenner et al. (1981) have defined soft soils as soils that are normally consolidated or slightly overconsolidated clayey formations, i.e., geologically recent fine soils, while Vermeer & Neher (1999) have proposed that soft soils are normally consolidated clays, or clayey silt and peat. Soft soils are common in coastal and lowland areas and are found throughout the world (Leroueil et al., 1990). Usually, they are of very recent geological origin, having been formed since the last phases of the Pleistocene, in the last 20.000 years (Leroueil et al., 1990), corresponding to the last glacial period. The glaciers melted and progressively retreated towards the inland, corresponding to a general rise in sea level associated with the progressive heating of the earth. This recovery in the sea level has controlled the process of formation of soft soils. Depending on the local topography and hydrography, the sedimentation environment can be classified as marine, deltaic, lacustrine, or coastal (Leroueil et al., 1990).

The soft soils that will be studied here are from Portugal and Chile, more precisely from Baixo Mondego area (Coimbra region) and Magallanes area, respectively. The former one has a fluvio-marine sedimentation environment while the latter has a marine and lacustrine depositional environment (Uribe, 1982; Coelho, 2000; Correia, 2011; Carrasco, 2014). Besides the apparent differences, they have similar geological and geotechnical properties as presented in the next sections. At the end of the chapter, a final discussion will be presented aiming to identify the similarities between both soft soils.

2.2 Magallanes Soft Soils

It is important to mention that the Magallanes region is located in the southern part of Chile, with only 0.9% of Chile's population (INE, 2017), an economic activity that represents 1.15% of the nation and a construction activity that represents only 1.4% of the country according to Banco Central de Chile, 2016. Therefore, in the southern zone there is an absence of important engineering projects, and as a result, the geological and geotechnical information regarding the soils of such regions are not well characterised (Donoso, 2006; Villarroel & Damianovic, 2008; Foncea, 2009; Chia, 2010; Vasquez, 2012; Carrasco, 2014; Vasquez et al., 2014) Nevertheless, there are few studies published focusing on the characteristics and properties of the Magallanes soil, especially on soft soils. In the next sections, it is presented a summary of the main features of the soft soils located in the Magallanes region, focusing on the geological characteristics, physical properties, and mechanical behaviour.

2.2.1 Geological Characteristics

The Magallanes area corresponds to a sequence of sandstones and claystone of approximately 800 m of thickness, consisting of a strata with a small dip towards the north (Otero et al., 2012) and has been interpreted as an estuary deposit (Rojas & Le Roux, 2010; Otero et al., 2012). The sediments that gave rise to this formation came from the erosion of the west proto-cordillera (Graham, 2009) that was lifted by a process of convergence of active tectonic plates until the end of the Miocene, and this last process generated a series of folds in the Magallanes area. Thus, the Magallanes area is a foreland basin and is characterised by a powerful sequence of fine, sandy marine sediments ranging from the lower Cretaceous to the Miocene, covered by layers from the Upper Tertiary continental (Miocene - Pliocene) and some thin episodes of shallow water marine life. This sequence lies on a nozzle series which in turn rests on a basement (Figure 2.1).

Repeated advances and retractions of glacier ice, proglacial lake formations and eventual interglacial periods formed in the area, leaving sediment overlap along the Strait of Magallanes. Glaciotectonic deformation around the centre and north of the Strait affected thick successions of glacial sediments, glaciofluvial, glaciolacustrine, and glaciomarine. The transition to warmer environments had a major impact on the area, as expressed by the presence of peat deposits in depressions caused by glacial movement or by glacial holes (kettles).

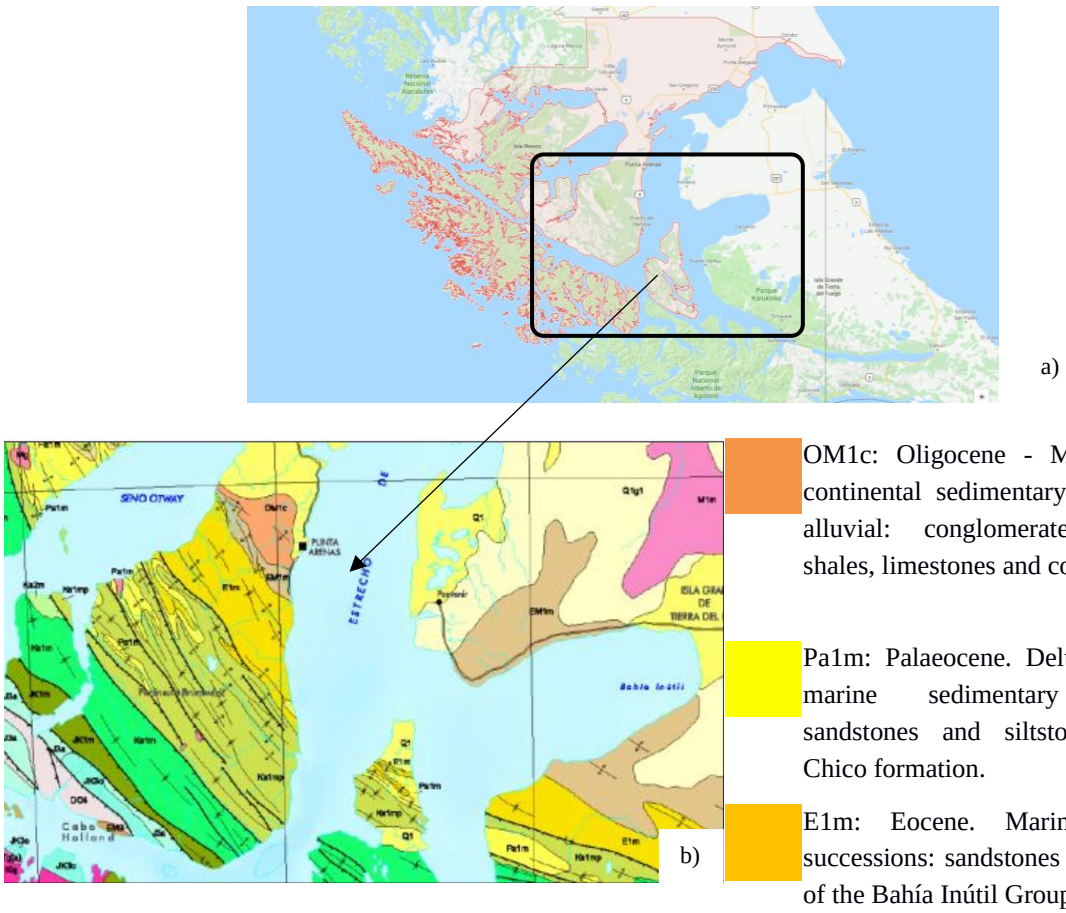

Figure 2.1: Magallanes Geological Maps: a) Location of Punta Arenas, Magallanes (Google Maps©); b) Geological Map (adapted from Sernageomin, 2003)

The type of structure and formation of the glacial sediments depends on the material (sand, silt, clay), the flow regime, the stress to which they are subjected, and the water content. Sediments under permafrost conditions behave as brittle materials. Sandy sediments in low flow regime may present continuous undulated layers, while soft sediments, clayey silt type with high water content, origin as stratification structures recumbent as contortioned stratification fluid leaks, and drying polygons, among others (Carrasco, 2014).

Punta Arenas, Magallanes, is located in the northeastern part of the Brunswick Peninsula, characterised by sedimentary rocks which have been gently folded and deposited in the Magallanes basin during the late Tertiary era, whose layers vary between 0º and 10º in the northeast direction, with some exceptions, (Uribe, 1982). The Quaternary deposits that were originated during the advance and retractions of the Holocene and Pleistocene glaciers lay over the Tertiary sediments.

Punta Arenas is in the delta of the Las Minas River, which sometimes floods inside the unlevel between the fall of the river and the sea level. This area, before the urbanization, was characterised by being flooded, so it is possible to find sediments of all kinds. This delta, being active, is

influenced by the upper part of the basin of the Las Minas River, which was considered an alluvial risk zone between May 1990 and March 2012.

In summary, Punta Arenas area can be considered after the Last Maximum Glacier (LMG) as a thawing valley, delineated to the west by lateral moraine cords that lined up sub-parallelly north-south with the old glacial margins, which end at the north in canals that drain into the Strait of Magallanes. Between this strait and the current coastline, there are different types of glacial and postglacial sediments, varying in lateral and vertical successions, thus constructing a complex stratigraphy of thrust tills, basal tills, flow tills, sandy deltas, wash plains, varved clays, peat, in addition to fine and coarse river sediments of different compaction (Carrasco, 2014).

2.2.2 Physical Characteristics

The information available regarding the physical characteristics of the soft soil of Magallanes area are focused on the physical properties such as particle size distribution, mineralogical composition, plasticity as well as the organic matter content. In the following sections, each of these characteristics are described.

2.2.3 Physical Properties

The physical properties of soils are influenced by the relative proportions of each of the three phases of a soil: solid, liquid, and gaseous. The physical indices usually evaluated experimentally, are the water content, the unit weight, and the specific gravity of soil particles. Based on these 3 basic physical indices, other physical properties of the soil were estimated, namely, the void ratio and the dry unit weight. Regarding the Magallanes soft soil, the natural water content, w_{nat}, ranged between 9.2 and 36% for the first 6m depth (Figure 2.2 and Table 2.1), with an average value of 22.6% (Vasquez, 2012). Results from the test were evaluated from intact samples collected in the field using Chilean standard NCh151 (1979) (oven drying method at 105°C). The in-situ unit weight of such soils (NCh1516, 1979) ranged from 17 to 21 kN/m^3, with an average value of 19.18 kN/m^3 (Vasquez, 2012 and Table 2.1). In fact, these values are a little higher for soft soils but in agreement with the natural water content. The third basic physical index reported was the specific gravity of the soil particles, G_s. It was measured according to the procedure described in the Chilean standard NCh1532 (1980). The mean value of the specific gravity of soil particles was 2.672 (Vasquez, 2012 and Table 2.1).

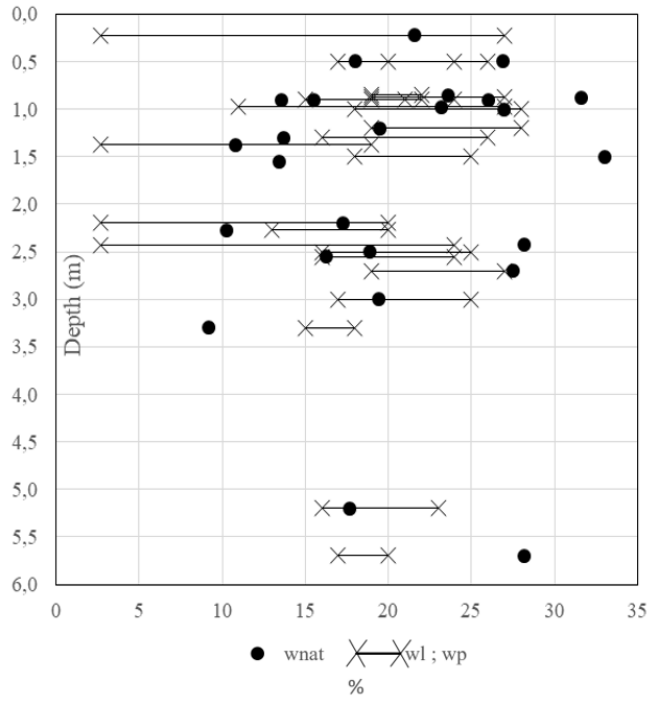

Figure 2.2: Atterberg Limits and water content of Magallanes soft soils (adapted from Donoso, 2006)

Based on the average values of these three basic physical properties, other physical properties of the soil were estimated by Vasquez (2012), and the following values were obtained (Table 2.1): the void ratio, e_0, ranges between 0.56 to 1.35 with an average value of 0.87, and the dry unit weight, γ_d, changed from 11.2 to 17.3 kN/m^3, with an average value of 14.6 kN/m^3.

Table 2.1: Physical index properties – average values for the first 6 m. depth (Vasquez, 2012)

Sample	w_{nat} (%)	γ_{sat} (kN/m^3)	G_s	e_0	γ_d (kN/m^3)	w_p (%)	w_L (%)
Varvada Clay (z = 1m)	20	17	2.63	1.35	11.2	19.7	28.6
Varvada Clay (z = 3m)	19	19.2	2.63	0.77	15	25.4	53.8
Lana Plant clay	36	18.2	2.7	1.06	13.1	21.2	40.3
Chiloé-Briceño clay	18	21	2.7	0.56	17.3	12.2	23.4
Cereco clay	23	20.5	2.7	0.63	16.6	16.4	33.3

It is also important to mention that the water table is located near the soil surface as observed in in-situ drill hole tests (Vasquez, 2012).

In general, it can be said that Magallanes soft soils (MSS) exhibit a low water content combined with a high unit weight, characteristics that are not typical for soft soils. However, it should be emphasized that these characteristics are only for samples collected from the first 6m depth, thus, may not represent the entire deposit. As it will be shown below, when the geological characteristics are considered together with the grain size distribution, organic matter content, and mechanical behaviour, it will be clear that the soils in Magallanes area are soft soils (Figure 2.3).

2.2.4 Particle Size Distribution

The grain size distribution of soil particles according to their dimensions was evaluated on soil samples resulting from either residues of intact samples or from small parts of a large volume sample. As presented in Figure 2.4, Donoso (2006) took fifteen samples to characterise the grain size and composition of Magallanes soft soils, collected in different places inside the city of Punta Arenas (10 of the samples are from Chiloe-Briceño clay identified in black in Figure 2.4). Vasquez (2012) has also characterised the grain size composition of Magallanes soft soils collected in 4 different places, and the results are summarised in Table 2.2.

Figure 2.3: Examples of Magallanes soft soils (adapted from Donoso, 2006): a) and c) MSS in natural State; b) and d) till stratigraphic profile

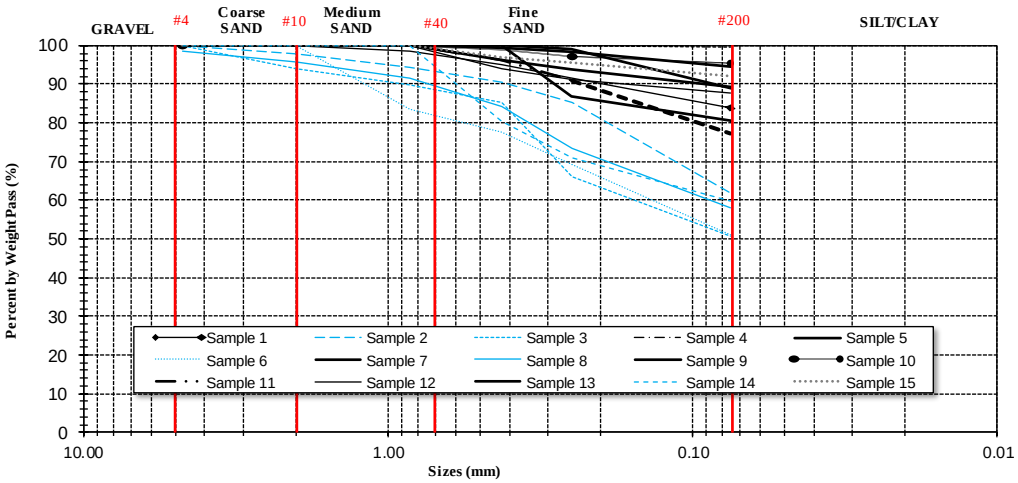

Figure 2.4: Particle size distribution of Magallanes soft soils (adapted from Donoso, 2006)

Table 2.2: Results of different samples of Magallanes soft soils (Vasquez, 2012)

	Varvada Clay	Lana Plant Clay	Chiloe-Briceño Clay	Cereco Clay
Sand	11	0	5	2
Silt	81	85	83	84
Clay	8	15	12	14
PI	28,4	19,1	11,2	16,9
Activity (A)	3.55	1.27	0.93	1.21

In summary, it can be said that, in average terms, Magallanes soft soils showed a grain size distribution marked by the predominance of the silt fraction (≈ 83.25%), with the clay fraction ranging from 8 to 15%, and sand from 0 to 11%, (Table 2.2).

2.2.5 Mineralogical composition

The mineralogical composition of the soil and its clay fraction may provide valuable information of its origin, as well as allow the prediction of some of its physical and mechanical properties. X-ray diffraction (XRD) tests were used to obtain important characteristics about the structure of any crystalline substance, element, or compound (Bonito, 2008). As presented in Table 2.3 the mineralogical composition was carried out by direct means, rather than the traditional indirect clay minerals evaluation through Atterberg limits which only give signs, sometimes ambiguous, of the predominant clayey fraction. The mineralogical identification study was carried out with X-Ray Diffraction equipment, SIEMENS D5000, from the Department of Physics of the University of Chile (Villarroel & Damianovič, 2008; Vasquez, 2012). The analysis was qualitative (Table 2.3), therefore the amount of clay minerals found was not determined, but it was identified that the peaks of vermiculite and montmorillonite are stronger than the others. Vasquez (2012) has demonstrated that the Magallanes soft soils exhibit two major types of clay minerals: vermiculite and montmorillonite. As written above, the identification of clay minerals may be important to anticipate the engineering properties of the soil. Mitchell & Soga (2005) and Gonzalez de Vallejo (2004) have identified three main groups of clay minerals: kaolinite, illite, and smectite (including montmorillonite). In general, smectites are expandable, kaolinites are stable, while illites exhibit a collapsible behaviour (Gonzalez de Vallejo, 2004). In Figure 2.5, it is possible to observe evidence of the expansion of the soil of Magallanes with pavement lifting, suggesting the presence of smectites.

Table 2.3: Summary of XRD results of Magallanes soft soils (clay minerals identified in bold)

Vasquez, 2012 [a)]	Vasquez, 2012 [b)]	Jordan et al., 2008 [c)]	Villarroel & Damianovic, 2008 [c)]
Quartz	Quartz	Quartz	Quartz
Vermiculite	Albite	Albite	Rutile
Montmorillonite	**Vermiculite**	Microcline	Albite
Graphite	Faujasite	**Kaolinite**	**Muscovite**

Note: a) Cereco Clay; b) Varvada Clay; c) Other MSS samples

Figure 2.5: Uprising of the pavement in El Ovejero, Punta Arenas (adapted from Vasquez, 2012)

2.2.6 Organic matter and plasticity

The organic matter has a strong influence on the physical and plasticity characteristics of a soil, which is reflected on its mechanical behaviour (Coelho 2000; Correia 2011). Thus, it is of upmost importance to know the organic matter content of Magallanes soft soils.

From the bibliographic review, it was possible to identify that the Varvada clay presents an organic matter content that ranges from 10 to 30% (Vasquez, 2012). For the other Magallanes soft soils, there is no information available regarding the organic matter content, but, from the geological studies it is expected that such soils have organic matter in a content not negligible.

The plasticity characteristics of the Magallanes soft soils are described in detail by Vasquez (2012) and Donoso (2006), as presented in Table 2.1 and Figure 2.2, respectively. It may be found that the plastic limit ranges from 2.7 to 25.4%, while the liquid limit ranges from 18 to 53.8%, equivalent to an average plasticity index of 21.85%. When the plasticity index is related with the clay fraction (average of 11.5%, presented in Table 2.2, it is found that the Magallanes soft soils present an average activity of 1.9, which is typical of a smectite clay mineral. This is in according to the mineralogical composition.

From Table 2.1 it is possible to observe that the natural water content of Lana Plant clay is very near to the liquid limit, suggesting that this soil shows a reduced undrained shear strength, behaving as a normally consolidated or slightly overconsolidated soil. If the water content reaches the liquid limit, the soil could turn into an unstable fluid soil.

2.2.7 Mechanical Behaviour of Magallanes Soft Soil

The classical soil mechanics theory analyses the mechanical behaviour of soils according to different individual perspectives, such as compressibility, primary and secondary consolidation, and stress-strain-shear strength (Coelho, 2000). Such properties will be described in the next sections based on the works published by Donoso, (2006) and Vasquez, (2012).

2.2.7.1 Compressibility and consolidation results

The compressibility and consolidation characteristics of the Magallanes soft soils were evaluated by oedometer tests performed on intact samples collected at different locations (Vasquez, 2012). The oedometer tests were performed under the procedures described in the standard ASTM D 2435-02 (2003). Figure 2.6 summarises the results obtained for the Varvada clay, Lana Plant clay, Chiloe – Briceño clay and Cereco clay.

The Varvada clay behaves like a normally consolidated (NC) sample as mentioned by Vasquez (2012), however, the results in Figure 2.6a) seem to indicate that the samples at the depth of 1m and 3m are slightly overconsolidated (OCR ≈ 3). As expected, the compressibility indices (C_r and C_c) and the natural void ratio decrease as the depth increases (Vasquez, 2012). In terms of primary consolidation, Vasquez (2012) observed that the consolidation coefficient, c_v, increases with the vertical pressure: for stresses lower than 50 kPa, c_v is around 45 m^2/year, while for stresses higher than 200 kPa the c_v decreases to values lower or equal to 10 m^2/year (Vasquez, 2012).

The Lana Plant clay behaves as a slightly overconsolidated soil (OCR > 2), exhibiting a very low recompression index (Figure 2.6b). This behaviour agrees with the consolidation indices that shows values of 75 m^2/year for the overconsolidated state, decreasing to values lower or equal to 5 m^2/year in the normally consolidated state (Vasquez, 2012).

The Chiloe – Briceño and Cereco clays present a very similar behaviour. Both soils behave like a normally consolidated soil (OCR ≈ 1) exhibiting a compressibility index lower than the other clays, reflecting its nature (both soils are tills). The coefficient of consolidation is continuously decreasing with the increase of the vertical effective stress, as expected for a normally consolidated soil (Vasquez, 2012).

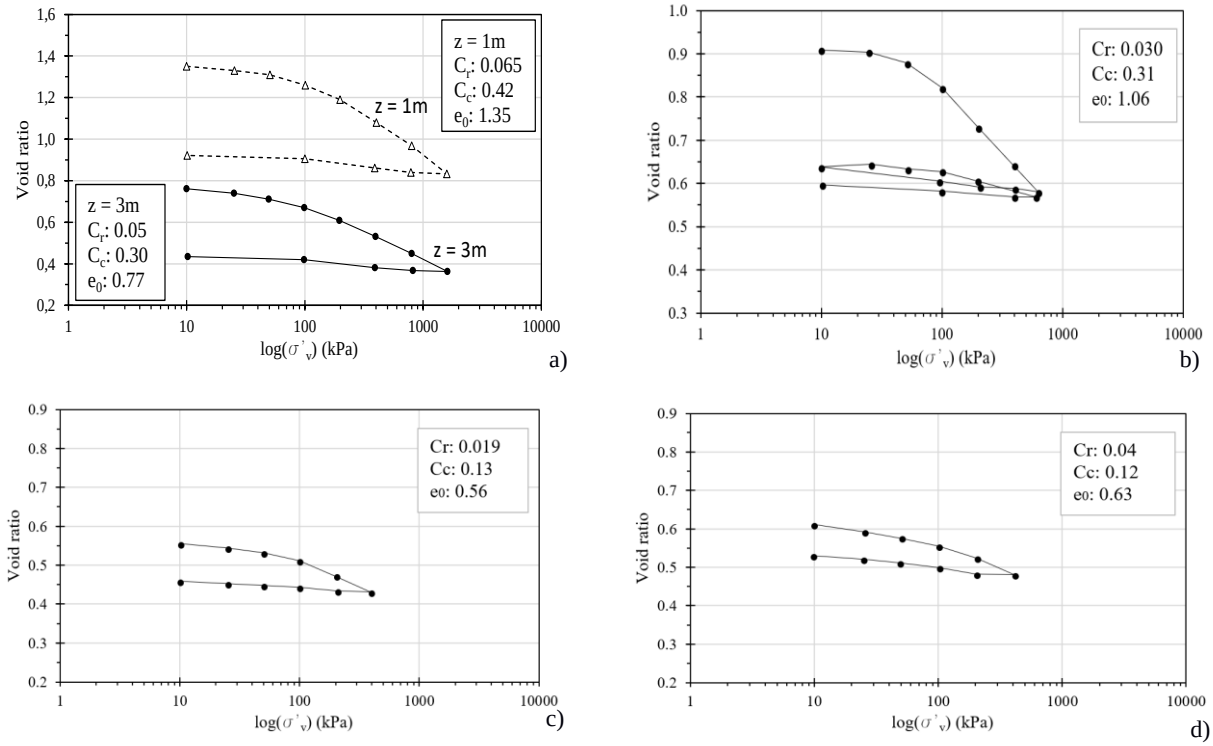

Figure 2.6: Consolidation Curves of Magallanes soft soils (adapted from Vasquez, 2012): a) Varvada Clay; b) Lana Plant clay; c) Chiloe – Briceño clay; d) Cereco clay

The Table 2.4 summarises the main results obtained from the oedometer tests. It is observed that the soft soils of aquatic environment are those that present higher initial void ratio and compressibility index. For the basal till, the result reported the lowest re-compressibility index, C_r and the lowest initial void ratio, e_0 (Vasquez, 2012).

Table 2.4: Compressibility characteristics of Magallanes soft soils (adapted from Vasquez, 2012)

Sample	Sedimentation Environment	e_0	C_c	C_r
Varvada Clay (z = 1m)	Aquatic high energy	1.35	0.42	0.065
Varvada Clay (z = 3m)	Aquatic/Lagoon	0.77	0.30	0.05
Lana Plant clay	Flooded fluvial	1.06	0.31	0.03
Chiloé- Briceño clay	Basal tills	0.56	0.13	0.019
Cereco clay	Thrust tills	0.63	0.12	0.04

2.2.7.2 Stress-strain-shear strength behaviour

The stress-strain behaviours of the MSS were studied by Vasquez (2012). Several triaxial tests were made on intact samples retrieved from in-situ boring samples. Once extracted, the samples were trimmed in the laboratory to the final dimensions of 50 mm in diameter and 100 mm in height. Figure 2.7 shows some of the laboratory procedures adopted; a full description of the laboratory procedure is described in Vasquez (2012).

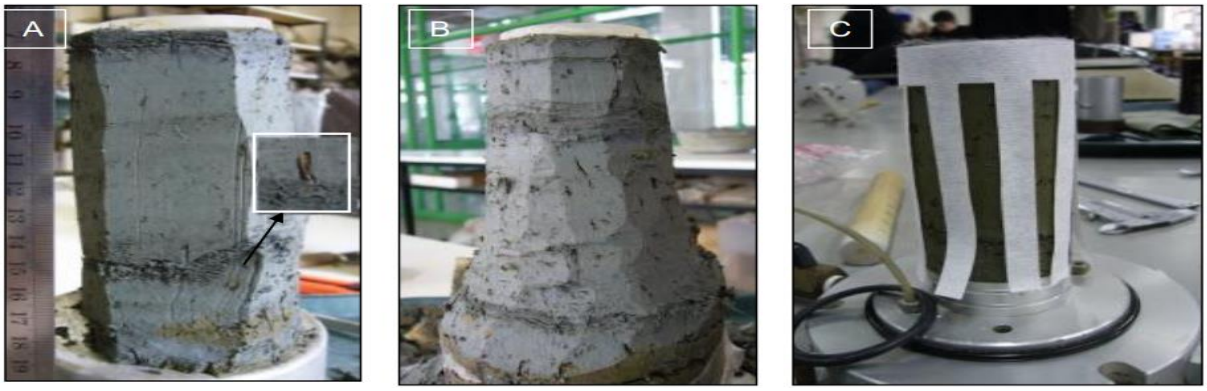

Figure 2.7: Sample preparation of Magallanes soft soils (adapted from Vasquez, 2012): a) organic matter and stratification detail; b) sample preparation; c) paper to accelerate the saturation

The triaxial tests performed were Consolidated Isotropically Undrained Tests (CIU). The samples were submitted to confining pressures of 100, 200, and 300 kPa. The undrained shear stage was performed under a constant strain rate of 0.13 %/min, referring to the sample height.

Figure 2.8 shows that the shear strength and the excess of pore water pressure increase with the confining pressure. It is also observed that the excesses of pore water pressure developed during the undrained shear are positive (contractive behaviour), which agrees with the normally consolidated or slightly overconsolidated state of the samples. The effective stress path shown in Figure 2.9 reflects this behaviour, i.e., the effective stress path moves to the left, corresponding to a positive excess pore water pressure, evolving to the failure. The shape of the curves of normalized q-ε_a and Δu-ε_a are approximately homothetic independently of the confining pressure (Figure 2.8), i.e., suggesting that the Cereco clay exhibits a normalized behaviour.

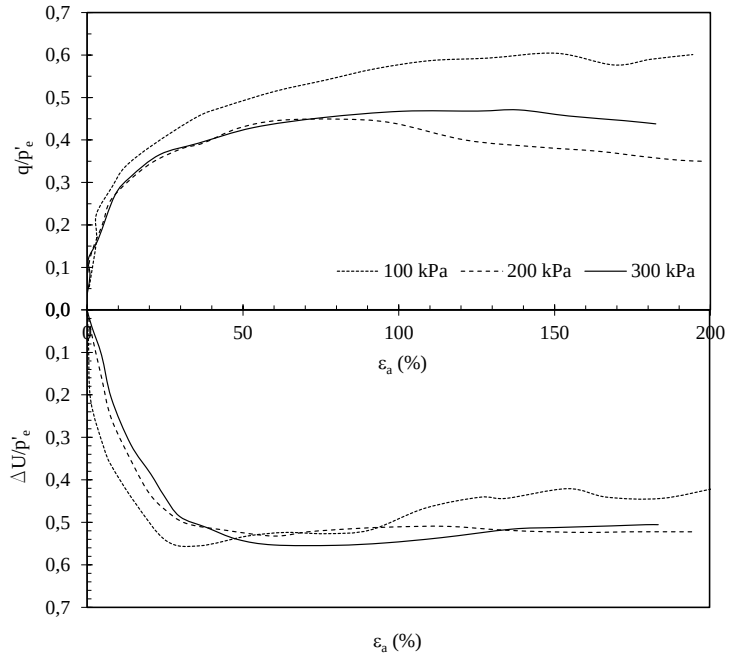

Figure 2.8: Normalized q-ε_a and Δu-ε_a plot obtained in CIU triaxial test for Cereco clay (adapted from Vasquez, 2012)

The Figure 2.9 presents the effective stress path and the Mohr-Coulomb failure envelope for the Cereco clay, with the shear strength parameters, $c' = 0$; $\emptyset' = 35^{o}$ (Table 2.5). For a normally consolidated soil, the Mohr-Coulomb coincides with the critical state line (CSL), characterised by its slope, $M = 1.418$, as presented in the same figure. The shear strength parameters obtained maybe higher for soft soils, but they agree with its grain size composition (Table 2.2).

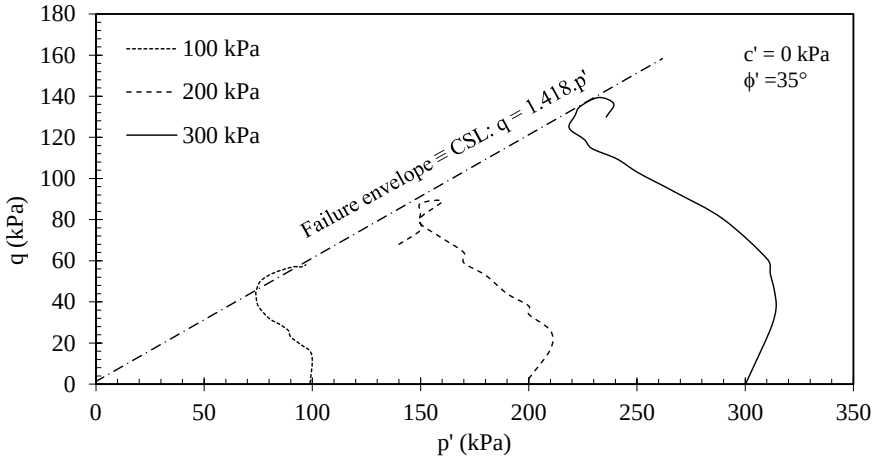

Figure 2.9: Stress paths obtained in CIU triaxial test for Cereco clay (adapted from Vasquez, 2012)

Table 2.5: Shear strength parameters (adapted from Vasquez, 2012)

Sample	c' (kPa)	ϕ' (º)	M
Varvada Clay (OC)	26	22	-
Varvada Clay (NC)	0	26	1.027
Chiloé- Briceño clay	15	30	-
Cereco clay	0	35	1.418

2.2.8 Summary of Magallanes soft soils properties

Table 2.6 presents a summary of the main geological, physical, and mechanical characteristics of the Magallanes soft soils.

Table 2.6: Geological, physical, and mechanical characteristics of Magallanes soft soils

Geological Description	
Macroscopic description	Blue grey colour with irregular lenses of silt and sand, abundant remains of plant material, metallic smell [(1)]
Sedimentary environment	Marine - Lacustrine [(1)]
Geological Period of Formation	Holocene - Pleistocene
Mineralogical Composition	Quartz, Albite, Vermiculite, Montmorillonite, Kaolinite, Muscovite [(1-4)]
Physical Properties	
Specific Gravity of Soil	2.67 [(1)]
Water Content	9.2 - 36% [(1-4)]
Void Ratio	0.56 - 1.35 [(1)]
Saturated unit weight	17 - 21 [(1)]
Grain size composition	Sand: 0 - 11%; silt: 81 - 85%; clay: 8 - 15% [(1)]
Plasticity Index	w_P = 2.7 - 25.4%; w_L= 18 - 53.8%; PI ≈ 21.85% [(1)]
Activity	1.9 [(1)]
Organic Matter	10% - 30% [(1)(a)]
Soil classification (UCSC)	CL, SM, ML [(4)]
Mechanical Characteristics	
Overconsolidation ratio	1 - 3 [(1)]
Compression Index	0.12 - 0.42 [(1)]
Swelling Index	0.019 - 0.065 [(1)]
Consolidation coefficient	NC: 5 - 10 m^2/year; OC: 45 - 75 m^2/year [(1)]
Effective Cohesion	0 - 26 kPa [(1)]
Shear Strength Angle	22 - 35º [(1)]
Undrained Shear Strength	20 - 34 kPa [(1,3)]

References: [(1)] Vasquez, 2012, [(2)] Jordan et al., 2008, [(3)] Vivar, 2013, [(4)] AustroUmag, 2018
Notes: [(a)] Only for Varvada clay samples.

2.3 Portuguese Soft Soils

Recently, a study focused on the characterisation of Portuguese soft soils was carried out by Esteves (2014), who has reported information from different sources, establishing the essential properties of the geological, physical, and mechanical behaviour (compressibility and stress-strain-shear strength) of soft silt-clay formations that exist in Portugal, (Figure 2.10). Other important studies have been performed on soft soils located in the north of Portugal, namely, Leça: (Aguiar, 1992; Furtado, 1995; Gomes and Ladeira, 1991), Ria de Aveiro: (Aguiar, 1992, Bonito, 2008, Esteves 2014), in the central region mainly Baixo Mondego: (Hindle, 1994; Phillipson, 1994; Soares, 1995; Coelho, 2000; Correia, 2011) and in the southern part of Portugal, Baixa de Santo André (Silva, 1984) and Baixo Tejo (Marreiros and Carneiro, 1995)

In the next sections, a summary of the main features of the Portuguese soft soils will be presented, focusing on the geological characteristics, physical properties, and mechanical behaviour.

Figure 2.10: Main soft soil deposits in Portugal (Esteves, 2014)

2.3.1 Geological Characteristics

The Portuguese soft soils have essentially two main sedimentary environments, estuary, or lagoon (Esteves, 2014). Estuaries are bodies of water located in coastal re-entrances, located at the mouth of rivers, in which the sea penetrates and circulates internally (Carvalho & Carvalho, 2005). Further investigation has shown that in Portugal the Minho, Leça, Mondego, Tejo, and Sado rivers can be characterised as estuaries, those are places where there is a strong predominance of soft clayey silt alluvium (Esteves, 2014). Lagoons are aquatic extensions, developing parallel to the coast and isolated from it by mountain/sand-dune ranges. In Portugal, examples of lagoon sedimentary environments are the Baixa de Santo André (Silva, 1984) and the Ria de Aveiro. The last one is a large lagoon area, with a length of about 50 km, where the term "Ria" comes from a river valley subject to the water of the sea.

The Leça soft soil has a hydrographic basin of approximately 185 km^2, with a narrow and elongated shape with a dominant direction NE-SW. This basin is confined at north by the hydrographic basin of the Ave River, and at the east and south limited by the Douro River.

The Ria de Aveiro corresponds to an extensive lagoon area, approximately 50 km in extension. The first sediments of this lagoon dated from 200 million years ago, when, after fracture, the euro-Asian and north American plates started to separate and the space between them was invaded by

sea water. In terms of stratigraphy, the Ria de Aveiro lagoon is composed of gneisses and migmatites (Proterozoic), as well as granitoids (Palaeozoic), in the northern end, and schists (Proterozoic) in the other zones (Rocha, 1993) cited by (Esteves, 2014). The soft soil deposit was formed in transition environments, corresponding to recent alluvial deposits of the Holocene period, made of successive layers of silty mud or clayey, muddy sand and sand. The deposit thickness is variable, reaching the 40m depth, and the water table varies with season, although almost always superficial (Esteves, 2014). Aguiar (1992) reported the presence of shells and plant fossils. The soft soil deposit lays on a cretaceous formation and composed mainly by sandstones, clays, and limestone.

The Mondego River has a hydrographic basin of about 6670 km^2 presenting a dominant northeast-southwest orientation. Along its way, the river receives the water from its effluents like Dão in the right bank, Alva Ceira, Ega, Arunca, and Pranto, on the left bank. Much of the way to Coimbra, Alto Mondego, consists of a valley embedded in metamorphic rocks and granite. The terminal section, designated by Baixo Mondego, with about 40 km in extension, crosses an alluvial plain. As Coelho (2000) points out, from the geological point of view, the soft soil of Baixo Mondego has a sedimentary environment similar to those in other Portuguese alluvial deposits, namely the fluvial transport of sedimentary material due to the rock erosion at upstream, and their deposition, downstream, where the river velocity is lower. The mentioned deposition process was developed in the deep valleys excavated during the last glacial era, being accompanied by the gradual but sustained rise of sea level during the last few thousand years. According to the same author, the mineralogical, grain size and organic compositions of these soft soils reflect the geological processes involved in its formation. In terms of mineralogical composition, the deposit has a large amount of quartz, mica, and kaolinite, which agrees with the granite found in the Alto Mondego valley. The significant presence of organic matter in the deposit is a result of the intensification of life during the period of its formation and is further accentuated by the maritime influence on the sedimentary environment, which is easily identified by the numerous fragments of marine organisms found in the deposit at various depths (Coelho, 2000).

The estuary of Tejo River has a narrow and deep mouth of the channel, with west-east orientation, followed at upstream by a dissymmetric widening elongated to north-east. The inner part of the estuary, the widest and shallow, is located immediately on the extension of the lower Tejo valley. The Tejo estuary is resulted from the sea level variations due to successive cooling (glaciers) and heating earth periods (Marreiros and Carneiro, 1995).

Baixa de Santo André is in the Alentejo coast, corresponding to another lagoon on the Portuguese coast. The Lagoon of Baixa de Santo André was formed due to the appearance of a coastal sand

dune that blocked the mouth. The existence of wider beaches than the existing ones allowed the formation of a dunar system concordant with the coast, which blocked even further depressions. The sedimentation that occurred along the geological history of the lagoon is of the fluvial marine type, developed during the Holocene period. The soft soil deposit is composed of clayey muds and silty muds alternating with sands, with a thickness that may reach up to 24 m. Table 2.7 summarises the geological characteristics of some of the soft soils in Portugal. All soft soils described in Table 2.7 contain organic matter in the range of , a characteristic that is typical of recent organic alluvial deposits (Silva, 1984).

Table 2.7: Geological characteristics of several Portuguese soft soils

Geological Description	**Rio Leça**	**Ria de Aveiro**	**Baixo Mondego**	**Baixo Tejo**	**Baixa de Santo André**
"Mother"-rock	granites, schist and greywackes [(2)]	granites, schists and some greywackes, calcareous [(2)]	granite, schist, and some greywackes, sandstones and calcareous [(1)]	schists, greywackes, sandstones, calcareous and some granite [(7)]	calcareous, greywackes, marls, schist, sandstones [(8)]
Sedimentary Environment	Alluvial and Estuary [(2)]	Deltaic Transition [(2)]	Alluvial and Estuary [(1)]	Alluvial and Estuary [(7)]	Marine fluvial and lagoon [(8)]
Geological Period of Formation	Holocene [(2)]	Holocene [(2)]	Holocene [(1)]	Holocene [(7)]	Holocene [(8)]
Thickness	≤20 a 27 m [(2)]	≤20 m [(2)]	≤23 m [(6)]	≤58 m [(7)]	≤24 m [(8)]

References: [(1)] Coelho (2000); [(2)] Aguiar (1992); [(3)] Furtado (1995); [(4)] Gomes & Ladeira (1991); [(5)] Ladeira & Gomes (1991); [(6)] Several authors; [(7)] Marreiros & Carneiro (1995); [(8)] Silva (1984); [(9)] Correia (2011)

2.3.2 Physical Characteristics

The studies developed for the Portuguese soft soils (Leça, Ria de Aveiro, Mondego River, Tejo river and Baixa de Santo André), have considered the evaluation of the physical characteristics, including the classification of the soils. The main physical properties of the soil, the grain particle size distribution, its mineralogical and chemical composition, and the organic matter present in the soil will be presented in detail in the following sections.

2.3.3 Physical properties

Regarding the physical properties, the main physical indices were, the specific gravity of the soil particles, the water content, and the unit weight (Table 2.8).

The specific gravity values reflect the nature of the mineralogical composition of the soils. The natural water content of the soft soils is in general very high, indicating that the soils are in a saturated condition. The saturated unit weight of all soils is in general low (12 – 18.5 kN/m^3),

with high water content and the presence of organic matter. These physical indices are typical of recent organic alluvial deposits.

Table 2.8: Summary of the index properties of some Portuguese soft soils

Physical Properties	**Rio Leça**	**Ria de Aveiro**	**Baixo Mondego**
G_s	2.58 - 2.64 (2)	2.45 – 2.72 (2)	2.43 - 2.63 (6); 2.55 (9)[a]; 2.50-2.62 (1)
w_{nat}	44 - 60% (2)	30 – 89% (2)	56 - 110% (6); 80.87 (9)[a]; 55 - 127% (1)
γ_{sat}	14.6 - 16.9 kN/m^3 (2)	12 - 18.5 kN/m^3 (2)	13.8 - 16.7 kN/m^3 (6); 14.56 kN/m^3 (9)[a]; 12.8 - 16.1 (1)

References: (1) Coelho (2000); (2) Aguiar (1992); (3) Furtado (1995); (4) Gomes & Ladeira (1991); (5) Ladeira & Gomes (1991); (6) Several authors; (7) Marreiros & Carneiro (1995); (8) Silva (1984); (9) Correia (2011)
[a] analysis at z = 2.5 m.

2.3.4 Particle size distribution

The grain size distribution of soil particles according to their dimensions was evaluated on soil samples resulting from either residues of intact samples or from small parts of a large volume sample.

For the Baixo Mondego soft soil, the fine fraction (< #200) of the soil was also evaluated through a laser granulometer (Correia, 2011). The results obtained for the particle size distribution are presented in Table 2.9.

Table 2.9: Particle size distribution of some Portuguese soft soils

Rio Leça	**Ria de Aveiro**	**Baixo Mondego**	**Baixo Tejo**	**Baixa de Santo André**
silt: 75 - 80% (2) clay: 5% (2) sand: NA	silt: 84% (2); 51 - 84% (10) clay: 10% (2); 10 - 31% (10); sand: 6 - 28% (10)	silt: 32 - 90% (1); 71% (9)[a]; clay: ≤25% (1); 8 - 12% (9)[a]; sand: 17-21% (9)[a] ≤35% (1)	Material bellow #200 mesh > 70% - 90% (7)	silt: 40% - 90% (8); clay: ≤25% (8) sand: NA

References: (1) Coelho (2000); (2) Aguiar (1992); (3) Furtado (1995); (4) Gomes & Ladeira (1991); (5) Ladeira & Gomes (1991); (6) Several authors; (7) Marreiros & Carneiro (1995); (8) Silva (1984); (9) Correia (2011); (10) Esteves (2014)
[a] analysis at z = 2.5 m.

In summary, it can be said that on average, all soft soils have a predominance of the silt fraction with an important clay amount and some sand fraction. These characteristics are consistent with the deposition conditions observed during the geological formation of the deposits, typical of recent alluvial deposits.

2.3.5 Mineralogical Composition

The mineralogical composition of a soil, in particular of its clay fraction, may provide valuable information of its origin, as well as allow the prediction of some of its physical and mechanical properties. X-ray diffraction (XRD) tests were used to identify the minerals present in the Portuguese soft soils, of which the results that are presented in Table 2.10. For the Baixo Mondego soft soil, it was performed not only a qualitative but also a quantitative measurement of clay minerals (Correia, 2011).

From the analysis of the results, it is possible to verify that all the soft soils studied have quartz and kaolinite in their mineralogical composition, reproducing the geological history of the soils, namely the sedimentary environment. Quartz is the predominant mineral, hiding the diffraction of other minerals in clay minerals. To have a more accurate evaluation of the clay minerals, for the soft soil of Baixo Mondego, Coelho (2000) and Correia (2011) have performed specific XRD tests on samples containing only clay (< 2μm) particles showing mostly kaolinite and vermiculite.

Table 2.10: Mineralogical composition of some Portuguese soft soils

Characteristics	**Rio Leça**	**Ria de Aveiro**	**Baixo Mondego**	**Baixo Tejo**	**Baixa de Santo André**
Macroscopic Description	fine, homogeneous, dark, micaceous, and organic [2]	fine, homogeneous, dark, micaceous, and organic [2]	fine, homogeneous, dark, micaceous and organic [6] shells [1]	Clay mud, soft soil and shells [7]	clayey, organic, dark, soft and shells [8]
Mineralogical Composition	Quartz, kaolinite, muscovite, and feldspar [2]	Quartz, kaolinite, muscovite, and feldspar [2]	Quartz, kaolinite, muscovite, calcite [1], vermiculite, iron chlorite [9]	NA	Quartz, illite, kaolinite, montmorillonite, feldspar [8]

References: [1] Coelho (2000); [2] Aguiar (1992); [3] Furtado (1995); [4] Gomes & Ladeira (1991); [5] Ladeira & Gomes (1991); [6] Several authors; [7] Marreiros & Carneiro (1995); [8] Silva (1984); [9] Correia (2011); [10] Esteves (2014)
[a] analysis at z = 2.5 m.

2.3.6 Organic matter and plasticity

As written previously, all Portuguese soft soils contain organic matter in significant proportions, a characteristic that is typical of recent alluvial deposits. Moreover, it is well known that the organic matter has a strong influence on the physical and plasticity characteristics of a soil, which is reflected on its mechanical behaviour (Coelho, 2000; Correia, 2011). Thus, the evaluation of the organic matter content is of upmost importance.

As it may be seen from Table 2.11, the organic matter of Portuguese soft soils is around 10%, in agreement with the sedimentary environment. For two of the Portuguese soft soils (Baixo Tejo and Baixa de Santo André), there is no information available regarding the organic matter content,

however, from the geological studies (section 2.3.1) it is expected that such soils contain organic matter in significant proportions.

The plasticity characteristics of the Portuguese soft soils are summarised in Table 2.11. It may be found that the plastic limit ranges from 16 to 59%, while the liquid limit ranges from 50 to more than 100%, equivalent to an average plasticity index of 30%. When the plasticity index is related to the clay fraction (≈ 20%, section 2.3.2), it is found that the Portuguese soft soils present an average Activity of 1.5, which is typical of illite (muscovite) and vermiculite clay minerals (Mitchell & Soga, 2005). This agrees with the mineralogical composition (Table 2.10). The activity values higher than 2 reported by the same authors should be interpreted with caution because they are not in agreement with the clay mineral composition. Thus, it is possible to conclude that the clay fraction of the Baixo Mondego soft soil contains not only kaolinite, but also vermiculite, illite, and some iron chlorite.

As observed for the Magallanes soft soils, the Portuguese soft soils have a natural water content very near the liquid limit, suggesting that these soils show a low undrained shear strength and behave as a normally consolidated or slightly overconsolidated soils.

2.3.7 Mechanical Characteristics

The knowledge of the behaviour of a soil is only complete when, in addition to the geological and physical characteristics, the mechanical behaviour is also known. In the next sections, a summary of the main features regarding the compressibility, primary and secondary consolidation characteristics, as well as the stress-strain-shear strength behaviour of some Portuguese soft soils are presented.

2.3.7.1 Compressibility and consolidation results

The compressibility and consolidation characteristics of some Portuguese soft soils were evaluated by oedometer tests performed on intact and laboratory reconstituted samples.

In terms of stress, with the exception of the superficial crust of some soft deposits, all Portuguese soft soils are in a normally consolidated or lightly overconsolidated state, which agrees with the fact that these soils are geologically very recent - Holocene period, (i.e., with less than 120.000 years old). Regarding the compressibility, all Portuguese soft soils exhibit high compressibility, expressed by the $C_c \approx 0.5$ and $C_r \approx 0.06$ values, related with the high natural water content and

void ratio. It must be pointed out that the compressibility related with creep/secondary consolidation is usual for these soft soils, which is linked with the fact that these soils are geologically very recent and are organic soils (Figure 2.11 a-b presents the compression curve at the end of primary consolidation, EOP, and after 72h). The compressibility is also characterised by its anisotropy (higher compressibility index in the horizontal direction) due to the sedimentary environment and grain size composition of the soils (Correia 2011).

Table 2.11: Organic matter and plasticity of some Portuguese soft soils

	Rio Leça	**Ria de Aveiro**	**Baixo Mondego**	**Baixo Tejo**	**Baixa de Santo André**
Organic Matter	8 - 11% (2)	9 - 10% (6); 3 - 9.8% (7)	2 - 13% (1); 7.96% (9);	NA	NA
Plastic Limit	23 - 46%(10)	19 - 59(9)	42.80% (9); 30-44% (1)	16 - 43% (11)	NA
Liquid Limit	57 - 72% (2)	31 - 53% [c](2,3); 77% (1)	71.03% (9); 60 - 109% (1)	50 - 70% (6)	50 - 188% (5)
Plasticity Index	17 - 22% (2)	≤35% (1); ≤13% [c] (2,3)	28.2% (9); 26 - 66% (1)	20 - 35% (6)	30 - 125% (5)
Activity	3.4 - 4.4 [a]; 2 – 3 [b]; ≤1 [b](2)	3.5 [a]; 1.9 [b]; 1.9 [d](1)	1.19 (9); 0.42 – 0.72 (1)	NA	NA
Soil classification (UCSC)	OH (2)	CL, ML, OL (3); OH (1,8)	MH [c](9) OH(1) high plasticity	MH, CH and ML(6)	CH, CL, MH, ML, OH (5)

References: (1) Coelho (2000); (2) Aguiar (1992); (3) Furtado (1995); (4) Gomes & Ladeira (1991); (5) Ladeira & Gomes (1991); (6) Several authors; (7) Marreiros & Carneiro (1995); (8) Silva (1984); (9) Correia (2011); (10) Esteves (2014)
Observations: [a] results obtained on the samples tested in their natural state; [b] results obtained on samples previously air-dried; [c] results conditioned by the elimination of the organic matter in the drying process for the preparation of the sample, reducing the plasticity characteristics; [d] results obtained on samples previously dried in an oven (100°C)

The consolidation characteristics presented by the Portuguese soft soils are in general low, exhibiting a c_v of the order of 10 m^2/year. It is important to mention that the consolidation coefficient estimated from back-analysis studies (several authors cited by Coelho 2000) showed that in field the consolidation time is much faster than the one evaluated from the oedometer tests, which may be related to the presence of thin layers of silty sand or sandy silt in such deposits due to the sedimentary environment.

Table 2.12: Compressibility, consolidation, and permeability characteristics of some Portuguese soft soil.

	Rio Leça	**Ria de Aveiro**	**Baixo Mondego**	**Baixo Tejo**	**Baixa de Santo André**
OCR	1.4 - 1.6 (2)	1.5 (2)	1.4 – 3 (9)[a]; 6 (1)[c]; 1 – 1.3 (1)[d]	≥1 for Z≤3m (6)	1 (5)
Swelling Index (C_r)	0.06 - 0.08 (2)	0.09 (3); 0.02 - 0.09 (11)	0.04 - 0.16 (6); 0.065 (9); 0.055 – 0.165 (1)	NA	NA
Secondary Cons. Coef. [b]	C_α/C_c = 0.038-0.040 (2); C_α = 0.019-0.021 (2)	C_α/C_c = 0.044 (3); C_α = 0.002-0.022 (3)	C_α/C_c = 0.046 (9); C_α = 0.002-0.022 (6); C_α = 0.010 - 0.082 (1)	NA	NA
Compression Index (C_c)	0.48 - 0.55 (2)	0.13 - 0.7 (8,4); 0.5 (3)	0.24 - 1.13 (6); 0.41 - 1.24 (1); 0.55 [e] - 0.75 [f] (9)	0.12 - 0.9 (6)	0.25 - 1.2 (5)
Consolidation Coefficient (c_v)	13 - 22 m^2/year (3); 1.3 m^2/year (2)	0.2 - 32 m^2/year (4); 13 - 22 m^2/year (12,2); 0.2 – 38.5 m^2/year (11)	2 - 130 m^2/year (6); 0.7 – 3 m^2/year (1); $c_v^{field} >>> c_v^{lab}$	0.3 - 2.2 m^2/year (6)	NA
Permeability Coefficient (k)	(0.1 - 4) x 10^{-9} m/s (2)	(1 - 12) x10^{-9} m/s (2)	4x10^{-10} -2x10^{-7} m/s (5); (3.9 -20.7) x 10^{-10} (9)	(0.5 - 6.5) x10^{-10} (6)	NA

References: (1) Coelho (2000); (2) Aguiar (1992); (3) Furtado (1995); (4) Gomes & Ladeira (1991); (5) Ladeira & Gomes (1991); (6) Several authors; (7) Marreiros & Carneiro (1995); (8) Silva (1984); (9) Correia (2011); (10) Esteves (2014)
Observations: [a] on surface; [b] Consolidation Index ; [c] z = 0m ; [d] z ≥ 3.5 to 20m; [e] vertical direction; [f] horizontal direction.

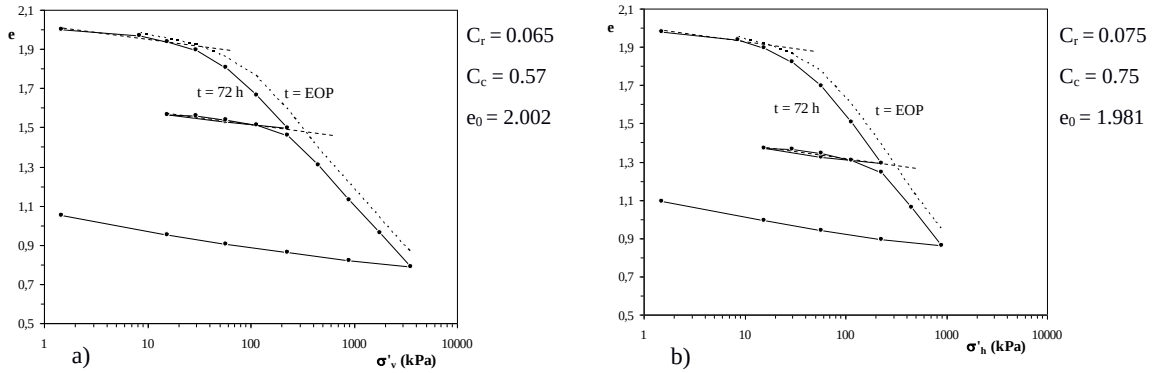

Figure 2.11: Oedometer test results for the Baixo Mondego soft soil: a) intact sample tested on vertical direction; b) intact sample tested on horizontal direction (Correia 2011)

2.3.7.2 Stress-strain-shear strength behaviour

The stress-strain behaviour of the Portuguese soft soils was studied by several authors as presented In Table 2.13, where the main results are summarised. The mechanical behaviour was characterised through laboratory triaxial tests complemented with in situ tests. The triaxial tests were performed on intact samples as well as on laboratory reconstituted samples. The triaxial tests performed were isotropically and anisotropically consolidated, sheared in drained and undrained conditions under different stress-paths. A detailed description of the triaxial tests, including the laboratory procedures, can be seen in the references presented in Table 2.13.

The undrained shear strength is in general low (< 50 kPa), typical of recent alluvial deposits, notwithstanding the fact that when normalised by the overburden effective stress it presents a high value due to the relatively low effective stress. The same behaviour was observed for the undrained stiffness modulus, which is in general low as expected for normally consolidated soft soils.

In general, the Portuguese soft soils are normally consolidated soils, which is consistent with their pore water pressure A-parameter (≥ 0.5) and cohesion in effective stresses (≈ 0). The shear strength angle in effective stresses is high, which is not in accordance with the plasticity characteristics, however, it reflects the grain size composition of such deposits (mainly silty soils with an important sand fraction).

Table 2.13: Mechanical behaviour of Portuguese soft soil

Characteristics	**Rio Leça**	**Ria de Aveiro**	**Baixo Mondego**	**Baixo Tejo**	**Baixa de Santo André**
Cohesion (c')	0 [a]; 30 kPa [a](2)	0 (5) - 20 kPa (2)	0 - 5 kPa (6) 0 (1)	NA	NA
Friction Angle (max) (ϕ')	41 - 44º [a]; 35º (2)	31º (2) 27º - 34º (11) -	37 - 42.5º 36.4 - 37.8 (1) 41.5 -36.3(1)	NA	NA
Undrained Shear Strength (S_u)	S_u/σ'_{vc} = 0.4 [a](2) 0.4 - 0.7 [b](2)	S_u/σ'_{vc} = 0.38 - 0.50 [e](2) 0.15 - 0.25 [d](2) 0.15 - 0.70 (5) S_u = 26 - 35[d](7) S_u = 44.2 – 68.5[d](6)	S_u/σ'_{vc} = 0.15 - 0.25 [e](1) 0.42 – 0.17(1) S_u = 20 - 69 kPa[j](6)	S_u = 20 - 35[d](7)	S_u = 32 - 40 kPa[d](8) S_u = 9 - 40 kPa[d](8)
Undrained Stiffness Modulus (E_u)	E_u/S_u = 200 - 300 [a,c](2) E_u/S_u = 200 – 300 [b,c](2)	E_u/S_u = 300 - 700 [e,c](2) E_u/S_u = 1200 - 1600 [d,c](2)	E_u/S_u = 100 - 400 [a,c](6) E_u/S_u = 150 - 500 [b,c](6)	E_u = 400–6000 kPa[c](7)	NA
A (Skempton)	0.7 - 0.9 [a]; 0.3 - 0.5 [b](2)	0.4 - 0.9 [e]; 0.9 [d](2)	0.4 - 0.6 [a,f]; 0.8 [b,f](6) ; ≈ 0 [e] 0.57 – 1.12 (1) 0.04 – 0.61 (1)	NA	NA

References: (1) Coelho (2000); (2) Aguiar (1992); (3) Furtado (1995); (4) Gomes & Ladeira (1991); (5) Ladeira & Gomes (1991); (6) Several authors; (7) Marreiros & Carneiro (1995); (8) Silva (1984); (9) Correia (2011); (10) Esteves (2014)
Observation: [a] normally consolidated soil; [b] overconsolidated; [c] Eu determinate for ε_a=0.1%; [d] results of triaxial extension tests; [e] results of triaxial compression tests; [f] results of triaxial extension tests. [g] results from vane – test.

Figures 2.12 and 2.13 illustrates the stress-strain-shear strength behaviour of the Baixo Mondego soft soil under undrained shear in compression and extension. The samples were submitted to confining pressures of 100, 200, and 300 kPa. The shear stress-strain and the excess of pore water pressure-strain plots show that the shear stress and the excess of pore water increase with the confining pressure. During the undrained shear, the normally consolidated samples develop positive excesses of pore water pressure, following an effective stress path to failure. However, for the samples under extension, at the start, the development of negative excesses of pore water

pressure was observed, showing that the samples increase in volume. However, as the shear was done under undrained condition the samples can only achieve failure developing positive excesses of pore water pressure (Correia, 2011). The results showed that the stress-strain-shear strength behaviour depends on the stress path compression, or extension, being obtained a shear strength angle of 37º in compression, and 32º in extension.

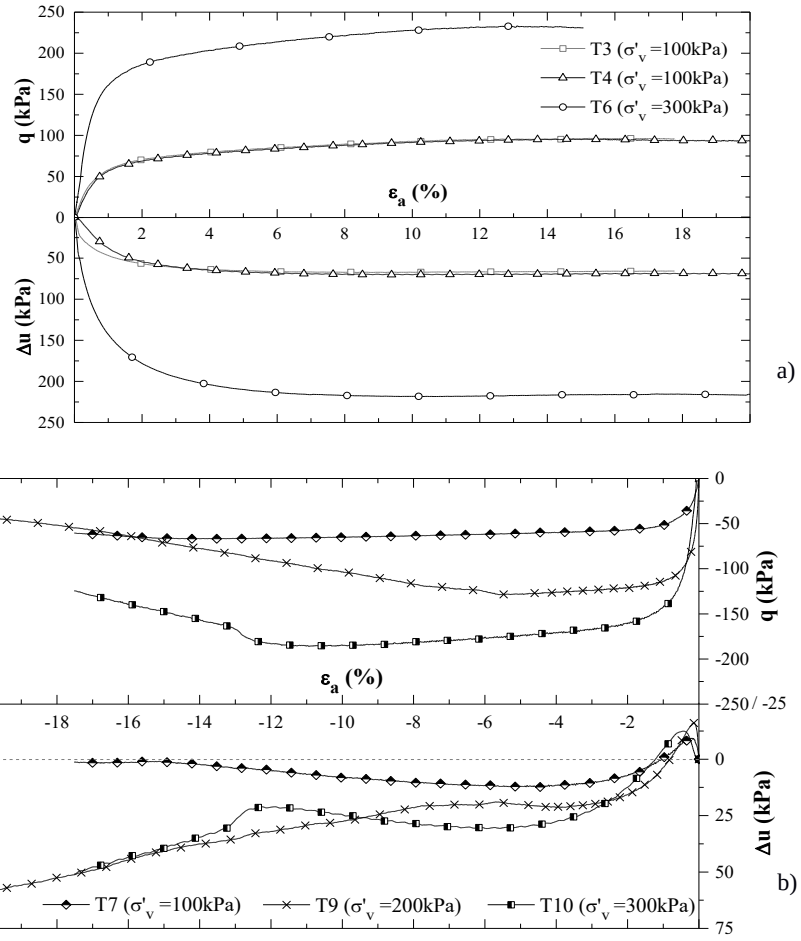

Figure 2.12: q-ε_a and Δu- ε_a plot obtained in CIU triaxial tests for Baixo Mondego soft soil: a) compression shear; b) extension shear (Correia, 2011)

2.3.8 Final remarks

Along the previous sections, a brief description of the soft soils from Magallanes area and from Portugal were done. Besides the natural differences, there are geological and geotechnical properties very similar which must be highlighted. A special emphasis given to the comparison between the Magallanes soft soils and the soft soil from Baixo Mondego because this will be the base material used in the laboratory work.

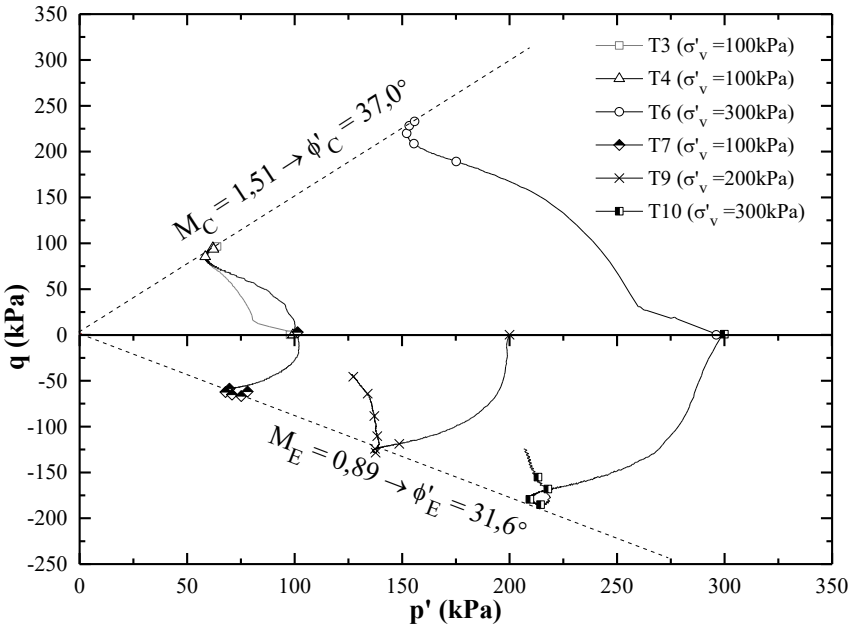

Figure 2.13: Stress paths obtained in CIU triaxial tests for Baixo Mondego soft soil (Correia, 2011)

Geologically, soil Magallanes soft soil (MSS), and Baixo Mondego soft soil (BMSS) are very recent alluvial deposits formed in the Holocene period. In both cases, the sedimentary environment is marine but, in the MSS has a lacustrine nature, while in the BMSS has an estuary origin. However, in both deposits there are irregular thin layers of silty sand or sandy silt material, with a high impact on the consolidation properties, as well as a significant organic matter which strongly influences the plasticity characteristics and the natural physical indices, in the special $w_{nat,}$ e_0. The mineralogical composition is similar apart from the clay minerals: montmorillonite is only present in the MSS.

Regarding the physical characteristics, it may be concluded that the MSS when compared with the BMSS exhibit a lower natural water content and void ratio and a higher saturated unit weight because the MSS are in a slightly overconsolidated state, while the BMSS are in a normally consolidated state. Nevertheless, these differences, the grain size composition is very similar, i.e., in both deposits the silt is the dominant fraction (≥ 70%).

In terms of mechanical characteristics, both soft soils exhibit similar compressibility properties, even if the compressibility is a little bit lower for the MSS due to their slightly overconsolidated condition. Can be related with the higher value of the effective cohesion of the MSS. The shear strength angle in effective stresses is lower for the MSS when compared with the BMSS, in agreement with the grain size composition: the MSS have a lower sandy fraction. Although these differences, both soft soils have a very low undrained shear strength, typical of recent alluvial deposits.

Apart from some natural differences between both soft soils, there are similarities between them. So, the experimental study, developed in the present work the BMSS is expected to be extrapolated with caution, to the MSS.

CHAPTER 3 – LITERATURE REVIEW

This chapter will address four important topics of this work. The first is the fundamental concepts of chemical stabilisation of soft soils unreinforced and reinforced with fibres. Then the mechanical behaviour of these composite materials under monotonic loading and, subsequently, under cyclic loading will be characterised. The chapter ends with the definition of the yield surface of natural and cemented clay.

Population expansion has increased the soil occupancy density, resulting in the need to occupy weak geotechnical foundation soils characterised by low shear strength and high deformability. In order to allow construction in such soils, ground improvement methods have been developed (Cajada, 2017). One of the ground improvement methods that has been applied successfully is the Chemical Stabilisation of Soils (CSS), in which the natural soil is mixed with stabilising binders, and in some cases mixed also with fibres to improve the tensile behaviour of the composite material (Chemical Stabilisation of Soils Reinforced with Fibres, CSSRF).

The CSS technique has been effectively used in practice for soil improvement in numerous engineering projects, such as transportation infrastructures, embankment and building foundation, liquefaction mitigation, slope stabilisation (Ali et al., 1992).

It is known that the improvement of soils with the use of stabilising binders increases the stiffness and strength of the non-stabilised soils but creates a material with high brittleness and low tensile and flexural strength. Thus, the inclusion of short fibres into the mixture intends to overcome such limitations of the CSS (Correia et al., 2017), i.e., the CSSRF technique arises as a response to the inability of the stabilised material to withstand loading in conditions of excessive strain, as well as when the composite material is under tensile stresses. Nowadays, there are several types of fibres that may be used as short reinforcement elements such as synthetic fibres, natural fibres and fibres produced from waste materials. Synthetic fibres can be divided into several subcategories since they can be made of polypropylene, nylon, plastic, fibreglass, asbestos, metals, and others. Among these, polypropylene fibres are often selected because of their competent mechanical and durability characteristics. Natural fibres may come from fruits

(coconut and banana fibres) or plants such as bamboo, sisal, or hemp. The major concern about natural fibres is related with their durability and tendency to lose resistance over time due to environmental conditions. Although synthetic fibres present greater strength and durability than natural fibres, natural fibres are advantageous from an environmental point of view.

As stated above, this chapter present a brief framework of the mechanical behaviour of CSS and CSSRF techniques under monotonic and cyclic loading as summarised in Figure 3.1.

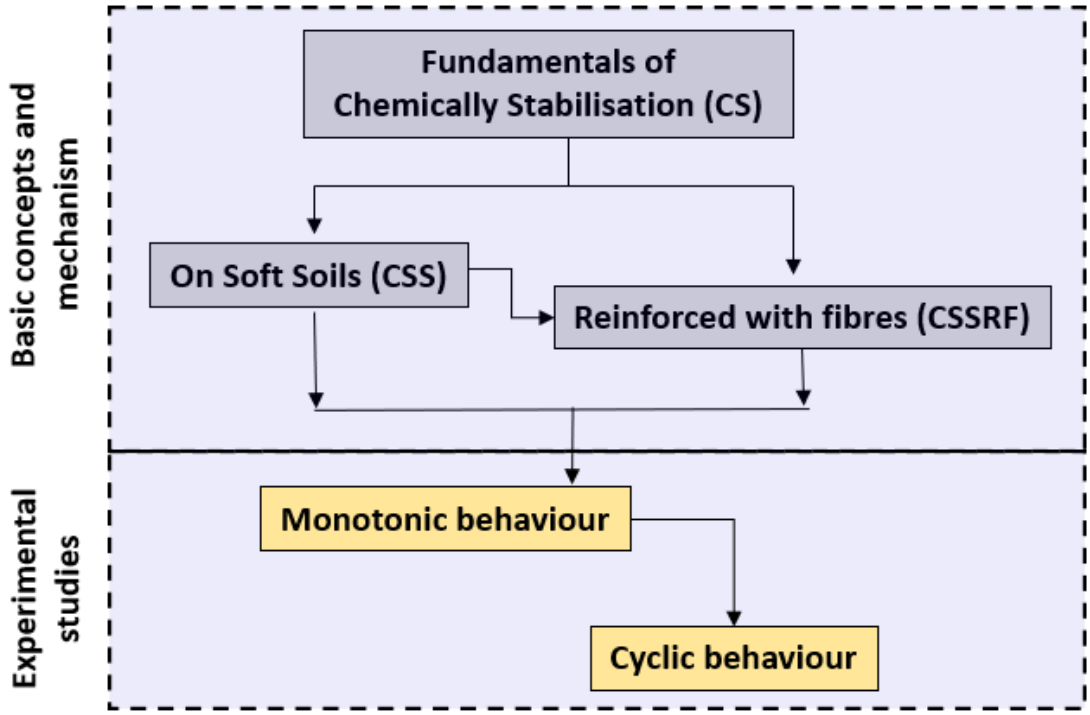

Figure 3.1: Flowchart of sections 3.1 to 3.4

The results of the present work aim to increase the knowledge of such composite materials under different loading conditions and to support the development of more realistic constitutive models that can predict the behaviour of cement-based stabilised soils especially when reinforced with fibres and under cyclic loading conditions. Indeed, when applying numerical methods to solve soil mechanics problems, one of the problems is how to define a three-dimensional yield surface in its principal stress space (van Eekelen, 1980). The yield surface is the boundary that distinguishes between elastic and plastic behaviour, i.e., it defines where destructuration of the material begins. However, van Eekelen (1980) said that the fact that a yield condition is expressed in the three stress invariants does not guarantee that it can give a reasonable description of the actual behaviour of the material. This is even more important when dealing with artificially stabilised soils reinforced with fibres and under cyclic loading, where the information about the yield surface and constitutive models is scarce. In the literature, few research works related to the definition of yield surface under monotonic/cyclic loading were found. This fact justifies the

inclusion in the literature review of some studies related with reconstituted clays and artificially cemented clays as it will be presented in the last section of the chapter.

The following sections include the principles of CSS and CSSRF, the mechanical behaviour under monotonic and cyclic loading, and the yield surface definition.

3.1 Concept and mechanism of Chemically Stabilised Soils (CSS)

The chemical stabilisation of soils consists in in-situ mixing the natural soil with materials that exhibit binding properties (from now on simply referred to as binders). The binders will develop physico-chemical interactions with soil's particles and water enhancing the mechanical properties of the soil, namely, to increase its strength and stiffness and decrease its permeability and compressibility. The in-situ mixture soil-binder-water and the properties of the composite material produced depend on many parameters. Along this section, some of the most important parameters will be characterised in the light of the current state of knowledge.

3.1.1 Type of binder

The most common binders used in the chemical stabilisation technique are Portland cement and quicklime, applied alone or mixed with other additives/binders (Porbaha, 2000; Kitazume and Terashi, 2003; Edil and Staab, 2005). However, other binders are becoming nowadays a valid alternative to Portland cement and quicklime, such as granulated blast furnace slag, fly ash, and other industrial by-products. Many of these "new" binders have been developed for specific purposes (for example, to deal with organic soils and/or soils with high water content), while other have been developed because of environmental issues pursuing sustainable solutions for the construction sector (Axelsson et al., 2002; Janz and Johansson, 2002; Kitazume and Terashi, 2003; Edil and Staab, 2005).

The blast furnace slags come from iron manufacturing, and they are a nonmetallic by-product. It is mostly composed of calcium oxide, silica and aluminium oxides (Kamei et al., 2018). Slags are a material with latent hydraulic properties, i.e., the physico-chemical interactions with water take place in the presence of an activator (in general, the $Ca(OH)_2$ that may came from alkalis or sodium silicate) and may last for several weeks. The reactivity of slag depends on its composition, the physical structure of the minerals (which must be amorphous) and their fineness (expressed by the Blaine surface area). It is essential to mention that slags as a binder are included in the green geotechnical solutions (Kamei et al., 2018).

Fly ash used in this experimental plan was a recovered by-product obtained from gas-fired and coal-fired power plants (Indraratna, 1995). Its composition is very variable containing calcium oxide, silica and aluminium oxides, among other oxides. Fly ash is a material with pozzolanic properties, i.e., does not develop physico-chemical interactions when mixed with water. However, when the fly ash is finely powdered and in the presence of water, fly ash reacts at normal temperature with dissolved calcium hydroxide ($Ca(OH)_2$ from an external source) as long as it exists in free form. In this case, the physico-chemical interactions are very slow, developing over months, sometimes years (Coutinho, 1988). With the increase in temperature, the physico-chemical interactions are accelerated, leading to a faster gain in mechanical strength. Fly ash reactivity depends on its composition (if the CaO content is higher than 10% it may exhibit also hydraulic properties, NP EN 197-1:2001, NP EN 450-1:2005), the physical structure of the minerals (which must be amorphous) and their fineness (expressed by the Blaine surface area). The fly ash "solution" is cheaper and eco-friendly binder suitable for large-scale chemical stabilisation projects (Makusa, 2013).

Quicklime used in the chemical stabilisation of soils is produced from limestone rock, in industrial kilns at high temperatures. It is mainly composed of calcium oxide (> 90%) with other oxides. Quicklime is a material with hydraulic properties, i.e., the physico-chemical interactions with water are spontaneous, promoting a fast enhancement of soil mechanical properties. Its reactivity depends on its composition (content of calcium oxide) and its fineness (the smaller, the more reactive is the quicklime). The major drawback regarding quicklime is associated with the raw-materials extraction, energy consumption and CO_2 emissions.

Portland clinker is an artificial product obtained from a well-proportioned mixture of limestone and clay or similar raw materials. After reducing to a very fine powder (milling) and being very well homogenised and well dispersed, the mixture is kiln-fired to the beginning of fusion (clinkerisation) in a rotary kiln at high temperatures. Finally, the Portland cement is obtained from a mixture of Portland clinker with approximately 5% of gypsum, which may contain other additives. After grinding, it exhibits a particle size distribution between 1-100μm and a Blaine specific surface of approximately 300-450 m^2/kg (E 378-1993). Portland cement is mainly composed of calcium oxide (CaO), silicon oxide (SiO_2), aluminium oxide (Al_2O_3) and iron oxide (Fe_2O_3) with small quantities of other compounds. Portland cement is a material with hydraulic properties, i.e., it is a finely grinded inorganic material that when mixed with water develops spontaneous physico-chemical interactions (hydration reactions) originating a paste that sets and hardens (NP EN 197-1:2001). As for the quicklime, Portland cement reactivity depends on its composition and its fineness (the smaller, the more reactive is the Portland cement). The Portland

cement is, nowadays, the most used additive in chemical stabilisation of soils due to its versatility but has high environmental impact associated to its production (high energy and raw-material consumption process, high CO_2 emissions: 900 kg of CO_2 per ton of Portland cement, Benhelal et al., 2013). This fact justifies the development of new binders/additives that correspond to an efficient and sustainable use of raw materials, and a reduction in CO_2 emissions – thus contributing to meet the United Nations Sustainable Development Goals, European Union, Portugal and Chile energy targets goals (UN, 2019; EU, 2020; PNEC, 2020; ENE, 2012).

Nevertheless the binder type selected, the binders can be introduced into the soil in the dry state or in the form of grout (binder previously mixed with water), corresponding to the dry or wet variant of the chemical stabilisation technique, respectively. The main advantage of the dry method is that it promotes a decrease of the water content in the stabilised soil, allowing to achieve higher mechanical strength with smaller quantities of binder. Moreover, in this variant the reflux losses are almost negligible, and the construction equipment is lighter. The main advantages of the wet variant are related to homogeneity the soil-binder mixture and the versatility with regard to the nature and characteristics of the soils, being possible to apply from soft soils to soft rocks (Edil and Staab, 2005; Kempfert and Gebreselassie, 2006).

3.1.2 Binder physico-chemical interactions

The physico-chemical interactions developed between the binder-water and soil's particles modify the mechanical behaviour of the chemically stabilised soil (or composite material). These changes are highly dependent on the type and binder content and soil's characteristics and conditions (Terashi, 1997). Understandably, the choice of binder that best stabilises the soil is influenced by the characteristics of the natural soil, through which it is possible to predict which type of interactions will occur. These interactions can be grouped into three categories (Correia, 2011):

- hydration reaction (or primary reaction);
- pozzolanic reaction (or secondary reaction); and
- ion exchange.

Among these, the first two types of interactions have a greater contribution in modifying the mechanical behaviour of the stabilised soil. The hydration reactions are the ones that occur between the binder and the water present in the soil, which are spontaneous for certain types of binders. In general, these reactions will stop within a few hours. Then, pozzolanic reactions

develop between the pozzolanic minerals present in the soil, the binders and the water. These secondary reactions are very slow and can develop over the months and years (Correia, 2011). Together with these reactions, clay particles present in the soil may change their structure by ion exchange, contributing to soil stabilisation. However, the stabilising effect associated with ion exchange is of less importance compared to hydration and pozzolanic reactions (Correia, 2011). Nevertheless, all of these interactions produce a stabilising effect on the soil, either by the production of reaction products that bind soil's particles or by changes promoted in soil structure. The stabilising effect can, in any case, be understood as soil cementation. The term cementitious reactions or bonds should be understood as referring to these three interactions (Correia, 2011). In the following sections these three interactions are described in more detail.

3.1.2.1 Primary and Secondary reactions

The hydration and the pozzolanic reactions that occur during the chemical stabilisation process are strongly dependent on the type of binder and its reactivity. The reactivity of a binder is described as the ability of the material to combine/interact with water. As stated previously, when this capacity is high, the binder is said to be hydraulic (e.g., Portland cement and quicklime), in which case hydration reactions occur spontaneously. When the reactivity of a binder is modest, the hydration reactions only occur if they are activated, classifying the binder as latent hydraulic (e.g., granulated blast furnace slag). When this reactivity is almost null, the binder does not exhibit any type of primary reaction, classifying the binder as pozzolanic (e.g., fly ash).

The following equations describe the main reactions of a soil stabilised with Portland cement. The choice of Portland cement is justified by the fact that it is the most commonly used binder in chemical stabilisation of soils (EuroSoilStab, 2002; Horpibulsuk, 2001; Kitazume and Terashi, 2002; Edil and Staab, 2005; Åhnberg, 2006). The chemical reaction developed with Portland cement can be summarised in the following Equations:

$$\mathbf{6(CaO).2(SiO_2) + 6H_2O \rightarrow 3(CaO).2(SiO_2).3(H_2O) + 3Ca(OH)_2} \quad \text{Equation 3.1}$$

$$\mathbf{4(CaO).2(SiO_2) + 4H_2O \rightarrow 3(CaO).2(SiO_2).3(H_2O) + Ca(OH)_2} \quad \text{Equation 3.2}$$

$$\mathbf{Ca(OH)_2 \rightarrow Ca^{2+} + 2(OH)^-} \quad \text{Equation 3.3}$$

$$\mathbf{Ca^{2+} + 2(OH)^- + (SiO_2 \text{ or } Al_2O_3) + H_2O \rightarrow CaO.SiO_2.H_2O \text{ or } CaO.Al_2O_3.SiO_2.H_2O} \quad \text{Equation 3.4}$$

The previous equations only show the reactions concerning tricalcium ($3CaO.SiO_2$) and bicalcium ($2CaO.SiO_2$) silicates (Equations 3.1 and 3.2) since these materials are responsible for about 75%

of the constituents of Portland cement and are the ones that most contribute to the mechanical strength increase (Correia, 2011). At the same time as this primary hydration reaction is carried out, the dissolution of part of the calcium hydroxide ($Ca(OH)_2$) occurs (Equation 3.3). Calcium hydroxide can be combined with the silica (SiO_2) and aluminium (Al_2O_3) minerals present in the soil (Equation 3.4), giving rise to a secondary pozzolanic reaction (a reaction that develops at a reduced speed and is partly responsible for the increase of the strength over time).

The main products resulting from the above reactions are a gel of hydrated calcium silicates ($CaO.SiO_2.H_2O$), which crystallize as needles, entangled and sticking to each other and to the soil's particles (building a hard solid skeleton), ensuring that the soil's density and strength are increased. If aluminium minerals are abundant in the soil, then the gel produced during the pozzolanic reaction will be a hydrated calcium silico-aluminates-compound ($CaO.Al_2O_3.SiO_2.H_2O$), which is very similar to the hydrated calcium silicate's mineral.

Portland cement is responsible for a quick increase in strength (about 50% of Portland cement reacts up to the 3rd day and 60% up to the 7th day), while Pozzolanic reactions, which occur at a slow rate, are responsible for the increase of the strength over time (Coutinho, 1988; Janz and Johansson, 2002). The hydration reaction is an exothermic reaction responsible for increasing temperature and promoting pozzolanic reactions.

If the soil contains organic matter, the development of the reactions described above can be strongly constrained. Organic matter is mainly composed by humus and humic acids, contributing significantly to raising the soil's water content, increasing its porosity and reducing the soil's pH. Their presence has, in general, a negative impact in terms of soil stabilisation, but such effect is not yet fully understood. However, based on some works (EuroSoilStab, 2001; Axelsson et al., 2002; Janz and Johansson, 2002; Edil and Staab, 2005), it is known that:

- the humic acids and other groups of acids, react with calcium hydroxide giving rise to insoluble products which precipitate on the surface of the particles, inhibiting the pozzolanic reactions and the consequent increase of mechanical strength;

- humic acids promote a decrease in potential hydrogen, pH, causing the pozzolanic reactions, and therefore the increase in strength, to take place at a slower rate.

- there is the potential for organic materials to affect the composition and structure of the hydrated calcium silicates that form in the hydration and pozzolanic reactions, impacting the strength development;

- because of its high-water retention capacity, the presence of organic matter can limit the amount of water available for hydration and pozzolanic reactions, delaying the gain of strength;

- organic matter promotes the increase in porosity, i.e., a reduction in the number of solid particles per volume, which means a minor stabilising effect for an equal amount of binder.

3.1.2.2 Ionic exchange

The clay particles present in soil can change their structure by ion exchange, effect that may contribute to soil stabilisation. It should be noted, however, that this effect plays an important role when in the presence of eminently clayey soils stabilised with small amounts of binder. As it will be shown later, this effect is not very expressive for the soil studied in the present work, because silt is the predominant fraction. Nevertheless, the ion exchange that takes place in a soil is briefly described below.

From the mineralogical point of view, the clay particles are composed of clay minerals that are generally hydrated silicates. These hydrated silicates are organized in tetrahedral or octahedral sheets, stacked to form in a hexagonal pattern. These sheets may be associated in various ways leading to non-crystalline minerals groups (e.g., allophane and imogolite) or crystalline mineral groups (e.g., kaolinite, illite montmorillonite, chlorite, and vermiculite, Gomes, 1988; Correia, 2011). The clay particles have important features due to their tiny dimensions and for showing a shape similar to small long plates. Therefore, the clay particles have huge specific surfaces, meaning that a large percentage of the constituent molecules and negative ions are located on their surface.

Due to the arrangement of its molecular structure, the clay particles have negative electric charges on the faces and positive on the edges. It must be said the clay particle has an electrically active surface (usually negatively charged), or by other words, electrical forces control the clay particles behaviour, far exceeding the effect of gravitational forces (Matos Fernandes, 2006). To maintain electrical neutrality, clay particles attract salts cations dissolved in water, such as Na^{+}, K^{+}, Ca^{2+}, Al^{3+}, and others from the surrounding environment, as well as water molecules. The ions and water molecules closest to the particle's surface are subjected to very high stresses and are practically in a solid state. Each particle can attract several layers of water molecules and ions until it gets electrically neutralized. This water is designated as adsorbed water (Matos Fernandes, 2006). However, both the water molecules and the adsorbed ions are not part of the clay structure, varying their presence around the clay particle depending on the type of clay mineral, soil’s water

content, salts dissolved in soil water, the equilibrium established at each point between attractive and repulsive forces, etc. (Matos Fernandes, 2006). These will therefore have an impact on the relative arrangement of the clay particles. Thus, if the soil water content is high, the balance between attractive and repulsive forces is established for considerable distances between clay particles, each surrounded by a thick cloud of adsorbed water. A soil with low consistency, high void ratio and porosity will be obtained. If the predominant clay mineral is montmorillonite, this is even more pronounced given its very high specific surface area (Correia, 2011).

The ion exchange capacity, i.e., the number of ions, particularly cations, which a clay mineral or clay can exchange is an important property of clay minerals. The ion exchange process is a stoichiometric process whereby each equivalent exchange ion from the clay mineral or clay causes the release of a previously fixed equivalent ion. For equal concentrations, some cations are exchanged more strongly than others. Hence, they can be ordered in sequences, lyotropic or Hofmeister series, which in the case of the most frequent cations has the following sequence:

$$\mathbf{Al^{3+} > Ba^{2+} > Ca^{2+} > Mg^{2+} > NH_4^+ > K^+ > Na^+ > Li^+}$$

The greater the valence of a cation, the greater its exchange power will be. Thus, a cation with higher valence replaces another cation of lower valence adsorbed by the particle (for example, Na^+ is replaced by Ca^{2+}). In the case of cations of the same valence state, it is observed that the greater its ionic radius (size) is, the greater its exchange will be (Gomes, 1988; Lindh, 2004).

Ionic exchange can convert a dispersed clay into a clay of a flocculated structure of low plasticity (Figure 3.2). A clay dispersed structure is characterised by pronounced parallelism between the water-filled particles, separated by adsorbed water layers. On the surface of the particles, there is a concentration of positive ions (cations), usually potassium (K^+) and sodium (Na^+). Soil stabilisation with lime or Portland cement introduces mainly calcium ions (Ca^{2+}), whose source is calcium hydroxide ($Ca(OH)_2$), which differ in valence and size from the ions adsorbed by the clay (as described in the lyotropic series). Ion exchange occurs and calcium cations replace almost all of the potassium and sodium cations that initially were adsorbed on the surface of the clay particles. This ion exchange reduces the thickness of the cloud of water adsorbed by the particles (resulting from the need to maintain the electrical equilibrium), which causes the change of the original structure of the clay, inducing its flocculation. Consequently, the consistency of the soil increases, and the plasticity is strongly reduced. This phenomenon occurs in a period that varies with the type of clay mineral, ranging from 24 to 72 hours (Lindh, 2004; Correia, 2011).

The ion exchange capacity of the clay mineral, is determined by the specific surface area of the clay particles and the type of clay (Åhnberg et al., 1995; Chu and Yin, 2006). In addition, Portland

cement has a lower capacity for ion exchange than quicklime due to large amounts of potassium (K^+) and sodium (Na^+) ions released during the cement hydration reactions. These potassium and sodium ions reduce or inhibit exchange with the potassium and sodium ions adsorbed by the clay particles (Janz and Johansson, 2002). On the other hand, the hydration reaction of Portland cement gives a smaller amount of calcium hydroxide (which constitutes a source of Ca^{2+} cations) than quicklime.

Figure 3.2: Explanation of change due to cation exchange (after Little 1997) (adapted from Lindh, 2004)

3.1.3 Characteristics of binders (stabilising agents)

In terms of mechanical behaviour, identifying the best binder(s) in terms of mechanical behaviour to be applied in soil stabilisation depends on the characteristics of the natural soil and the binder, which determine the type of physico-chemical interactions established between soil particles, binder(s) and water. Other factors such as the technical and economic criteria, the environmental impacts associated with binder use, and previous experience must also be evaluated.

It is an essential condition of the stabilisation that at least one of the binders is hydraulic (most soil improvement works are performed with Portland cement), which should generally be taken as the base binder. Other materials may be added to the base binder in the form of additives (e.g., slag, fly ash, silica fume, other industrial by-products). Thus, it is possible to maximise the technical-economic requirements with the environmental advantages of reusing industrial by-products. In any case, the material selected to be used as a binder must have reactive properties, allowing the enhancement of the mechanical properties of the soil (Janz and Johansson, 2002). The reaction products must also be resistant to time and chemical and physical attacks. It must be emphasised that industrial by-products must not include heavy metals or other ecologically harmful elements (this is also valid for other binders) (Correia, 2011; EuroSoilStab, 2001; Janz and Johansson, 2002; BS EN 14679, 2005). In addition, special care must be taken when using industrial by-products because their properties may vary significantly due to changes in the raw materials and in the production process (Correia, 2011).

Among the several soil characteristics, organic matter is one of the critical factors in the choice of the binder. The binders that best stabilise inorganic soils are not necessarily equal to all organic

soils. Thus, the introduction of filer into the organic soil may be convenient in terms of stabilisation since the filer allows the increase in the number of particles per volume to which the binder can bind, which contributes to the construction of a strong solid skeleton, increasing the stabilisation effect (Janz and Johansson, 2002; BS EN 14679, 2005, Edil and Staab, 2005). The introduction of filer has an extra positive effect in cost reduction since it allows to achieve the same stabilising effect (measured in terms of strength) for a lesser binder quantity (Edil and Staab, 2005). The process of choosing the best binder(s) to be applied in soil stabilisation should always be preceded by a laboratory study, where the performance of the soil-binder mixture is verified, both from a mechanical and environmental point of view (EuroSoilStab, 2001, BS EN 14679, 2005). In the laboratory study, it is necessary to consider the characteristics described above (natural soil and binders) and the mixing and curing conditions, which should seek to reproduce as accurately as possible the field conditions without compromising the quality of samples prepared in the laboratory. Terashi (1997) summarised the factors that influence the strength of the improved soil into four categories: characteristics of the binder (stabilising agent); characteristics and conditions of soils; mixing conditions; and curing conditions (Table 3.1). Although several factors affect the curing process, temperature greatly influences the speed of the reactions between the soil and the binder (higher temperature corresponds to a higher rate of development of the reaction and consequently on the strength development). Curing of the samples in laboratory should be done, preferably, in controlled temperature chambers, reproducing the field temperature. However, this procedure is not always possible to adopt in the laboratory, leading to laboratory/field result discrepancies. Even if a temperature-controlled chamber is used, the volume of soil involved in a laboratory sample differs from the volume of soil stabilised in the field. Thus, the heat released in the soil/binder reactions produces different scale effects in the laboratory and field (the temperature will drop more slowly in the field than in the laboratory).

Table 3.1: Factors that influence the strength of the improved soil (Terashi, 1997)

Description	Characteristics
Characteristics of stabilising agent	Type of binder (stabilising agent); Quality; Mixing water and additives.
Characteristics and condition of soils	Physico-chemical and mineralogical properties of soil; Organic content; pH of pore water; Water content.
Mixing Conditions	Degree of mixing; Timing of mixing; Quantity of binder (stabilising agent).
Curing conditions	Temperature; Curing time; Humidity; Wetting/drying, freezing/thawing.

In addition to these factors, other aspects may influence the analysis and interpretation of the results of the laboratory tests such as the size and shape of the samples tested in the laboratory, the type of water used, the presence of percolation, etc. It may even happen that the binder that best stabilises the soil in laboratory may not be the most effective in the field. Some works showed differences in laboratory/field results, expressed in unconfined compressive strength, ranging from 1/1 to 5/1 (Kitazume and Terashi, 2002). Based on laboratory studies and some field results published by several authors (Åhnberg et al., 1995, Carlsten and Ekström, 1997, Japan Geotechnical Society 0821, 2000; EuroSoilStab, 2002; Axelsson et al., 2002; Janz and Johansson, 2002; Kitazume and Terashi, 2002; Åhnberg et al., 2003; Edil and Staab, 2005 and BS EN 14679, 2005), the best efficient binders to stabilise different types of soils are presented in Tables 3.2 and 3.3.

Regardless of the binder chosen, it should be applied in quantities not lower than a minimum in order to have an effective mechanical effect. The minimum amount of binder to be mixed with clayey soils is in the range of 30 - 50 kg/m^3 (Terashi, 1980; Uddin, 1994; Horpibulsuk, 2001), while a minimum of 70 kg/m^3 should be used in the presence of organic soils (Babasaki, 1997; Axelsson et al., 2002).

In a study conducted by Axelsson et al. (2002) on the stabilisation of a mud and different types of binders (Portland cement, quicklime, blast furnace slag and fly ash), the authors concluded that stabilisation of the mud should preferably be performed with Portland cement alone, while in the case of peat, a mixture of Portland cement with blast furnace slag is more efficient. In the case of mud, the total amount of binder should be between 100 - 200 kg/m^3, and in the case of peat between 150 - 250 kg/m^3.

Table 3.2: Efficiency of binders in different stabilised soft soils (adapted from Åhnberg et al., 1995)

Binder	Soil									
	Clayey silt	Clay-Silt	Clay	Quick Clay	Salt clay	Sulphite Clay	Mud clay	Muddy Clay	Mud	Peat
Quicklime	●	+	●	+	+	-	●	●	-	-
Portland Cement - Quicklime (75%-25%)	+	+	+	+	+	+	+	●	●	●
Portland Cement (100%)	++	++	+	++	+	+	+	+	+	+

Inefficiency ● Normally + Efficiency ++ Great efficiency

Table 3.3: Efficiency of binders in different stabilised Nordic soft soils according to the UCS at 28 days (adapted from EuroSoilStab, 2001)

Binder	Silt (O.M = 0-2%)	Clay (O.M = 0-2%)	Organic Soil (O.M = 2-30%)	Peat (O.M = 50-100%)
Cement	+	●	●	+
Cement + gypsum	●	●	+	+
Cement + slag	+	+	+	++
Quicklime + cement	+	+	●	-
Quicklime + gypsum	+	+	+	-
Quicklime + slag	●	●	●	-
Quicklime + gypsum + slag	+	+	+	-
Quicklime + gypsum + cement	+	+	+	-
Quicklime	-	+	-	-

Inefficiency ● Normally + Efficiency ++ Great efficiency

The current section has reviewed the factors and mechanisms that affect chemically stabilised soils. The following section will be addressed the basic concepts and mechanisms that act in stabilised soils but now reinforced with fibres.

3.2 Concept and mechanism of Chemically Stabilised Soils Reinforced with Fibres (CSSRF)

As stated previously, the chemical stabilisation of a soil produces a composite material characterised by a brittle behaviour and low tensile and flexural strength (Sukontasukkul and Jamsawang 2012; Correia et al., 2015; Venda Oliveira et al., 2016). It cannot be used in seismic zones or when materials are exposed to horizontal displacements (such as deep-mixing columns placed beneath embankments and slopes) or lateral earth pressures (as for deep-mixed soil walls). In such situations, flexural/tensile strength is needed to avoid tension failure. One possible solution is to add short fibres to the soil-binder-water mixture in a similar way as used in concrete (Venda Oliveira et al., 2016).

Examples of soil reinforced with natural elements can be found on the wall of Mesopotamia (1400 BC), where soil layers were reinforced with root layers in a construction similar to some sections of the Great Wall of China and on roads built by Incas in Peru, where the wool from the wild vicuña (Lama vicugna) was used as reinforcement (Casagrande, 2001).

An important example of the influence of fibres in chemically stabilised soils can be seen in a study carried out in roads of Louisiana, United States of America, with soils mainly composed of clay and silt with low strength and stiffness characteristics like the BMSS and requiring a higher quantity of Portland cement (Gaspard, 2000; Coelho, 2000). This high amount of binder results in higher heat of hydration that produces excessive micro-cracks due to high shrinkage strain. Adding fibre to a soil–cement may enhance its mechanical characteristics (Maher and Ho, 1993;

Sobhan et al., 1999; Gaspard and Mohammad 2002; Khattak and Arashidi 2006) and results showed that the fibre reinforcement at optimum fibre percentage may resist the tensile or shrinkage crack formation in the soil–cement mixtures for road bases thereby, improving the structural capacity and performance of pavements.

As stated at the beginning of the chapter, the fibres can be divided into three types: natural, synthetic and fibres produced from waste materials. Natural fibres may come from fruits (such as coconut and banana fibres), or plants such as bamboo, sisal or hemp. The major concern about natural fibres is related with their durability and tendency to lose resistance over time due to degradation induced by the environmental conditions. Synthetic fibres can be made of polypropylene, nylon, plastic, fibreglass, asbestos, metallic, and others. Although synthetic fibres present greater strength and durability than natural fibres, natural fibres are advantageous from an environmental point of view. Nowadays fibres derived from waste materials are becoming popular because of their advantages in terms of sustainability.

The chemical stabilisation of soils reinforced with fibres consists in in-situ mixing the natural soil with binders and with fibres. The binders will develop physico-chemical interactions with soil's particles, fibres and water enhancing the mechanical properties of the soil. It is important to state that the tensile strength of the fibres can only be mobilised for a certain strain/deformation level, which implies destructuration of the composite matrix (Venda Oliveira et al., 2018). By other words, for an effective mobilisation of the fibres the breakage of some cementation bonds must happen. The presence of the fibres will therefore have an impact on the mechanical behaviour of the composite material which depends on several parameters. Along this section, the main important parameters will be characterised in the light of the current state of knowledge.

3.2.1 Mechanism of reinforcement with fibres

Falorca and Pinto (2011) studied how fibres interact with particles of a non-chemically stabilised soil using optical and scanning electron microscopes. The study showed that the fibres do not fail by tensile during shear but are stretched, and some damage may occur (Figure 3.3). The damage is fundamentally due to fibre indentation, with no cutting. It is believed that the damage mainly arises during compaction as a result of high impact energy. The fibres lose their straightness and finish with numerous bends (angularities).

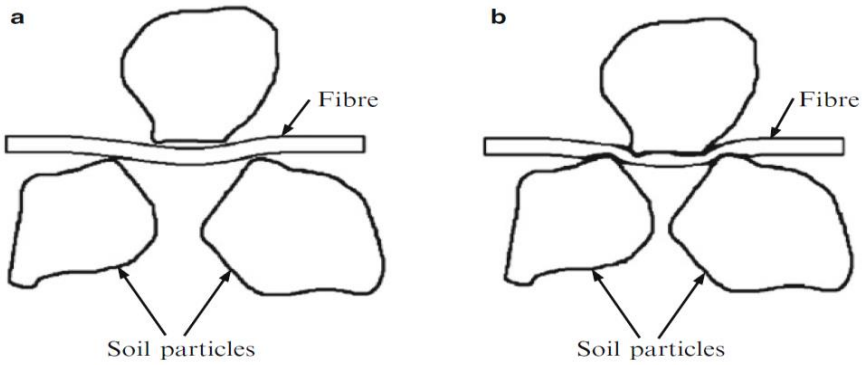

Figure 3.3: Interaction mechanism between fibre and soil particles: a) the fibre prevents the soil particles from packing tightly a until fibre stretch and imprinting occur; b) increasing the capacity to hold the particles and therefore allowing adhesion to develop (adapted from Falorca and Pinto, 2011)

Tang et al. (2007) presented a scheme that shows the mechanism developed between the fibres and the particles of an unstabilised soil (Figure 3.4). Through this study, it was possible to conclude that there are clay particles glued to the surface of the fibres, thus contributing to the increase of the frictional strength between the soil and the fibres. In this way, the fibres are prevented from sliding by mobilizing their tensile strength, preventing failure surfaces' continuous formation. The random distribution of the fibres forms a three-dimensional network that binds the soil matrix, reinforcing it.

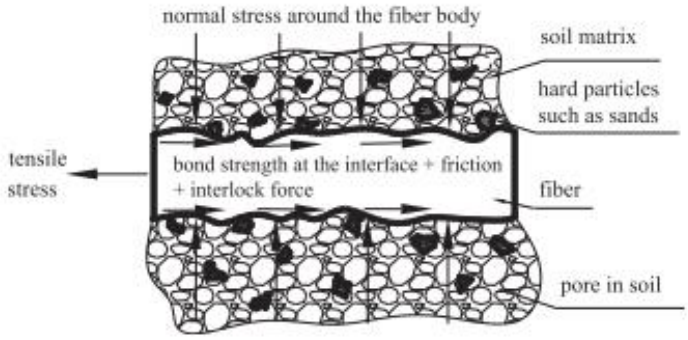

Figure 3.4: Sketch of mechanical behaviour at the interface between fibre surface and soil matrix (Tang et al., 2007)

When the soil is chemically stabilised, there are very complex and varied factors that affect the behaviour of the stabilised soil reinforced by the addition of fibres. The mechanical properties of CSSRF depend on the interaction soil-fibres, which are related to several aspects, with the most important ones being related to the level of cementation induced by stabilisation and the characteristics of the fibres (e.g. length, thickness, stiffness, etc.). For low cementation level the soil type has also an important role since it is known that, in general, granular soils confer better anchorage conditions to the fibres than fine soils. Indeed, for soils stabilised with low binder

content (less than 10%), there are important deformations since the beginning of the loading, given the "reduced" stiffness of the solid skeleton. As the deformations evolve there is a progressive mobilization of the fibres, which contribute to the increase of the strength capacity of the composite material since the rupture/failure occurs for higher levels of deformation, compatible with the effective mobilization of the fibres (Cai et al., 2006; Tang et al., 2007; Consoli, 2011; Park, 2011; Estabragh et al, 2012; Sukontasukkul and Jamsawang, 2012; Olgun, 2013; Güllü and Khudir, 2014; Lemos et al., 2021). However, for soils stabilised with high binder content (> 10%), the deformations up to failure are very small due to the "high" stiffness of the solid skeleton. For such low levels of deformation, the fibres are not mobilised, so the strength (at rupture/failure) is controlled by the cementitious matrix. In this case (high binder content), the fibres are effectively mobilized to post-rupture deformation levels (Khattak and Alrashidi, 2006; Consoli et al., 2009a; Sukontasukkul and Jamsawang, 2012; Lemos et al., 2021).

In any case, in order to mobilise the fibres, there must be a relative displacement between fibres and solid skeleton, generating shear stresses on the fibres surface (along the fibre-stabilised soil interface), which leads to the effective mobilisation of the tensile strength of the fibres. That is, the development of shear stresses on the surface of the fibres allows the transfer of stresses from the cementitious matrix to the fibres, with obvious impact on the mechanical behaviour of the composite material.

3.2.2 Characteristics of the fibres (reinforcement elements)

A fibre is a unit of matter characterized by flexibility, fineness and a high ratio of length to thickness (or diameter). Also considered a general term that refers to all filaments, yarns, staples, bristles/hairs, buffings, chips, crumbs, and other similar highly flexible entities (Shukla, 2017).

The fibres can be natural (Figure 3.4), synthetic (Figure 3.5), or produced from waste materials (Figure 3.6). There are many natural fibres, such as wood chips, bamboo, sisal, palm grasses, banana, manila, cotton, corn stalks, oat and flax straws (Shukla, 2017; Rao and Balan, 2000; Raymond 2002; Tang et al. 2007; Gosavi and Patil, 2004; Abuel-Naga et al., 2006; Mattone, 2005; Marandi et al., 2008; Abtahi et al., 2010; Islam and Iwashita, 2010; Ramesh et al., 2010; Hejazi et al., 2012). Table 3.4 shows the mechanical properties of some natural fibres. For these specific three fibres, coir fibres have the smallest tensile strength but keeps this property in wet conditions (Shukla, 2017; Rao and Balan, 2000), while bamboo fibres are robust in tension but have a low modulus of elasticity.

The main advantages of natural fibres are their low cost and being an environmentally friendly material. The limitations of using natural fibres are related with durability and biodegradability (for instance, the coir fibres have a low resistance to alkaline environments), which induces a progressive loss of strength over time (Shukla, 2017).

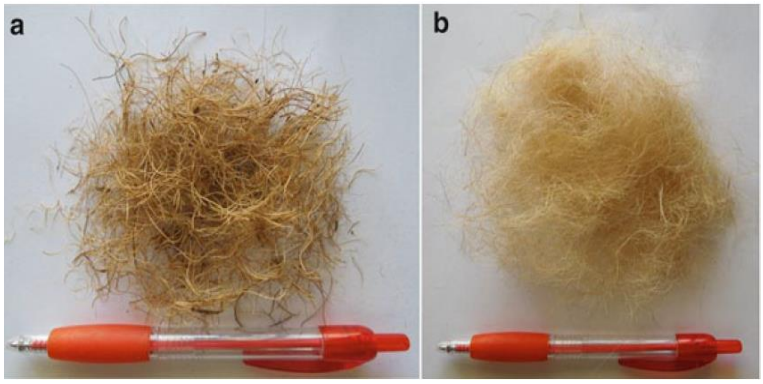

Figure 3.4: Natural fibres: (a) coir fibres, (b) jute fibres (Shukla, 2017)

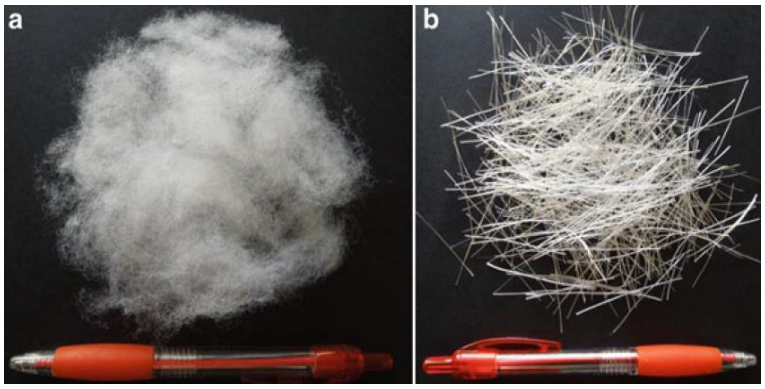

Figure 3.5: Synthetic fibres: (a) polypropylene (PP) fibres, (b) glass fibres (Shukla, 2017)

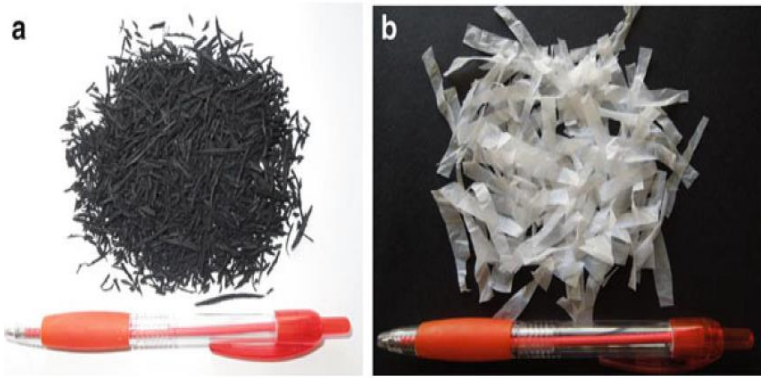

Figure 3.6: Waste fibres: (a) old/used tyre fibres, (b) waste/used plastic fibres (Shukla, 2017)

Table 3.4: Physical/mechanical properties of some natural fibres (Biswas et al. 2013; Shukla, 2017)

Fibre type	Tensile strength (MPa)	Modulus of elasticity (GPa)	Strain at failure (%)
Coir (brown/white)	165-237	3.79-3.97	38.7-41
Jute	331-414	28.43	2.6
Bamboo	615-862	35.45	4.1

Regarding synthetic fibres, the focus will be put on the properties of polymeric fibres (Table 3.5) since they are often selected as reinforcing elements of stabilised soils because of their competent mechanical and durability characteristics. The PET fibres have the highest mechanical properties (higher tensile strength and stiffness), while the PVC fibres show the lowest mechanical properties. According to Hoover et al. (1982) and Shukla (2017), synthetic fibres have two advantages over natural fibres: the production is easy, and most synthetic fibres are not biodegraded, i.e., the mechanical properties are unchanged in long-term.

Table 3.5: Typical properties of polymeric fibres (adapted from Shukla, 2017)

Fibre types	G_s	Melting Temperature (ºC)	Tensile strength (MPa)	Modulus of elasticity (GPa)	Strain at failure (%)
PP	0.91	160 - 165	400 – 600	1.3 – 1.8	10 – 40
PET	1.22 – 1.38	260	800 – 1200	12 – 18	8 – 15
PE	0.91 – 0.96	100 - 135	80 – 600	0.2 – 1.4	10 -80
PVC	1.38 – 1.55	160	20 – 50	2.7 – 3	50 – 150
PA	1.05 – 1.15	220 - 250	700 – 900	3 – 4	15 - 30

PP-Polypropylene; PET-Polyester; PE-Polyethylene; PVC-Polyvinyl chloride; PA-Nylon/Polyamide.

Finally, regarding the fibres produced from waste materials their origin is varied: they can be produced from old used tyres, from plastic waste, from industrial waste or even from waste of natural fibres (such as human and animal hair). As mentioned before, the use of waste fibres has a positive impact in terms of sustainable development.

Table 3.6 summarises the main properties of some synthetic and natural fibres, describing the fibres by its specific gravity (G_s); the average length (L); equivalent diameter (D), tensile strength (σ_f); strain at failure/rupture (ε_r) and tensile modulus (E_f).

Table 3.6: Main properties of some natural fibres (adapted from Shukla, 2017)

	Type	G_s	L (mm)	D (mm)	σ_f (MPa)	ε_r (%)	E_f (GPa)
Glass [5]	S	1.7	10-15	0.02	300		
Processed cellulose (PC) [6]	N	1.5	3	0.015	500		50
Coir [7]	N	1.07	15	0.25	102		2
Jute [8]	N	1.47	7-9	0.005-0.025	331-414		
Date palm [9]	N	0.92	295	0.42	123	5.10	2.47

Note: S: Synthetic fibre; N: Natural fibre
References: [1] Kaniraj and Havanagi (2001); [2] Consoli et al., (2009); [3] Choudhary, AK (2015); [4] Park (2009); [5] Lovisa et al., (2010); [6] Khattak and Alrashidi (2006); [7] Babu et al., (2008); [8] Spritzer et al., (2015); [9] Sarbaz et al., (2014).

The mobilisation of the tensile strength of the fibres is dependent on of the fibre-soil interface properties, which are influenced by friction, bonding force, matrix suction and interface morphologies (Tang et al. 2007; Gelder and Fowmes, 2016).

The effective mobilisation of the fibres does not depend solely on the properties of the fibres-soil stabilised interface but also on the characteristics of the fibres themselves. Regarding the fibre

characteristics, the following parameters are the most important: fibre type and material (natural/synthetic/waste); fibre shape (monofilament, yarn, fibrillated, tape, mesh, etc.); fibre diameter and length and its aspect ratio (length to diameter ratio); specific surface area; tensile strength, longitudinal stiffness/modulus of elasticity and strain at failure; fibre texture (straight or crimped) and surface roughness (skin friction); water absorption; melting point; and durability (resistance to biological and chemical degradation) (Shukla, 2017).

Fibres produced from natural, or waste materials are more susceptible to water adsorption and to biodegradation than synthetic fibres, but present a surface with higher roughness allowing better interaction along the fibre-soil stabilised interface (Venda Oliveira et al., 2016 and 2022; Kalka 2013).

As mentioned above, the type of fibres is one of the characteristics that influence the behaviour of the material, which can be natural fibres, synthetic fibres and/or waste fibres. Kalkan (2013) studied the impact of adding waste fibres to a clayey soil. The results showed that the silica fume (a waste product obtained as a by-product of producing silicon metal or ferrosilicon alloys), scrap tyre rubber fibres (length ranging from 5 to10 mm; thickness ranging from 0.25 to 0.5 mm; width ranging from 0.25 to 1.25 mm) and silica fume-scrap tyre rubber fibre mixtures increase the UCS of clayey soil. The maximum value of UCS is obtained by addition of 20% silica fume and 2% fibres. The direct shear test results indicate that the maximum cohesion and internal friction angle values are also obtained by addition of 20% silica fume and 2% fibres.

Fibres with higher length or crimped ends allow a more effective anchorage of the fibres, and therefore a better mobilisation of the fibres tensile strength (Venda Oliveira et al., 2016; Consoli et al. 2003). Other effects such as the confining pressure are impossible to be studied in unconfined compression strength tests, clearly indicating the necessity of carrying out triaxial tests to fully understand the fibre-reinforced soil behaviour (Consoli et al. 2009b).

The fibre diameter and length and its aspect ratio (length to diameter ratio) have an influence on the mechanical behaviour of the composite material. Generally, fibre length becomes more important than fibre diameter in randomly distributed fibre-reinforced soils (Gowthaman et al., 2018). As the aspect ratio or the specific surface area of the fibres increases, the shear stresses transferred along the fibre-soil stabilised interface are lower, allowing a more effective anchorage of the fibres (Correia et al., 2015; Gowthaman et al., 2018). Kumar and Singh (2008) reported the improvement in unconfined compressive strength of fly ash with random inclusion of PP fibres. At an aspect ratio of 100, the unconfined compressive strength of fly ash increased from 128 to 259 kPa with increment in fibre content from 0 to 0.5%. The results showed that the variation of

unconfined compressive strength with fibre content is linear, while with aspect ratio, the variation is nonlinear in terms of increase. The optimum fibre length and aspect ratio were found as 30 mm and 100, respectively.

Fibres with better mechanical properties (higher tensile strength and stiffness and, in general, lower deformation at rupture/failure) require less deformation for their effective mobilisation (Venda Oliveira et al., 2016 and 2021; Michalowski and Zhao, 1996).

In the following sections of this chapter some experimental studies on CSS and CSSRF under monotonic and cyclic loading will be presented, highlighting the effect of fibre inclusion and the effect associated to cyclic loading.

3.3 Experimental studies on CSS/CSSRF under monotonic loading

In any geotechnical problem the parameters to consider are compressibility, permeability, and stress-strain-shear strength. This section will briefly analyse the results of some research works about those parameters under monotonic loading on soils chemically stabilised unreinforced and reinforced with fibres.

3.3.1 Definition of monotonic loading

A monotonic loading is a load applied slowly (a relative term) on the body mass such that it is not subjected to any motion (Islam, 2021). The load applied on the sample's body generates strains and stresses, which should be recorded and interpreted properly to understand the mechanical behaviour of the sample under monotonic loading. The characteristics usually evaluated when a sample is subjected to a monotonic loading are the stress-strain curve, the maximum stress (associated to rupture/failure) and the strain at rupture/failure (ε_r), and the stiffness usually defined for a stress or load equal to 50% of the stress or load at rupture/failure (E_{u50}). Along this section some research works will be presented using these parameters to characterise the mechanical behaviour of CSS and CSSRF under monotonic loading.

3.3.2 Change of physical geotechnical properties

As stated previously, it is important to consider that composite material properties change due to the stabilising effect induced by the binder. Some studies have shown that cement treatment leads to an increase in the plastic and liquid limits (e.g. Locat, 1990; Uddin et al., 1997; Petchgate et

al., 2001; Chew et al., 2004; Lee et al., 2005; and Ghee, 2006). Both Locat et al. (1996) and Chew et al. (2004) attributed the increase in the liquid limit to the presence of trapped water within the essentially hollow cemented-soil clusters. Chew et al. (2004) also attributed the increase in the plastic limit to the clustering of the soil particles to larger clusters of particles.

As shown in Figure 3.7, Ghee (2006) found that liquid limit increases after cement treatment but decreases with the effective pressure in curing consolidation. Ghee (2006) attributed this decrease to the squashing of the clusters, which reduces the amount of trapped water within the clusters. The void ratio changes during curing-consolidation may be accounted for by the decrease in volume of intra-aggregate pores.

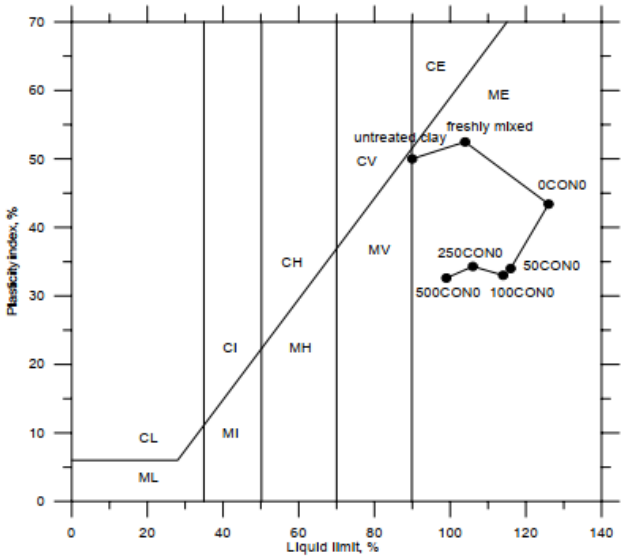

Figure 3.7: Plasticity chart for cement-treated clay under stress states during the curing period, the number indicate the effective curing stress in kPa and CON means curing-consolidation] (Ghee, 2006)

Correia (2011) concluded that adding a binder to a soil triggers physico-chemical reactions, which consume water. Therefore, the stabilised material is characterised by a lower water content than the original (non-stabilised) soil. In terms of unit weight, the chemical stabilisation induces its increase up to 15% (Porbaha et al., 2000; Horpibulsuk, 2001; Åhnberg et al. 2003; Åhnberg, 2006). However, this depends on the type of binder and is related to the quantity of reaction products produced, the density of the binders, and the water content (the lowest values are recorded for the wet variant of the deep mixing technique). In general, the void ratio of a chemically stabilised soil is reduced because some of the voids are now filled by products resulting from the physico-chemical reactions (Horpibulsuk, 2001; Åhnberg, 2006; and Lorenzo and Bergado; 2006).

3.3.3 Engineering behaviour

The mechanical behaviour of a chemically stabilised soil is strongly conditioned by structural changes induced by the stabilisation (usually characterised by a lower void ratio) due to the cementitious bonds between the solid particles which are responsible for constructing a stiff and hard solid skeleton. In this section the focus will be on these structural changes expressed in terms of compressibility, permeability, and stress-strain-shear strength.

3.3.3.1 Compressibility

As discussed, soil stabilisation involves stabilising agents (binder materials) added to soils to improve their geotechnical properties such as compressibility, strength, permeability, and durability. Many authors said that the chemical stabilisation of soils increase the strength and reduce the compressibility (Correia, 2011; Horpibulsuk, 2001; Makusa, 2013; Mamat, 2013). Chemical stabilisation decreases the recompressibility index (C_r) due to the fact that there is an increase in stiffness (stiffer solid skeleton). However, chemical stabilisation increases the Compression index (C_c) due to the fact that when the yield stress is exceeded the material tends to evolve to the non-stabilised soil behaviour (metastable behaviour). That is, when the yield stress is exceeded, destructuring occurs, characterised by an abrupt breakage of the cementitious bonds. In terms of yield stress, the chemical stabilisation promotes an increase of the yield stress compared to the pre-consolidation stress of the natural soil; this increase is due to the higher strength of the solid skeleton resulting from the cementitious bonds.

The introduction of fibres in the cementitious matrix does not introduce significant changes to the behaviour described above (Correia, 2011; Correia, 2015; Shukla, 2017). However, the study performed by Shukla (2017) with non-stabilised clayey soil reinforced with fibres concluded that the compressibility of the fibre-reinforced soil decreases with the increase of fibre content (Table 3.7).

Table 3.7: Compressibility index of unreinforced and coir fibre-reinforced black cotton soils, L= 15 mm, and diameter, D = 0.25 mm (Shukla, 2017)

Fibre content (%)	Compressibility index, C_c
0	0.51
0.5	0.43
1	0.40
1.5	0.33

Al-Akhras et al. (2008) examined the impact of nylon fibres on swelling of three non-stabilised clayey soils (CH, CH, and CL). The results from one-dimensional oedometer tests (Figure 3.8)

demonstrate that clayey soils with fibres have lower swelling potential and the swelling pressure than those without fibres.

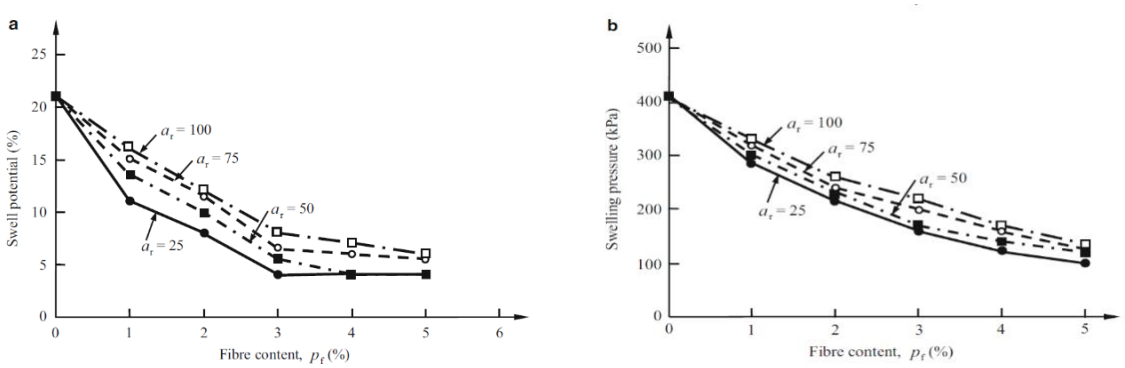

a) b)

Figure 3.8: Effect of nylon fibres on: (a) swelling potential; (b) swelling pressure of clayey soil (classified as CH with a liquid limit of 78% and plasticity index of 43%) (Adapted from Al-Akhras et al. 2008)

The stabilised material under conditions of perfect confinement (Figure 3.9) is characterised by exhibiting reduced compressibility until reaching the yield stress, which is considerably higher than the pre-consolidation stress of the original soil. These two facts are directly related to the high strength of the cementitious bonds (Uddin et al., 1997, Horpibulsuk 2001, Lorenzo and Bergado, 2004 and 2006, Correia, 2011). The post-yielding behaviour of the stabilised soil is generally characterised by greater compressibility than the original (non-stabilised) soil, reflecting the collapsible behaviour of stabilised soil with abrupt breakage of cementitious bonds (destructuring). Progressively, the behaviour of stabilised soil tends to that of the unstabilised soil (Correia, 2011).

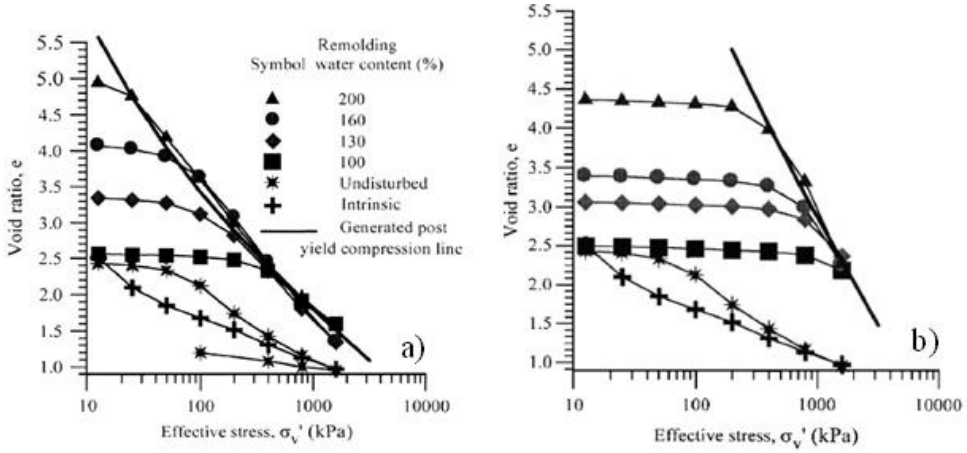

Figure 3.9: One-dimensional compression curves for different cement contents: (a) 5%, (b) 15% (adapted from Lorenzo and Bergado, 2006)

Figure 3.9 also shows that the yield stress decreases with the increase in the water content as a direct consequence of the increase in the void ratio; however, the pre-yield and post-yield compressibility seem to be indifferent to the water content change. This fact emphasizes the importance of the strength of the cementitious bonds in the mechanical behaviour of a stabilised soil.

3.3.3.2 Permeability

The permeability, or hydraulic conductivity, is a property of enormous interest since it controls the speed of dissipation of excess pore pressures, with impact on the drainage conditions (drained or undrained) to be considered in the strength analysis. In specific applications such as percolation control and impermeable barrier, permeability is the main functional requirement of chemical stabilisation.

Several researchers have studied the permeability of stabilised soils with various types of binders, applied in different quantities and in the dry or wet state, with divergent results, pointing some studies to an increase and others to a decrease in the permeability of the stabilised soil versus non-stabilised soil (Porbaha et al., 2000; Horpibulsuk, 2001; Kitazume and Terashi, 2002; Åhnberg, 2006; Lorenzo and Bergado, 2006; Yin and Fang, 2006). The ratio between the stabilised and non-stabilised soil permeability coefficients (k_e / k_o) can range from 0.01 to 1 (Chai, 2006). Such variations can be explained by the structural changes induced by the chemical stabilisation, which depend on the type and amount of binder, the pressure conditions, the type of soil and its water content.

The permeability decreases over time due to the development of the physico-chemical reactions. Figure 3.10 shows the results for some Swedish soils, stabilised with different binders and under different conditions (Åhnberg, 2003 and 2006). The results reflect the above comments, and it can be seen that the permeability of the stabilised soil increases with the water content, corresponding to a lower unconfined compressive strength, q_u which reflects the larger void ratio of the stabilised soil (Correia, 2011).

Few studies have been carried out to study permeability (hydraulic conductivity) in the case of fibre-reinforced non-stabilised soils. Miller (2004) agree that the increase of fibre content increases the hydraulic conductivity, Figure 3.11. The increase in hydraulic conductivity was most significant for fibre contents exceeding 1%. Plé et al (2012), also showed that with the increment of fibre content, the hydraulic conductivity also increases.

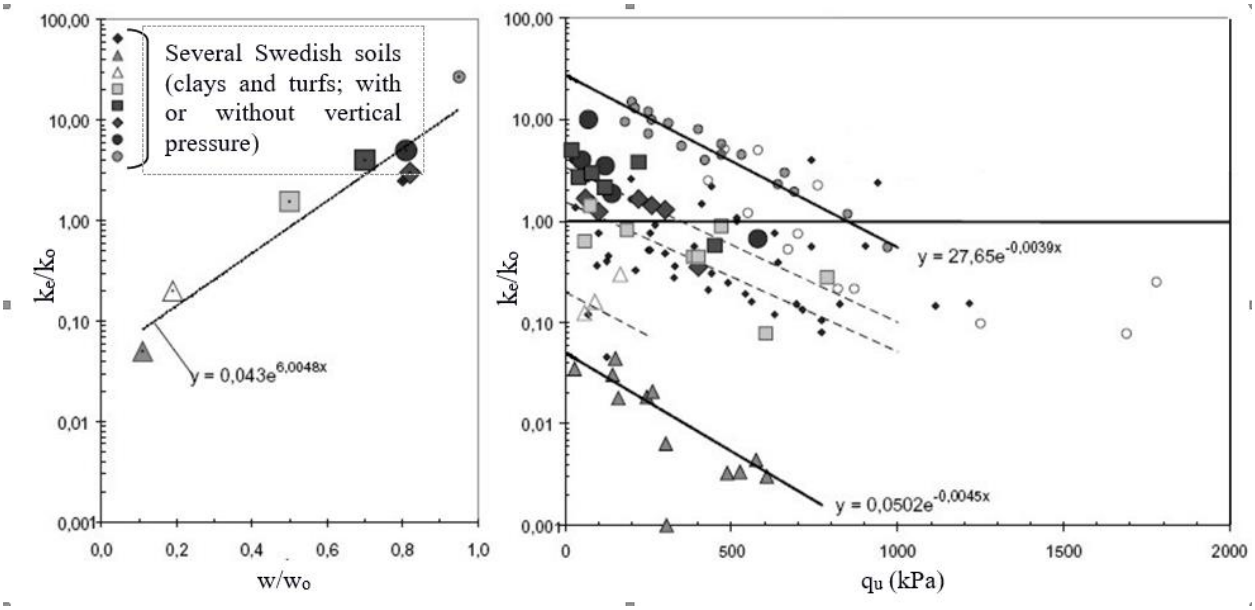

Figure 3.10: Changes in permeability after stabilisation: a) change in permeability vs change in water content; b) change in permeability vs strength (adapted from Åhnberg, 2003)

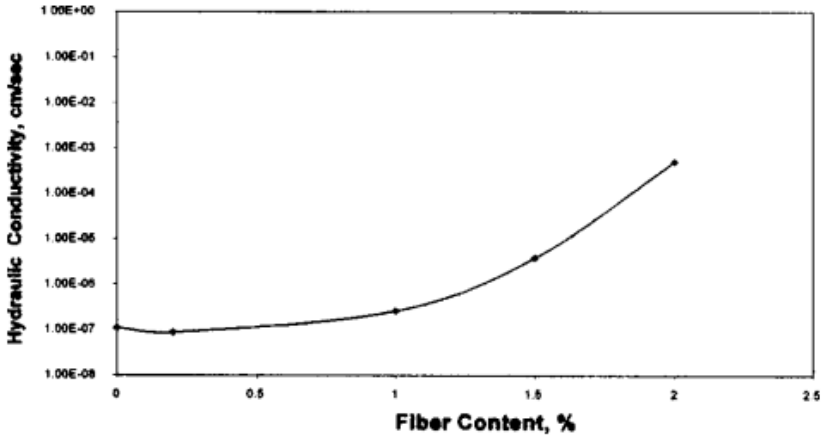

Figure 3.11: Hydraulic conductivity for various fibre contents (Miller, 2004)

3.3.3.3 Stiffness

The chemical stabilisation induces a solid matrix stiffer than that of the natural soil as a result of cementitious bonds. This effect is more significant the higher the binder content and the lower the water content (provided that there is enough water for the hydration reactions of the binders). The presence of organic matter tends to reduce the stiffness due to the fact that it prevents the establishment of some cementitious bonds with the solid particles. In general, granular soils exhibit greater stiffness than fine soils due to the larger size of the solid particles.

It was observed that soils stabilised with low binder content (less than 10%) show that the inclusion of fibres originates a decrease in stiffness (Tang et al., 2007). When the binder content increases the mechanical behaviour of the CSSRF depends on the soil type. Sandy soils stabilised with high binder content showed a decrease in stiffness with the inclusion of polypropylene fibres

(Consoli et al., 2009), whereas Khattak and Alrashidi (2006) observed an increase in stiffness in high plasticity clays stabilised with a 10% cement content and reinforced with polypropylene fibre content higher than 0.3%.

3.3.3.4 Stress-Strain-Shear Strength behaviour

Soil stabilisation improvement is commonly measured in terms of strength gain over time (curing). The strength can be evaluated by triaxial tests, and by unconfined compressive strength (UCS) tests to characterise the compression strength, or by direct tensile strength (DTS), or splitting tensile strength (STS) or flexural strength (FS) tests to characterise the tensile strength. As stated in Carlsten and Ekström (1997), JGS 0821 (2000), EuroSoilStab (2001) and Kitazume and Terashi (2002), the UCS test is taken as reference test for stabilised soils because the stabilised samples can stand alone, the testing procedure is simples and test results are obtained quickly. The UCS test is undrained and assumes no moisture loss during the test. It is important to mention that the shear strength evaluated in undrained triaxial tests is very similar to the strength evaluated in UCS tests since the stabilised samples are in a saturated condition in the triaxial tests; the samples in the triaxial will developed excess pore pressure that counteract the confining stress applied, leading to a state of near unconfinement. This is another reason that justifies the choice of UCS tests as the reference test for the mechanical characterisation of stabilised soils.

When a chemically stabilised soil is sheared in the triaxial test it is observed that the behaviour is dependent on the strength of the cementitious bonds between the solid particles while the confinement pressure is lower than the yield stress, then evolving to the behaviour to that of the unstabilised soil (Coop and Atkinson, 1993; Uddin et al., 1997; Cuccovillo and Coop, 1999, Malandraki and Toll, 2000 and 2001, Horpibulsuk, 2001, Lorenzo and Bergado, 2006). The behaviour is dependent on the parameters that control the strength development of the cementitious bonds and on the confinement pressure applied in the triaxial test. When the confining pressure exceeds the strength of the cementitious bonds, it produces changes in the structure of the stabilised soil and its behaviour tends to be identical to that of the original soil (unstabilised) since its strength depends only on the frictional component (Coop and Atkinson, 1993, Uddin et al., 1997; Malandraki et al. 1997; Cuccovillo and Coop, 1999; Horpibulsuk 2001; Åhnberg 2006; Correia 2011).

Thus, for confinement pressures below the yield stress of the stabilised soil (a common situation in most applications of the chemical stabilisation technique, Correia, 2011), the material under drained or undrained conditions begins to exhibit a very rigid behaviour because of cementitious

bonds. The rupture/failure is characterised by a peak corresponding to an abrupt loss of strength due to the breaking of the cementitious bonds. Post-peak rupture, and as the cementitious bonds are progressively destroyed, the behaviour tends to be identical to that of the unstabilised soil, (Coop and Atkinson, 1993; Udding et al., 1997; Cuccovillo and Coop 1999; Correia, 2011).

For large strain level, the failure envelope of the stabilised soil may be slightly above the original/unstabilised soil due to the increase of dilatancy, a direct consequence of changes in the "apparent" particle size of the stabilised soil which is coarser due to the cementitious bonds established between the solid particles (Lade and Overton, 1989). This behaviour is well illustrated by Horpibulsuk (2001) results (Figure 3.12), who have studied the Ariake clay (w_L = 120%, w_P = 57%, $w_{nat} \leq 130\%$) stabilised with Portland cement applied in a binder content of 12%.

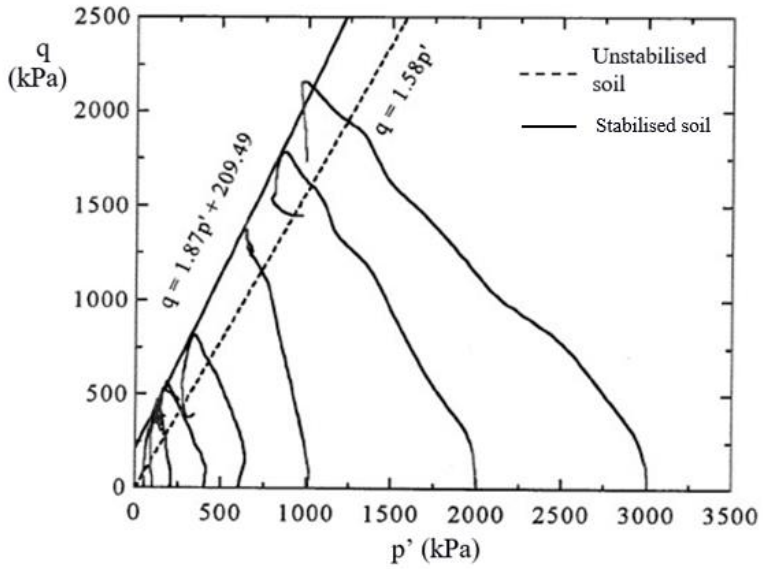

Figure 3.12: Undrained stress paths and failure envelope of samples stabilised with 12% of cement (yield stress = 380 kPa) (Horpibulsuk, 2001)

As proposed by Leroueil and Vaughan (1990), Coop Atkinson (1993), and Cuccovilo and Coop (1999), the mechanical behaviour of a soil stabilised for an high binder content (> 10%) may be summarised in the Figure 3.13. These authors indicate that the behaviour is fundamentally dependent on the initial state of the stabilised soil when compared with the limit state/yield surface and the critical state line (CSL) of the non-stabilised soil.

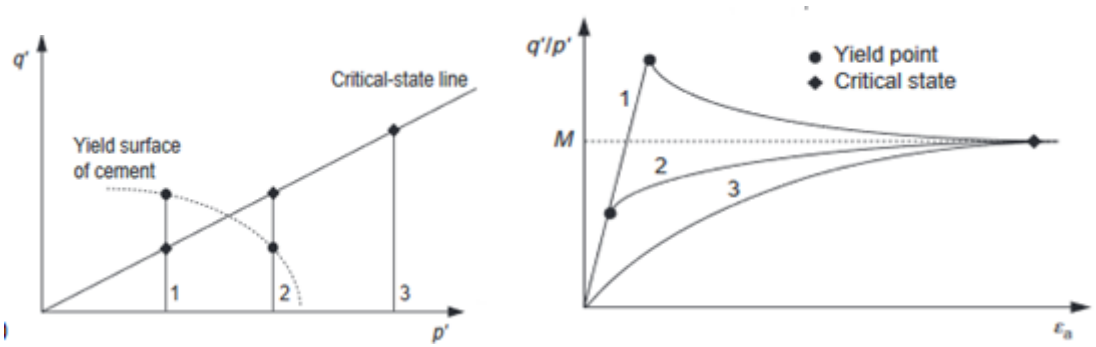

Figure 3.13: Mechanical behaviour of s soil stabilised with an high binder content (after Coop and Atkinson, (1993) adapted from Cuccovilo and Coop, (1999))

When subjected to triaxial shear testing, and for relatively low stress levels (inside the limit state/yield surface, curve 1 in Figure 3.13), the behaviour is brittle characterised by a quasi-elastic initial section, with a peak occurring for small strains and for stresses well above the limit state surface of the unstabilised soil. The behaviour up to the peak-failure is fundamentally dependent on the cementitious bonds. Post-peak, there is a sudden decrease in strength due to an abrupt breakage of these bonds, and the behaviour becomes dependent on the frictional strength. For large strains level, the behaviour evolves towards the critical state line of the unstabilised soil. By increasing the confinement stresses (curves 2 and 3 in Figure 3.13), the stabilised soil behaviour changes evolving to the unstabilised soil (the strength becomes dependent only on the frictional component).

Everything described above is related to a chemically stabilised soil (CSS) technique. However, this work also deals with the behaviour of chemically stabilised soils reinforced with fibres (CSSRF). In order to evaluate the effect of fibres on the mechanical behaviour of the composite material, some studies will be presented first for unstabilised fibre-reinforced soils and later on for stabilised fibre-reinforced soils.

Many authors have developed triaxial laboratory tests on samples that were reinforced using fibres to improve the engineering properties of several soils. A curved-linear or bilinear principal stress envelope was seen in laboratory triaxial compression experiments conducted by Maher (1988). Indeed, when a uniform rounded sand was tested (Figure 3.14a) it was observed a curved-linear envelope while for the case of a well-graded or angular sand (Figure 3.14b) the results showed that there is a crucial confining stress, or a threshold confining stress, i.e., the envelope is now bilinear.

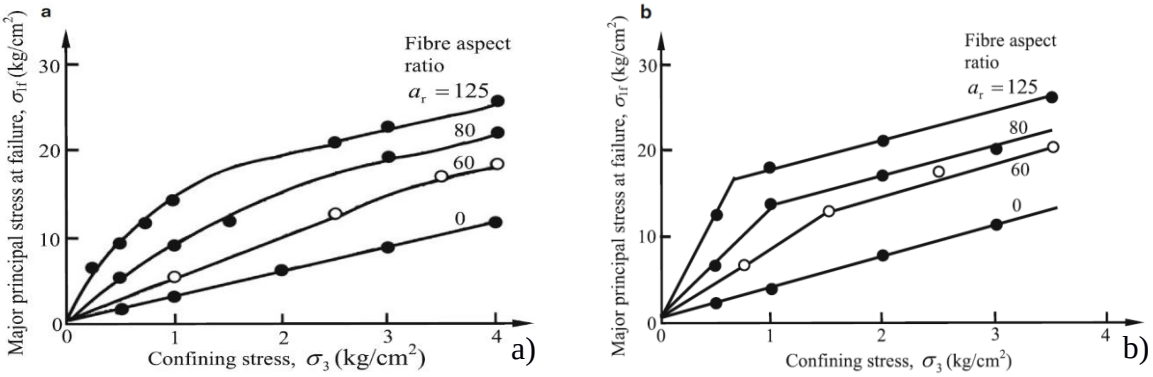

Figure 3.14: Principal stress envelopes from triaxial compression tests on reinforced sands: (a) Muskegon dune sand; (b) mortar sand (glass fibre content = 3%). (Adapted from Maher and Gray 1990)

Other authors, such as Consoli et al. (2003), found that adding polypropylene fibres to a sandy soil has almost a null impact on the friction angle but enhances the cohesion intercept.

Consoli et al. (2009b) performed triaxial test on a sandy soil unstabilised and stabilised with Portland cement and reinforced or not with polypropylene fibres. The authors found that in samples tested without binder, the fibres can increase the strength to high strains, while in samples stabilised with low binder content (< 7%), the reinforcement with fibres increases the peak strength and decreases the loss of strength after the peak-failure (Figures 3.15a-c). For a binder content of 10%, the results indicate that there is no mobilisation of the strength of the fibres (the material is very stiff) before failure. Thus, the fibres do not contribute to the increase of peak strength, Figure 3.15. Independently of the binder content used, the results show a significant increase in the ductility of the material with the inclusion of the fibres Figure 3.15.

The fibres increase the strength for binder contents up to 7% (Figure 3.15a-c), having a negative effect for higher binder content. These results show that a more deformable material (with low binder content) enhances the mobilisation of the tensile strength of the fibres, which does not occur at a higher level of cementation since, in this case, the solid skeleton is very stiff. This effect is well expressed in Figure 3.16.

As the composite material is monotonically loaded the shear stresses increase causing changes in the soil-fibre interface behaviour. As the hydrated reactions develop and interact with the fibre surface, the surface roughness and pull-out strength increase, allowing a better tensile mobilisation (Gelder and Fowmes 2016).

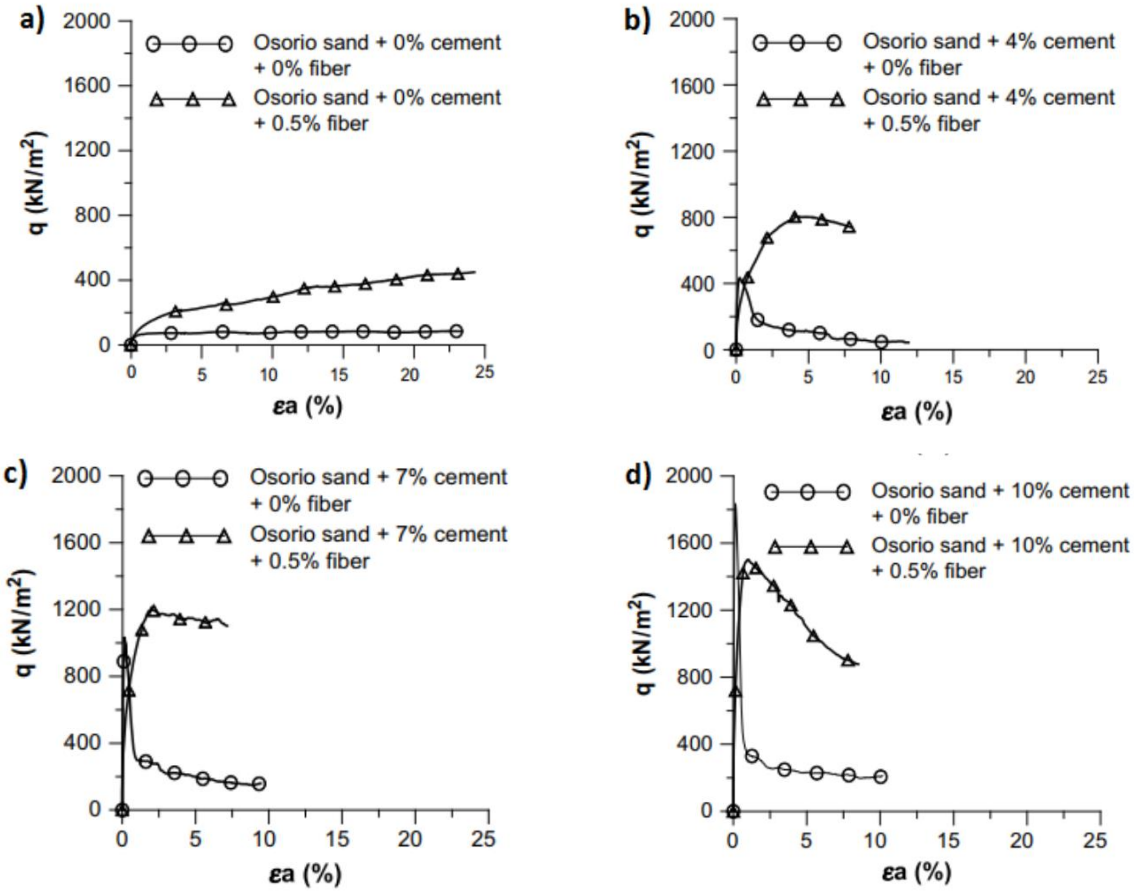

Figure 3.15: Deviator stress–axial strain triaxial response: (a) uncemented specimens, (b) 4% cement content. (c) 7% cement content and (d) 10% cement content (Consoli et al., 2009)

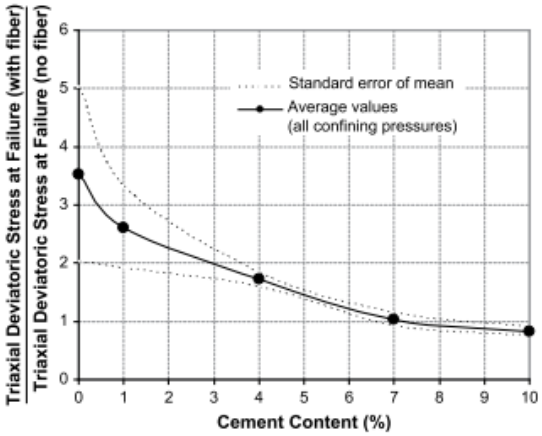

Figure 3.16: Effect of fibre-reinforcement on peak deviatoric strength of cemented sand (adapted from Consoli et al., 2009b)

So far, only some experiments on granular soils have been described. From now on the focus will be on fine-grained soils.

Figure 3.17 shows the laboratory research carried out by Tang et al. (2007) using a series of UCS tests on clayey soil, including different amounts of polypropylene fibres (12 mm long) and using

Portland cement for stabilisation. Test samples were compacted at the maximum dry unit weight and optimum water content, defined by the Proctor test.

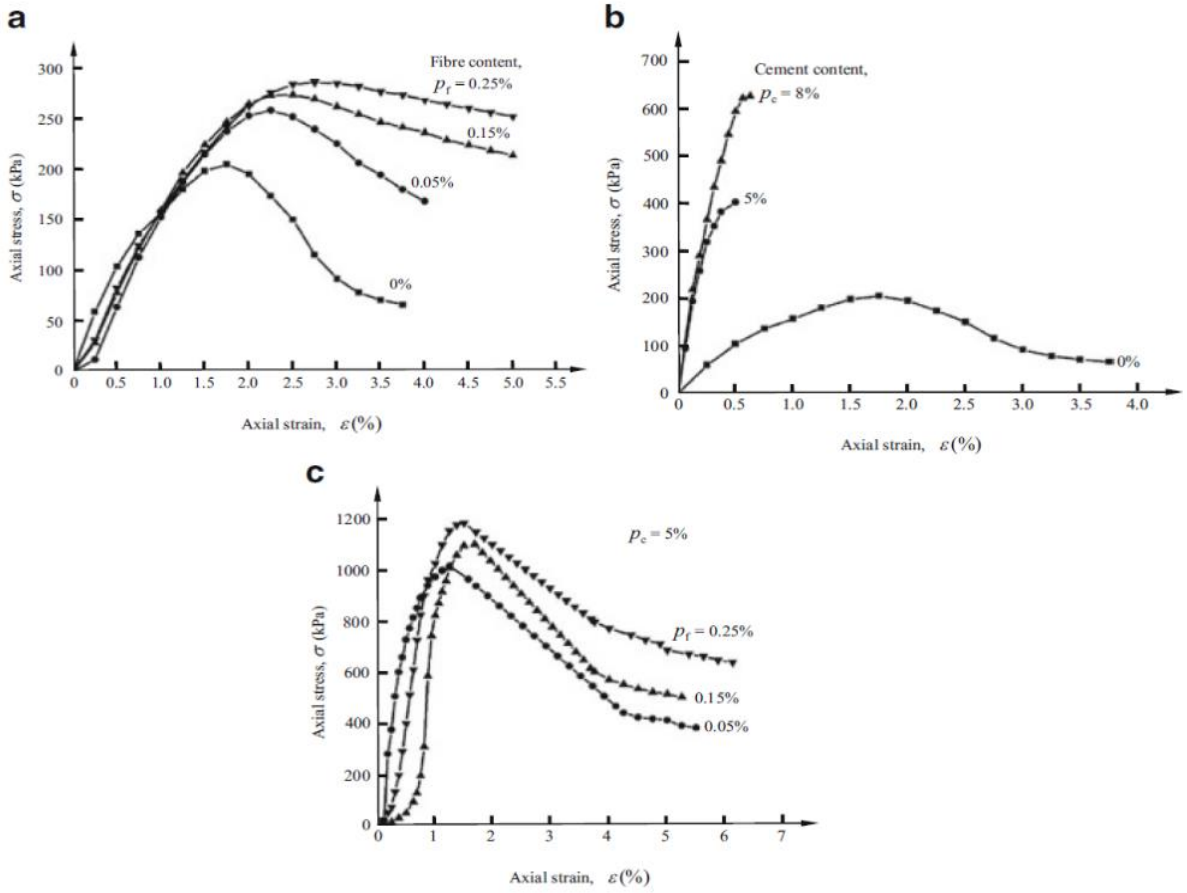

Figure 3.17: Stress-strain curves obtained from UCS tests: (a) fibre-reinforced uncemented clayey soil; (b) cement-stabilised clayey soil after 28 curing days; (c) fibre-reinforced cemented clayey soil for cement content of 5% and fibre content ranging from 0.05 to 0.25% after 28 curing days (Adapted from Tang et al. 2007)

The results indicate that the inclusion of fibres in stabilised and unstabilised soils induce an increase in the ductility of the material, i.e., the loss of post-peak strength decreases. Soil stabilised with cement alone exhibits a brittle behaviour and the rupture/failure mechanism started with the formation of wide and long tension cracks (Figure 3.18a). Fibre inclusion can change the behaviour of the composite material from brittle to a more ductile one. When the tension cracks started to appear, the fibres serve as ‘‘bridges’ avoiding the further opening and development of cracks and preventing samples from complete rupture/failure (Figure 3.18b-c). It is also observed that the tension cracks become gradually narrower and shorter with increasing the fibre content.

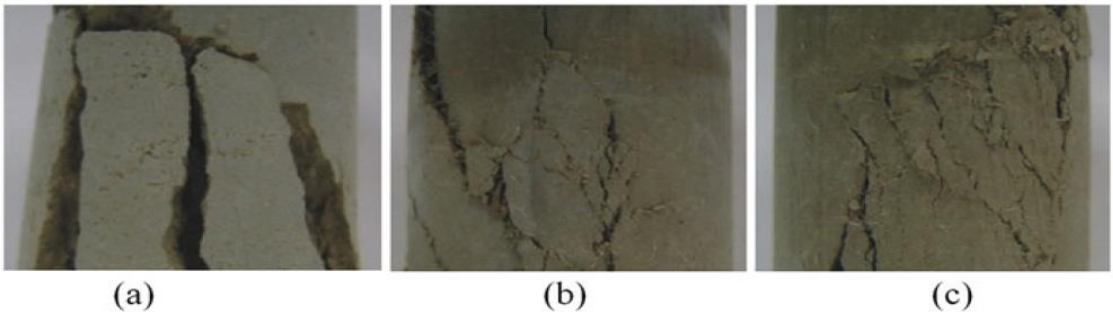

Figure 3.18: Effect of fibres on the failure pattern of cement-stabilised clayey soil in UCS tests for a cement content =8% and a fibre content of: (a) 0%; (b) 0.05%; (c) 0.25% (Tang et al. 2007)

The same authors have also studied the impact of the fibre content in the strength parameters, cohesion and internal friction angle. It was observed that the fibre addition and cement content play an important role in the development of the cohesion and angle of internal friction (Figure 3.19a-b). Both parameters increase with fibre content. For a constant fibre content, it was observed that the chemical stabilisation enhances both shear strength parameters.

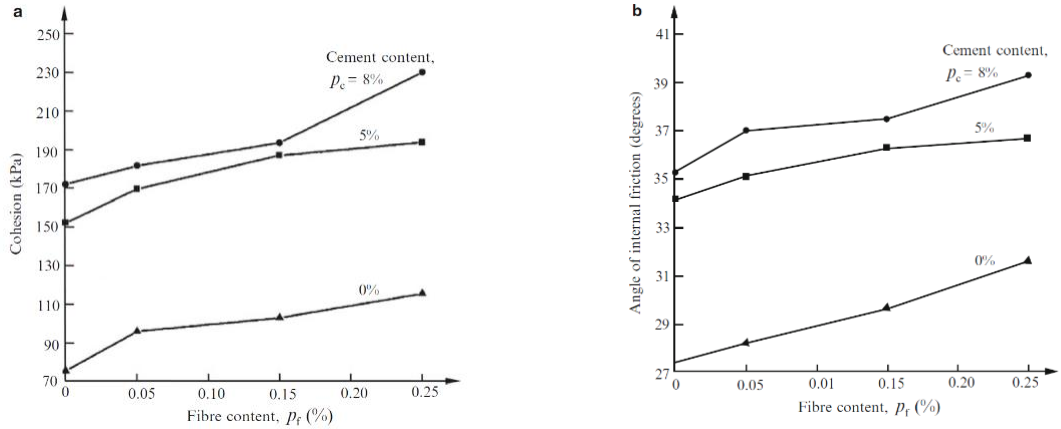

Figure 3.19: Variation of shear strength parameters with fibre content (p_f) for uncemented and cemented clayey soil after 28 days of curing: (a) cohesion *c'*; (b) angle of internal friction ϕ' (Tang et al. 2007)

As previously stated, adding fibres to a stabilised soil encourages the creation of bridges that prevent cracks/fractures from forming, changing the behaviour of the composite material from brittle to ductile (Tang, 2007; Correia et al., 2017; Shukla, 2017).

Zaimuglu and Yetimoglu (2012) have studied the impact of randomly dispersed polypropylene fibre reinforcement (12 mm length, 0.05 mm diameter) on fine-grained soil (MH, high plasticity soil). The results of the UCS tests showed an increase of the unconfined compressive strength with the fibre content (Figure 3.20). However, the rate of increase in unconfined compressive strength is not substantial for a fibre content greater than 0.75%.

Regarding the shear strength, the behaviour of reinforced soils without cement is divided into three phases: the soil regulates the behaviour in the first phase; the matrix and reinforcement control the behaviour in the second phase; and the fibres govern the behaviour in the third phase (Zaimoglu and Yetimoglu 2012).

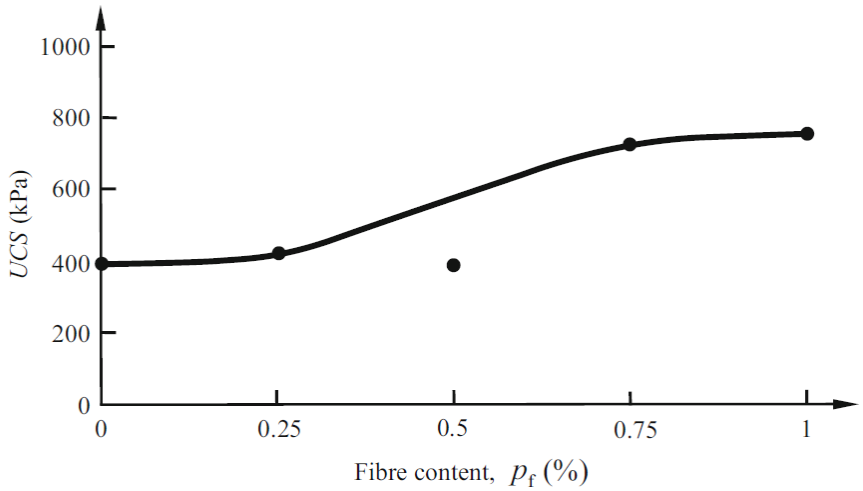

Figure 3.20: Effect of fibre content on unconfined compressive strength of fine-grained soil (Adapted from Zaimoglu and Yetimoglu 2012)

Another author who worked with non-granular soils was Feuerhermel (2000). The author compared the behaviour of three soils, clay, sand, and sand-silt, with and without cement and reinforced with polypropylene fibres. In the case where the mixtures were without binder, it was concluded that polypropylene fibres increased its strength, which is more evident for the more granular soils (Figure 3.21).

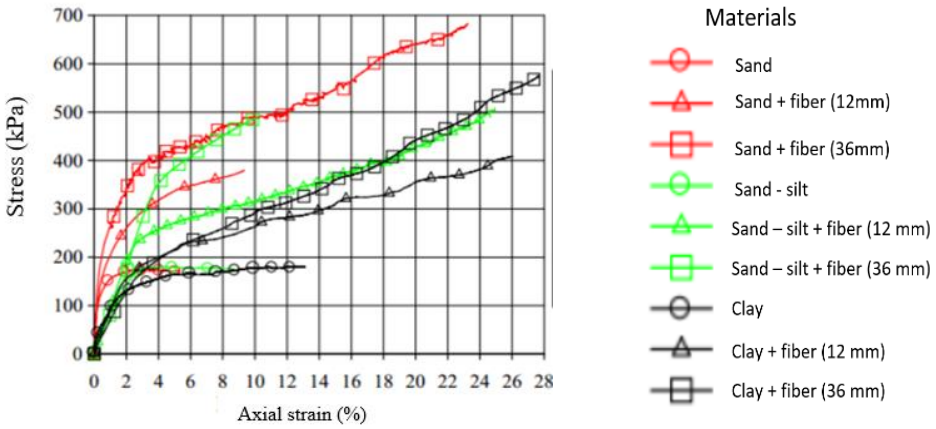

Figure 3.21: Stress-strain curves for samples without binder (adapted from Feuehermel, 2000)

In the case where the mixtures were stabilised, the introduction of polypropylene fibres promotes a change in the post-peak behaviour due to the "adhesion" of the fibres to the matrix (fibre-solid matrix interaction) (Figure 3.22).

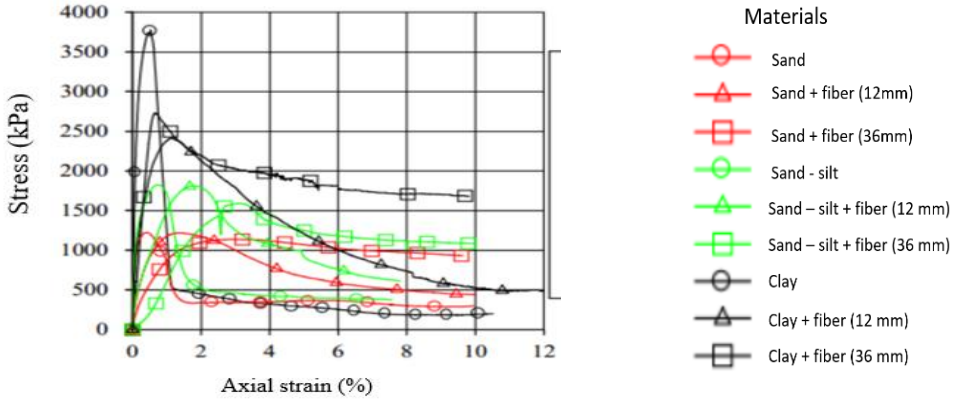

Figure 3.22: Stress-strain curves for samples stabilised (cement) (adapted from Feuehermel, 2000)

Contrasting with the general published results, Feuerharmel (2000) observed a decrease of the unconfined compressive strength due to the inclusion of fibres into the stabilised material, which is more noticeable for the clayey soil, Figure 3.23.

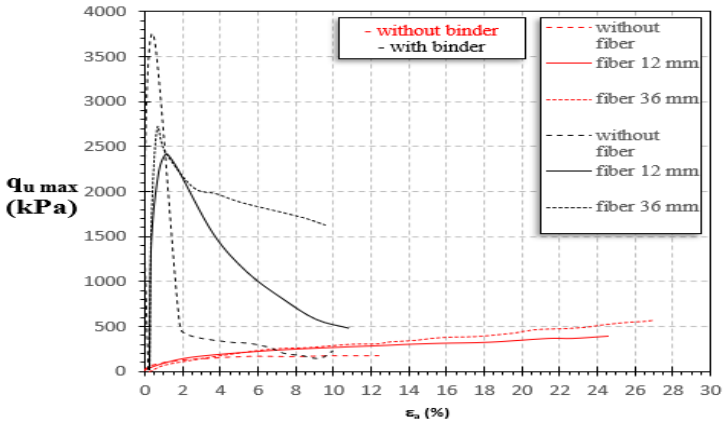

Figure 3.23: Stress-strain curves for samples with cement or without cement, in the case of clay (adapted from Feuerharmel, 2000)

Ingles and Metcalf (1972) carried out a series of UCS tests on different stabilised soils and said that the unconfined compressive strength increases linearly until a certain lime content (about 8%) and increase with time due to physico-chemical reactions (Figure 3.24a-b).

Jiang et al. (2010) studied the effect of fibre content and fibre length (Figure 3.25a-b) on the unconfined compressive strength of a clayey soil. The results showed that the increase in fibre content higher than 0.3% has a detrimental impact and that the best length of the fibres is 15 mm.

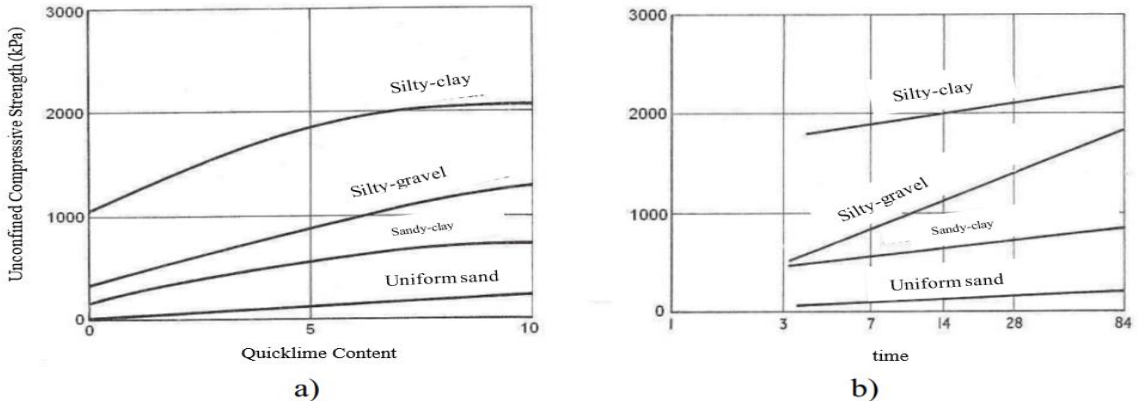

Figure 3.24: Unconfined compressive strength for several soils: a) quicklime content; b) curing time (adapted from Ingles and Metcalf, 1972)

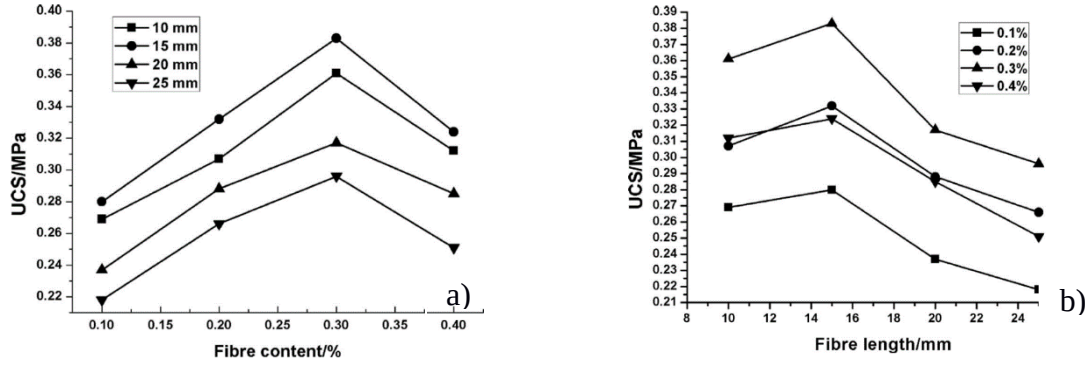

Figure 3.25: Effect of (a) fibre content and (b) fibre length on UCS of fibre reinforced soil (Jiang et al., 2010)

Correia et al. (2015) studied the effect of the binder and fibre quantity on the mechanical behaviour of a stabilised soft soil reinforced with polypropylene fibres. The compression behaviour was characterised by UCS tests while the tensile behaviour was characterised by split tensile strength (STS), direct tensile strength (DTS) and flexural/bending strength (FS) tests. The results showed that an increase in binder content (Figure 3.26) promotes an increment in the stiffness, the compressive and tensile strength, but have a lower impact on the stabilised soil reinforced with fibres. In Figure 3.26, It was observed also a decrease of the peak strength, both under compression and tension (DTS tests), which is explained by the fact that the fibres do not allow some cementation bonds to be established with the soil particles. However, an addition of 50-75 kg/m^3 of fibres leads to an improvement in the mechanical characteristics, in relation to both lower and higher quantities of fibres, indicating that this may be close to the optimum value. The authors have also observed that the impact of the addition of fibres on the strength depends on the failure mechanism imposed on each test: in FS tests the impact of the fibres is significant, while in the DTS tests the inclusion of fibres has a negligible effect.

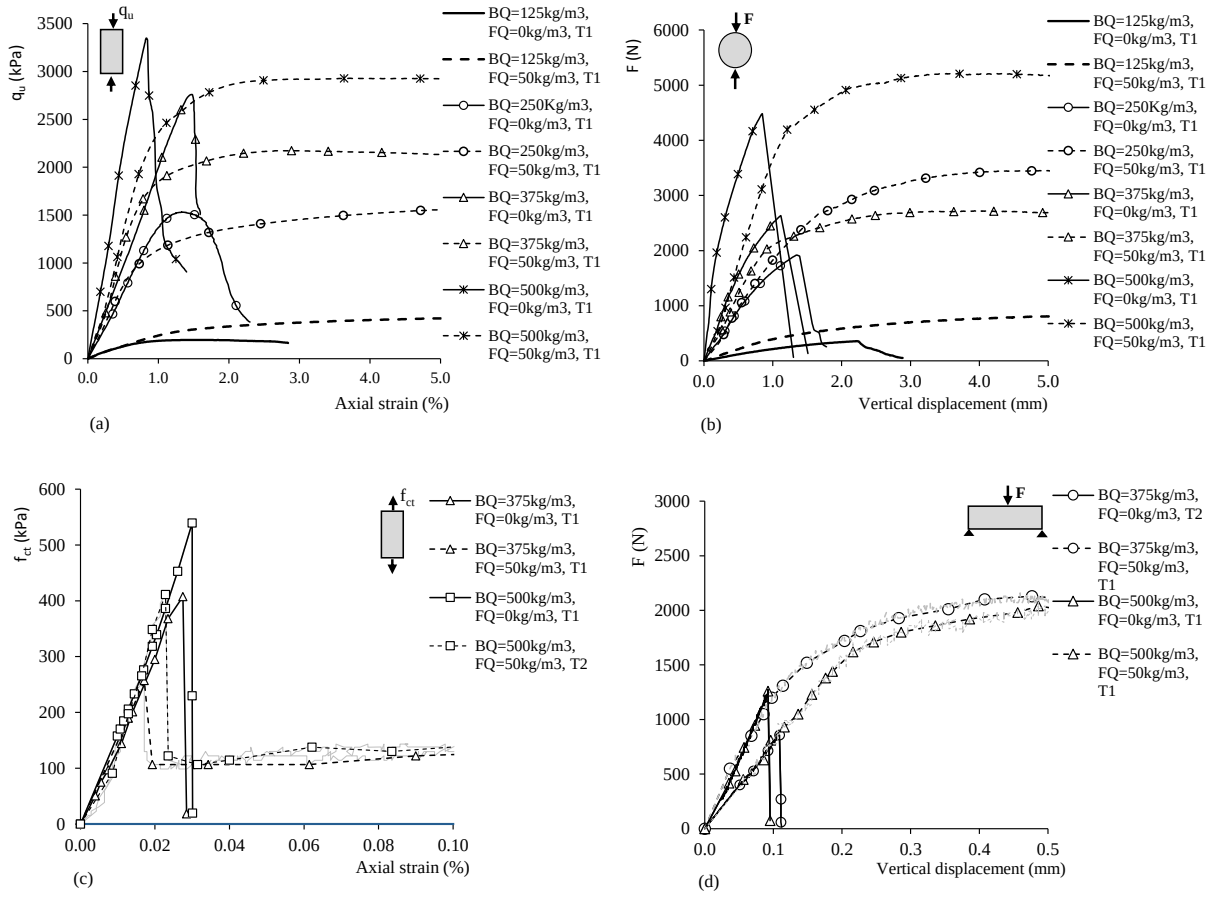

Note BQ: binder quantity; FQ: fibre quantity; q_u: unconfined compressive strength; f_{ct}: tensile strength; F: Load.
Figure 3.26: Stress-strain and load–displacement curves. Effect of binder quantity, both with and without polypropilene fibres (FQ = 50 kg/m^3): (a) UCS test; (b) STS test; (c) DTS test; (d) FS test. (Correia et al., 2015)

In general, the effect of the fibre quantity on the stiffness, compressive and tensile strength are not proportional to the amount of fibres added to the paste. In fact, the inclusion of a low quantity of polypropylene fibres into the soil-binder mixtures tends to decrease the stiffness, decreases the loss of strength after peak and changes the behaviour from brittle to more ductile (Figure 3.27).

Correia et al. (2017) have performed a similar study to the previous one nonetheless now making use of steel fibres. The results showed that choosing a different fibre type (higher mechanical properties but lower specific surface area when compared with polypropylene fibres) will have impact on fibre mobilisation, which is depending on the failure mechanism of each test, Figure 3.28. In general, the binder content has a similar effect on the strength development but the presence of a low quantity of steel fibres had a detrimental effect in terms of UCS and a negligible impact on the STS, while a beneficial effect was found for DTS and FS.

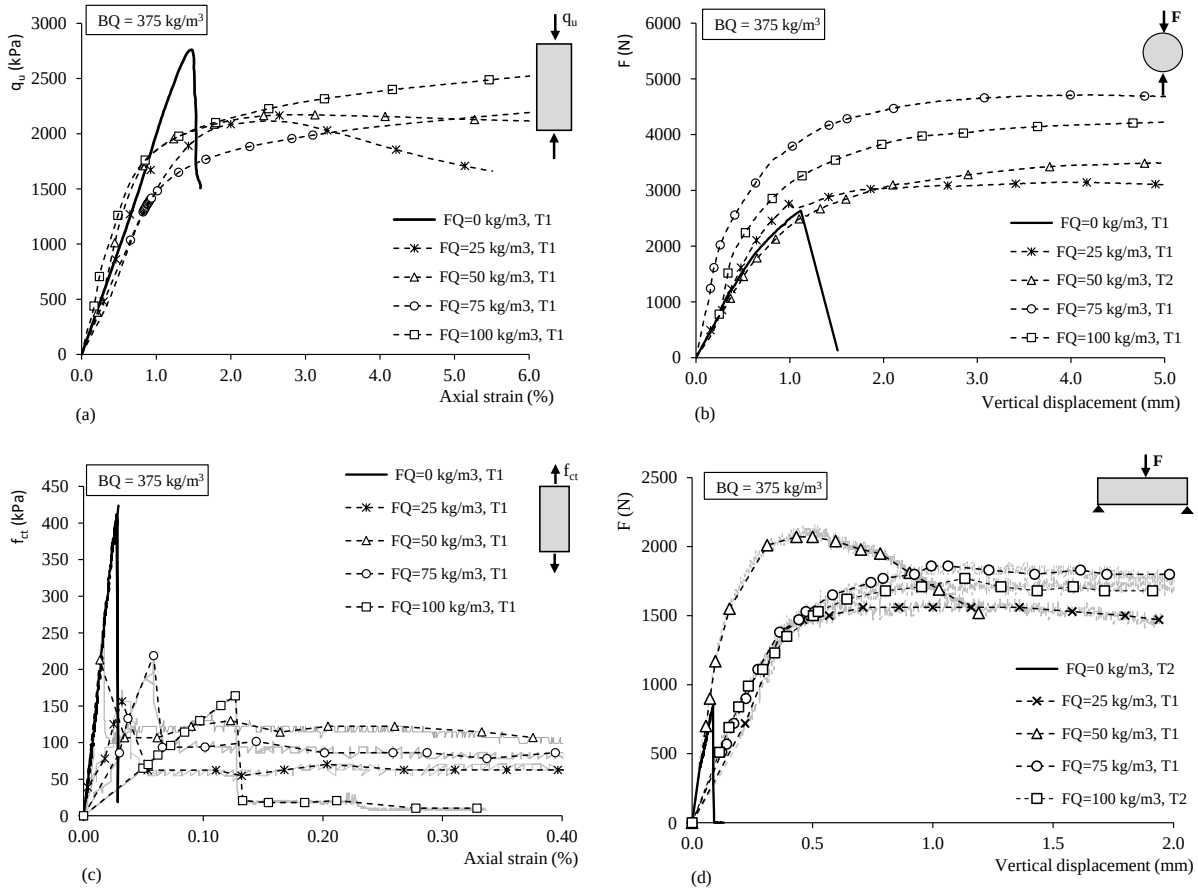

Note BQ: binder quantity; FQ: fibre quantity; q_u: unconfined compressive strength; f_{ct}: tensile strength; F: Load.
Figure 3.27: Stress-strain and load–displacement curves. Effect of polypropylene fibre quantity: (a) UCS test; (b) STS test; (c) DTS test; (d) FS test. (Correia et al., 2015)

In Figure 3.28 illustrates, with the reinforcement with steel fibre quantity was increased, the UCS, STS and FS tests revealed a decrease in brittleness, while the DTS tests showed brittle behaviour with an abrupt and complete loss of tensile strength after failure. The authors explained such behaviour due to the failure mechanism of the DTS test, which induced a sudden transfer of the applied load from the stabilised soil matrix to the fibres, leading to breakage of the steel fibres or pull-out of the fibres because of an insufficient anchorage length. The authors have described the failure mechanism of the tests: UCS and STS tests induced a compressive-based failure mechanism with a low mobilisation of the steel fibres for the peak strength; for the DTS and FS tests a clear tension crack is imposed, even for low strain levels, allowing an effective mobilisation of the tensile strength of the fibres that crosses the crack; moreover, in the FS and STS tests a vertical crack was initiated on one face and evolved to the other face slowly, allowing a progressive mobilisation of the tensile strength of the fibres crossing the crack and producing a non-linear strain field along the failure surface.

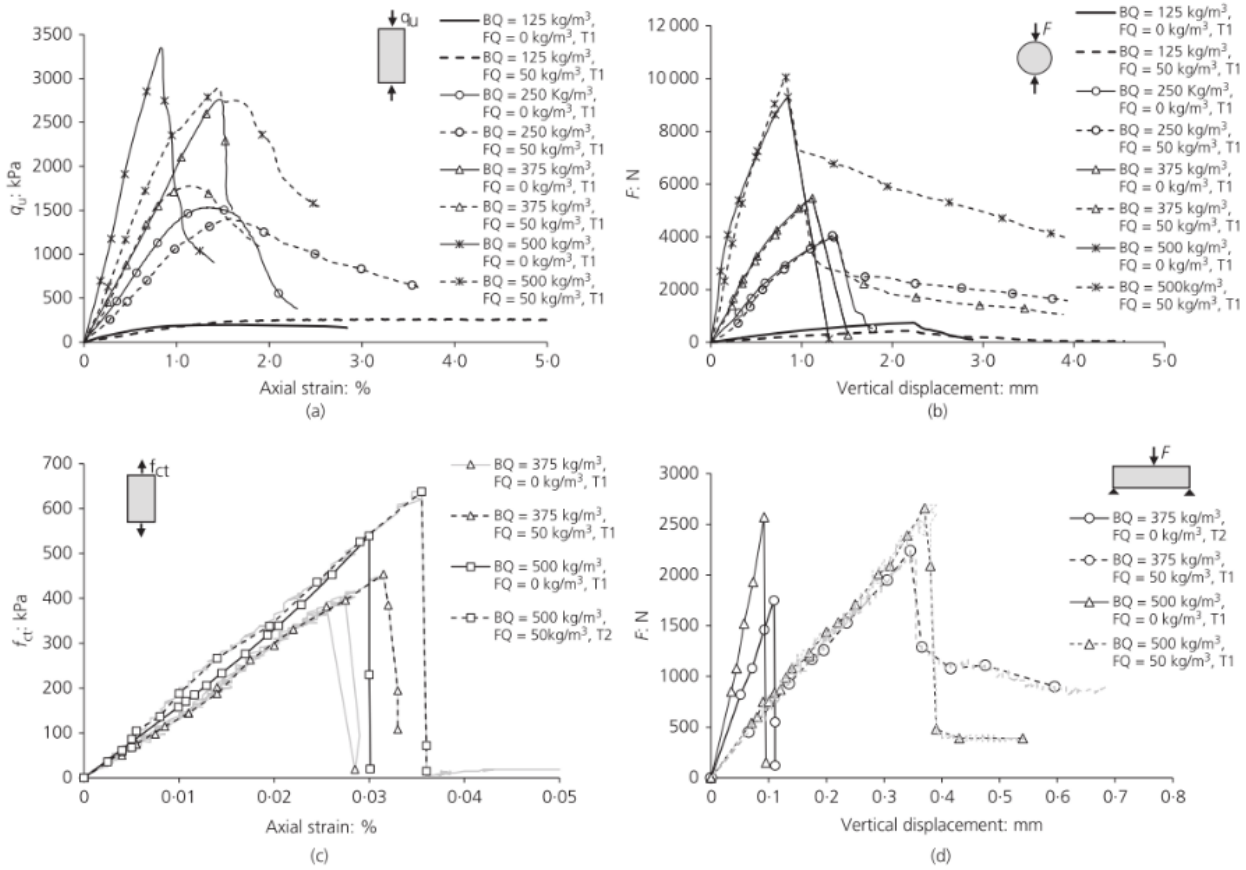

Note BQ: binder quantity; FQ: fibre quantity; q_u: unconfined compressive strength; f_{ct}: tensile strength; F: Load.
Figure 3.28: Stress-strain and load–displacement curves. The effect of BQ, without and with steel fibres (FQ=50 kg/m^3): (a) UCS test; (b) STS test; (c) DTS test; (d) FS test (Correia et al., 2017)

3.3.4 Concluding remarks

When a monotonic loading is applied to soils stabilised with low binder content (less than 10%) it was observed that the inclusion of fibres originates an increase in compressive and tensile strength (Cai et al., 2006; Tang et al., 2007; Consoli et al., 2011; Park, 2011; Estabragh et al, 2012; Olgun, 2013), a decrease in stiffness (Tang et al., 2007), an increase of the residual strength (Tang et al., 2007; Sukontasukkul and Jamsawang, 2012) and an improvement of ductility of the composite material (Tang et al., 2007; Estabragh et al., 2012; Correia et al., 2015; Correia et al., 2017). When the binder content increases there are some modifications on the mechanical behaviour. Sandy soils stabilised with high binder content showed a decrease in peak compressive strength with the inclusion of polypropylene fibres (Consoli et al., 2009), whereas Khattak and Alrashidi (2006) observed a reduction in the tensile strength in high plasticity clays stabilised with a 10% cement content and reinforced with polypropylene fibre content higher than 0.3%. The few studies on the inclusion of steel fibres in a soil stabilised with high binder content (higher than 10%) show a reduction in flexural strength (Sukontasukkul and Jamsawang, 2012), while the

use of steel fibres in a low plasticity soil stabilised with 4% lime causes an increase in compressive strength (Güllü and Khudir, 2014).

3.4 Experimental studies on CSS/CSSRF under cyclic loading

Throughout time, several solutions have been developed to improve the mechanical behaviour of soils with poor geotechnical characteristics. Several experimental works have been carried out to support this evolution, focusing on analysing soil behaviour (mainly its load capacity and deformability) subjected to monotonic and cyclic loading (Cajada, 2017). In the case of monotonic loading behaviour, extensive information exists as was shown in the previous section. The present section aims to present some experimental works focusing on studying the impact of cyclic loading on the mechanical behaviour of soils chemically stabilised unreinforced and reinforced with fibres.

Stabilised soils have been used to enhance the performance of geotechnical constructions exposed to cyclic loading induced from different sources such as traffic, industrial equipment, offshore vibrations, and even earthquakes. In general, tests on stabilised soil samples (without fibres) have shown that increasing the number of load cycles causes progressive degradation of the cementation bonds, increases accumulated permanent strains (Chauhan et al., 2008; Yang et al., 2008; Viana da Fonseca et al., 2013) and decreases stiffness (Sharma and Fahey, 2003). When fibres are added to stabilised soils subjected to cyclic loading, the fibres change the soils' behaviour from brittle to ductile (Tang et al. 2007; Estabragh et al. 2012) while increasing residual strength due to the fibre's tensile strength mobilisation for higher strain levels (Tang et al. 2007; Sukontasukkul and Jamsawang 2012).

3.4.1 Definition of cyclic loading

In this section, it is appropriate to discuss and clarify the differences between a dynamic and cyclic loading. Briefly, a dynamic load is applied in a fast way (a relative term) such that the body mass is subject to a motion, and the resistance to the load are provided by the stiffness, viscosity, and inertia of the body. A load that repeats itself (in magnitude) in a regular time interval (frequency) is termed as a cyclic load. It could be monotonic (if applied very slowly) or dynamic (if applied faster) (Islam, 2021). O'Reilly and Brown (1991) have defined the term 'cyclic loading' as suggesting a system of loading that exhibits a degree of regularity both in its magnitude and frequency. Loading systems that are approximately cyclic in this sense are indeed encountered in

practice. Many machines and even offshore structures transmit fairly rhythmic stress pulses to their foundations.

One point that should be emphasised is that the behaviour of soils under cyclic loading seems to be highly complex. Some of the most sophisticated models have failed to provide accurate predictions under generalised cyclic stress conditions (O'Reilly and Brown, 1991). Accordingly to O'Reilly and Brown (1991) some of the reasons that may justify such results are due to the effect of stress reversals during the cyclic loading as well as to the rate-dependent response of soils. 'Stress reversal' refers to a shift in the sign of the stress rise/increment, not to the stress itself. O'Reilly and Brown (1991) have shown an example: *'an increase in stress magnitude followed by reduction would, in this sense, be a stress reversal even though all stresses continue to act in the same direction.* The same author explained that in terms of 'stress increase', it is difficult to define, when considering three-dimensional stress-states especially with principal stress rotation, the general distinction between loading and unloading for simple stress paths such as those experienced during triaxial tests at constant confining pressure.

Figure 3.29 shows the idealised behaviour of elements of dry granular soils subject to regular drained cyclic during stress-controlled loading between two shear stress-states, S1 and S2.

O'Reilly and Brown (1991) have said that the irreversible or plastic strain generated over time tends to decrease during the cyclic loading. The soil eventually finds an equilibrium for this loading pattern. At this point, the recoverable strain encountered throughout a cycle greatly exceeds the plastic strain increase. It is characterized as quasi-elastic or 'resilient'.

According to O'Reilly and Brown (1991), the influence of the 'rate of loading and strain' on the soil's strength and stiffness comes from two sources: viscous interparticle's action and time-dependent dissipation of excess pore pressures produced by loading.

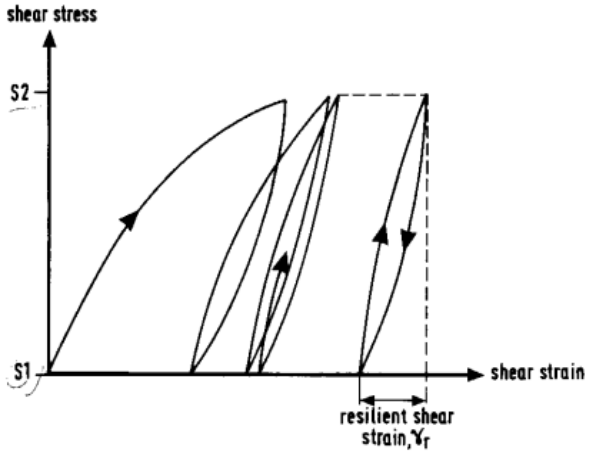

Figure 3.29: Typical development of shear strain during a repeated load test and definition of resilient shear strain (adapted from O'Reilly and Brown, 1991)

3.4.2 Engineering behaviour

The behaviour of a stabilised soil under cyclic loading is characterised not only by the features presented in section 3.3 (mainly, interpreting stress-strain curve, $q_{u\text{-}max}$, $\varepsilon_{ax\text{-}rupt}$, E_{u50}), but also by during cyclic stage, the evolution of the axial permanent strains ($\varepsilon_{ax\text{-}perm}$), as well as by the post-cyclic behaviour (which may be characterised by the same features as the ones presented in section 3.3).

Chauhan et al. (2008) studied the effect on the shear strength of adding coir and polypropylene fibres to a silty sand stabilised with a fly ash content of 30% (to be applied as a subgrade). Due to instrument and time constraints, all specimens were tested to 10,000 cycles. Results from cyclic triaxial tests indicate that the permanent axial strain increases with the number of load cycles (Figure 3.30a), while the resilient modulus (i.e., is a ratio of the applied stress and recoverable strain at a particular load/stress) decreases (Figure 3.31b) for both reinforced and unreinforced materials. From Figure 3.30a it may be seen that up to 10,000 cycles, the 10% failure strain criterion (as anticipated for the subgrade for pavement in rural area) was not reached, indicating that it would take additional load cycles to attain the failure strain criterion. In the case of Figure 3.30b), the resilient modulus decreases more noticeable for the reinforced materials indicating that as the number of load cycles increases the irreversible or plastic strain generated over time tends to decrease, which is good for a subgrade reinforced soil. Coir fibres show better resilient response than synthetic fibres due to their higher coefficient of friction. Moreover, the same authors have also studied the impact of the confining pressure on triaxial samples and have concluded that both the permanent strains and resilient modulus in reinforced and unreinforced materials decrease with confining pressure (Chauhan et al., 2008).

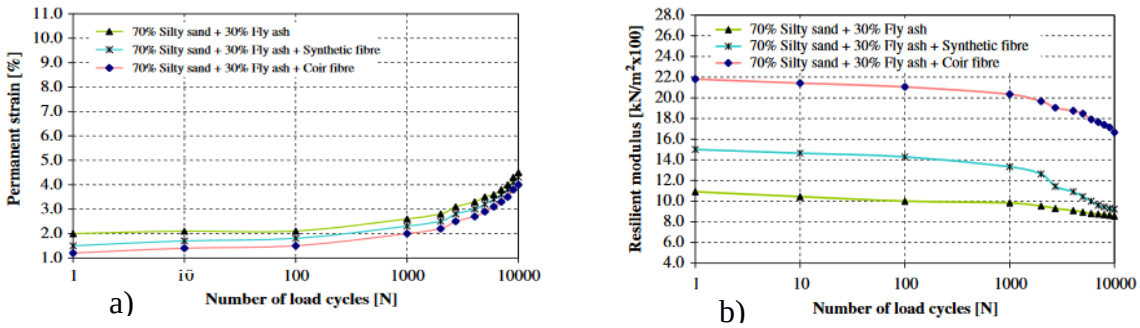

Figure 3.30: Cyclic triaxial results at deviator stress of 120 kN/m^2 and confining pressure of 75 kN/m^2 for silty sand (SM) mixed with fly ash: a) Permanent strain; b) Resilient modulus (Chauhan et al., 2008)

Dall'Aqua et al. (2010) carried out a study to identify the behaviour of adding polypropylene fibres (in a content of 0.2, 0.3 or 0.4%) to a clayey soil stabilised with Portland cement (binder

content of 4 or 6%) subjected to repeated loading. All samples were prepared at optimum water content and maximum dry density. Before starting the repeat test the samples were subjected to a ten-minute initial 'conditioning' where an axial stress of 10 kPa was applied. The repeated test were performed as follows: an axial stress of 100 kPa was applied during 10.000 load cycles; each load cycle is two seconds long: one-second load period followed by one-second rest period. Sample's deformation is shown in Table 3.8.

Table 3.8: Permanent deformation for kaolinite (clay) reinforced with fibre and stabilised with cement (adapted from Dall'Aqua et al., 2010)

Composites of materials	3.600 cycles	10.000 cycles
Kaolinite	4.5	5.2
Kaolinite + 0.2% F23	1	2
Kaolinite + 0.3% F23	1.1	1.9
Kaolinite + 0.4% F23	1.3	2.8
Kaolinite + 4% cement	0.7	0.9
Kaolinite + 4% cement (soaked specimen)	Failed	Failed
Kaolinite + 4% cement + 0.3% F23	2.6	3
Kaolinite + 4% cement + 0.3% F23 (soaked specimen)	5.2	6
Kaolinite + 6% cement	0.6	0.9
Kaolinite + 6% cement (soaked specimen)	Failed	Failed
Kaolinite + 6% cement + 0.3% F23	1.3	1.5
Kaolinite + 6% cement + 0.3% F23 (soaked specimen)	0.9	1.4

A typical deformation-load cycle relationship (for 28 days) is shown in Figure 3.31. The authors observed that fibres or cement when applied alone reduces substantially the deformations, which is in accordance with previous findings (Table 3.8). However, when combining both effects, cement stabilisation and fibre reinforcement, it was observed that samples with fibres have more deformations than those samples tested without fibres. This is presumably due to poor soil stabilised-fibre bonding. However, the reinforced stabilised samples were the only mixes which could undergo soaking tests where the bond strength and friction between the stabilised clay and fibre were no doubt helping to maintain the integrity of the samples.

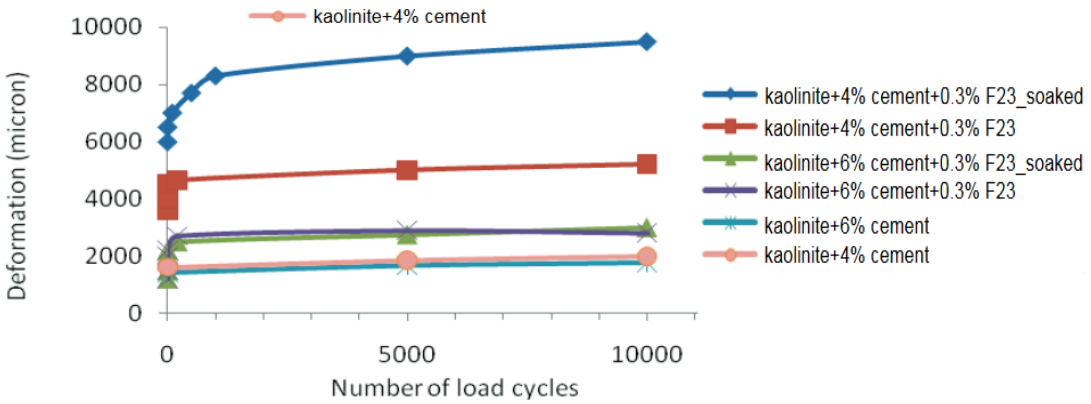

Figure 3.31: Repeated axial load test results for kaolinite with fibre and cement after 28 days (adapted from Dall'Aqua et al., 2010)

Moreover, Viana da Fonseca et al. (2013) also working with silty-sand artificially cemented, found that for long-term cyclic triaxial tests with a high number of load cycles there is a continuous increase in the accumulated permanent deformations (Figure 3.32).

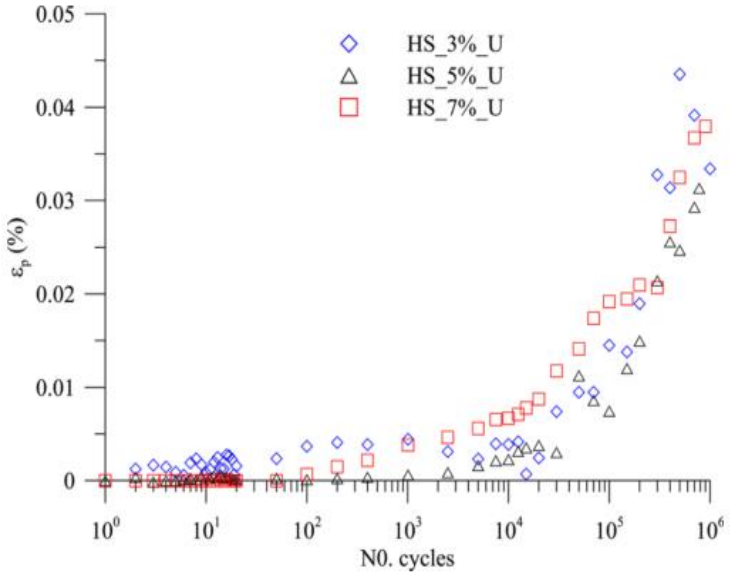

Figure 3.32: Evolution of the permanent deformation with the number of load cycles for three undrained (U) tests at higher stress (HS) levels of a silty-sand soil stabilised with 3, 5 and 7% of Portland cement (adapted from Viana da Fonseca et al., 2013)

The authors concluded that the cyclic behaviour of stabilised samples should be investigated for a large number of load cycles. From Figure 3.33, the uncemented specimen (LS_0%_D which means lower stress level, cement content of 0%, and testing in drained condition) showed a continuous increase in the accumulated permanent deformation without any sign of stabilisation conversely to what should be expected from a granular material, while the resilient modulus is almost constant, Figure 3.34. As stated by the authors, the high scatter observed in the undrained test stabilised with 7% of cement (LS_7%_U) is due to the very low strain values developed in this test. It was observed that the resilient moduli decrease with the cement content, indicating that cement has a significant effect in the stiffness increase. In terms of the evolution of the resilient modulus with the number of cycles, a slight increase was observed in the cemented samples after 10,000 cycles, despite the cement degradation indicated by the plastic strains. This means that the development of plastic deformation does not seem to affect so much the stiffness as it does on the plastic (accumulated) deformations (Viana da Fonseca et al., 2013).

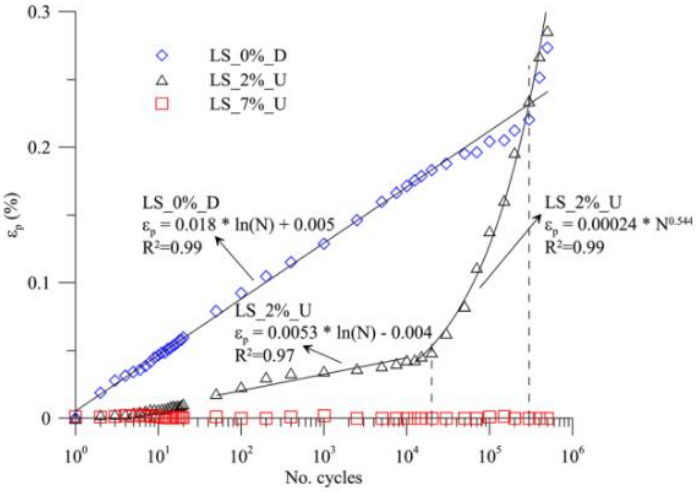

Figure 3.33: Evolution of the accumulated permanent deformation with the number of cycles. (Viana da Fonseca et al., 2013)

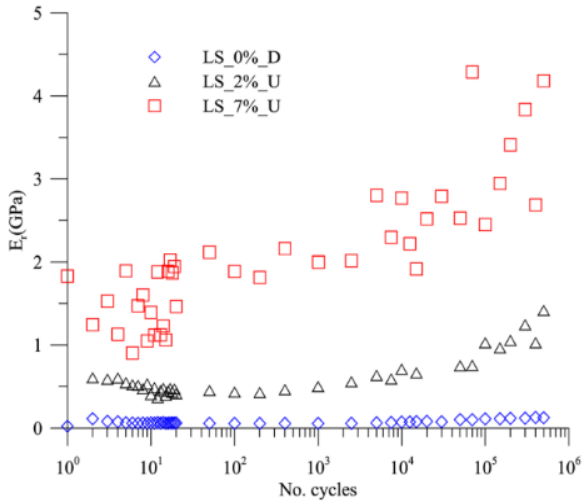

Figure 3.34: Evolution of the resilient modulus with the number of cycles. (Viana da Fonseca et al., 2013)

Venda Oliveira et al. (2017) studied the effect of cyclic loading on the behaviour of a soft soil chemically stabilised with Portland cement and blast furnace granulated slag (proportion 75/25) and reinforced with steel fibres. Samples were submitted to UCS cyclic tests for a deviatoric stress level of 55% of the maximum unconfined compressive strength ($q_{u\text{-}max}$), frequency of 0.5 Hz, with an amplitude of ± 4% of $q_{u\text{-}max}$. The results indicate the permanent axial strain increases with the number of load cycles up to 5,000 cycles, showing a linear trend for logarithmic scale as indicated in Figure 3.35. For a higher number of cycles the effect on the $\varepsilon_{ax\text{-}perm}$ tends to diminish, and for values higher than 5,000 cycles the $\varepsilon_{ax\text{-}perm}$ remains almost constant. This behaviour agrees with the results of a stabilised clay reinforced with the polypropylene fibres from Sukontasukkul and Jamsawang (2012), Correia et al. (2015), Consoli et al. (2011 and 2013) and Park (2011). The behaviour observed seems to be linked to some local breakage of the cementitious bonds and the

consequent transfer of stresses from the cement matrix to the steel fibres, which, due to their high axial stiffness, are mobilized for low strain levels. Beyond 5,000 cycles the results suggest that the cyclic loads have been absorbed by the fibres, which are still in elastic behaviour, justifying the constant values observed for the permanent axial strain.

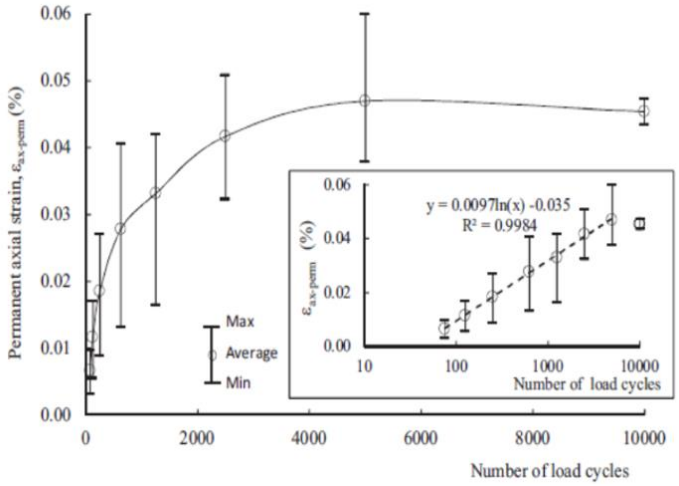

Figure 3.35: Evolution of accumulated axial deformation with the number of cycles (Venda Oliveira et al., 2017)

Moreover, the same authors have also studied the impact of the cyclic loading on the post-cyclic stress-strain behaviour through UCS tests performed just after the end of the cyclic stage. The value of the maximum unconfined compressive strength increases with the number of load cycles (Figure 3.36).

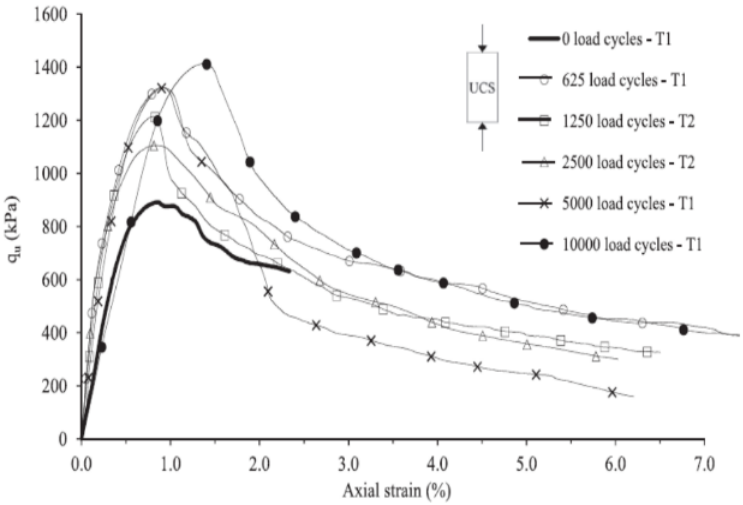

Figure 3.36: Effect of number of cycles on stress-strain curves of UCS tests performed after the cyclic stage (Venda Oliveira et al., 2017)

Such behaviour is probably linked to the increased of axial deformation during the cycle stage, allowing the mobilisation of fibre tensile strength which seems to compensate the breakage of the cementitious bonds during cyclic loading. However, the number of cycles have a lower impact on

the post peak strength since the results exhibit a similar trend to that obtained from the monotonic UCS tests. As a result, the difference between the peak and the post peak strength tends to increase with the number of cycles. The similarities in the post peak strength trends may be related with the equal fibre content used in the sample preparation, since it is expected that for high strain levels the tensile strength of the majority of the fibres has already been mobilised (Venda Oliveira et al. 2017).

Venda Oliveira et al. (2018) studied the influence of cyclic loading on the behaviour of several soils chemically stabilised with Portland cement unreinforced and reinforced with polypropylene fibres. All UCS samples were prepared with a binder quantity of 175 kg/m^3, a water-binder ratio of 5.3 and a fibre quantity of 0 and 10 kg/m^3. Soils differ in grain size composition: soil A (100% of sand) and B (65% of sand) are sandy soils; soil C, D and E have different content of clay+silt particles, 56% for soil C, 64% for soil D and 73% for soil E; additionally, soil E displays a high organic matter (OM) content of 10.3% (Figure 3.37).

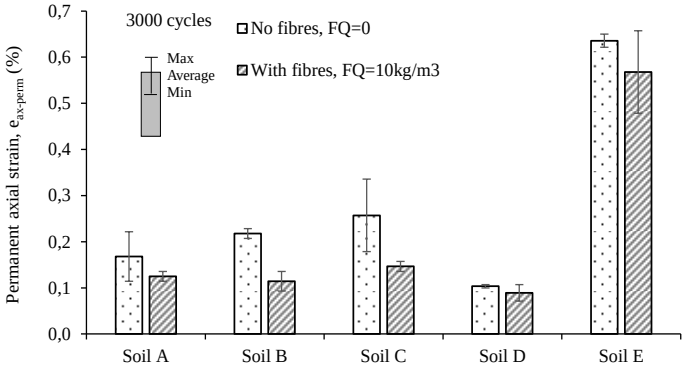

Figure 3.37: Effect of soil type on the accumulated permanent axial strain for 3.000 load cycles. (Venda Oliveira et al., 2018)

The results show that the inclusion of fibres in the composite material has a positive effect on the cyclic behaviour, decreasing the accumulated permanent axial strain, while the increase in the amount of clay + silt particles and the organic matter content has a detrimental effect (Figure 3.38). Moreover, it was observed also the effect of the cyclic stage on the brittleness depends on the soil type, thus, coarser soils show an increase in the brittleness while an increase in the organic matter content promotes a slight increase in the ductility (Figure 3.38). The cyclic stage induces an increase in the mechanical characteristics (strength and stiffness) of the composite material; indeed, the deterioration of the solid skeleton during the cyclic stage is partially compensated by the mobilization of the tensile strength of the fibres due to the strain level imposed by the cyclic loading. The improvement of the stabilised materials due to the cyclic stage is higher for unreinforced soils than for fibre-reinforced

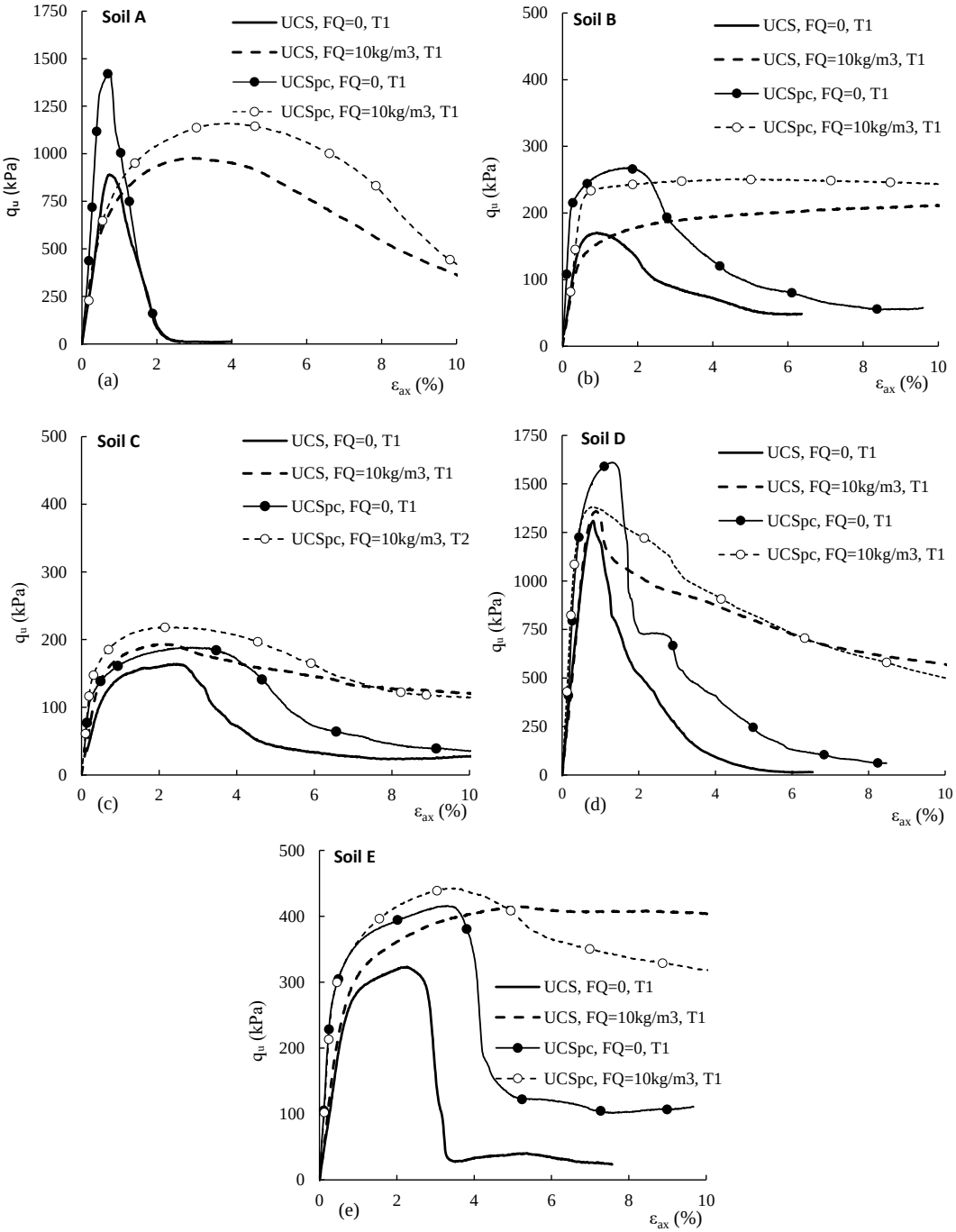

Figure 3.38: Effect of soil type and reinforcement with polypropylene fibres on the stress-strain curves of the UCS tests carried out before (UCS) and after the cyclic stage (UCSpc). a) Soil A; b) Soil B; c) Soil C; d) Soil D; e) Soil E. (Venda Oliveira et al., 2018)

soils and is more significant for the stiffness than unconfined strength. Independently of the soil analysed and the reinforcement or not with fibres, the cyclic loading induces the increases of the strength of the stabilised soil, and this effect is more significant in soils with a high sandy fraction (Soil A) (Figure 3.38). The case of Soil E represents a soft soil with similar characteristics to the soil used in this work and results shown that fibres enhance the q_u and adding fibres not shown a remarkable difference.

Festugato et al. (2013) performed cyclic simple shear experiments on mining tailings (sandy silt with clay traces), stabilised with Portland cement (5%) and reinforced with polypropylene fibres (0 and 0.5%), Figures 3.39 and 3.40. The presence of fibres causes the cemented material to harden under monotonic shear. After the load cycle stage, fibres have promoted an increase of the shear stress of cemented samples.

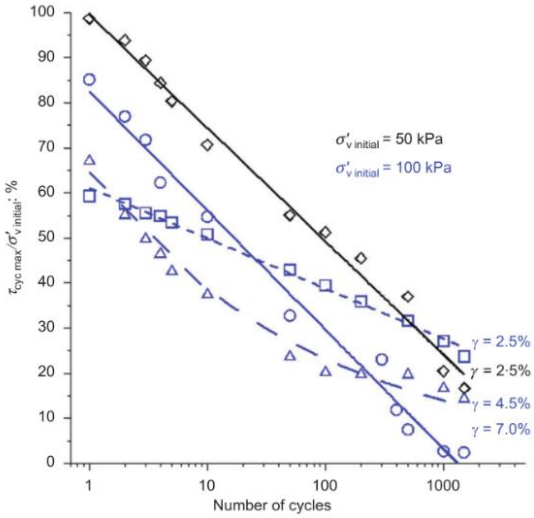

Figure 3.39: The ratio of cyclic maximum shear stress to initial effective vertical stress $\tau_{cyc\,max}$ /$\sigma'_{v\,initial}$ against the number of cycles of strain-controlled tests conducted at 100 kPa and 50 kPa initial effective vertical stress for unreinforced cemented mine tailings (Festugato et al., 2013)

Unreinforced and reinforced cemented samples were exposed to controlled shear strain (γ) of 2.5, 4.5 and 7.0%. As the Figures 3.39 and 3.40 indicate, raising the initial effective vertical stress enhances shear strength for the reinforced case. Increasing the applied shear strain increases early load cycle shear stress values, while decreases later load cycle shear stress values.

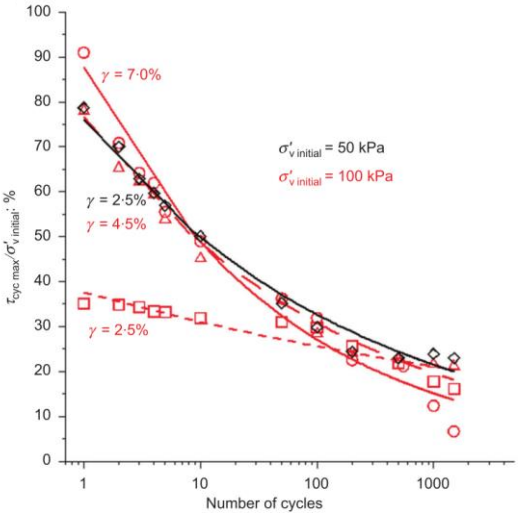

Figure 3.40: Ratio of cyclic maximum shear stress to initial effective vertical stress $\tau_{cyc\,max}$ /$\sigma'_{v\,initial}$ versus the number of cycles of strain-controlled tests under 100 kPa and 50 kPa of initial effective vertical stress for fibre-reinforced cemented mine tailings (Festugato et al., 2013)

Khattak and Alrashidi (2006a) carried out a series of splitting tensile strength tests under monotonic and cyclic conditions on four cohesive soils stabilised with Portland cement (binder content of 10%) and reinforced with polypropylene or processed cellulose fibres (fibre content of 0, 0.15, 0.30 and 0.50%). The results indicated that the maximum stress to failure for the fibre stabilised soil are significantly higher than for the unreinforced stabilised soil. The post-peak stress-strain behaviour indicates that the inclusion of the fibres increases the energy to failure (toughness). Both increases in tensile strength and toughness of the reinforced stabilised soil indicate high resistance to tensile cracking. The authors stated that this behaviour depends on type of soil and fibre, and fibre content. Regarding the splitting tensile cycle tests results it was observed that the addition of fibre reduces the plastic deformation and either maintained or increased the resilient modulus.

Ahmed and Naggar (2018) studied a sandy soil stabilised with a mixture of recycled bassanite and Portland cement (applied in different ratios, 1:1, 2:1, 4:1, 8:1, and in a content of 5, 10, 15 and 20%) and reinforced with shreds of waste tire (with dimensions of 2, 4, 8 and 10mm, applied in a content of 0.5, 1, 2 and 4%). UCS and splitting tensile strength tests were performed under monotonic and cyclic conditions. The results showed that the strength of the treated soil increased with the binder content but decreases as the binder content increases, and the addition of shredded waste tire improved the tensile strength of the treated soil, but slightly reduced its compressive strength. Cyclic loading resulted in significant degradation of strength for stabilised samples, however, incorporation of shredded tire waste reduced this degradation. It was also observed that the size of shredded waste tire had negligible effect on cyclic strength of the composite material.

Venda Oliveira et al. (2021) based on cyclic UCS tests have analysed the effect of the frequency of the cyclic loading on the behaviour of a stabilised sandy soil, unreinforced and reinforced with polypropylene and sisal fibres. The authors have observed that in terms of the unconfined compressive strength, the frequency has a low impact on the unreinforced material, contrary to the effect on the reinforced material, which induces a decrease in strength for a frequency of 1.0 Hz and an increase in strength for frequencies of 2.0 and 4.0 Hz for both types of fibres. Moreover, the inclusion of fibres induces a decrease in the accumulated permanent axial strain obtained at the cyclic stage; this reduction is more significant for a frequency of 1.0-2.0 Hz and with the use of sisal fibres, due to the greater roughness and higher mechanical properties of these type of fibres (Figure 3.41).

Goulart (2019) have performed a similar study to the one done by Venda Oliveira et al. (2022), using the same soil and studying the effect of the frequency of the cyclic loading, but now it was used cyclic splitting tensile strength test. The results showed that in terms of the load-

displacement behaviour, the presence of the fibres induces a more ductile tensile behaviour that is characterized by a second peak strength and by a residual strength (Figure 3.42). Under cyclic loading it was observed that the inclusion of fibres promotes a significant reduction in the accumulated plastic axial displacement as the frequency increases (Figure 3.43). This is more expressive for the synthetic fibres due to a higher number of randomly distributed fibres (strong interlocking density). The cyclic loading induced a higher post-cyclic tensile strength for the sisal fibres but a more ductile tensile mechanical behaviour for the polypropylene fibres.

Indeed, investigations on the cyclic loading of composite materials are rare and almost always with unreinforced materials under compression. Cyclic loading of unreinforced stabilised soils causes the gradual breakdown of the cemented matrix structure, increasing plastic deformations (Chauhan et al., 2008; Yang et al., 2008; Viana da Fonseca et al., 2013) and a decrease in the stiffness and yield stress (Sharma and Fahey, 2003; Subramaniam and Banerjee, 2014).

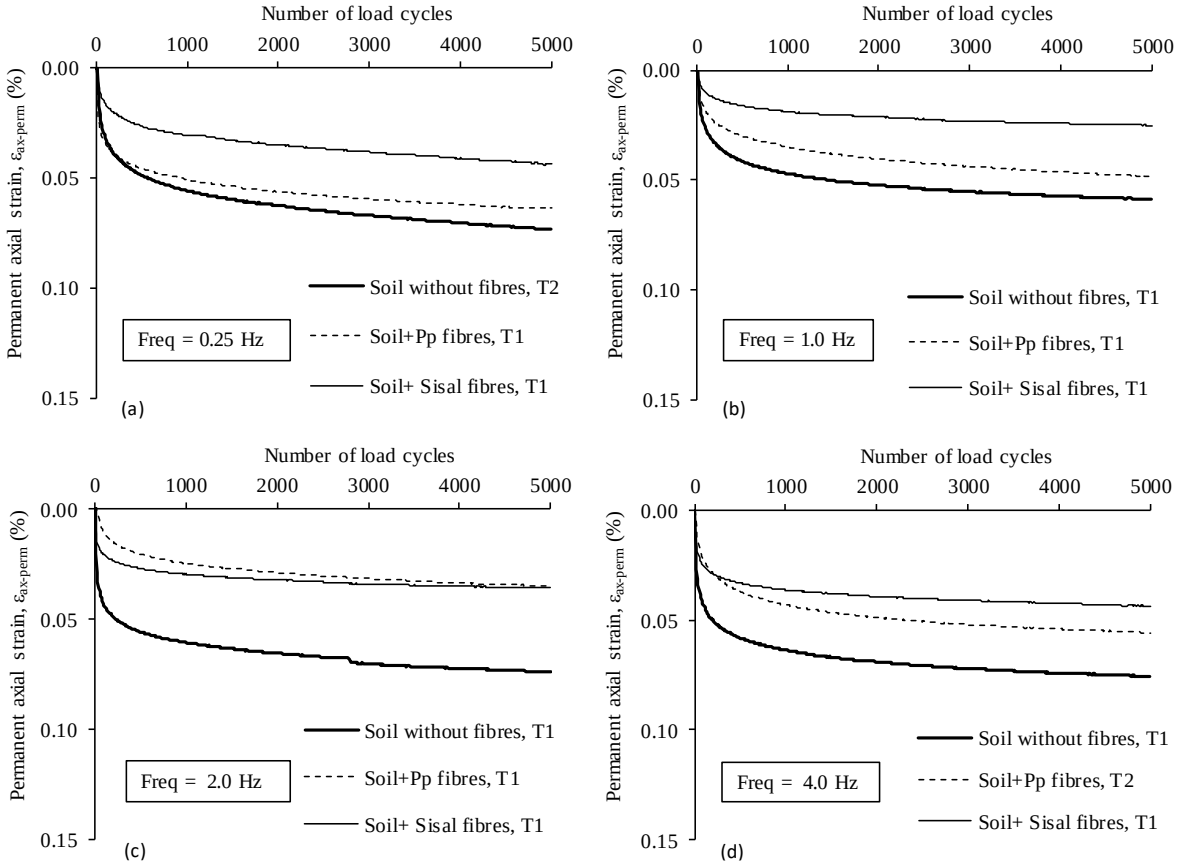

Figure 3.41: Effect of the frequency on the accumulated permanent axial strain with the number of load cycles for a frequency of: a) 0.25 Hz; b) f 1.0 Hz; c) 2.0 Hz; d) 2.0 Hz (Venda Oliveira et al., 2021)

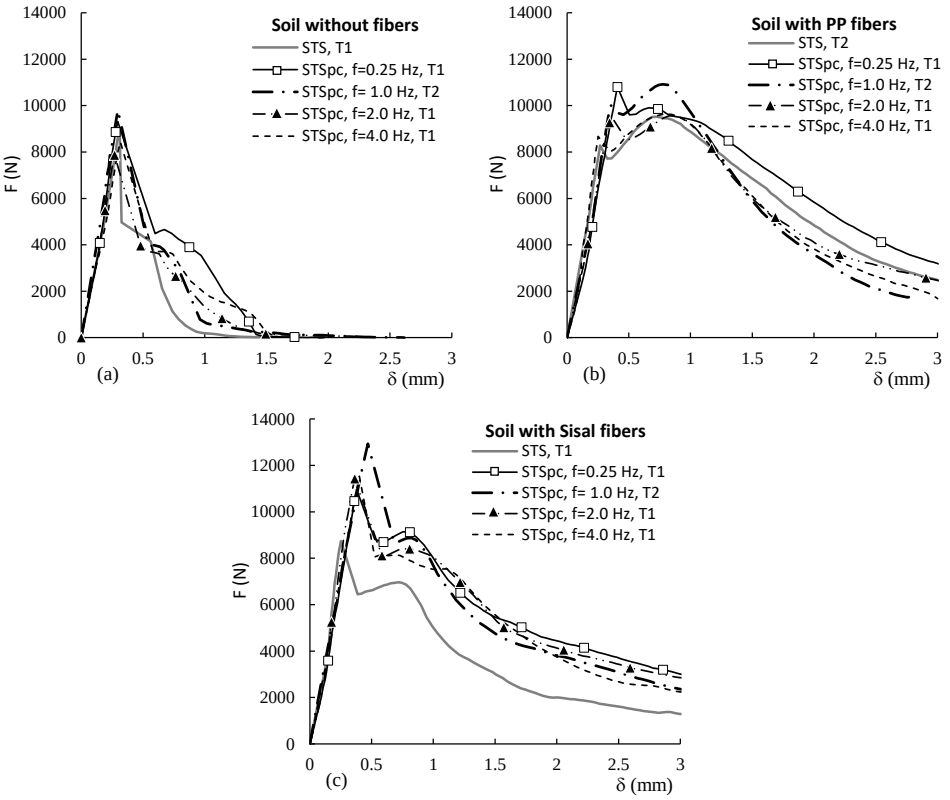

Figure 3.42: Effect of the frequency on the load-displacement curves of the splitting tensile strength tests carried out before (STS) and after the cyclic stage (STSpc) for: a) unreinforced stabilised soil; b) stabilised soil reinforced with polypropylene fibres; c) stabilised soil reinforced with sisal fibres (Goulart, 2019)

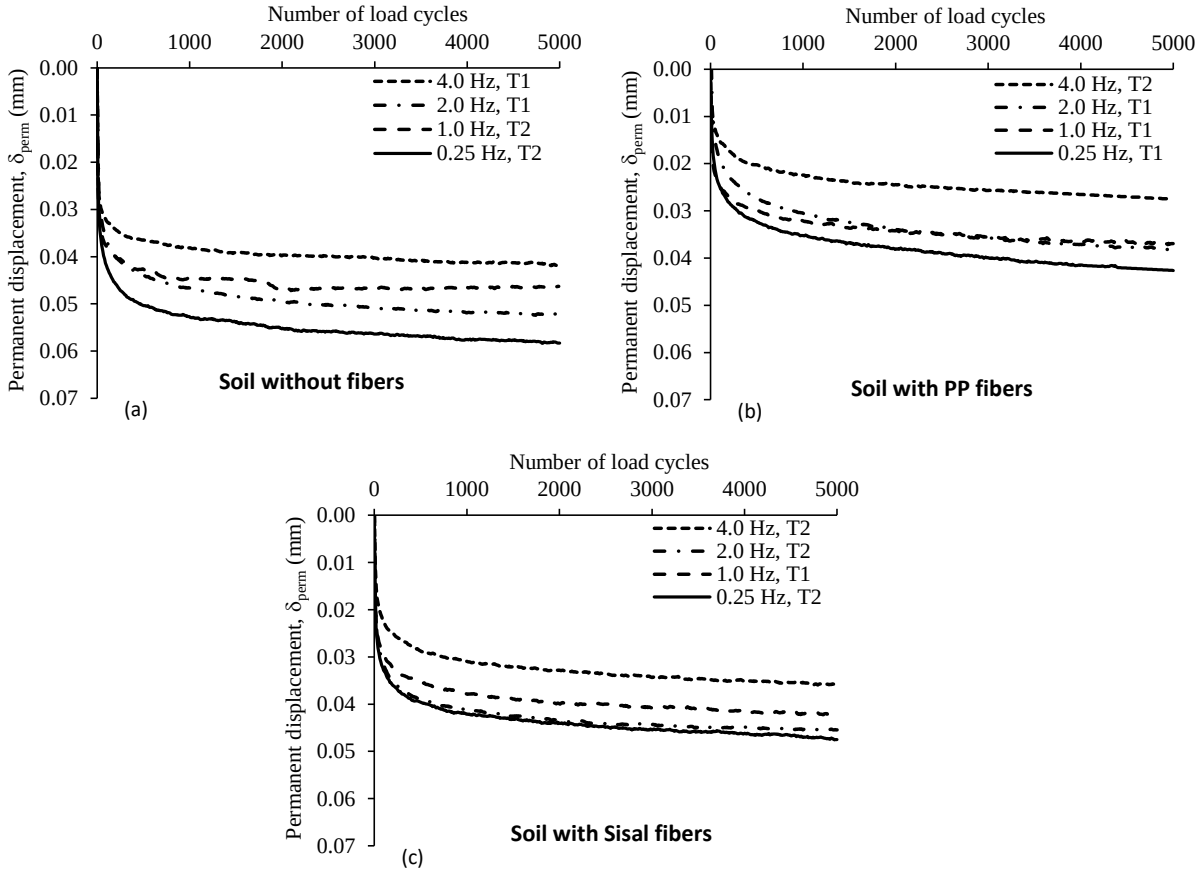

Figure 3.43: Effect of the frequency on the accumulated plastic displacement with the number of load cycles for: a) unreinforced stabilised soil; b) stabilised soil reinforced with polypropylene fibres; c) stabilised soil reinforced with sisal fibres (Goulart, 2019)

In summary, it has been observed that plastic deformations grow with load cycles, with the most significant increase occurring during the initial cycles (Dall'Aqua et al., 2010; Venda Oliveira et al., 2017; Venda Oliveira et al., 2018) or for a large number of load cycles (Chauhan et al., 2008; Viana da Fonseca et al., 2013). The results of the plastic deformations are contradictory, with Khattak and Alrashidi (2006) and Chauhan et al. (2008) observing a decrease in the plastic strains from splitting tensile cyclic load tests, while an increase was measured in other works (Dall 'Aqua et al., 2010; Venda Oliveira et al., 2017). These observations altogether with the literature review regarding the CSSRF under cyclic loading showed that:

(i) knowledge is limited, and some of the results require further investigation.

(ii) the few works available are mainly based on a single type of cyclic test (UCS);

(iii) the effect of cyclic loading parameters (such as cyclic load frequency, cyclic load mean value and amplitude) on mechanical behaviour of a stabilised and fibre-reinforced soil is less studied;

(iv) there are no constitutive models able to simulate accurately the cyclic behaviour of the CSSRF.

Thus, it is important to better understand the stress-strain-yielding behaviour of chemically stabilised soils unreinforced or reinforced with fibres to develop more realistic constitutive models that may reasonably predict the behaviour of such composite materials. The following section will present some research on the yield surface of cement-based stabilised soils unreinforced or reinforced with fibres. Due to the few numbers of studies, it was decided to include some of the results for natural and structured clays (which may exhibit a behaviour closer to cement-based stabilised soils).

3.5 Definition of Yield Surface

The phenomenon of yielding in clay soils is well known, and the detailed discussion on concepts involved yielding on soft clays can be found in several research works (Roscoe and Schofield's, 1963; Wong and Mitchell 1975; Tavenas and Leroueil, 1980; Graham et al. 1983; others). The definition of the yield surface is important because it separates the "elastic" behaviour from the "plastic" behaviour (Figure 3.44), i.e., the yield surface defines where the destructuration starts. Atkinsons (1990) described that yielding should be restricted to show the end of the elastic range. Other authors, such as Vaughan (1985), define yield stress as a stress state in which material

shows a discontinuity in its mechanical behaviour. Malandraki and Toll (1996) agree with this last concept saying that when the stress-strain changes, the yield happens.

Thus, it is of upmost importance to define the yield surface even for chemically stabilised soils unreinforced or reinforced with fibres. Unfortunately, regarding fibre-reinforced stabilised samples there is little information on this subject. Such information is essential to better understand the mechanical behaviour of such materials, a necessary condition to develop more realistic constitutive models to reasonably predict the cement-based stabilised soil behaviour. As stated previously, the present research work aims to contribute to the increase of knowledge in this area.

Knowing that there is limited information about the yielding surface of fibre-reinforced chemically stabilised by cement samples, in the following sections it will be addressed some related experiences on natural and cemented clays.

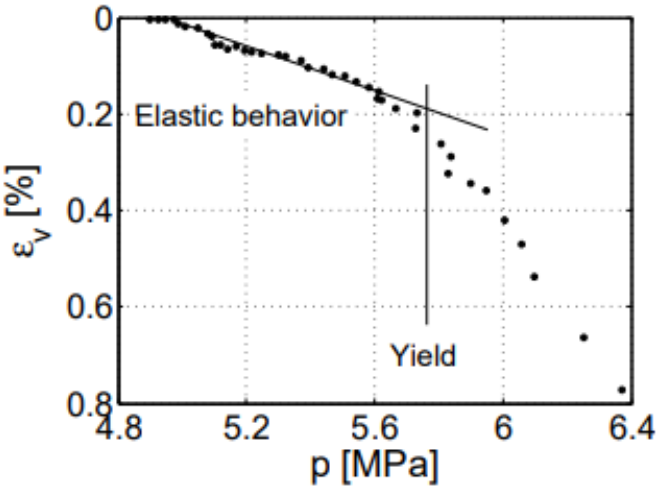

Figure 3.44: Yield locus of Leda clay established by Mitchell (1980)

3.5.1 Natural clays

It has been observed that when natural clays are subjected to changes in effective stress, they show a rather stiff (or “elastic”) behaviour at the beginning followed by considerable elastoplastic deformations. In stiff or “elastic” region, the stress vector remains within a domain in the stress space, the boundary is called the "yield locus" (e.g., Mitchell, 1970; Wong and Mitchell, 1975). Roscoe et al. (1958) describes the yield surface concept as an effective tool for forecasting natural soil behaviour for soft clays. Also, other authors using reconstituted clays mentioned that during the loading, the stiffness of the soil changes from overconsolidated “elastic” to normally consolidated “plastic”, which has practical applications for analysing geotechnical problems, as

for example embankment foundation behaviour (Tavenas and Leroueil 1980; Folkes and Crooks 1985) and slope behaviour (Tavenas and Leroueil 1977).

Baracos et al. (1980) investigated the yielding of a highly plastic natural inorganic clay from Winnipeg, Canada. Yield envelopes were determined from drained triaxial tests on anisotropically consolidated samples sheared along various stress paths. The yield envelopes were well-defined for the shear failure of the soil structure but were poorly defined for conditions of increasing octahedral stress. Graham et al. (1983) have continued Baracos et al. (1980) study on Winnipeg clay. They performed an oedometer, K_0 triaxial and drained triaxial tests at different stress ratios on normally and lightly overconsolidated clay samples (Figure 3.45).

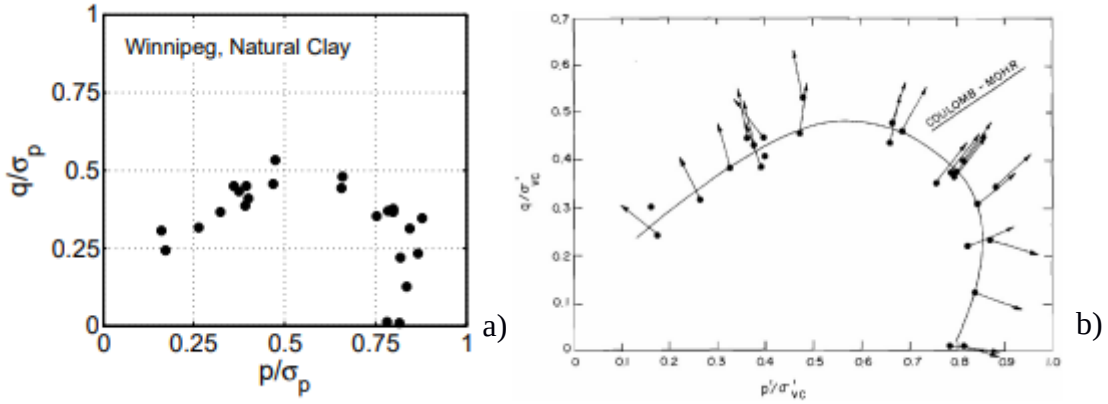

Figure 3.45: Yield points for Winnipeg Natural clay: a) normalized stress space; b) normalized stress space with plastic strain vectors (adapted from Graham et al. (1983))

In addition to the resulting yield surface, Graham et al. (1983) also showed that the plastic strain vectors are not always normal to the yield surface which is indicated a non-associated flow rule. Figure 3.45 summarises both the yield surface and the plastic strain vectors. Although yield stresses have been determined by plotting different quantities, Graham et al. (1983) found that the yield values obtained from various graphs were usually quite similar. Consequently, they concluded that the yield stresses indeed constitute an inherent component of soil behaviour (Figure 3.45).

Mitchell (1970) performed completely drained triaxial tests for different bedding plane orientations (horizontal, vertical, and inclined 45° to the horizontal) to study the effect of soil anisotropy. He concluded that a yield curve for natural Leda clay might be constructed. Such curves were not the same for samples orientated in various orientations during testing owing to apparent anisotropy. Figure 3.46 illustrates the volumetric yield locus is generally similar in shape to that for Leda clay (Mitchel, 1970 and Parry, 1973)

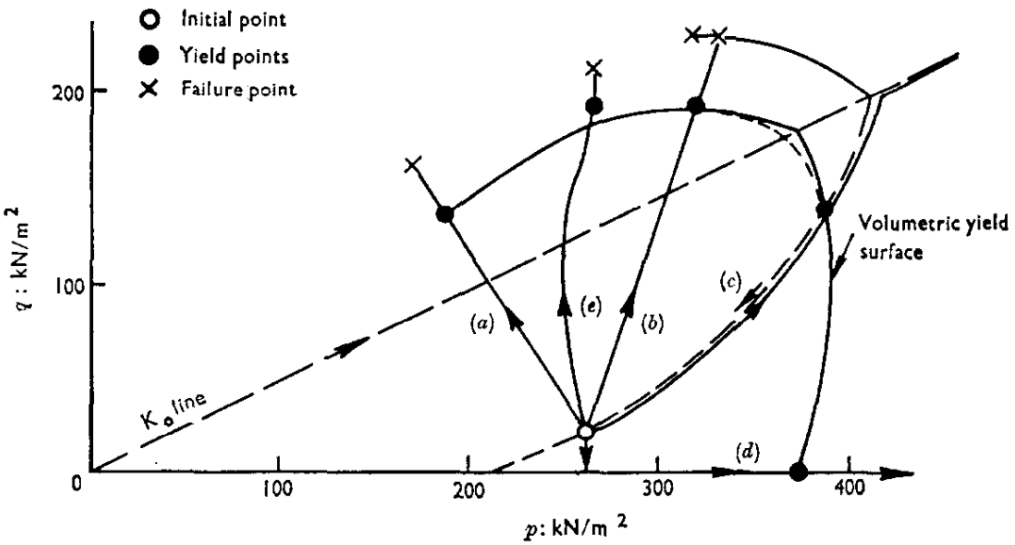

Figure 3.46: Volumetric yield locus for OCR = 1.6 (Parry, 1973)

3.5.2 Cemented Clays

As stated before, yielding can be interpreted as the starting point of irrecoverable or plastic strains. However, this is often difficult to define experimentally. Hence, yielding is usually identified by a discontinuity in the stress-strain behaviour. This section discusses the yielding of cemented or artificially bonded soft soils.

Vaughan (1988) mentioned that natural cemented clays start to fail (first yield) when bonds begin to break, the second yield occurs when it increases the stress applied and the bonds are already broken. Maccarini (1987) worked with artificially bonded soils and identified the first yield at the end of the linear part of the curve of deviator stress versus axial strain. Bressani (1990) used a log-log scale plot to define the yield surface by observing the changes in the stress-strain behaviour.

Silveira et al. (2012) and Correia (2011) have performed drained and undrained triaxial shear tests on a soft soil stabilised with Portland cement mixed with granulated blast furnace slag (proportion

3:1, binder quantity of 175 kg/m^3). The samples were isotropically consolidated for confining pressures of 50, 150 and 250 kPa. It was observed that for low values of the consolidation stresses, the stabilised soil samples exhibit a nearly linear initial path, which is limited by a well-defined structural yield point, at which plastic strains intensify (Silveira et al., 2012, Correia, 2011), in agreement with the previous findings of Malandraki and Toll (2000 and 2001). For the undrained triaxial tests, the authors have used two different yield criteria that are in well agreement between each other: bi-log plot of the undrained tangent stiffness modulus with the axial strain and the plot of the axial strain with the mean effective stress (Figure 3.47a-b). Regarding drained triaxial tests, similar results were obtained with the following two yield criteria: plot of the axial or volumetric strain with the mean effective stress (Figure 3.48a-b).

Silveira et al. (2012) and Correia (2011) describe that the yield is the point at which the cementitious bonds begin to break, followed by a brittle failure characterized by the abrupt breakage of the cementitious bonds and the resulting decrease in shear stress.

The following section will present in more detail the different criteria used to identify the yield loci/zone in the case of artificially cemented soils.

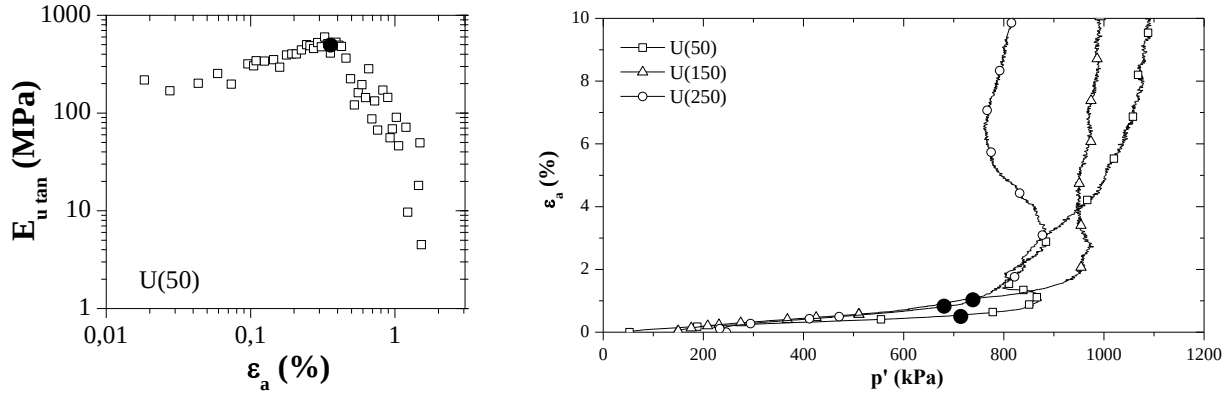

Figure 3.47: Yield loci in the plot: a) tangent undrained deformability modulus with the axial strain; b) axial strain with the mean effective stress (Silveira et al., 2012)

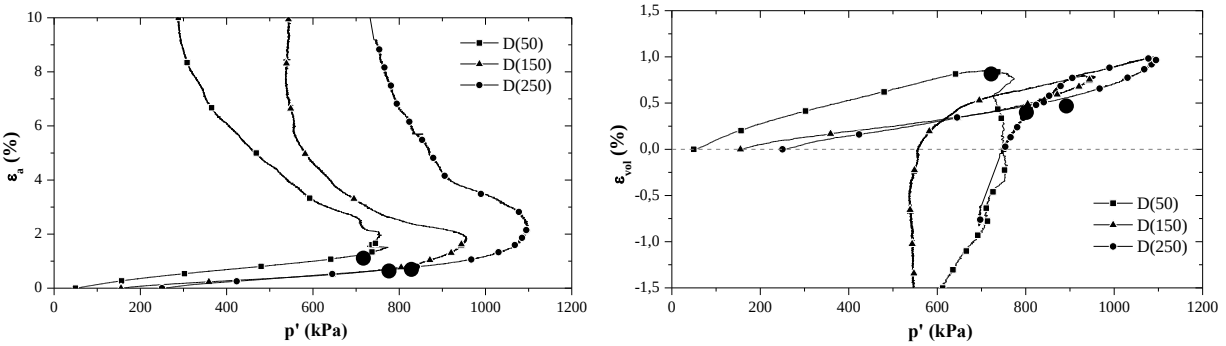

Figure 3.48: Yield loci in the plot: a) axial strain with the mean effective stress; b) volumetric strain with the mean effective stress (Silveira et al., 2012)

3.5.3 Criteria to identify the yield loci

3.5.3.1 Criteria (ε_{vol} vs. p') and (ε_a vs. p')

Different yield criteria are typically used because the yield loci definition is ambiguous. According to Mouratidis and Magnan (1983), the most likely yield loci is a trend variation in the evolution of volumetric strain (ε_{vol}) as a function of mean effective stress (p'). This methodology is similar to the Casagrande method used to calculate the preconsolidation pressure (Jamiolkowski et al. 1985). Venda Oliveira and Lemos (2014) have studied the shape of the yield surface and have concluded that it may also be complemented by analysing the trend variation in the evolution of axial strain (ε_a) with mean effective stress (p').

Venda Oliveira and Lemos (2014) performed drained triaxial tests to identify the yield zone of an inorganic sandy lean clay with medium plasticity to be used in isotropic and anisotropic elastoplastic models.

Figures 3.49 and 3.50 show the results of drained triaxial tests of samples isotropically or anisotropically consolidated for a stress ratio q/p' of 1. The authors have defined the yield zone making use of two distinct criteria, evolution of the axial or volumetric strain with the mean effective stress, where the yield loci is related with the end of the first linear trend of such plots.

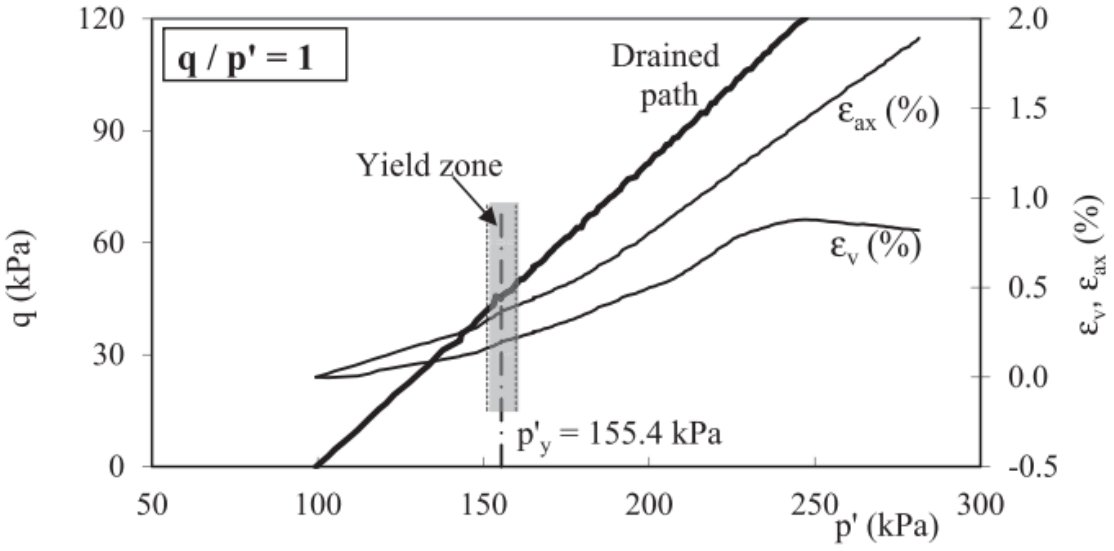

Figure 3.49: Identification of yield zone in an inorganic sandy lean clay based on drained triaxial tests performed for a q/p'=1 in a sample isotropically consolidated (Venda Oliveira and Lemos, 2014)

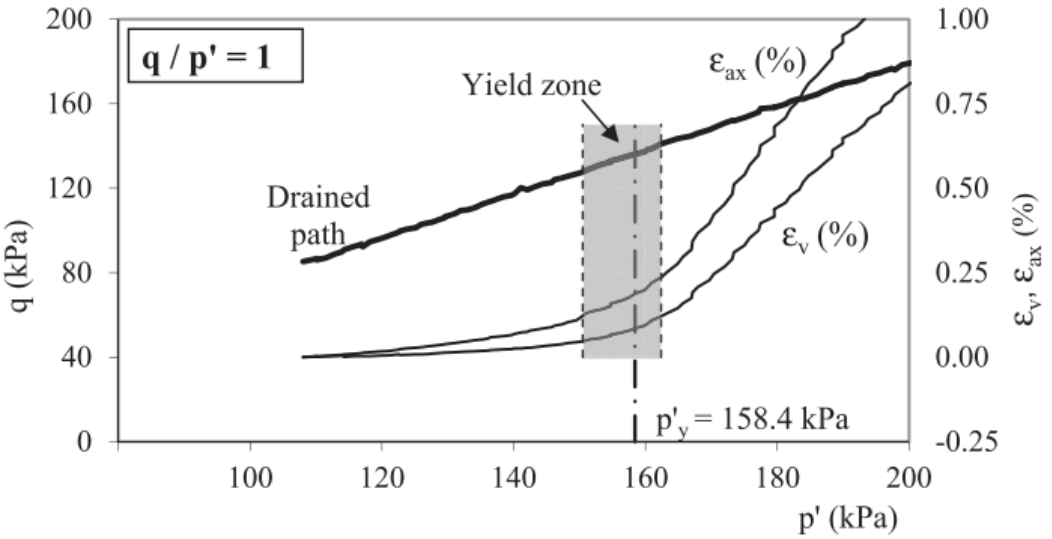

Figure 3.50: Identification of yield zone in an inorganic sandy lean clay based on drained triaxial tests performed for a q/p'=1 in a sample anisotropically consolidated (Venda Oliveira and Lemos, 2014)

Santos et al. (2021) studied the application of different yield criteria on the definition of the yield surface of a chemically stabilised soft soil. The soil used is very similar to the one selected for this work, i.e., it is a clayey silt organic soil that was stabilised with Portland cement (binder quantity of 250 kg/m^3). The authors have performed four drained triaxial tests with different stress paths (q/p' of 3 and 4) combined with one undrained triaxial test and one isotropic compression test, aiming to intersect the yield surface at different points (Figure 3.51 and 3.52). For both representations, and for all tests, it was possible to identify an approximately linear initial path followed by a sudden variation of the trend, in a similar way as observed by Mouratidis and Magnan (1983) and Graham and Lau (1988). The end of this linear path can be understood as the start of structural yield, point at which plastic strains intensify (Malandraki and Toll, 2001).

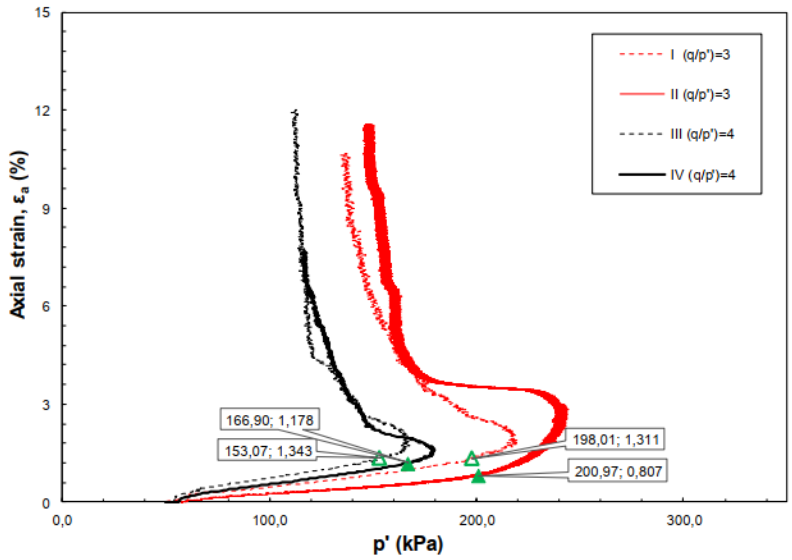

Figure 3.51: Yield Criteria defined in the mean effective stress vs axial strain plot (Santos et al. 2021)

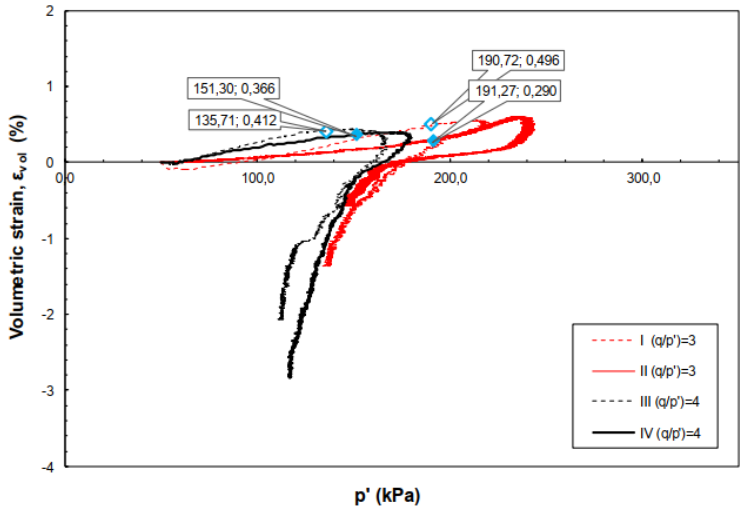

Figure 3.52: Yield Criteria defined in the mean effective stress vs volumetric strain plot (Santos et al. 2021)

3.5.3.2 Criterion (q/p' vs. $\delta\varepsilon_{vol}/\delta\varepsilon_s$)

The research of Coop and Wilson (2003) allows an understanding of the phenomena of dilatancy in materials, where in addition to the frictional part, there is also a contributing element related with volume change (at peak stress state). For artificially cemented soils there is also a cohesive part due to cementitious bonds between particles.

The behaviour of these cemented soils was studied by Coop and Atkinson (1993) who have showed that initially in the (q/p' vs $\delta\varepsilon_{vol}/\delta\varepsilon_s$) plane, there is an almost vertical stretch in the curve, considered elastic, where q/p' increases and $\delta\varepsilon_{vol}/\delta\varepsilon_s$ is almost constant (Figure 3.54). However, as can be seen in the figure, it is also possible that this line is steeper which may be possible from the change of the Poisson's ratio or the occurrence of plastic strain due to the application of confining stress before the shear plastification point of the sample.

More recently (Cruz, 2008) validated the yield criterion mentioned above that requires interpretation of the stress-dilatancy curve (q/p' – $\delta\varepsilon_{vol}/\delta\varepsilon_s$). From Figure 3.53 it is possible to observe that the plastic strain point of the samples can be determined with higher precision mainly in tests with higher cementation and lower confining stresses.

Santos et al. (2021) have also applied this criterion to identify the yield point/zone in a cement stabilised clayey silt organic soil, as described previously. Figure 3.54 shows the results obtained from the drained triaxial tests using this criterion. The results show an approximately linear path until plastic deformations start to occur and the trend of the curve drastically changes. The initial path followed by the samples is practically the same for all tests, which is related with the same

elastic parameters (namely, the same Poisson's ratio). At large strains all samples seem to gradually tend to the critical state ($\delta\varepsilon_{vol}/\delta\varepsilon_s = 0$), as noticed by Cruz (2008).

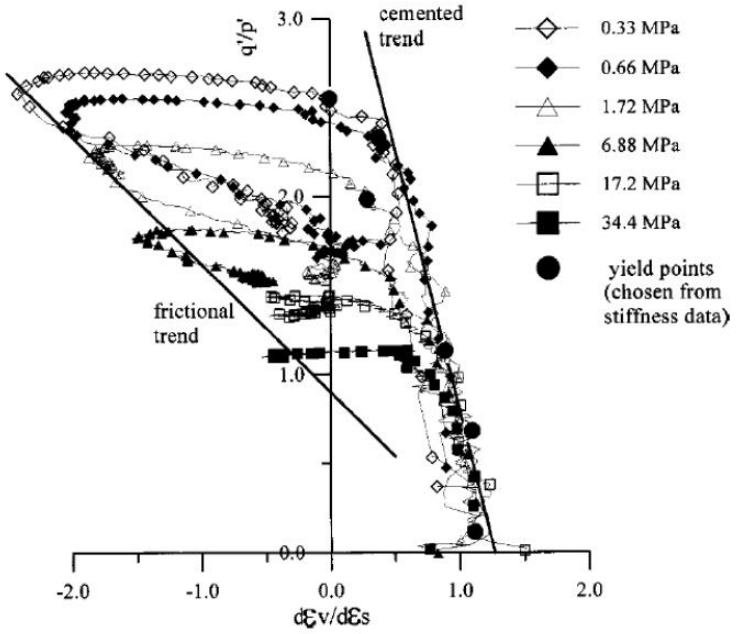

Figure 3.53: Yield Criteria defined by dilatancy (ratio of volumetric and axial strain) vs ratio of deviatoric stress and mean effective stress (Cruz, 2008)

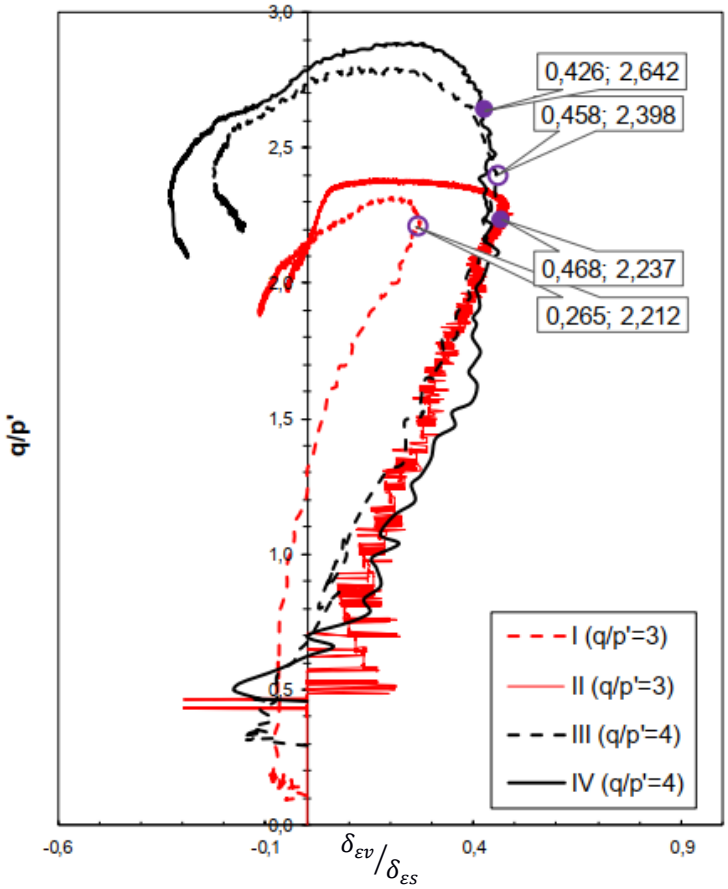

Figure 3.54: Yield criteria defined by dilatancy (ratio of volumetric and axial strain) vs ratio of deviatoric stress and mean effective stress (Santos et al., 2021)

3.5.3.3 Criterion ($E_{u\text{-}tan}$ vs ε_a)

For the undrained triaxial tests Malandraki and Toll (1996 and 2000) have observed that the evolution of the undrained tangent stiffness modulus ($E_{u\text{-}tan}$) with axial strain (ε_a) is characterized by an initial stiffness plateau limited by a well-defined yield point, identified as the point of structural yielding, i.e., the point from which plastic deformations intensify, as presented in Figure 3.55.

As it was shown by Silveira et al. (2012) and Correia (2011), when this yield criterion was applied to a soft soil stabilised with Portland cement mixed with granulated blast furnace slag (proportion 3:1, binder quantity of 175 kg/m^3), the results obtained fit well with other yield criteria, as previously demonstrated in section 3.5.3.1.

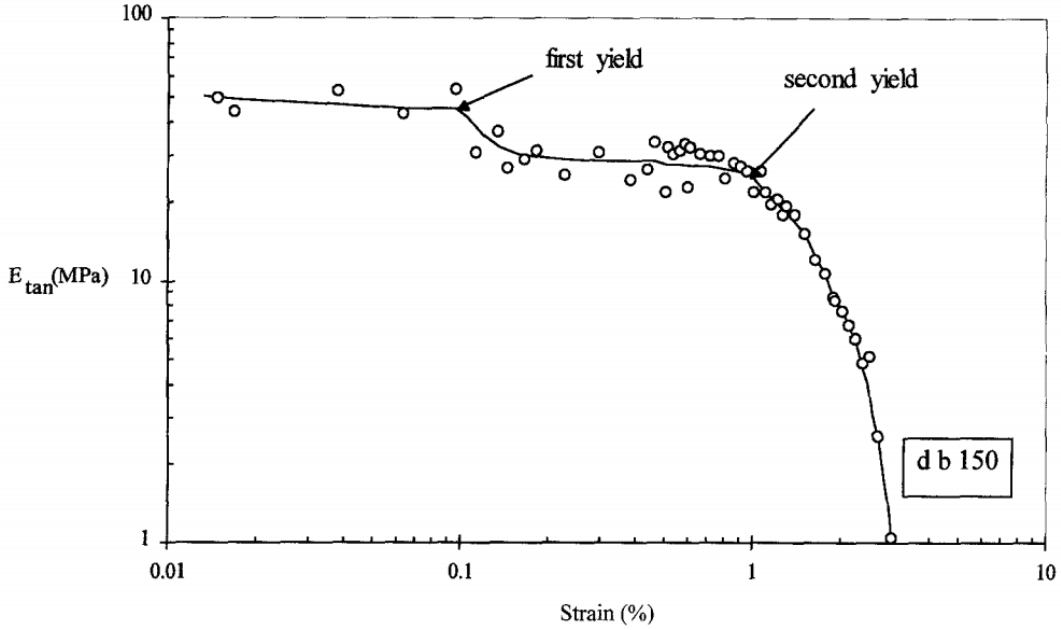

Figure 3.55: First yield and second in $E_{u\text{-}tan}$ - ε_a plot (Malandraki and Toll, 1996)

CHAPTER 4 - MATERIAL CHARACTERISATION AND TESTING PROGRAM

This chapter characterises all materials used in the study, namely the soft soil collected in the Baixo Mondego area in the centre region of Portugal, as well as the binders used for the chemical stabilisation and the fibres selected for reinforcement. Following the laboratory procedure adopted in the preparation of the chemically stabilised samples, reinforced or not with fibres, as well as the testing equipment used to perform all tests are described. In the last section, the testing program is presented in detail.

4.1 Baixo Mondego soft soil characterisation

4.1.1 Introduction

The materials characterisation starts with the base material, the soft soil. For the soft soil of Baixo Mondego, data from the particle size distribution, specific gravity, plasticity limits and organic matter content will be presented and interpreted in the following sub-sections.

4.1.2 Particle size distribution

According to their dimensions, the grain size distribution of soil's particles is evaluated on soil samples resulting from either residue of intact samples or small parts of a large volume sample. The grain size distribution was assessed following the procedures described in specification E196 (1966) of the LNEC.

For this purpose, the specification E 196-1966 describes the conditions under which the particle size study should be performed according to the soil's particles dimensions, namely sieving (treatment of the coarse fraction) and sedimentation (treatment of the fine fraction). The results for the soft soil of Baixo Mondego indicate that the soil is composed of 14% clay, 64% silt, and

22% sand particles. However, to compare the results, the laser granulometer test was performed (Figure 4.1, curves identified as T1 to T4).

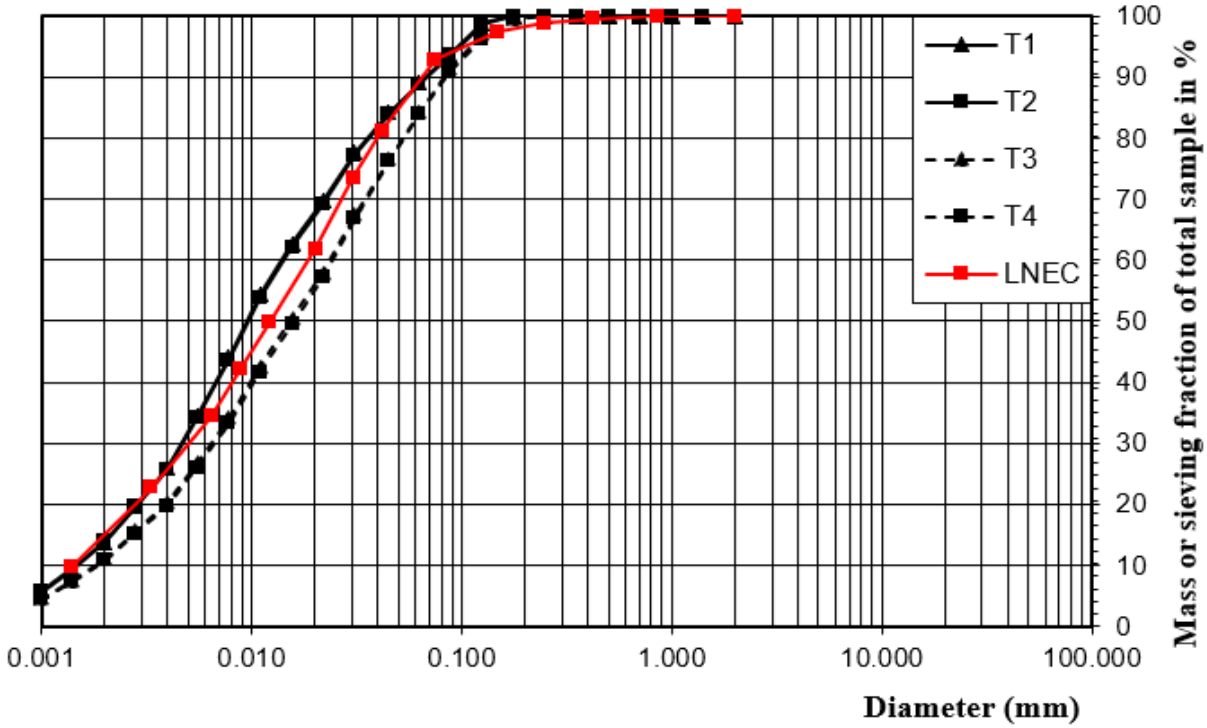

Figure 4.1: Particle size distribution of Baixo Mondego soft soil

Although Laser granulometer is not a widespread technique in the geotechnical environment, the results obtained compared to conventional methods showed satisfactory results, having as advantages its speed and effectiveness (Venda Oliveira et al., 2018). The Laser granulometer method does not have process standardisation, so the analysis occurred according to the guidance of the equipment operation manual and took as reference the procedure described in standard ISO 13320-1 (1999). The equipment used was the Coulter LS-230 laser granulometer from the Sedimentology Laboratory of the Earth Sciences Department of the University of Coimbra, which allows particle size analysis from 0.4 to 2000μm. The results (Figure 4.1 and Table 4.2) indicated that the soil consists of 20.7% sand, 71.3% silt, 8.0% clay, values that agree with the ones obtained from the traditional method. In Figure 4.2 shows the frequency distribution of particles observed in the laser granulometer tests.

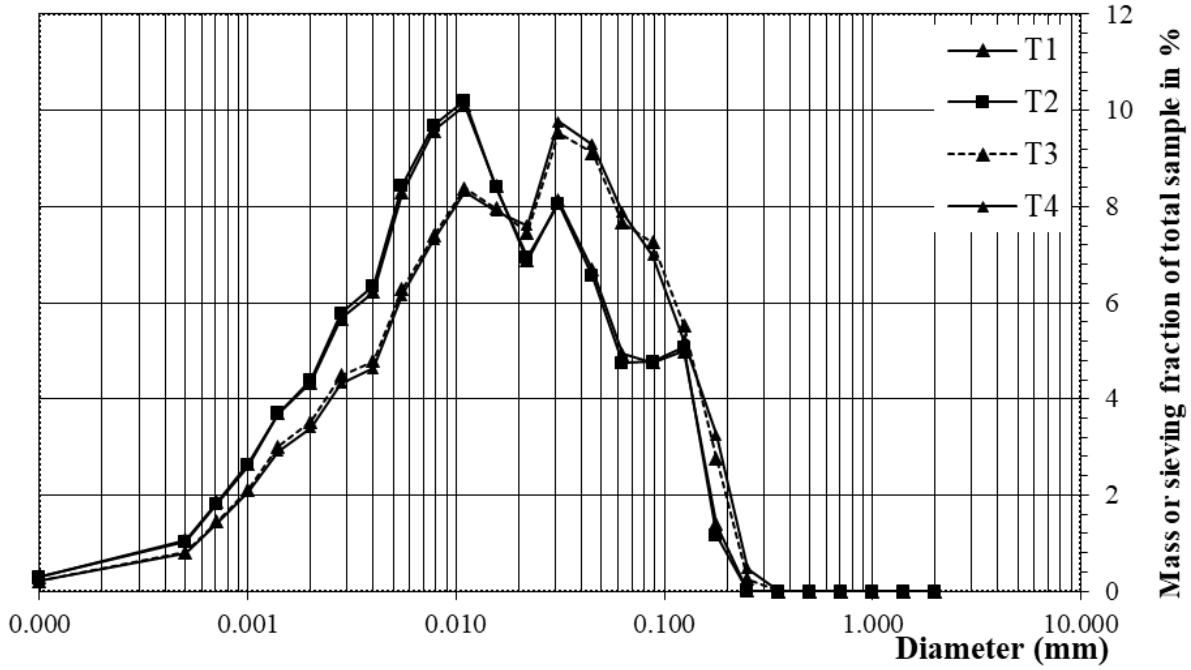

Figure 4.2: Frequency distribution of the laser granulometer tests for Baixo Mondego soft soil

Table 4.1: Particle size results of Baixo Mondego soft soil

	T1	T2	T3	T4	Average	LNEC
% Clay	13.83	13.92	11.13	10.83	12.43	14
% Silt	74.37	74.10	71.78	71.92	73.04	64
% Sand	11.79	11.98	17.09	17.25	14.53	22

In summary, it can be said that, on average, the soft soil of Baixo Mondego has a predominance of the silt fraction (≈ 70%), with an important sand fraction (≈ 20%) and some clay fraction (≈ 10%). These characteristics are consistent with the deposition conditions observed during the geological formation of the deposit, typical of recent alluvial deposit, values in agreement with previous studies as presented in Chapter 2.

4.1.3 Specific gravity

As recommended in standard NP-83 (1965), the determination of the solid-particle density (G_s) considered data obtained in three different pycnometers. The density value is obtained by the ratio between the density weight of solid particles (γ_s) and the density weight of distilled water (γ_w). From this test, values were 2.56, 2.60, and 2.56, giving an average value of 2.57.

4.1.4 Organic Matter Content

This method estimates soil's organic matter based on gravimetric weight change associated with high-temperature oxidation of organic matter. After initial oven drying at 50ºC, the samples are

ignited in a muffle furnace for 24 hours at 400ºC. The percent weight loss during the ignition step is reported as Organic Matter (OM) – Loss on Ignition (OM-LOI), in % of weight loss, as explained in the following equation. In this work, eight measurements were carried out to obtain the mean value of OM, which is around 8.13% using Equation 4.1, and this value agrees with the previous studies as presented in Chapter 2.

$$O.M = \frac{W_d^{50℃} - W_d^{400℃}}{W_d^{50℃} - W_{caps}}$$ Equation 4.1

4.1.5 Atterberg Limits

The following table shows a comparison of the previously analysed values for the Baixo Mondego soil, which values are approximated.

The plasticity limits or *Atterberg limits* correspond to the water content that establishes the boundary between different types of soil behaviour. The liquid limit (w_L), corresponds to the water content above which the soil behaves as a liquid; the plastic limit (w_p), establishes the limit between the zones of mouldable and friable behaviour; and the shrinkage limit (w_s), coincident with the water content below which the soil dries out at a constant volume.

The tests for the present geotechnical characterisation focused only on the determination w_L and w_p following the NP 143 (1969) using the Casagrande apparatus for w_L and rolling a soil's sample between the palms of the hands and a flat glass plate for w_p. As a result, the following values were obtained for the soft soil of Baixo Mondego: w_L= 72.4% (Figure 4.3), w_p= 24.5%, and PI = 47.9% which are close to the limits determined by Correia (2011) and other authors.

Figure 4.3: Liquid limit chart of Baixo Mondego soft soil

4.1.6 Soil Classification

Table 4.2 summarizes the main geotechnical characteristics of the soft soil of Baixo Mondego. Based on these characteristics it is possible to classify the soil. In terms of grain size composition, the soil can be classified by Ferret's triangle as a silt loam (Figure 4.4). In terms of Unified Soil Classification System (USCS, ASTM D2487), the soft soil of Baixo Mondego is classified as a CL – OH.

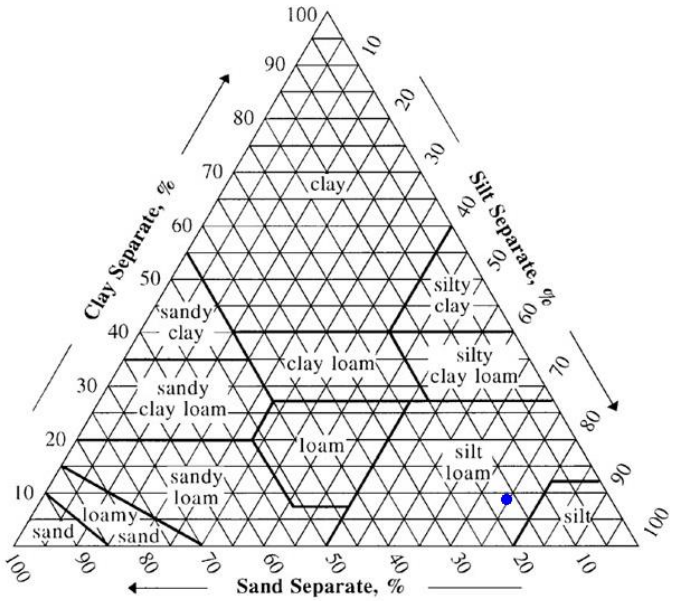

Figure 4.4: Ferret's Triangle for Baixo Mondego soft soil

Table 4.2: Summary of Baixo Mondego soft soil's characteristics

Properties	Present studio
Sand	12.43%
Silt	73.04%
Clay	12.43%
Organic Matter	8.13%
Plastic Limit	47.9%
Liquid Limit	72.4%
w_{nat}	80.6%
Plasticity Index	24.5%
Activity	1.15
Soil classification: UCSC	CL - OH

4.2 Binders

In the following sub-sections will be presented the main characteristics of all binders selected for the experimental study: Portland cement, blast furnace slag, fly ash and eggshell. In the choice of binders, it was decided to use the most commonly used binder and the most versatile

as regards the soil's type, Portland cement. In an attempt to obtain a more environmentally friendly binder, other types of binders were studied as partial substitutions for Portland cement, all of them industrial by-products. Thus, it was considered blast furnace slag (a nonmetallic coproduct produced in the process. It consists primarily of silicates, aluminosilicates, and calcium-alumina-silicates). Fly ash (by-product of burning coal) which is a binder with pozzolanic properties, i.e., the reaction with water is only processed while certain conditions are maintained. Finally, eggshell (a food industry by-product) was considered given its high CaO content and chemical composition similar to quicklime, which can act as an excellent partial substitute for Portland cement.

4.2.1 Portland cement

The binders to be used in the chemical stabilisation of a soil are an important factor since they are the ones that promote the physico-chemical interactions with soil particles and water resulting a composite material with a mechanical behaviour better than the natural soil. This designation was given in 1824 by an English builder named Joseph Aspdin because the buildings in England at that time were in greyish coloured stone originating from Portland.

The main binder selected for the present study is Portland cement Type I 42.5 R (EN-197-1, 1966), characterised by the chemical composition presented in Table 4.3, with a specific gravity of 3.18 and a specific surface of 326.3 m^2/kg according to the manufacture's data. The binder exhibits hydraulic properties due to the high $CaO:SiO_2$ ratio (Taylor, 1997), meaning that the binder reacts spontaneously in the presence of water.

Table 4.3: Chemical characterization of Portland Cement Type I 42.5 R (manufacturer's data)

Chemical Compounds	%
CaO	62.88
SiO_2	19.00
Al_2O_3	5.15
Fe_2O_3	3.19
SO_2	3.14
MgO	2.16
K_2O	1.29
Na_2O	0.10

4.2.2 Blast Furnace Slag

Blast Furnace Slag is a by-product of the manufacturing of iron in a blast furnace where iron ore, limestone and coke are heated up to 1500ºC. When these materials melt in the blast furnace two products are produced – molten iron, and molten slag. The molten slag is lighter and floats

on the top of the molten iron. The molten slag is mostly composed by silicates and alumina from the original iron ore, combined with some oxides from the limestone.

The process of granulating the slag involves cooling the molten slag through high-pressure water jets. This rapidly quenches the slag and forms granular particles generally no larger that 5 μm in diameter. The rapid cooling prevents the formation of larger crystals, and the resulting granular material comprises some 95% non-crystalline calcium-aluminosilicates.

The granulated slag is further processed by drying and then ground to a very fine powder, which is ground granulated blast furnace slag. Grinding of the granulated slag is carried out in a rotating ball mill. Different forms of slag product are produced depending on the method used to cool the molten slag. The chemical composition of blast furnace slag used in this study is presented in Table 4.4.

Table 4.4: Characterisation of blast furnace slag (manufacturer's data).

Chemical Compounds	**(%)**
SiO_2	43.06
Al_2O_3	11.63
Fe_2O_3	1.01
CaO	33.62
MgO	5.74
MnO	1.70
K_2O	1.02
SO_3	0.99

4.2.3 Eggshell

Eggshells are major domestic waste products from the food industry. By literature review, it is seen that eggshells are rich in CaO and share the same chemical composition as lime (Singh and Arora, 2019). Hence, they can be used as an economical replacement for lime. The eggshells used in the present study were collected from restaurants, local food joints and poultry farms. Eggshells were thoroughly mixed, washed with clean water and dried at air temperature (in sunshade) for 48 h. Eggshells were then grinded in a laboratory ball mill to obtain uniform and fine eggshell powder and then sieved through 425μm sieve for further laboratory investigations. The specific gravity of eggshell powder was found to be 1.34, and its chemical composition was established based in the literature review as presented in Table 4.5.

Table 4.5: Characterisation of eggshell (Singh & Arora, 2019).

Chemical Compounds	**(%)**
CaO	95 - 99
Al_2O_3, SiO_2, Cl, Cr_2O_3, MnO and Cu_2O	1 - 5

4.2.4 Fly Ash

The fly ash was obtained from a coal-fired power plant in Mindanao. As per ASTM C168, it is classified as Class F, that is the fly ash is safe for use in the environment regarding leaching. Fly ash is an industrial by-product obtained by collecting dust from the combustion gases of from furnaces fed with pulverized or ground coal. In fact, when burning coal, the combustible part burns instantly, while the non-combustible part (called coal impurities), consisting essentially of clay quartz and limestone, partially melts. Some of these particle's agglomerate and solidify into small spheres of amorphous matter. The smaller particles are carried away by the flow of combustion gases and can be captured before they escape into the atmosphere. Ash can be captured by electrostatic precipitators electrostatic precipitators, which capture the smaller particles, or by mechanical collectors. In Table 4.6 presents the chemical composition of a fly ash produced in Portugal (Sines Production Sines production plant) which was used in this Study. Besides the components shown there, there are others that occur in small quantities, such as TiO2, PO2, among others (Correia, 2011). It should be noted that some ashes may contain radioactive substances which collect the larger particles (Temuujin, 2019).

Table 4.6: Characterisation of Fly ash (manufacturer's data)

Chemical Compounds	Values (%)
CaO	4
SiO_2	55
Al_2O_3	22
Fe_2O_3	7
MgO	2
SO_3	0.48
K_2O	2
Na_2O	0.70

4.3 Fibres

One of the objectives of this study is to assess the effect of monotonic and cyclic loading on the behaviour of the soft soil of Baixo Mondego chemically stabilised reinforced or not with fibres. Despite the fact that there are several types of fibres (natural, metallic and synthetic as described in chapter 2), it was decided to take advantage of the large experience acquired at the Geotechnics Laboratory of the University of Coimbra with the polypropylene fibres. Thus, for the present study synthetic fibres were chosen, composed of extremely thin polypropylene multifilament. These fibres are produced by BEKAERT, model DUOMIX M12, which have a length of 12mm, a diameter of 32μmwith a density of 110 million fibres/kg. The manufacturer's catalogue indicates the use of these fibres for inclusion in reinforced concrete with the ultimate aim of minimising cracking problems, also referring to the ease with which they are mixed by pumping or spraying. The geometric and mechanical properties of the fibres are summarised in

Table 4.7. Polypropylene fibres are considered non-biodegradable (Carvalho et al., 2014; Xie et al., 2018).

Table 4.7: Characteristics of polypropylene fibres

Length, L (mm) *	12
Diameter, D (μm) *	32
Aspect ratio (L/D) *	375
Tensile strength (MPa) *	250
Elasticity modulus (GPa) *	3.5-3.9
Surface texture roughness[&]	Lower
Biodegradability *	Not biodegradable
Density (g/cm^3) *	0.905

[&] Agboola et al. (2021). * manufacturer's data.

4.4 Sample Preparation

In this section the experimental soft soil chemically stabilised and reinforced sample preparation procedure for all tests will be presented in detail. At first the experimental samples preparation procedure for Unconfined Compressive Strength (UCS), Split Tensile Strength (STS), Direct Tensile Strength (DTS) and Flexural Strength (FS) tests are presented. After, the laboratory procedure adopted for the oedometer and triaxial samples are also described.

4.4.1 UCS, STS, DTS test Sample Preparation

Before the mixture of the soil with the binder and the fibres, the soil was homogenised appropriately to reduce its natural variability and guarantee the tests' required reproducibility. The soil-water-binder mixtures, both unreinforced and fibre-reinforced, were prepared based on the procedure stated in EuroSoilStab (2001) , Correia (2011) and Venda Oliveira (2018) , which is described in the following steps:

i) In order to adjust the natural water content of the soft soil to the target water content in the study (113%), distilled water was added and mixed with the specified binder content producing a slurry;

ii) The remoulded soft soil sample and the slurry were thoroughly mixed using a mechanical mixer at a speed of 142 rpm for 4 min, in order to obtain a homogeneous soil-water-binder paste. In the case of the fibre-reinforced samples, the required quantity of polypropylene fibres was progressively added to the slurry during the first minute of the mixture;

iii) The homogeneous paste was introduced into a cylindrical PVC mould in three layers;

iv) Each layer was lightly pushed down by a circular wooden disc and tapped 20 times against a rigid table. The top surface of each layer was lightly scarified before the introduction of a new layer. At the bottom there was a non-woven geotextile filter;

v) Samples were cured inside a room with a temperature (20±2ºC) and humidity (95±5%) control during the specified curing time (of the reference value was 28 days);

vi) At the end of the specified curing time the samples were removed from the mould and then both surfaces were trimmed in order to obtain specimens with a height/diameter ratio of 2 for UCS, DTS, and STS tests.

For the different tests, cylindrical PVC moulds with different dimensions were used, more precisely: UCS - diameter 37 mm and height 85 mm; STS and DTS - diameter 70 mm and height 140 mm. The laboratory procedure is the same for these three tests, except the quantity of materials which considers the dimensions of the moulds.

4.4.2 FS Test Samples preparation

The preparation of these samples followed the two first steps described for the preparation of UCS, STS and DTS samples, with the necessary adaptations due to the new type of mould (metallic parallelepiped mould with inner dimensions of 100mm × 100mm × 400 mm). The metallic parallelepiped mould was brushed with release agent oil to allow demoulding without compromising the quality of the sample, and the mould edges were filled with solid vaseline to guarantee their water tightness. The homogeneous paste was introduced into the parallelepiped mould in three layers, each one statically compacted with a rectangular compaction plate (the number of blows was previously adjusted in order to have the same unit weight). Like for UCS, STS and DTS, samples were cured inside a room with a temperature (20±2ºC) and humidity (95±5%) control during the curing time but now, after three curing days samples were demoulded but remained in the same curing room until the end of the curing time.

4.4.3 Oedometer samples preparation

The characterisation of the compressibility and consolidation behaviour of the soft soil chemically stabilised and reinforced with fibres was carried out by oedometer tests. The oedometer tests were performed according to the British Standard BS 1377-5 (1990). Due to the fact that the soil once stabilised may exhibit high yield stress, it was decided to use the 50 mm diameter oedometer ring and the high capacity oedometer equipment (allowing a maximum vertical stress of 24.8 MPa) existing at the Geotechnics Laboratory of the University of

Coimbra. This device (Figure 4.5), whose maximum load capacity is 450 kg, with a lever ratio of 11.04:1, using a rigid metallic ring with a diameter of 70 mm and a height of 19 mm, allowing a maximum stress to the sample of 12.6 MPa.

The oedometer samples were prepared in the laboratory following the two first steps described for the preparation of UCS, STS and DTS samples, with the necessary adaptations. Due to the reduced height of the oedometer ring (19 mm) it was decided to use an auxiliary part (Rodrigues, 2003; Correia, 2011) which accommodates the oedometer ring and a metal tube of the same diameter (70 mm), Figure 4.6a. The inner surface of the oedometric ring is greased with vaseline to prevent vertical friction between materials. After the mechanical mixing the homogeneous paste was introduced into this mould in three layers, sufficient to produce an oedometer sample. Each layer was statically compacted with a circular compaction plate (the number of blows was previously adjusted in order to have the same unit weight). The top surface of each layer was lightly scarified before the introduction of a new layer. In the 70mm diameter samples, the mould is inverted, the auxiliary part is removed and with the help of a wire saw and a spatula, the edges of the samples are carefully rectified. In the case of samples with a diameter of 50mm, the auxiliary part was not used, and after the mould is inverted, the compacted sample is slowly extracted while clamping carefully the oedometer ring in the centre (Figure 4.6b). At the end, with the help of a wire saw and a spatula, the edges of the samples are carefully rectified (Figure 4.6c).

After the oedometer sample was prepared, it was assembled in the oedometer cell with paper filter and porous stone on both ends. The oedometer cell is filled with distilled water and the sample was cured inside a room with a temperature (20±2ºC) and humidity (95±5%) control during the curing time specified.

a)

b)

Figure 4.5: Oedometer operative equipment

Figure 4.6: Oedometer preparations procedure (Correia, 2011)

4.4.4 Triaxial samples preparation

The characterisation of the stress-strain-strength behaviour and the yield surface study of the soft soil chemically stabilised and reinforced with fibres was carried out by triaxial tests. The triaxial tests were performed according to the British Standard BS 1377-8 (1990). The preparation of these samples generally follows the steps described for the preparation of UCS samples, with the necessary adaptations due to the new type of test. Due to the fact of having to ensure the saturation of the triaxial samples, the curing of the samples was carried out under submerged conditions inside a room with temperature (20±2ºC) control. After the samples were demoulded, they were carefully trimmed in order to have a final height of 76mm (equivalent to a height/diameter ratio of 2), Figure 4.7a the sample was weighted and from the cutting parts it was measured the water content.

After the sample was rectified (Figure 4.7b), it is placed in the triaxial apparatus (stress-path cell) between two paper filters and porous stones (previously saturated), ensuring drainage both at the base and at the top. The sample is then covered by a membrane - taking care to prevent any air bubbles - which, using two rubber rings (o-rings), is attached to the base. Other two rubber o-rings are placed around the top piece to ensure that the membrane is securely fixed. A load cell is adjusted to the top of the sample, and the triaxial cell is closed and filled with water. The triaxial test may start.


a)

b)

Figure 4.7: Sample rectification

4.5 Laboratory testing equipment description

This section will briefly explain the equipment used in the research to carry out the UCS, DTS, STS, FS, oedometer, triaxial and Pundit tests, explaining the deduction of their formulation to interpret the results.

4.5.1 Unconfined Compressive Strength (UCS) tests

The UCS tests were performed under the standard NP EN 12390-3 (2011). After completion of the curing phase (28 days), the samples were demoulded, weighed, and placed in the testing machine. At first it was used the monotonic WYKEHAM FARRANCE LTD Tristar 5000kg Stepless Compression Testing Machine (Figure 4.8) and in a second phase it was used the ELDYN GDS TRIAXIAL EQUIPMENT (Figure 4.9) which allows monotonic and cyclic loading unconfined conditions. UCS tests were performed by imposing a constant strain rate of 1%/min to the sample height.

Figure 4.8: UCS Test in Wykeham Farrance equipment


a)


b)

Figure 4.9: UCS a) a sample without fibres, b) a sample reinforced with fibres in GDS ELDYN equipment

According to Head (1985) and Young and Mullins (1991), the mechanical strength increases with the strain rate, and a value in the range 0.5 and 2%/min should be adopted (Head, 1985; BS 1377-7, 1990; ASTM D2166, 2000), referred to the height of the sample, varying according to the type of soil (when the material is more rigid, it should be the adopted strain rate). Since this is a chemically stabilised soft soil, a conservative value of 1%/min was adopted a lower strain rate in the UCS tests.

During the UCS test the vertical load and axial displacement were automatically recorded (measured using a load cell and a displacement transducer, respectively). After the sample was removed from the testing machine, two piece of samples samples were taken to control its final water content.

The unconfined compressive strength (q_u) is obtained by using Equation 4.2, where F denotes the applied load and A the cross-section area of the sample:

$$q_u = \frac{F}{A} \qquad \text{Equation 4.2}$$

The maximum load recorded during the test corresponds to the maximum compressive strength ($q_{u\ max}$) of the composite material. The respective stress-strain plot was built from the quantities measured during the test (force and displacement vertical) and based on the geometry of the sample (height and diameter). The axial strain (ε) was calculated from the displacement variation ($\Delta\delta_v$), assuming the simplifying assumption of uniform distribution of the strain on the sample (Equation 4.3), where h denotes the initial sample's height.

$$\varepsilon = \frac{\Delta\delta_v}{h} \cdot 100 \qquad \text{Equation 4.3}$$

The compressive stress was calculated using Equation 4.1, where the area (A) should be corrected (A_{corr}, Equation 4.4), to consider the radial strain experienced by the sample (Head, 1985).

$$A_{corr} = \frac{\pi \cdot D^2}{4 \cdot \left(1 - \frac{\varepsilon}{100}\right)} \qquad \text{Equation 4.4}$$

Figure 4.10 shows the general aspect of a UCS test.

Each UCS test is characterised by:

i) the stress-strain curve;

ii) the maximum compressive strength (q_{u-max});

iii) the axial strain at failure (ε_{a-rupt});

iv) the undrained secant deformability modulus defined for 50% of q_{u-max} (E_{u50});

v) the final water content measured immediately after the UCS test (w_f).

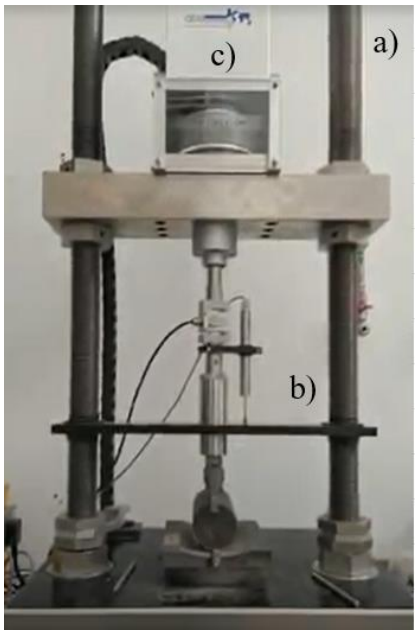

Figure 4.10: GDS ELDYN equipment a) frame b) external displacement; c) load cell

4.5.2 Direct Tensile Strength (DTS) test

DTS test samples were tested according to ASTM CRD-C 164-92 (1992). One day before the end of the curing time (day 27), the sample was removed from the thermohygrometric chamber and weighed, and rigid tops were glued on (to fix the "claws" of the press), using epoxy resin for this purpose. In the following day, the sample was placed in the test machine (SERVOSIS MUF 404/100 universal press visible in Figure 4.12 and in the ISISE equipment Figure 4.11).

Figure 4.11: DTS Test using the universal device in mechanical lab

The DTS test was performed by imposing a strain rate of 0.06%/min, relative to the height of the sample. This value was chosen because it corresponds to the lowest value possible to apply in the testing machine used, being this a conservative procedure. Once the test was finished, samples were taken to calculate the final water content. During the test, the vertical load and the axial deformation were automatically recorded (measured using a load cell and a displacement transducer, respectively). A Figure 4.12 shows some details concerning this type of tests.

Figure 4.12: DTS Test using the Servosis device

The tensile strength (f_{cd}) is obtained by Equation 4.5, where F designates the load applied and A the cross-section area of the sample at the moment of load application.

$$f_{cd} = \frac{F}{A} \qquad \text{Equation 4.5}$$

As in the UCS tests, the cross-sectional area of the sample should be corrected using Equation 4.4, which now experiences phenomena of reduction of its cross-section area. It should be noted that now the strains are in the opposite direction to those of the UCS tests, although in both cases they are represented as positive.

The maximum force recorded during the test corresponds to the maximum tensile strength of the sample, f_{cd-max}. Each DTS tests is characterised by:

i) the stress-strain plot;

ii) the maximum tensile strength (f_{cd-max});

iii) the axial strain at failure/rupture ($\varepsilon_{a-rupt,}\varepsilon_r$);

iv) the undrained secant deformability modulus defined for 50% of f_{cd-max} (E_{u50});

v) The final water content measured immediately after performing the DTS test (w_f).

4.5.3 Split Tensile Strength (STS) test

STS tests were performed following the guidelines of the standards NP EN 12390-6 (2011) and NP EN 13286-42 (2011), imposing a constant strain rate of 0.07 mm/min (0.1%/min, relative to the sample diameter). After 28 days of curing, the samples were placed in the testing machine (WYKEHAM FARRANCE LTD Tristar 5000kg Stepless or ELDYN GDS TRIAXIAL EQUIPMENT) and tested up to levels of deformation which verified the separation of the sample n two blocks. During the test, the applied load (F), and the vertical displacement (δ_v, measured according to the direction of load). At the end of the tests, samples were taken to determine the final water content.

This type of test, also known as the Brazilian test, was developed by Professor Lobo Carneiro for tests on concrete (Carneiro, 1943), being later adopted to test other type of cementitious materials, likewise this case. Simple to perform because it involves the same equipment and sample similar to those used in UCS tests. The basic principle of this test involves the evaluation of the tensile stresses produced perpendicularly to the “loading” diameter by two opposing loads that compress a cylindrical sample (Figures 4.13, 4.14).

Figure 4.13: Split Tensile Test (display)

These loads are applied along two rigid contact lines. The maximum tensile strength (f_{ct}) can be derived by Equation 4.6, where F is the maximum applied load, L the length of the sample contact line and d the vertical dimension of the sample in the cross-section, which in the case of the cylindrical sample coincides with the diameter (Figures 4.15).

$$f_{ct} = \frac{2 \cdot F}{\pi \cdot L \cdot d}$$ Equation 4.6

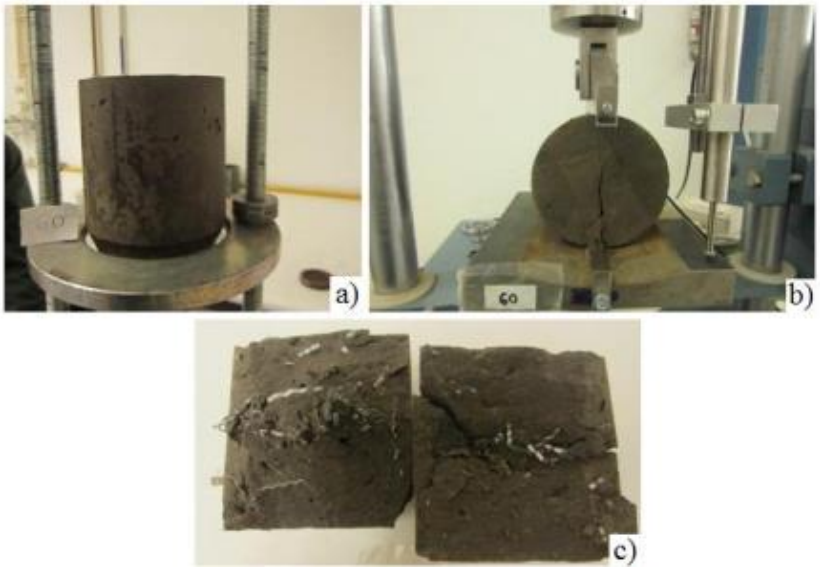

Figure 4.14: Test example (adapted from Teles 2013)

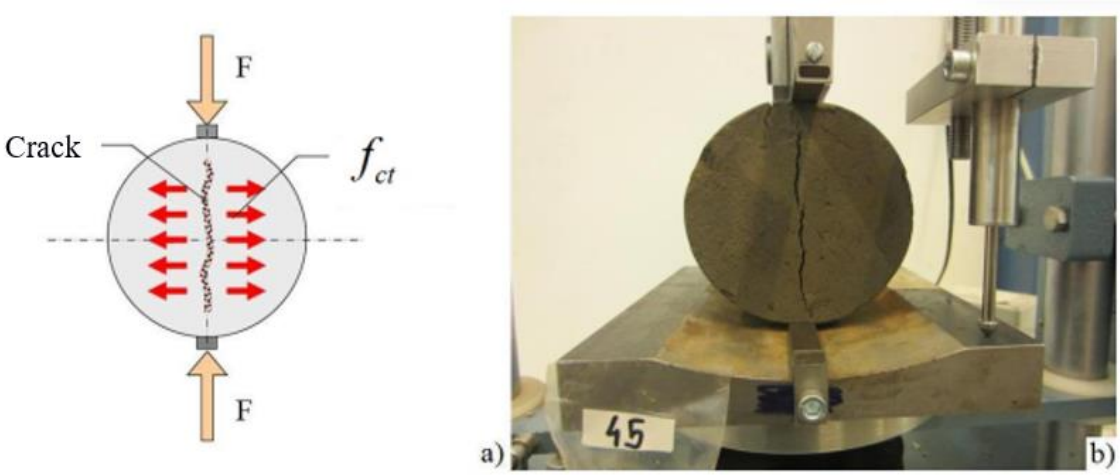

Figure 4.15: Split tensile test (adapted from Teles 2013)

The deduction of Equation 4.6 can be seen in Frocht (1948) and Teles (2013). Force-vertical displacement plots were built for STS tests, contrary to the stress-strain plots shown in the analysis of the UCS and DTS tests. Note that, even if the stresses could be constantly calculated by application of Equation 4.6, there is no interest in relating them to strains because the main tensile strains occurs in a perpendicular plane to the load application plane and, in the STS tests performed, those deformations were not measured .

For this reason, f_{ct} values refer always to the maximum load. Therefore, the quantification of the sample stiffness by simple analysis of the slope of the curves seems inappropriate (Teles, 2013).

Each STS test is characterised by:

i) The force-vertical displacement ($F - d$) curve;

ii) The maximum tensile strength by diametrical compression (f_{ct}) calculated with Equation 4.6;

iii) The vertical displacement at rupture/failure (δv);

iv) The final water content measured immediately after the STS test (w_f).

4.5.4 Flexural Strength (FS) Test

The FS tests, regulated by the standard NP EN 12390-5 (2009), were performed after the curing time was completed on parallelepiped samples in the testing machine SERVOSIS MUF 404/100. The samples were carefully positioned in the machine under the standard as mentioned earlier. Despite the care taken during the preparation and assembly of test samples in the respective test equipment, it is not at all possible to guarantee the perfect verticality of the

sample, either because the tops (or the sides of the parallelepiped samples) may not be perfectly flat, parallel to each other and perpendicular to the axis of the test piece, or because there may be a slight initial eccentricity concerning the point of load application.

The selected deformation speed was 0.01%/min**,** relative to the transversal lateral dimension of the sample (100 mm). During the FS test, the vertical load and the deflection at mid-span were automatically recorded (measured according to the direction of force application). At the end of the test, the sample was removed from the testing machine, and two samples were taken to control its final water content. Figure 4.16 shows aspects related to the FS test.

The simple or one point bending test consists of submitting a prismatic sample to a bending moment using rollers placed above and below it (Figure 4.17). With the maximum applied load, *F*, the flexural strength, f_{cf} is calculated by Equation 4.7, which details of its deduction can be seen in Teles (2013).

$$f_{cf} = \frac{3 \cdot F \cdot L}{2 \cdot d_1 \cdot d_2^2} \qquad \text{Equation 4.7}$$

where L represents the distance between supports ($3 \cdot d$ = 300mm) and d_1 and d_2 are the lateral dimensions of the sample (d_1=d_2 = d = 100mm).

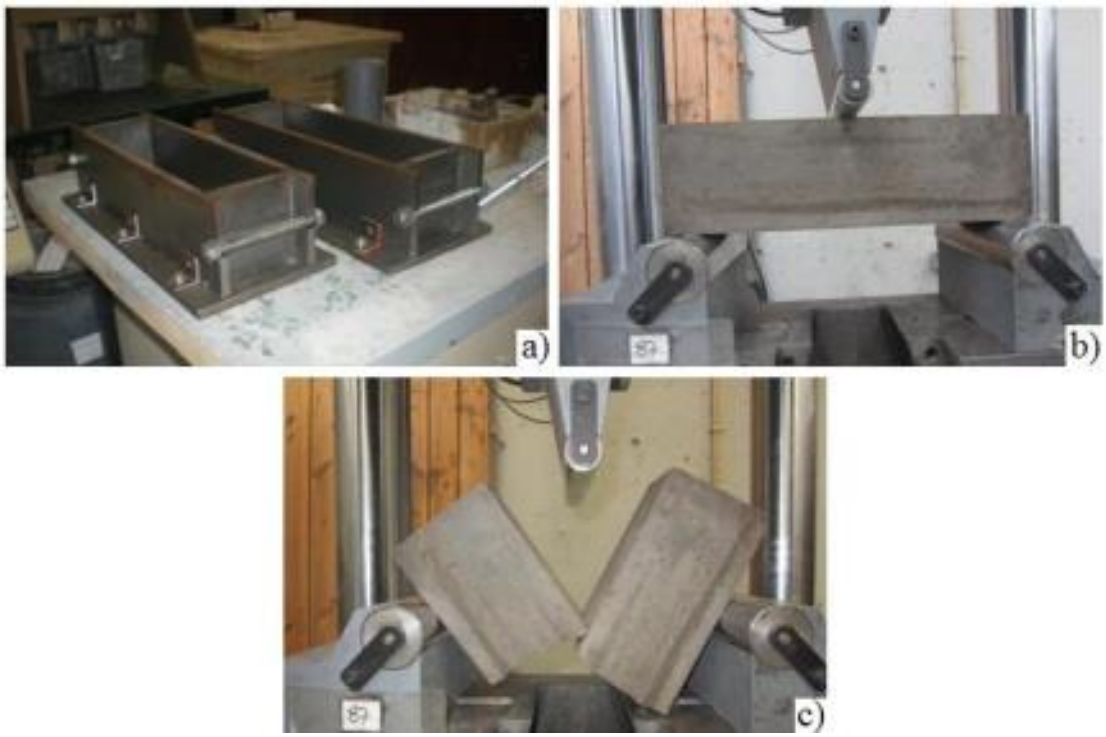

Figure 4.16: Flexural Test (adapted from Teles, 2013)

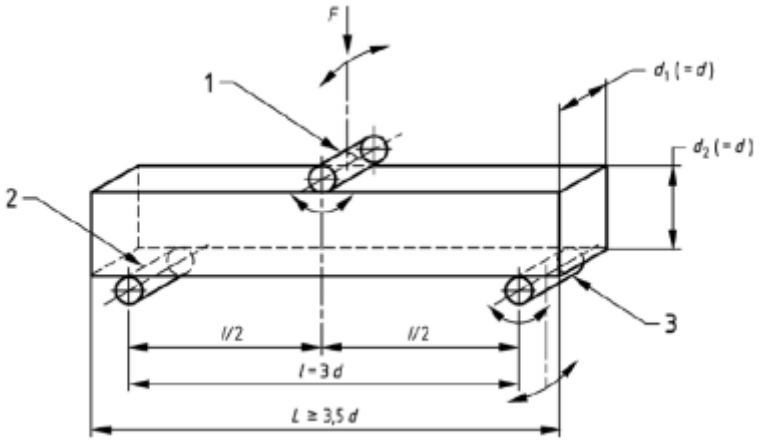

Figure 4.17: Diagram of definition the geometry and reactions of Flexural Test (FS)

Although the simple bending test is not the most appropriate for calculating the deformability modulus since the deformations that should be measured do not occur in the loading vertical plane, the value can be estimated as follows. Considering the prismatic sample is homogeneous and the material exhibits a linear elastic behaviour, by applying the concepts of strength of materials, it is possible to quantify the maximum deflection occurring at mid-span (Figure 4.18 and Equation 4.8).

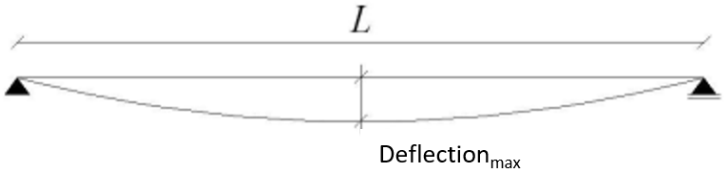

Figure 4.18: Free body diagram of FS illustration

$$deflection\ max = \frac{FL^3}{48EI} \qquad \text{Equation 4.8}$$

Considering the values that the dimensions and the moment of inertia, I, assume for the samples under study (d = 100mm = 0.1m; L = 3×d = 3×100 = 300mm = 0.3m; I = 8,333×10-6 m^4), the modulus of deformability, E can be obtained by development of Equation 4.9, as presented below:

$$deflection\ max = \frac{F \times 0.3^3}{48 \times E \times 8.333 \times 10^{-6}} \Leftrightarrow E$$
$$= 67.5 \times \frac{F}{deflection\ max} \qquad \text{Equation 4.9}$$

Once the maximum force and the deflection at mid-span are known it is therefore possible to estimate the deformability modulus. It should be noted that the use of Equation 4.9 to calculate

the deformability modulus would only be interest if the samples could be considered homogeneous.

Each FS test is characterised by:

i) the force-deflection (F - d) curve;

ii) the strength to bending (f_{cf});

iii) the deflection at rupture/failure;

iv) the final water content measured immediately after the flexural test (w_f).

4.5.5 Oedometer Test

The oedometer apparatus is one of the most widely used in geotechnics to characterize the consolidation and compressibility of a soil and consists simply of the reproduction in the laboratory of the one-dimensional compression phenomenon, through the application of a vertical load to a sample confined laterally, since the stresses and the water flow are established only in the vertical direction (Terzaghi, 1996). The load is applied to the sample in different steps and the evolution of settlements is recorded over time.

The oedometer tests were performed according to the British Standard BS 1377-5 (1990) on oedometer apparatus (Figure 4.19 and Figure 4.6) existing at the Geotechnics Laboratory of the University of Coimbra. Two types of oedometers were used, normal and high loading capacity oedometers, i.e., maximum loading capacity of 128 and 450 kg, respectively. The oedometers used are a mass loading system with a loading arm with a multiplicative factor of 11.04.

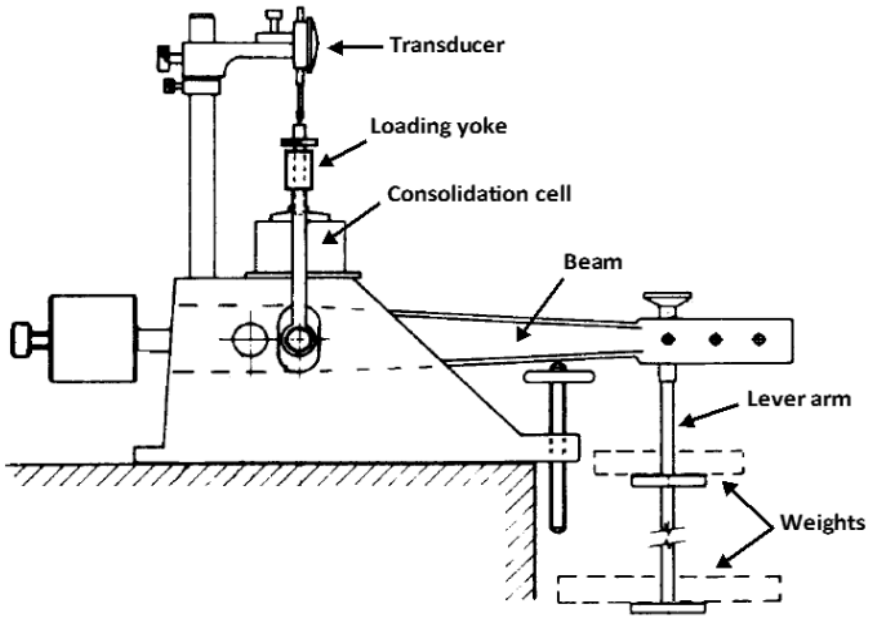

Figure 4.19: Schematic view of Oedometric device (Head, 1985)

The oedometer rings have a diameter of 70 or 50 mm but a height of 19mm in both cases. Once the sample is prepared, as described in section 4.4.3, the oedometer cell is assembly in the oedometer apparatus, oedometer arm is adjusted, the calibrated linear vertical displacement transducer (LVDT) is placed, and sample loading begins. For the present case, each loading/unloading step lasts approximately 0.5h, enough time to the end of the primary consolidation phenomenon since the nature of the stabilised samples, which exhibit very high stiffness and given the thickness of the sample (19mm), the excess of interstitial pressure dissipates quickly.

Each oedometer test allow to characterise by:

i) the compressibility parameters, namely, indices of recompressibility (C_r) and compressibility (C_c), yield stress (σ'_y);

ii) coefficient of consolidation (c_v);

iii) compression curves, i.e., the evolution of the void ratio with the effective stress (*e-log* σ'_v).

It was decided to characterise the compressibility through the recompressibility (C_r) and compressibility (C_c) indices, since they are parameters independent of the effective stress value, i.e., they are characteristic parameters of the composite material.

4.5.6 Triaxial Test

The triaxial equipment used in this work is in the Geotechnical Laboratory of the University of Coimbra and is presented in Figure 4.20. This is a Bishop and Wesley (1975) triaxial equipment, which allows testing specimens with 38 mm in diameter and 76 mm in height diameter and 76 mm high, with a maximum deviator stress limit of 1000kPa. The soil specimen is isolated from the fluid present in the triaxial chamber by a latex membrane and settles on the pedestal which is connected to the equipment's piston. The piston allows the pedestal to move vertically in both directions and the movement is controlled by a pump capable to generate a constant axial constant axial deformation, the Constant Rate Strain Pump (CRSP), which is the instrument responsible for generating the axial load. The water pressures applied both in the back and outside of the (cell) are controlled by a volumetric meter and by an air-water interface respectively. The pressures present at the air-water interface and the volumetric meter are generated by a compressed air system, whose highest value guaranteed in the Laboratory Geotechnics Laboratory of Coimbra University for a correct operation is 800kPa the air-water interfaces. An external air-water interface is also used, which allows manual pressure control.

pressure control, which can be connected to the top of the sample, making it possible to control different pressures at the bottom and at the top of the sample. With the exception of the latter, all the equipment is controlled and monitored by a computer, through the Triax software, developed by Toll (1990). The applied pressures are measured by pressure transducers, the axial load is measured by the load cell and the change in sample volume is recorded by a volumetric meter. The vertical displacements, on the other hand, are measured by an external displacement transducer or, to complement this reading, by internal displacement transducers glued directly on the sample.

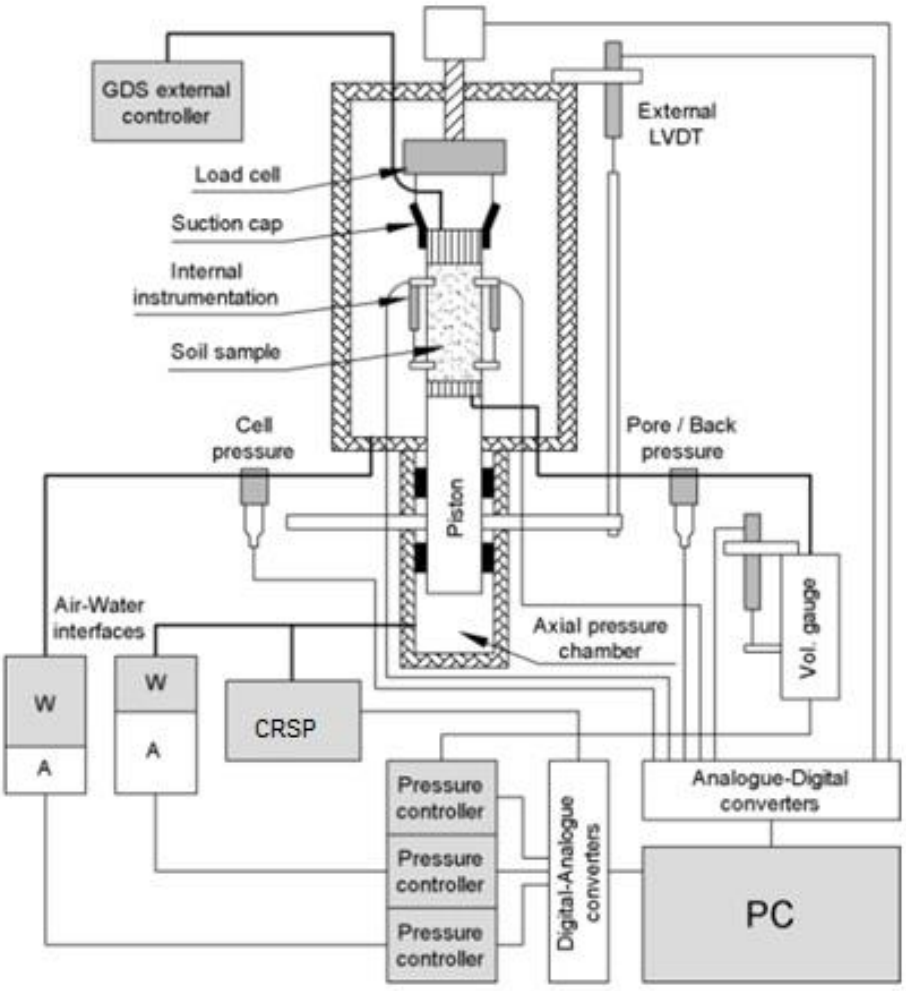

Figure 4.20: Schematic view of Triaxial Stress Path device (Gasparre, 2005 apud by Pedro, 2013)

These instruments are limited by their reading limit capacities, with the transducers used to read the pressure inside and outside the sample have a capacity of 1000kPa and the load cell a maximum reading capacity of 5000N. The volumetric gauge used for the measurement of volume variations has a capacity of 50cm^3 and the stroke limit of the external displacement transducer used for axial strain reading is 25mm. The internal displacement transducers have a reading capacity of about of 10mm. There are three triaxial apparatus existing at the

Geotechnics Laboratory of the University of Coimbra (Figure 4.21 and 4.22), two with a maximum cell pressure capacity of 1 MPa while the other allows a 8.5 MPa. All triaxial apparatus are stress-path cell type developed by Imperial College of London.

A detailed description of the operation of the equipment is presented in Venda Oliveira (1992); Coelho (2000) and Correia (2011).

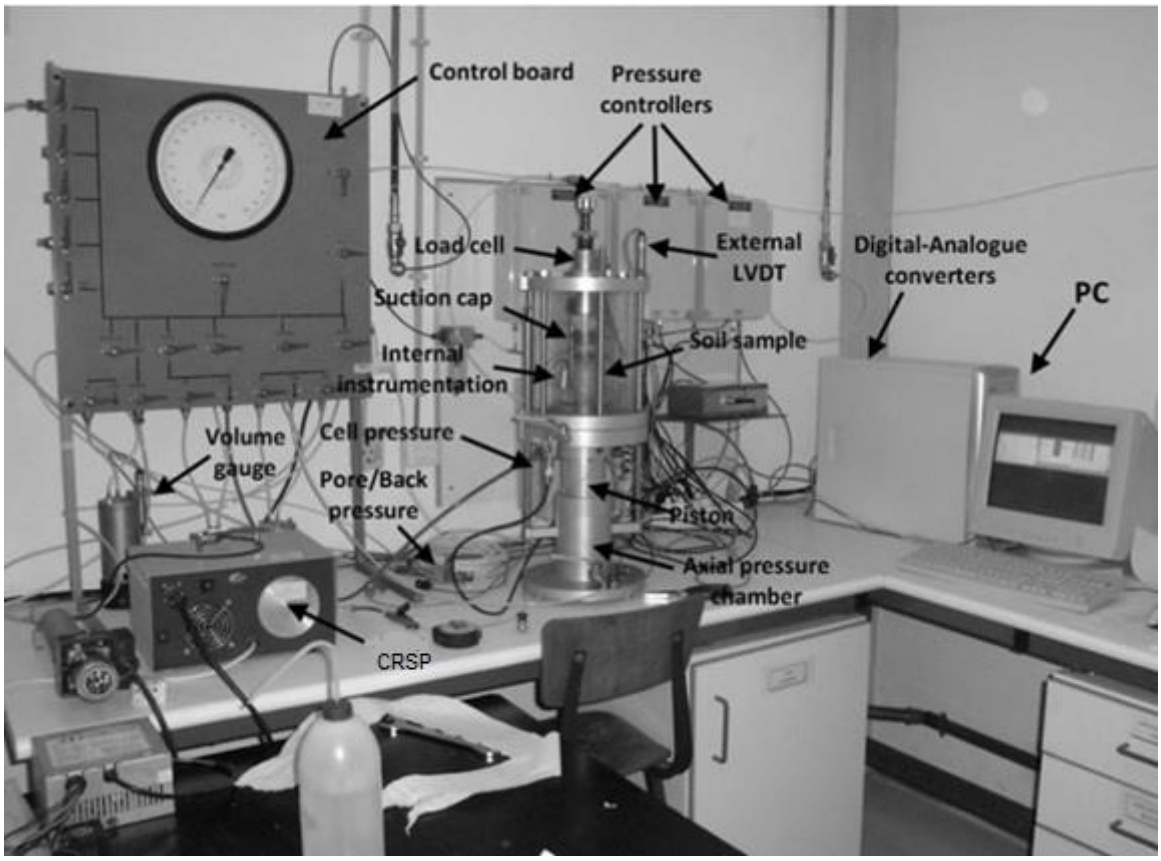

Figure 4.21: General view of Triaxial 1 equipment in University of Coimbra (adapted from Pedro, 2013)

a)

b)

Figure 4.22: Views from a) testing operation sample b) extended view of the triaxial stress path device

In summary, the available stress path cells allow the independent control of pressure in the cell (radial), pressure in the piston (axial) and pore-water pressure. A measurement of these pressures, as well as of the vertical and volumetric strains of the sample is performed by an automatic reading acquisition system, consisting of a load cell, electric pressure and displacement transducers, connected to a computer through an analog-to-digital signal (A/D) signal converter. The recorded values, in established periods of time are converted into force, pressure, displacement, and volumetric strain by applying previous calibrations.

The triaxial test may start. This first stage is the saturation of the sample, which is essential for the correct performance and interpretation of the triaxial test results. It is recommended to apply a minimum backpressure of 200 KPa (it was used a value of 450 kPa to allow the measurement of eventual negative values of excess pore pressure due the stabilised nature of the samples, 'equivalent' to overconsolidated soil), which ensures the dissolution of the air present in the soil's voids and, consequently, the sample's saturation (Egeli, 1980). The Skempton parameter measures the saturation, B $=\frac{\Delta u}{\Delta \sigma cell}$, assuming that the soil is saturated when its value is greater than or equal to 0.95. In practice, the assessment of saturation is done by subjecting the sample to an isotropic cell pressure, with the drainage valve closed. The values of the pressures, both back (Δu) and cell ($\Delta \sigma_{cell}$), are recorded. In all tests performed, values of B greater than 0.95 were obtained after 3 saturation days, so the samples were considered saturated. In the second stage of the triaxial test the samples were subjected to an isotropic consolidation stress (mean effective stress of 50, 200 and 350 kPa for the undrained/drained triaxial shear tests) by raising the cell pressure in a process that lasted one day (backpressure was kept constant at 450 kPa). The third and final stage consists of shear the samples on compression under undrained and drained conditions. The undrained triaxial shear tests were done under a constant axial strain rate of 1%/min, relative to the height of the sample. For the drained triaxial shear tests it was chosen a smaller value for the axial strain rate in order to prevent any excess pore pressure, i.e., a constant axial strain rate of 0.267%/min, relative to the height of the sample. The samples submitted to isotropic compression triaxial tests; the isotropic compression stage started immediately after the saturation stage. The isotropic compression triaxial test was done with a constant cell pressure rate of 20 kPa/h till a value clearly above the yield stress is reached (for the present study it was defined the isotropic effective compressive stress which had to be greater than at least twice the yield stress of the test.

4.5.7 Pundit Test

Elastic and density properties are dependent on the type of material, and these properties provide information about the strength of the material and its quality. Non-destructive tests such as Pundit (determination of ultrasonic pulse velocity) are used to determine good approximations of the elastic properties of materials. Pundit can be used to evaluate the homogeneity of a material, presence of voids, cracks or other internal imperfections or defects, changes in the material that may occur with time (i.e., due to the cement hydration) or damage from fire, frost or chemical attack (ASTM D 2845-05).

The Pundit test is regulated by the several standards such as EN12504-4, ASTM C 597-02 and ASTM D 2845-05, BS 1881-203, ISO1920-7:2004. In the present study it was adopted the procedure described in the standard ASTM D 2845-05. The pulse of the transmitter transducer is transferred to the sample by the contact medium and recognized by the receiving transducer on the opposite side. As the time between the generation and receiver of the wave is recorded by the electrical device, the wave velocity can be determined if the distance between transducers (transmitter and receiver) is known, Equation 4.10.

$$\text{Propagation pulse velocity} = \frac{Path\ length}{Transit\ time} \qquad \text{Equation 4.10}$$

In the Pundit the signal is generated and recorded by the computer, which is capable of amplifying, filtering, and viewing the signal. The computer also records the execution time and voltage amplitude.

Assuming that the sample behaves as an elastic material, the propagation velocity of a compression or primary (P) wave can be expressed as Equation 4.11.

$$V_p = \sqrt{\frac{M}{\rho}} = \sqrt{\frac{E(1-\nu)}{\rho(1+\nu)(1-2\nu)}} \qquad \text{Equation 4.11}$$

Where,

V_p: propagation velocity of a compression wave (m/s)

M: Constrained modulus (MPa)

E: Young's Modulus (MPa)

ρ: Density (kg/m^3)

ν: Poisson's ratio (-)

As opposed to the compression or primary (P) wave, the shear (S) wave causes only shear deformation without volume deformation, and the direction of the medium particle motion is perpendicular to the propagation direction. The propagation velocity of the S wave (V_s) in Equation 4.12 is determined by the shear elastic modulus and density of the medium (Hong et al., 2020).

$$V_s = \sqrt{\frac{G}{\rho}} \qquad \text{Equation 4.12}$$

Where, G is the shear elastic modulus (MPa) given by the following equation:

$$G = \frac{E}{2(1+\nu)} \qquad \text{Equation 4.13}$$

The fundamental components that affect the wave velocity are the elastic modulus and density. The wave velocity is proportional to the square root of the elastic modulus and inversely proportional to the square root of the density. The samples submitted to the Pundit test were the triaxial samples, having a cylindrical shape with a diameter of 37 mm and a height of 76 mm. In the present study it was used an ultrasonic pulse velocity equipment type PUNDIT LAB from Proceq, existing at the Department of Earth Sciences of the University of Coimbra. The Vp and Vs were recorded across the vertical direction. For the Vp it was used a 54 kHz primary wave transducer while for the Vs it was used 250 kHz shear wave transducer. The transducers are positioned at the centre of the sample's surface ends facing each other. At least 10 records were collected for the Vp or Vs propagation velocity. From the measured values of Vp and Vs, and knowing the sample's density, it is possible to determine good approximations of the elastic properties (E and ν) defined in Equation 4.14 and 4.15 of the chemically stabilised non-reinforced or fibre-reinforced soft soil, making use of the following equations:

$$E = [\rho * V_s^2 * (3 * V_P^2 - 4 * V_s^2)]/(V_P^2 - V_s^2)$$ Equation 4.14

$$\nu = \left[\frac{0.5\left(\frac{V_P}{V_s}\right)^2 - 1}{\left(\frac{V_P}{V_s}\right)^2 - 1}\right]$$ Equation 4.15

CHAPTER 5 – BASE TESTING CONDITIONS AND REFERENCES TESTS

5.1 Introduction

The present chapter aims to define the base testing conditions for the experimental study on chemically stabilised soft soil, with and without reinforced fibres. As described in Chapter 3, the test conditions have an influence on the mechanical behaviour of such composite materials. For such, first it was decided to study the chemically stabilised soft soils (CSSS), and to evaluate the impact of curing conditions, especially the immersed versus emersed cure, and applying a vertical stress during the curing period. It is also known that the binder can have an impact on the response of the stabilised soil. Therefore, the influence of the binder type (Portland cement) and the partial substitution of Portland cement by other more sustainable binder (such as blast furnace slag, fly ash and eggshell powder) is also studied. The curing time and the binder quantity are parameters that also influence the mechanical behaviour of the stabilised soil. Such influence is studied for curing times of 7 and 28 days and for two different binder quantities, 175 and 250 kg/m^3. Once the base conditions of the experimental study are defined (Portland cement I 42,5R, quantity 250kg/m^3, curing time of 28 days, without vertical stress and cured in a room in emerse condition), the study proceeds by carrying out the reference tests under static monotonic loading conditions, for chemically stabilised samples without and with fibres. These tests aim to define and characterise the behaviour in compression (UCS) and tensile (STS, DTS and FS) to be used as a reference for the next chapters.

5.2 Curing conditions effect

In this section, two parameters are studied individually. First, the effect of samples immersion in a water tank or samples storage in emerse condition in a curing room is investigated. Then the effect of a vertical stress applied during the curing period is also studied.

5.2.1 Immerse versus emerse curing conditions

As specified in the sample preparation procedures specified in Chapter 4, the samples are stored in a curing room with temperature (20 ± 2 ºC) and humidity (95 ± 5 %) control during the curing period of 7 days. In opposition to the emerse curing condition it was also studied the cure of the samples in an immerse condition, i.e., where the samples are immersed in a water tank at a controlled temperature (20 ± 2 ºC), Figure 5.1.

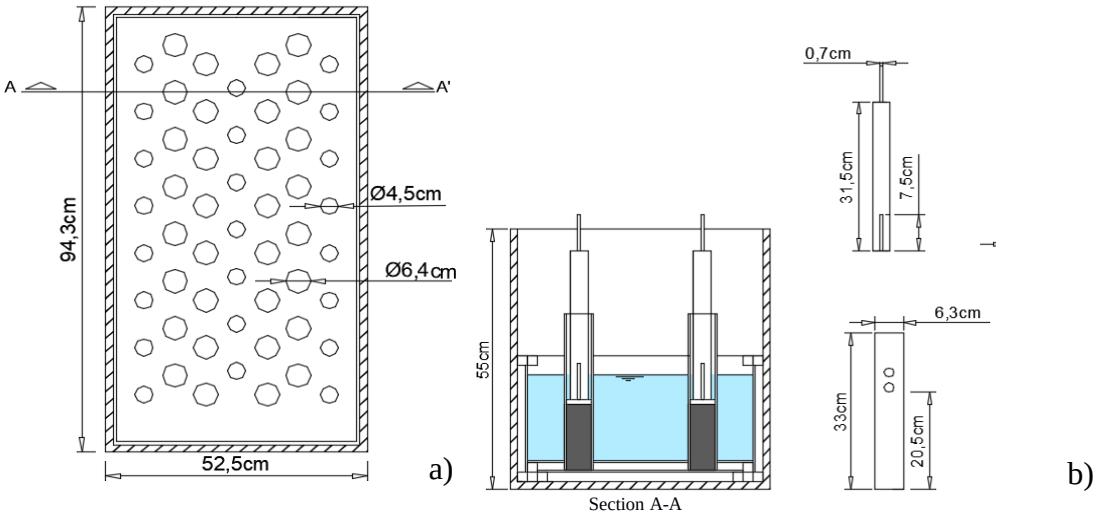

Figure 5.1: Curing tank and PVC moulds (dimensions in cm) adapted from Correia (2011)

The results for the tested samples in room (emersed) and tank (immersed or submerged) curing condition are listed in Table 5.1. Moreover, the stress-strain and $E_{u\text{-}sec}$ vs strain curves are plotted in Figure 5.2. The emerse curing condition results in 53.37% higher unconfined compressive strength ($q_{u\ max}$), although the undrained stiffness modulus value defined for 50% of $q_{u\ max}$ (E_{u50}) is slightly lower (27%) (Table 5.1 and Figure 5.2).

Table 5.1: Curing condition study (CI42.5 R; binder quantity = 250 kg/m^3; curing time = 7 days; vertical stress = 0 kPa)

Curing condition	ID	$q_{u\ max}$ (kPa)	ε_r (%)	E_{u50} (MPa)	w_f (%)
Emerse-room	TBC1	218.36	3.82	9.36	73.09
Immerse-tank	TBC6	142.37	3.07	15.58	74.19

It is also possible to verify that the final water content (w_f) of the emerse sample (room) is slightly lower than the immersed (in tank) sample, reflecting the free access to water of the immerse curing condition. However, by analysing the values of $q_{u\ max}$, this free access to water did not represent the development of more cementitious reactions. On the other hand, the results seem to indicate the existence of suction in the emerse samples, inducing a higher strength, which is in contraction

with the results obtained by Correia (2011) with similar soil and testing conditions. Therefore, the emersed curing condition is adopted in the remaining study.

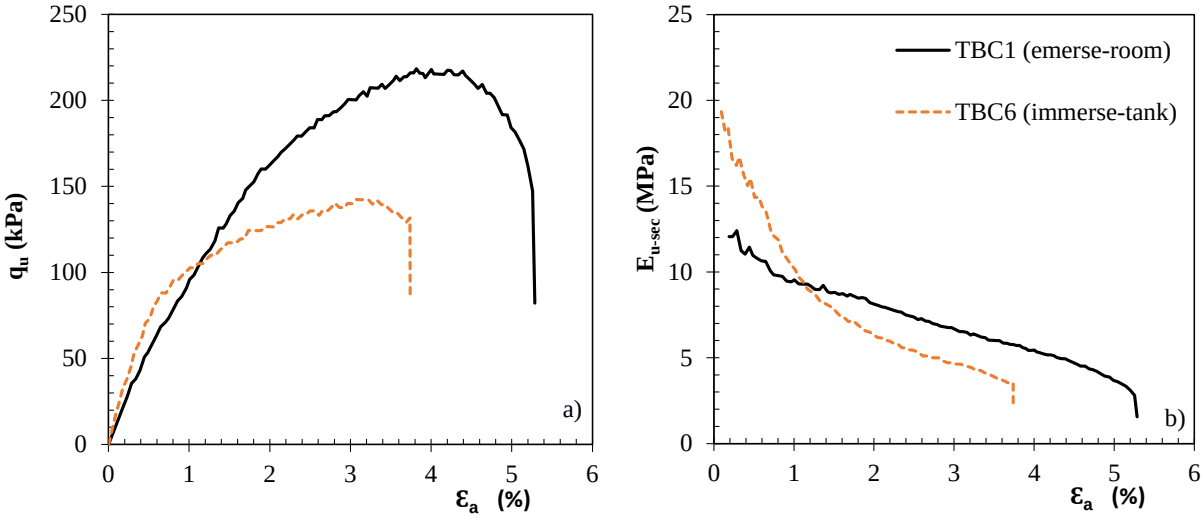

Figure 5.2: a) Stress–strain plot; b) $E_{u\text{-}sec}$ vs axial strain (CI42.5 R; binder quantity = 250 kg/m^3; curing time = 7 days; vertical stress = 0 kPa)

5.2.2 Effect of vertical stress during curing

The study of the vertical stress applied on the samples during the curing period aims to evaluate the possible improvement of the mechanical behaviour, measured by the increase of the unconfined compressive strength ($q_{u\ max}$), that is expected to occur with the increase of the vertical stress (Åhnberg et al., 2001; EuroSoilStab, 2001; Åhnberg, 2006; Correia, 2011).

The study of the vertical stress applied during curing was performed for equal stabilised samples but subjected to different vertical stress during the curing period (0 and 24kPa). The value 24 kPa aims to simulate the vertical stress equivalent to 5 m depth in the soft soil of Baixo Mondego (Correia, 2011), which was reproduced by considering weights on samples (Figure 5.1).

Nevertheless, the results obtained in the previous section, the study of the effect of the vertical stress is performed for both curing conditions, emerse and immerse. In both cases, the vertical stress was applied immediately after samples preparation (emerse samples) and immediately after their introduction in the curing tank for the immersed curing condition.

Table 5.2 and Figure 5.3 summarise the results obtained for immerse samples. The results show that by increasing the vertical stress in the curing period, there is an improvement in the mechanical behaviour of the samples, expressed by the increase of the unconfined compressive strength ($q_{u\ max}$) and undrained stiffness modulus at 50% of $q_{u\ max}$ (E_{u50}). This improvement can be explained by the fact the vertical stress promotes a smaller interparticle distance between the soil-binder particles, thus, promoting the development of a stronger and stiffer solid matrix, i.e.,

the vertical stress promotes the improvement of the mechanical behaviour. This is also visible in the slightly smaller water content (lower w_f) reflecting the development of a higher number of cementitious reactions and/or a lower void ratio promoted by the application of a vertical stress to the samples.

Table 5.2: Results of samples tested in immerse condition – effect of vertical stress, σ'_v (CI42.5 R; binder quantity = 250 kg/m^3; curing time = 7 days)

σ'_v (kPa)	ID	$q_{u\ max}$ (kPa)	ε_r (%)	E_{u50} (MPa)	w_f (%)
0	TBC6	142.37	3.07	15.58	74.19
24	TBC7	223.24	2.97	15.49	72.26
24	TBC8	233.80	3.55	21.36	72.79

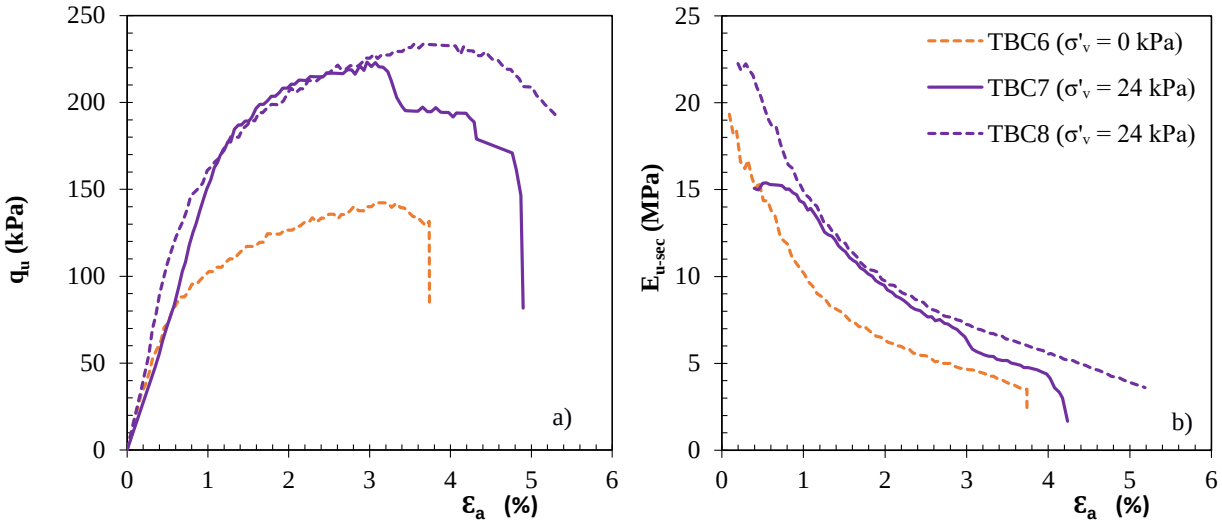

Figure 5.3: a) Stress–Strain plot; b) $E_{u\text{-}sec}$ vs axial strain (CI42.5 R; binder quantity = 250 kg/m^3; curing time = 7 days; σ'_v = vertical stress; curing condition = immerse in tank)

For the emerse case, similar conclusions can be drawn by analysing Table 5.3 and Figure 5.4. The application of a vertical stress during the curing period, even when in emersed condition, promotes the improvement of mechanical characteristics. This fact is justified by the same reasons as those presented for the immersed samples.

Table 5.3: Results of samples tested in emerse condition – effect of vertical stress, σ'_v (CI42.5 R; binder quantity = 250 kg/m^3; curing time = 7 days)

σ'_v	ID	$q_{u\ max}$ (kPa)	ε_r (%)	E_{u50} (MPa)	w_f (%)
0	TBC1	218.36	3.82	9.36	73.09
24	TBC11	228.68	2.08	26.36	73.26
24	TBC12	256.28	2.39	30.71	73.79

When comparing the results of immerse and emerse curing conditions, it is possible to see that the higher results are obtained for the emerse curing conditions as it was observed previously.

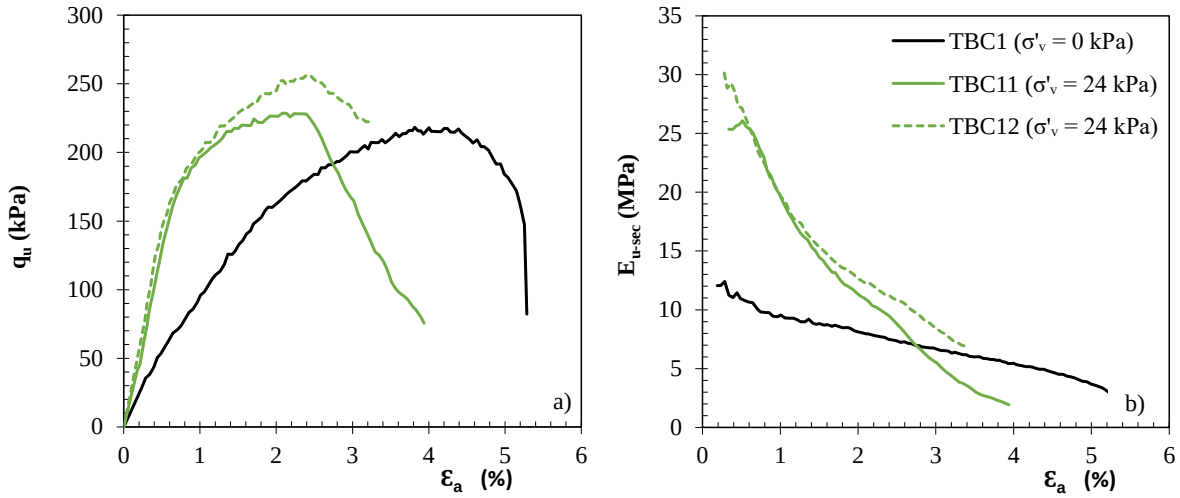

Figure 5.4: a) Stress–Strain plot; b) $E_{u\text{-}sec}$ vs axial strain (CI42.5 R; binder quantity = 250 kg/m^3; curing time = 7 days; σ'_v = vertical stress; curing condition = emerse/room)

Regarding the effect of applying a vertical stress during the curing period it may be concluded that the application of a vertical stress promotes the improvement of mechanical characteristics. However, as the number of weights available at the laboratory is limited, it was decided to continue the laboratory work without applying a vertical stress to the samples but under emerse (room) curing condition.

5.3 Study the effect of the binder quantity

This section aims to study the effect of the binder quantity on the mechanical behaviour of chemically stabilised samples prepared following the procedure described in Chapter 4 and cured in an emerse condition (room) and without the application of any vertical stress to the samples.

Many studies refer to the binder quantity as a key factor influencing the mechanical behaviour of a chemically stabilised soil (Chapter 3). As it was stated in Chapter 3, regardless of the binder type, it should be applied in quantities not lower than a minimum so that chemical stabilisation promotes an effective mechanical enhancement. For clayey soils, a minimum amount of 30 - 50 kg/m^3 has been proposed by Terashi (1980), Uddin (1994), Horpibulsuk (2001), while a minimum of 50 - 70 kg/m^3 is recommended for organic soils (Babasaki, 1997; Axelsson et al., 2002).

Axelsson et al. (2002) studied several organic soils (including mud and peat) and have concluded that the stabilization with Portland cement produces good results. The authors proposed that muddy (soft) soils should be stabilised with a binder amount of the order 100 - 200 kg/m^3, values that should increase to 150 - 250 kg/m^3 for the case of peat. Correia (2011) has carried out a study with the soft soil of Baixo Mondego stabilized with different quantities of Portland cement I 42.5R,

ranging from 75 to 250 kg/m^3. The author concluded that the mechanical behaviour of the stabilized material improves with the increase of the binder quantity, but have observed that this enhancement becomes smaller for binder quantities between 175 kg/m^3 and 250 kg/m^3. Based on such studies and considering the organic nature of the soil selected for the present study, it was decided to study only two binder quantities, 175 kg/m^3 and 250 kg/m^3.

Table 5.4 and Figure 5.5 show the results of the binder quantity (BQ) study. It may be concluded that as the binder quantity increases there is an improvement in the mechanical behaviour, expressed by an increase in the unconfined compressive strength ($q_{u\ max}$) and an increase in the undrained stiffness modulus at 50% of $q_{u\ max}$ (E_{u50}).

Table 5.4: Results of samples stabilized with different binder quantities (CI42.5 R; binder quantity = BQ; curing time = 7 days; vertical stress in curing conditions = 0 kPa; curing condition = room)

ID	BQ (kg/m^3)	$q_{u\ max}$ (kPa)	ε_r (%)	E_{u50} (MPa)	w_f (%)
TBC1	250	218.36	3.81	9.290	73.09
TBC4	175	112.55	8.12	3.578	75.34

This behaviour reflects that the increase of the binder quantity allows the development of a higher number of cementitious reactions, corresponding to higher water consumption, a fact clearly shown in the values of the final water content (w_f) in Table 5.4, which decreases with increasing binder quantity. A higher number of cementitious reactions corresponds to developing a denser and stiffer matrix, responsible for improving the mechanical properties of the composite material.

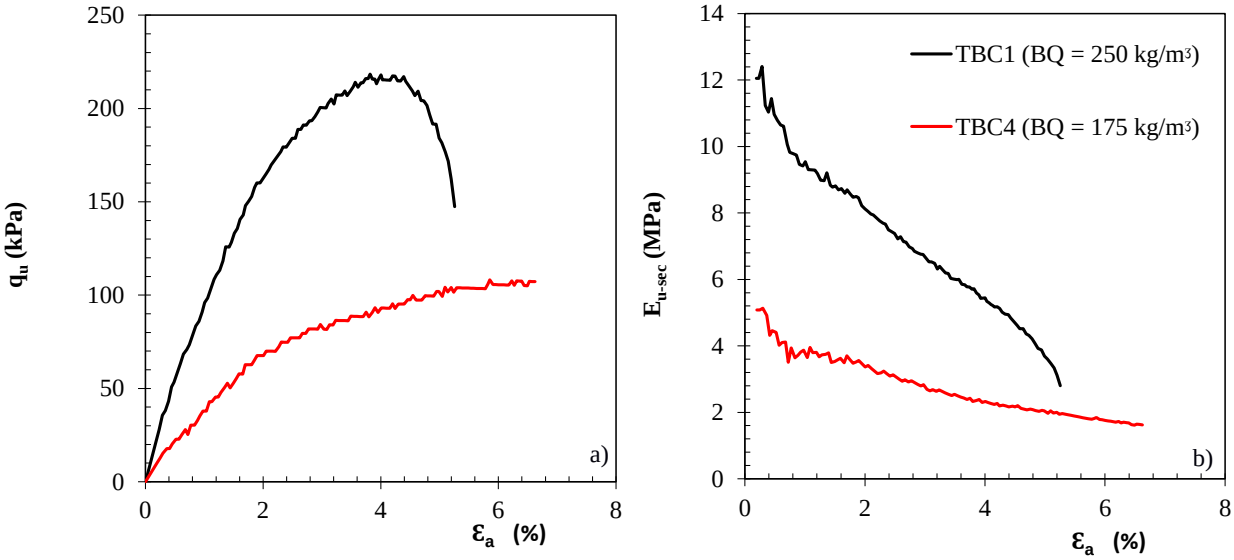

Figure 5.5: a) Stress–Strain plot; b) $E_{u\text{-}sec}$ vs axial strain (CI42.5 R; binder quantity = BQ; curing time = 7 days; vertical stress in curing conditions = 0 kPa; curing condition = room)

At the beginning of the experimental stage of this work, a series of tests was carried out looking for the effect of some key parameters in terms of chemical stabilisation of the soft soil of Baixo

Mondego. This was part of an international collaborative study involving the Tokyo Institute of Technology (TIT, Japan), Swedish Geotechnical Institute (SGI, Sweden), University of Coimbra (UC), Sapienza University of Rome (UR, Italy) and Port and Airport Research Institute (PARI, Japan), with the aim to study regional soils stabilized with regional and non-regional binders. The parameters binder type, water content during preparation and curing time were studied (Kitazume, 2020 and Villarroel, 2018). The results regarding the soft soil of Baixo Mondego stabilised with Portland cement I 42.5R, cured in immersed (tank) condition are summarized in Figure 5.6.

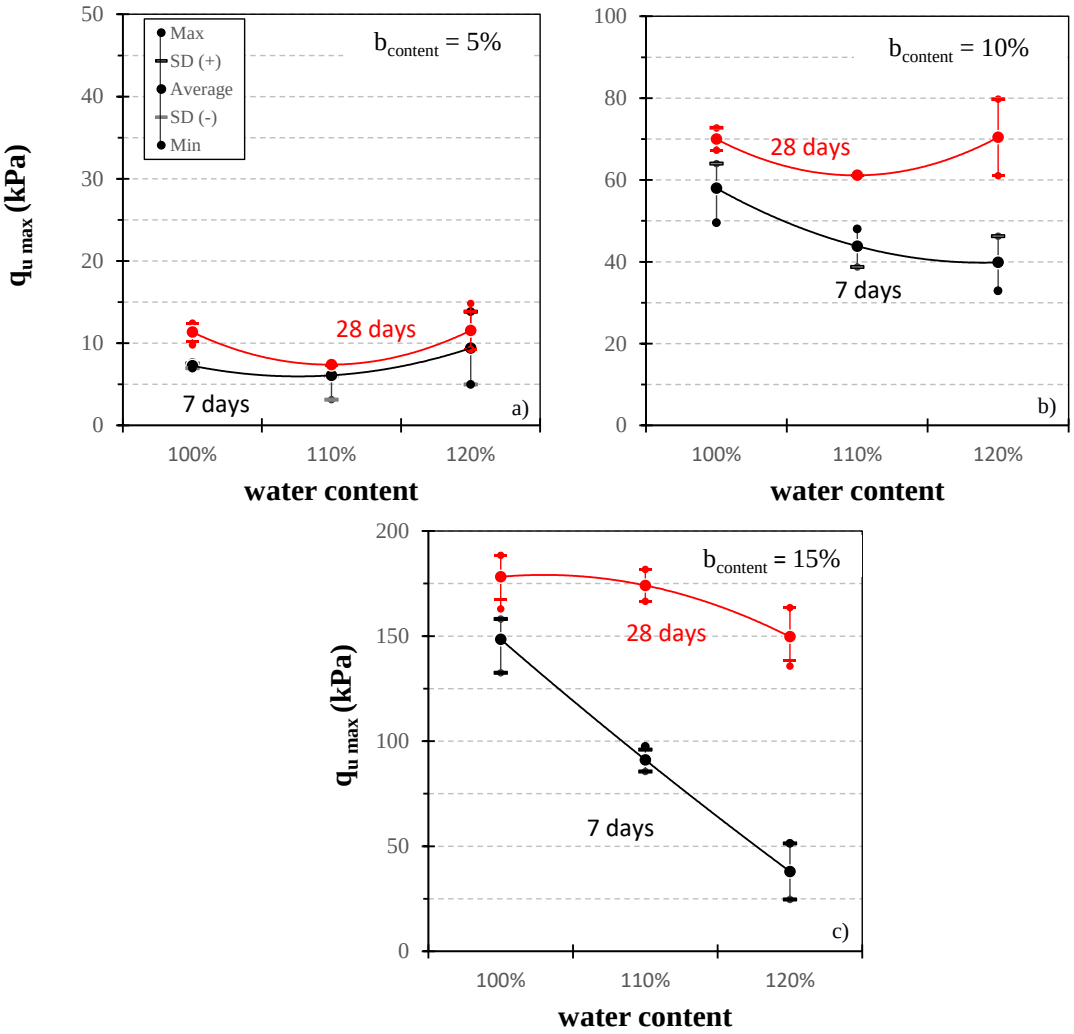

Figure 5.6: Effect of water content on the unconfined compressive strength for the Portland cement I 42.5R: a) $b_{content}$ = 5%; b) $b_{content}$ = 10%; c) $b_{content}$ = 15% ($b_{content}$ = binder content)

The results demonstrated clearly that there is a minimum binder amount so that chemical stabilisation promotes an effective mechanical enhancement: for the binder content of 5% the effectiveness of the chemical stabilization is almost negligible. From the Figure 5.6 it may also be seen that the water content plays an important role in the mechanical behaviour of the stabilised material. However, it was difficult to identify a clear tendency, but for the binder content of 15% (Figure 5.6 b), where it is clear the effects of the chemical stabilization, it may be seen that the

unconfined compressive strength decreases as the water content increase. This might be related to the fact that, for a saturated soil, the increase in water content promotes the increase of the void ratio of the material which means a more loose and "open" matrix (with the worst mechanical behaviour).

5.4 Study of the effect of the curing time

It is known that the soil-binder-water interactions develop over time (days, months, and even sometimes, years), impacting the mechanical characteristics of the stabilised soil (Correia, 2011). In the present section a study of the curing time effect is presented for stabilized samples having different curing times, 7 and 28 days. The results are presented in Table 5.5 and Figure 5.7.

Table 5.5: Results of stabilized samples – effect of curing time (CI 42.5 R; binder quantity = 250 kg/m^3; vertical stress = 0 kPa; curing condition = room)

ID	Curing time (days)	$q_{u\ max}$ (kPa)	ε_r (%)	E_{u50} (MPa)	w_f (%)
TBC1	7	218.36	3.82	9.36	73.09
TBC13	28	302.36	1.45	33.29	71.56
TBC14	28	288.80	1.25	33.92	71.86

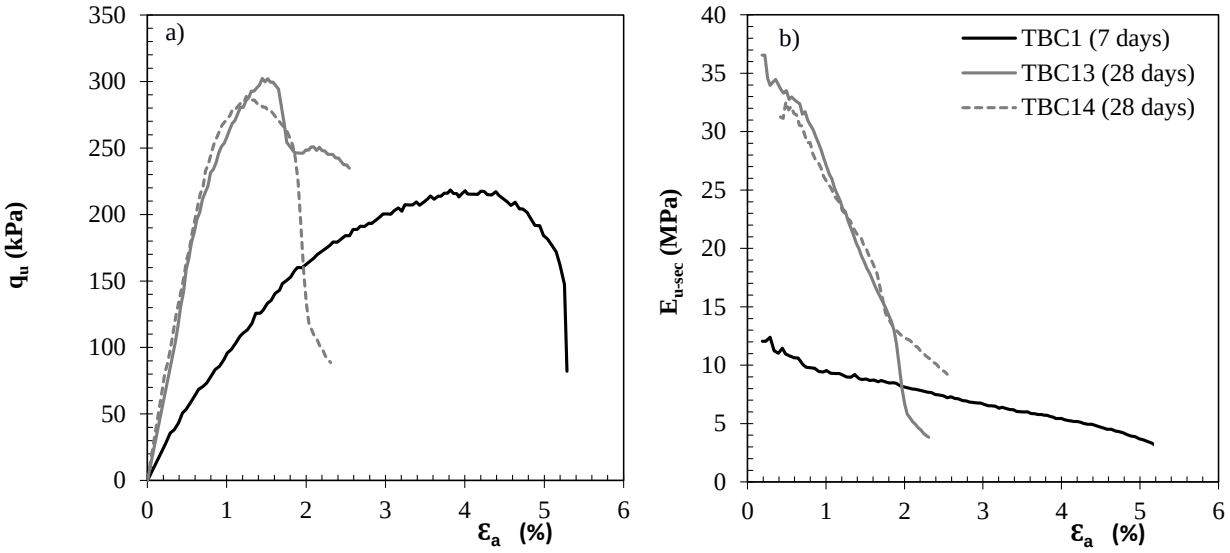

Figure 5.7: a) Stress–Strain plot; b) $E_{u\text{-}sec}$ vs axial strain (CI42.5 R; binder quantity = 250 kg/m^3; curing time = 7 and 28 days; vertical stress = 0 kPa; curing condition = room)

From the results it may be concluded the mechanical behaviour improves by increasing the curing time, as expected. This improvement is well expressed by the increase of the unconfined compressive strength ($q_{u\ max}$) and undrained stiffness modulus (E_{u50}). In terms of the axial strain at rupture (ε_r), it is observed a decrease as the curing time increases, i.e, the behaviour becomes more stiff. It is noticed that the higher the curing time, the more brittle is the samples' behaviour, characterized by a fast strength growth with an abrupt loss of the mechanical strength after rupture, behaviour that is much more pronounced for the curing time of 28 days in comparison to 7 days,

which agrees with results expressed by Correia (2011). The improvement of the mechanical behaviour with the curing time is related with the interactions between soil-binder-water which develop over time, conferring to the stabilised material a stronger and stiffer cemented matrix. This fact is well related with the w_f, where it was observed a decrease of the w_f as the curing time increases, due to a higher water consumption by the cementitious reactions.

5.5 Study of the effect of the binder type

The type of binder has a strong influence on the mechanical behaviour of a stabilised soil. In fact, it is due to the physico-chemical interactions triggered by the binder that the most significant mechanical changes in the stabilised soil are processed (EuroSoilStab, 2002; Janz and Johansson, 2002). Thus, it was decided to perform two studies, the first focused on the selection of the best Portland cement type to be used in the chemical stabilization, and in a second study the effect of a partial substitution of the Portland cement by other sustainable binders (blast furnace slag, fly ash and eggshell) will be evaluated.

5.5.1 Effect of the Portland cement type

Two Portland cement binders (hydraulic binders), produced at the company Cimpor-Souselas, Coimbra, were selected for the chemical stabilization of the soft soil of Baixo Mondego. The Portland cements chosen were, Portland cement type I 42.5R and Portland cement type II 42.5R, whose chemical characteristics are presented in Table 5.6. Table 5.7 and Figure 5.8 summarise the results for the soil stabilisation for the two Portland cement binders, both applied in a binder quantity of 250 kg/m^3. The samples were cured for 7 days in emerse condition without any vertical stress applied.

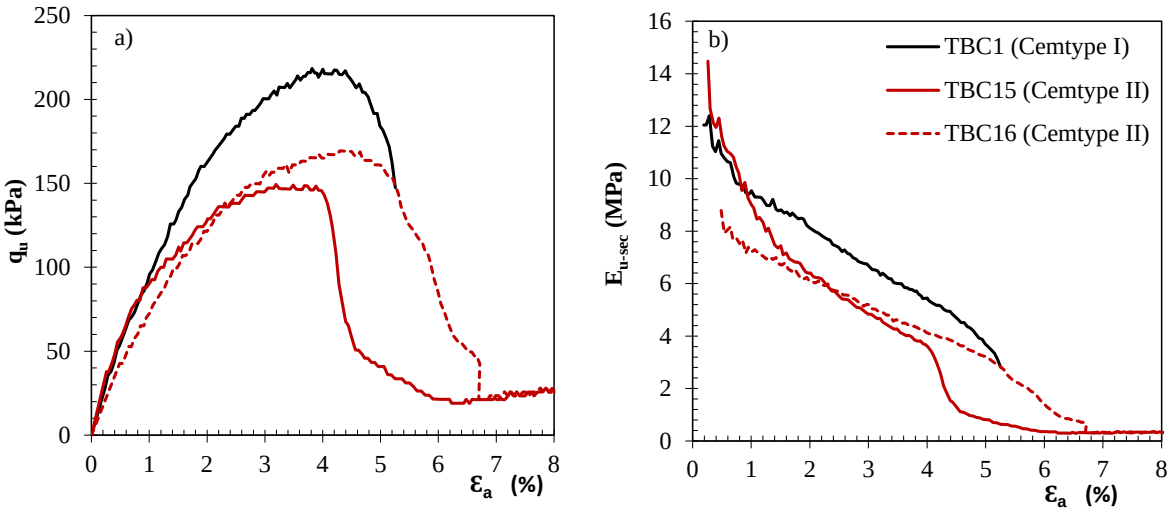

Figure 5.8: a) Stress–strain plot; b) $E_{u\text{-}sec}$ vs axial strain (binder quantity = 250 kg/m^3; curing time = 7 days; vertical stress = 0 kPa; curing condition = room)

As it can be seen, the best results (higher unconfined compressive strength and undrained stiffens) are obtained for the stabilisation with the Portland cement type I 42.5R. This can be explained by the fact that, as mentioned by Taylor (1997) and Coutinho (1988), the mechanical improvement promoted by an hydraulic binder is associated with the content of CaO, SiO_2 and Al_2O_3, being usually described by the ratio CaO/SiO_2 or simply by the amount of the compounds $CaO + SiO_2 + Al_2O_3$. As it may be seen from Table 5.6, regardless of the relationship considered, these are greater for Portland cement type I 42.5R, justifying the best results achieved with this cement (higher $q_{u\ max}$ and E_{u50}). A higher Portland cement reactivity corresponds to a higher water consumption, which is quite evident in the values obtained for w_f.

Table 5.6: Chemical characterisation of Portland cement Type I 42.5 R and Type II 42.5 R (manufacturer's data)

Chemical Compounds	Portland cement Type I 42.5 R	Portland cement Type II 42.5 R
CaO	62.88	61.08
SiO_2	19.00	19.31
Al_2O_3	5.15	4.31
Fe_2O_3	3.19	2.28
SO_2	3.14	2.96
MgO	2.16	2.38
K_2O	1.29	0.86
Na_2O	0.10	0.29

Table 5.7: Results of stabilized samples – effect of Portland cement type (binder quantity = 250 kg/m^3; curing time = 7 days; vertical stress = 0 kPa; curing condition = room)

Portland cement type	ID	$q_{u\ max}$ (kPa)	ε_r (%)	E_{u50} (MPa)	w_f (%)
Cemtype I 42.5 R	TBC1	218.36	3.81	9.29	73.09
Cemtype II 42.5 R	TBC15	149.39	3.19	6.91	74.34
Cemtype II 42.5 R	TBC16	169.33	4.29	7.59	74.7

5.5.2 Other binders - partial substitution of Portland cement

This section seeks to understand the effect of a partial substitution of Portland cement type I 42.5R by other binder (blast furnace slag, fly ash and eggshell powder) with the final aim to reduce the quantity of Portland cement used in the chemical stabilisation without compromise the mechanical behaviour of the composite material, i.e., contributing to find a more sustainable binder. The second binders are applied in proportions 95/5, 90/10 and 85/15, referred as the dry weight percentage of the Portland cement/second binder. In all cases, the binder quantity used was 250 kg/m^3, and the stabilised samples were cured for 28 days in an emerse (room) condition without any vertical stress.

Table 5.8 and Figures 5.9, 5.10 and 5.11 summarise the results obtained from the UCS tests performed. A first global analysis of the results shows that the partial substitution of Portland cement by blast furnace slag or fly ash leads to a decrease in the mechanical properties, namely,

reduction of unconfined compressive strength and undrained stiffness modulus, and increase of the axial strain at failure. In general, the final water content is higher than for the case of 100% Portland cement, which agrees with the deterioration of the mechanical properties observed (suggesting that cementitious reactions occur in a smaller number or less intensely).

Table 5.8 and Figure 5.9 presents the results concerning the Blast Furnace Slag (BFS) substitution from where it can be observed that regardless the blast furnace slag proportion, there is a deterioration in the mechanical behaviour ($q_{u\ max}$ and E_{u50}) of the stabilised samples when compared with the reference samples (Portland cement alone). The partial substitution of the Portland cement by Fly Ash (FA) leads to similar results (Table 5.8 and Figure 5.10), i.e., leads to a deterioration of the mechanical behaviour ($q_{u\ max}$ and E_{u50}) of the stabilised samples when compared with the reference samples (Portland cement alone). For the BFS substitution it seems that an increase of the second binder (slag) promotes less deterioration, while for the case of FA substitution, the results indicate an increase of the deterioration of the mechanical properties with the fly ash content increment. These results seems to be explained by the different nature of the binders (as presented in Chpater 3), being the slag a latent hydraulic binder requiring an activator (in general, the $Ca(OH)_2$ from Portland cement reactions) for the development of the hydraulic (primary) reactions, while fly ash is a pozzolanic binder where the physico-chemical interactions (secondary hydraulic reactions) developed very slowly justifying the poor mechanical performance as fly ash content increases.

Table 5.8 and Figure 5.11 show the results for eggshell addition. For this specific addition, it may be seen that when the Portland cement is partially substitute by eggshell an improvement of the unconfined compressive strength is observed when compared with the reference samples (Portland cement alone) whereas the undrained stiffness modulus decreased. Regarding the axial strain at failure, it may be seen that it increases with the partial substitution of Portland cement by eggshell, showing that the mechanical behaviour becomes slightly more ductile. This good behaviour of the eggshell may be explained by the high CaO content ($\geq$ 95%, Chapter 4) which boosts the Portland cement's hydraulic reactions and at the same time promotes pozzolanic reactions by combination with the silica and alumina present in the soil.

The results indicate (Figure 5.12) that the partial substitution of Portland cement by eggshell is beneficial in terms of mechanical behaviour, while contributing to the reduction of the environmental footprint associated with Portland cement. At first, the combination of Portland cement with eggshell seems to be a more sustainable solution, however, eggshell does not exist in powder form, requiring energy and mechanical actions (ball mill) to obtain it, which may compromise its environmental performance. More studies are needed to prove that eggshell

correspond to an effective sustainable solution. As such, it was decided to continue the studies with Portland cement only.

Table 5.8: Results of stabilized samples – effect of a partial substitution of Portland cement (binder quantity = 250 kg/m^3; curing time = 28 days; vertical stress = 0 kPa; curing condition = room)

Cement content (%)	Second binder content (%)	ID	$q_{u\ max}$ (kPa)	ε_r (%)	E_{u50} (MPa)	w_f (%)
Cement I 42.5 R						
100	0	TBC13	302.36	1.45	33.29	71.56
100	0	TBC14	288.80	1.25	33.92	71.86
Cement I 42.5 R + Blast Furnace Slag						
95	5	C95-BFS5_3	157.57	1.91	9.84	70.98
95	5	C95-BFS5_4	231.13	2.24	19.76	70.68
90	10	C90-BFS10_5	272.45	5.10	10.24	74.99
90	10	C90-BFS10_6	278.35	3.14	11.62	73.94
85	15	C85-BFS15_7	219.13	2.67	9.31	72.18
85	15	C85-BFS15_8	287.29	3.29	11.98	71.68
Cement I 42.5 R + Fly Ash						
95	5	C95-FA5_9	238.14	3.46	7.57	72.80
95	5	C95-FA5_10	222.91	1.83	2.93	72.50
90	10	C90-FA10_11	217.99	3.23	9.51	74.99
90	10	C90-FA10_12	202.11	3.81	7.54	73.10
85	15	C85-FA15_13	194.13	3.55	7.40	72.67
85	15	C85-FA15_14	197.95	3.71	5.74	72.17
Cement I 42.5 R + Eggshell						
95	5	C95-ES5_19	335.52	2.23	24.78	72.40
95	5	C95-ES5_20	384.88	2.76	20.23	72.10
90	10	C90-ES10_21	326.95	2.13	23.27	74.99
90	10	C90-ES10_22	358.94	2.93	19.77	73.94
90	10	C90-ES10_23	317.69	3.20	16.26	74.44
85	15	C85-ES15_24	257.17	1.66	18.08	71.98
85	15	C85-ES15_25	310.13	4.23	16.97	71.12
85	15	C85-ES15_26	329.95	4.60	32.16	73.20

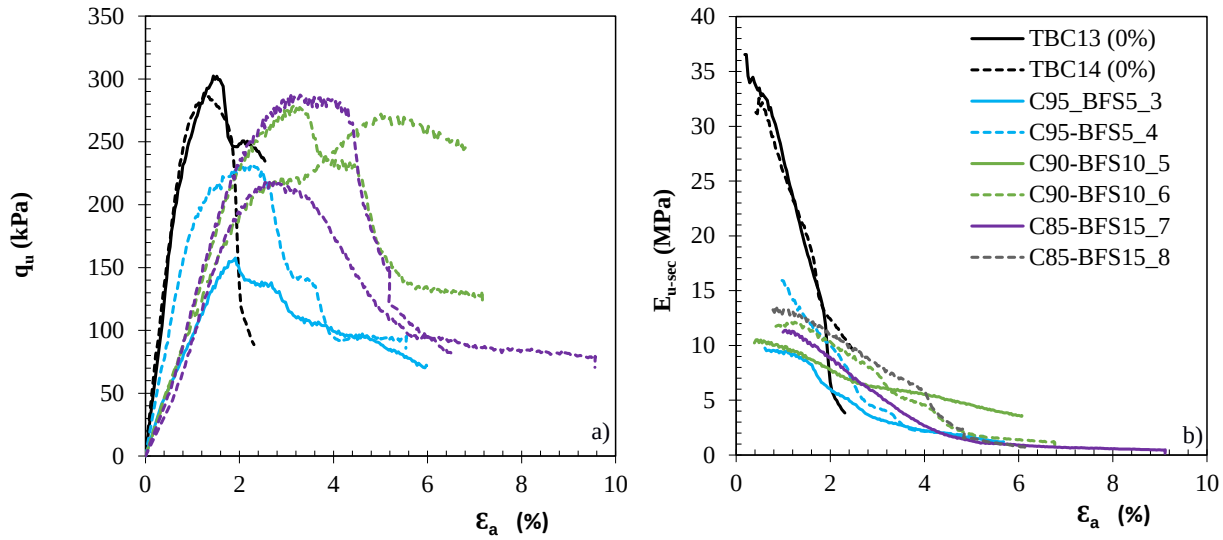

Figure 5.9: a) Stress–Strain plot; b) $E_{u\text{-}sec}$ vs axial strain (Blast Furnace Slag and CI42.5 R; binder quantity = 250 kg/m^3; curing time = 28 days; vertical stress = 0 kPa; curing condition = room)

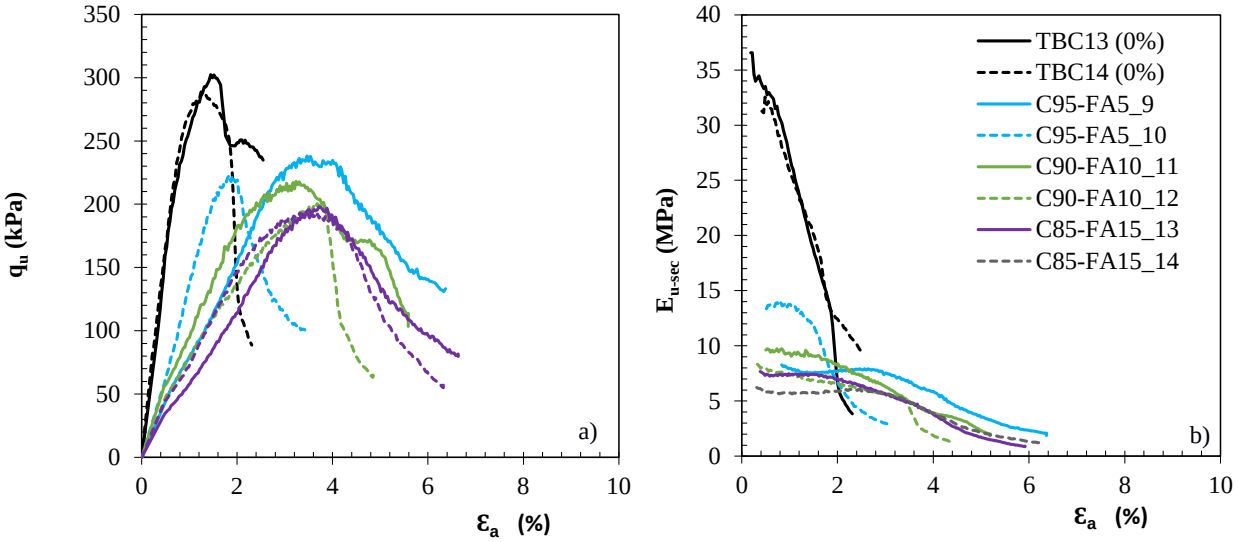

Figure 5.10: a) Stress–Strain plot; b) $E_{u\text{-}sec}$ vs axial strain (Fly Ash and CI42.5 R; binder quantity = 250 kg/m^3; curing time = 28 days; vertical stress = 0 kPa; curing condition = room)

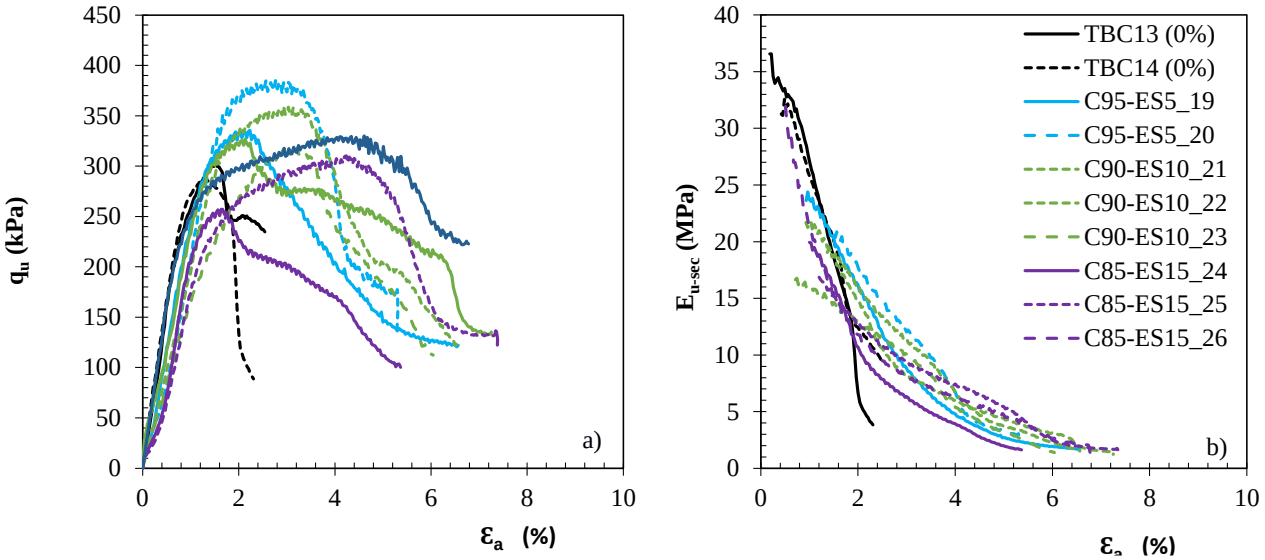

Figure 5.11: a) Stress–Strain plot; b) $E_{u\text{-}sec}$ vs axial strain (Eggshell Powder and CI42.5 R; binder quantity = 250 kg/m^3; curing time = 28 days; vertical stress = 0 kPa; curing condition = room)

From the studies carried out to define the base conditions, it may be concluded that the following conditions: the soft soil of Baixo Mondego is chemically stabilise with Portland cement type I 42,5R, applied in a quantity of 250kg/m^3, and the samples cured for 28 days in emerse (room) condition, without any vertical stress applied. The study proceeds by carrying out the reference tests under static monotonic loading conditions, for samples without and with fibres, following the conditions now established.

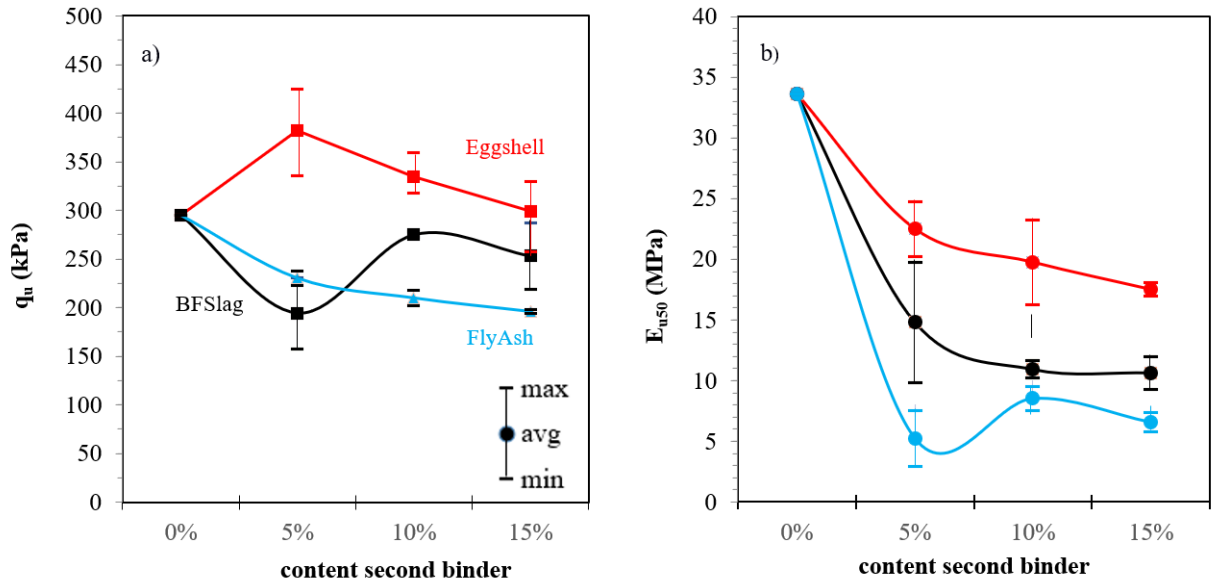

Figure 5.12: Summary of results regarding the partial substitution of Portland cement by different second binders: a) $q_{u\text{-}max}$ vs content of second binder b) Eu50 vs content of second binder

5.6 Monotonic Reference Tests

After defining the base conditions for the soft soil of Baixo Mondego chemically stabilise it is important to characterise the mechanical behaviour under monotonic loading conditions for samples without and with fibres. For such, compression and tensile strength tests were performed aiming to define and characterise the behaviour in compression (UCS) and tensile (STS, DTS and FS) to be used as a reference for the next chapters.

The stabilised samples were prepared following the procedures specified in Chapter 4, adopting the base conditions defined above. The samples were cured for 28 days in emerse condition (room with temperature, 20±2ºC, and humidity, 95±5%, control) without any vertical stress. For the fibre-reinforced stabilised samples, polypropylene fibres (described in Chapter 4) were added in a quantity of 10 kg/m^3.

The study starts with unconfined compressive strength (UCS) tests aiming to characterise the compressive behaviour of the composite material. Secondly, the definition of the tensile behaviour was done making use of direct tensile strength (DTS) tests as well as indirectly tensile strength tests, more precisely, splitting tensile strength (STS) tests and flexural (or bending) strength (FS) tests. Detailed explanations of these tests can be found in Chapter 4.

5.6.1 Unconfined Compressive Strength (UCS) reference tests

Table 5.9 and Figures 5.13 and 5.14 summarise the results obtained from the UCS tests performed on stabilised samples without and with the addition of polypropylene fibres. The results show that the addition of fibres modifies the mechanical behaviour, decrease the unconfined compressive strength, the stiffness, and the brittleness of the stress-strain behaviour of the composite material. The loss of unconfined compressive strength and stiffness due to the fibres addition may be explained by the fact that physical presence of the fibres prevents the development of some cementitious bonds within the composite matrix, producing a composite material will lower strength and stiffness. Regarding the stress-strain behaviour it may be seen that as the strain evolves the fibres are progressively mobilised minimizing the post-peak strength loss and thus giving to the composite material a ductile behaviour. The value of the residual strength depends on the fibres characteristics (namely, tensile strength, surface roughness, length), fibres quantity and failure mechanism imposed. From Figure 5.13 it is possible to see that both stabilised samples reinforced with fibres exhibit a very similar residual strength since it was added to the samples an equal quantity of the same fibres type. The results obtained are in well agreement with the findings from Correia et al. (2015), Venda Oliveira et al. (2016) and is also consistent with Kaniraj and Havanaji (2001) and Olgun (2013).

Table 5.9: UCS reference tests results for stabilised samples without and with polypropylene fibres (0 and 10 kg/m^3)

ID	Fibres	$q_{u\ max}$ (kPa)	ε_r (%)	E_{u50} (MPa)	w_f (%)
REF_UCS_1	No	302.36	1.45	33.29	71.56
REF_UCS_2	No	288.80	1.25	33.92	71.86
REF_UCS_1_F	Yes	293.87	4.55	14.32	70.62
REF_UCS_2_F	Yes	296.65	4.03	16.10	70.56

Regarding the water content measured immediately after the end of the UCS tests, the results indicate that the fibres addition promotes a slightly reduction of it which may be explained by some adsorption capacity of the fibres and/or by the fact that the fibres introduce some extra pores in the samples which may allow some additional drying of the samples during the UCS test.

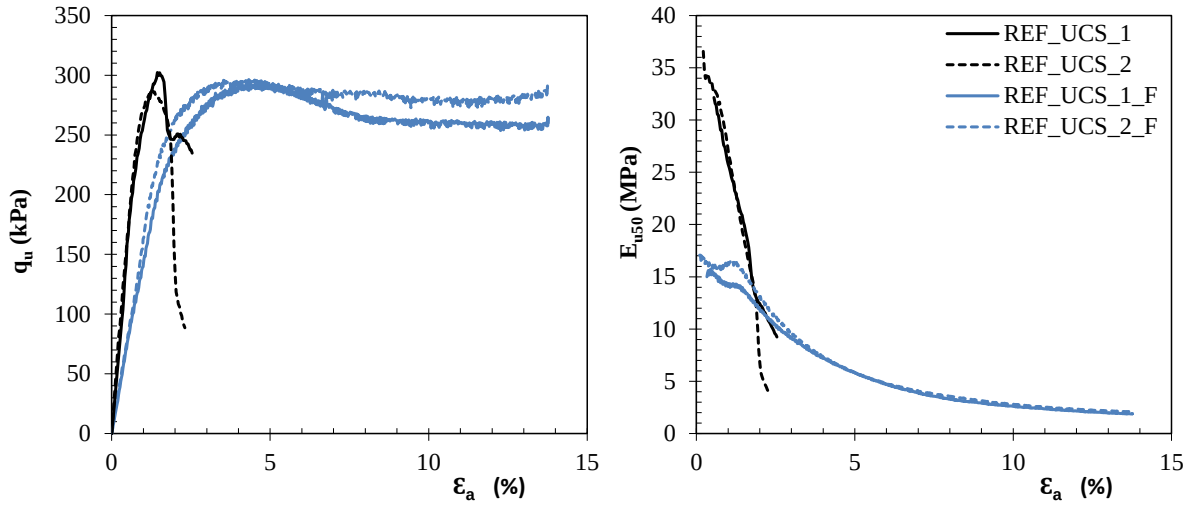

Figure 5.13: UCS reference tests results for stabilised samples without and with polypropylene fibres (0 and 10 kg/m^3): a) Stress–Strain plot; b) E_{u50} vs axial strain

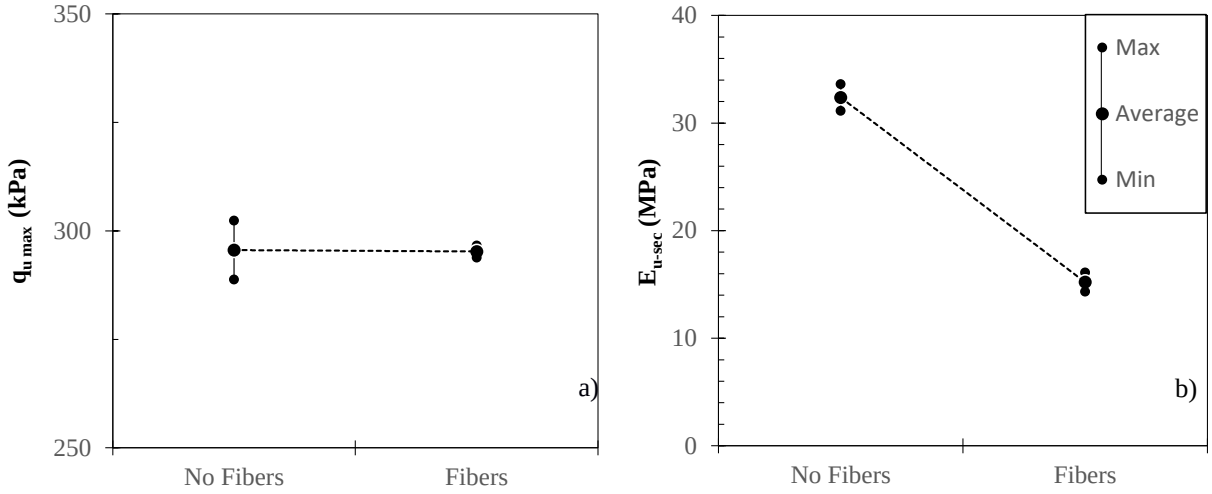

Figure 5.14: Influence of presence of polypropylene fibres in: a) unconfined compressive strength; b) E_{u50}

5.6.2 Split Tensile Strength (STS) reference tests

Table 5.10 and Figure 5.15 shows the results obtained for the STS tests performed on stabilised samples without and with the addition of polypropylene fibres.

Table 5.10: STS reference tests results for stabilised samples without and with polypropylene fibres (0 and 10 kg/m^3)

ID	Load, F (N)	δ_v (mm)	w_f (%)
REF_STS_1	1728	0.74	72.56
REF_STS_2	1640	0.74	72.91
REF_STS_1_F	1539	2.43	71.68
REF_STS_2_F	1451	3.03	71.58

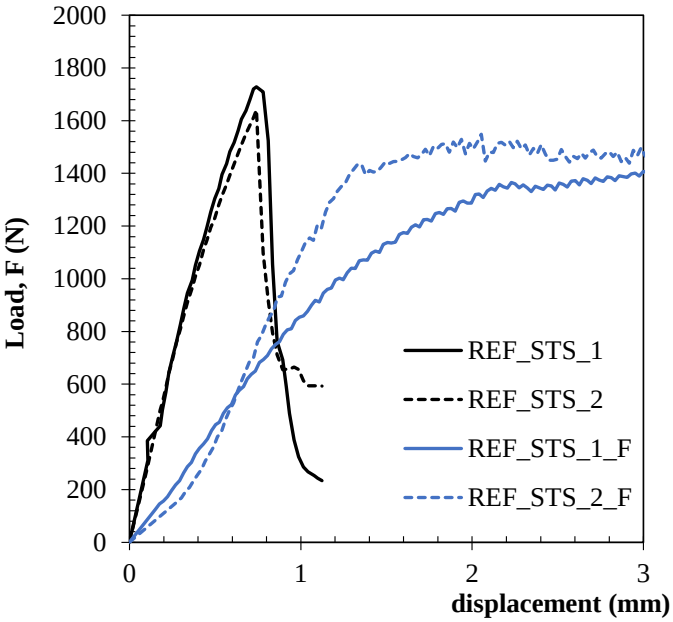

Figure 5.15: Load-displacement curves from STS reference tests for stabilised samples without and with polypropylene fibres (0 and 10 kg/m^3)

In general, the results slightly are in well agreement with the findings for the UCS tests, i.e., the fibres addition promotes a slight decrease of the load capacity (and indirectly, the tensile strength) of the stabilised samples and confers to the material a more ductile behaviour characterized by a progressive increase of the load capacity (without exhibiting an abrupt load loss after the peak) evolving to a considerable residual load capacity. Indeed, the physical presence of the fibres prevents the development of some cementitious bonds within the composite matrix, producing a composite material with lower load capacity. It is important to know the failure mechanism of the STS test which is characterised by an abrupt breakage of the cementation bonds, occurring for small vertical displacements, resulting in a vertical crack/failure plane that divides the samples into two semi-cylinder blocks (Figure 5.16). Taking in consideration these specific features, as the displacement evolves the vertical deformations concentrate on the vertical crack/failure plane which leads to a more effective mobilisation of the tensile strength of the fibres that cross this failure plane, which occurs since the beginning of the test. From Figure 5.15 it can be seen that as the vertical displacement increases the load capacity of the fibre-reinforced samples tends toward a very similar residual load capacity since it was added to the samples an equal quantity of the same fibres type. The results obtained are in well agreement with the findings from Correia et al. (2015), Venda Oliveira et al. (2016), Kaniraj and Havanaji (2001) and Olgun (2013).

Figure 5.16: Failure mechanism imposed in a STS test

Regarding the water content measured immediately after the end of the STS tests, the results follow the same trend as it was observed for the UCS tests, being valid the same explanations.

5.6.3 Direct Tensile Strength (DTS) reference tests

As described in Chapter 4, for the DTS test it is necessary to glue two cylindrical rigid plates to the ends (top and bottom) of the samples (Figure 5.17 a-b), a task that proved to be of some difficulty given the porous and wet nature of the ends of the stabilised samples.

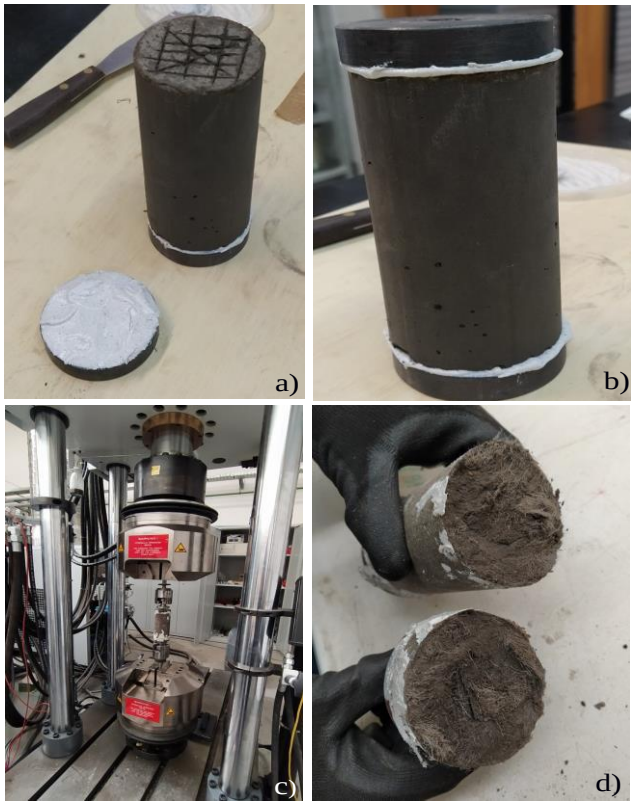

Figure 5.17: Pictures of different stages of DTS test: a) glue preparation; b) cylindrical rigid plates stick to the sample's ends; c) running a DTS test; d) sample after rupture

Indeed, it was necessary to test different glues before a good adhesion/gluing was assured. Once this problem was overcome, the DTS tests were carried out following the procedure described in Chapter 4, and the results are presented in the Table 5.11 and Figure 5.18.

The results of the DTS tests show that the stress-strain curves are characterised by a rapid growth in tensile stress, with tensile failure occurring suddenly with total loss of tensile strength. For the unreinforced stabilised samples, the tensile strength mobilised depends on the tensile strength of the cementitious bonds. However, when fibres are added to the stabilised samples the mechanical tensile behaviour changes substantially with a very significant increase in tensile strength. This tensile strength increase is due to the mobilisation of the tensile strength of the fibres that crosses the "horizontal" failure plane imposed by the DTS test. In Figure 5.17d) it is possible to identify clearly the fibres that were broken by tension, either by fibre breakage (the fibre's tensile strength was exceeded) or by insufficient bonding length of the fibres (pull-out breakage). Similar results were reported by Teles (2013), Custodio (2013) and Venda Oliveira et al. (2016).

Regarding the water content measured immediately after the end of the DTS tests, contrary to the previous reference tests, the water content seems to be not affected by the fibres addition. Perhaps this behaviour may be explained by the fact that after applying the glue it was necessary to wait one hour before running the DTS, which may have led the samples to similar water contents (note that the water content is lower in the DTS test than in the UCS and STS tests).

Table 5.11: DTS reference tests results for stabilised samples without and with polypropylene fibres (0 and 10 kg/m^3)

ID	f_{cd} (kPa)	ε_r (%)	w_f (%)
REF_DTS_1	106.54	0.07	68.97
REF_DTS_2	155.91	0.06	69.71
REF_DTS_1_F	370	0.10	69.65
REF_DTS_2_F	320	0.09	69.71

Comparing the tensile strength directly evaluated in the DTS tests with the strength indirectly evaluated in the STS tests (equation 4.6, unreinforced: f_{cd} = 112.3 or 106.5 kPa; fibre-reinforced: f_{cd} = 100.0 or 94.3 kPa), it is concluded that both tests provide very similar values for unreinforced samples, with substantial differences in the case of fibre-reinforced samples. Such discrepancies may be related to the different failure mechanism of the DTS and STS tests, which mobilize the fibres in a distinct way.

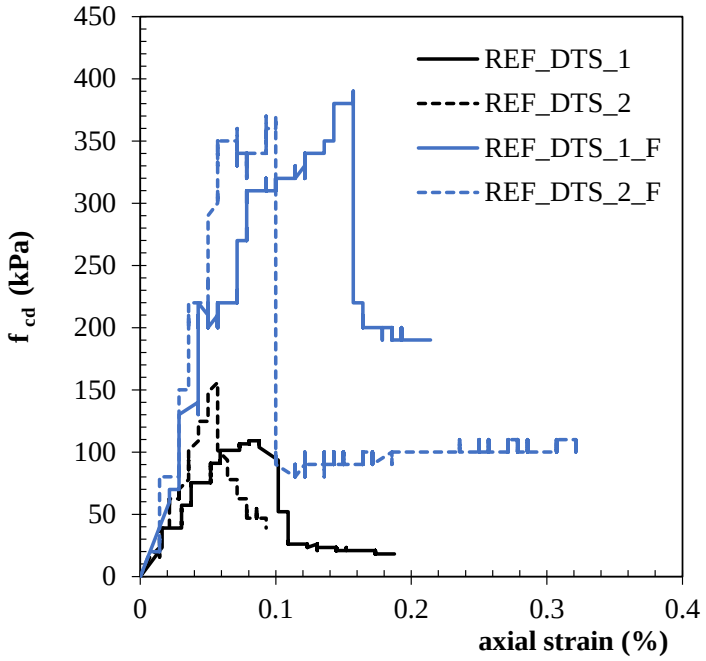

Figure 5.18: Stress–strain curves from DTS reference tests for stabilised samples without and with polypropylene fibres (0 and 10 kg/m^3)

It is important to mention that due to some DTS limitations, namely, the existence of a reduced number of cylindrical rigid plates and the fact that after each use they have to be heated in the muffle furnace to 200ºC followed by a cleaning process with an electric grinder, it was decided to not perform this specific test to characterise the mechanical tensile behaviour of the composite samples.

5.6.4 Flexural Strength (FS) reference tests

As described in Chapter 4, for the flexural (or bending) strength test a vertical load is applied at the middle of the top side/face of a parallelepiped sample, supported by two rollers at the bottom side/face, as presented in Figures 4.16 and 4.17. The FS tests were carried out following the procedure described in Chapter 4, and the results are presented in the Table 5.12 and Figure 5.19.

The results of the FS tests show that the load-vertical displacement curves are characterised by a continuous growth of the load till the peak failure (corresponding to the maximum load capacity or tensile strength if applying equation 4.7). The post-peak behaviour is characterised by an abrupt and total loss of load capacity (or tensile strength) of the composite samples. The results suggest that the addition of fibres to the stabilise samples promotes a decrease of the flexural/bending load-bearing capacity, which may be explained by the fact that only half of the fibres present in the vertical cross-section at mid-span are mobilised, i.e. the fibres on the tensioned side. This mobilisation of half the fibres does not seem to compensate the fact that the physical presence of

the fibres prevents the development of some cementitious bonds within the composite matrix, producing a composite material will lower strength and stiffness. Nevertheless the explanation proposed it is important to mention that the behaviour observed is in contradiction with the findings of Correia et al. (2015) and Venda Oliveira et al. (2016), thus, further FS tests are required. Moreover, as it may be seen in Figure 5.19, the load cell readings exhibit large variations, expressing the lack of sensitivity of the load cell to the values being measured, i.e., the load cell of the testing machine used is not adjusted to the type of material under study (the testing machine is usually used for testing concrete and steel). Thus, it is important to perform new FS tests with an equipment with a load cell suitable for the type of material under study.

Table 5.12: FS reference tests results for stabilised samples without and with polypropylene fibres (0 and 10 kg/m^3)

ID	Load, F (N)	δ_v (mm)	f_{cf} (MPa)	w_f (%)
REF_FS_1	301.24	0.69	135.56	70.43
REF_FS_2	332.30	0.59	149.54	69.13
REF_FS_1_F	137.58	0.45	61.91	68.34
REF_FS_2_F	192.29	0.29	86.53	69.70

Comparing the tensile strength directly evaluated in the DTS tests with the strength indirectly evaluated in the FS tests (Equation 4.7, unreinforced: f_{cf} = 135.6 or 149.5 kPa; fibre-reinforced: f_{cf} = 61.9 or 86.5 kPa), it is concluded that both tests provide very similar values for unreinforced samples, with substantial differences in the case of fibre-reinforced samples. As it was observed for the STS and DTS tests, the discrepancies observed in the FS and DTS tests may be related to the different failure mechanism of these tests, which mobilize the fibres in a distinct way.

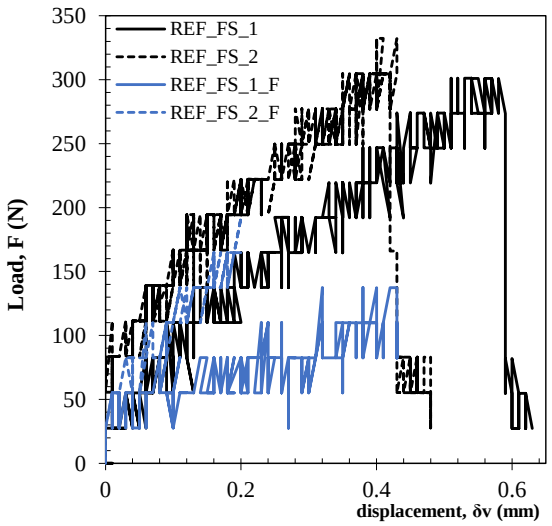

Figure 5.19: Load-vertical displacement curves from FS reference tests for stabilised samples without and with polypropylene fibres (0 and 10 kg/m^3)

Due to the FS limitations described above, related with the load cell sensitivity, and to the difficulty in ensuring that the sides/faces of the parallelepiped samples are perfectly flat, parallel to each other and perpendicular to the axis of the test sample, it was decided to not perform FS tests to characterise the mechanical tensile behaviour of the composite samples.

CHAPTER 6 – CYCLIC LOADING EFFECT - PARAMETRIC STUDY

6.1 Introduction

The presence of the fibres modifies the mechanical behaviour of the stabilised soil from brittle to ductile (e.g., Tang et al., 2010a; Estabragh et al., 2012), while an increase of the residual strength is generally observed due to the mobilisation of the tensile strength of the fibres for higher strain levels (e.g., Tang et al., 2010a; Sukontasukkul & Jamsawang, 2012a). However, this behaviour may change in the presence of cyclic loading induced by different actions, such as traffic loads, industrial machinery, vibrations on offshore structures and even earthquakes.

As stated previously in Chapter 3, based on some experimental studies with chemically stabilised soils unreinforced and fibre-reinforced under cyclic loading it has been observed: (i) an increase in the permanent deformations with the increment of the number of load cycles (Oliveira et al., 2018); (ii) the addition of fibres significantly increases the number of cycles and the magnitude of strain required to cause failure (Maher & Ho, 1993a); (iii) an increase in the unconfined compressive strength with the number of load cycles (Oliveira et al., 2018); and (iv) the effects on the strength depend on the binder content, the length and type of fibre and even the type of test used to evaluate the compressive and/or tensile strength (Correia et al., 2015b).

This Chapter aims to enhance the knowledge about the mechanical behaviour of a soft soil chemically stabilised with Portland cement without and with synthetic fibres under cyclic loading. For such it was developed a laboratory testing program focused on the study of the influence of several parameters of the cyclic loading (number of load cycles, frequency, amplitude, and level of stress of cyclic loading) on the mechanical behaviour of the composite material. The unconfined compressive strength (UCS) and splitting tensile strength (STS) tests presented in Chapter 5 are used as the monotonic reference behaviour.

The cyclic UCS and STS (CYC) tests are performed for different conditions of the cyclic loading, namely changing the following parameters: frequency (0.15, 0.25, **0.5**, 1, 2 and 4 Hz); number of

cycles (1.000, 2.500, **5.000**, 10.000, 50.000 and, 100.000); amplitude (5%, **10%**, 20% of the strength evaluated in the monotonic tests) and finally the level of stress (10%, 25%, **50%**, 75% of the strength evaluated in the monotonic tests). Values in **bold** refer to reference cyclic loading conditions, i.e., these values were kept constant when were studied the other parameters. The cyclic tests are composed of three stages as it will be defined later.

The procedures performed to prepare the samples for the UCS and STS tests are explained in section 4.4.1. All samples involved in the present parametric study were prepared based on the same laboratory procedure, as shown in Chapter 5. That is, samples were stabilised with Portland cement applied in a quantity of 250 kg/m^3, mixed with polypropylene fibres in a quantity of 10 kg/m^3, and cured for 28 days in a room with temperature (20±2ºC) and humidity (95±5%) control.

Along the next sections the results will be presented, beginning with the cyclic reference tests, followed by the parametric study. However, before starting it is important to mention that due to the experimental nature of the study, there is some scattering between the results of the different samples. Note that even when the laboratory procedure is followed strictly to make a homogenous composite material, the random distribution of fibres within the samples may result in certain local heterogeneities. Nevertheless, in this study, as it will be demonstrated, the variability of results is not statistically significant and is consistent with other findings published in the literature (Khattak & Alrashidi, 2006; Consoli et al., 2010; Correia et al., 2015a; Venda Oliveira et al., 2016; Venda Oliveira et al., 2018a; Huang et al., 2020; Duong et al., 2021).

6.2 Reference Cyclic Loading Tests

Before starting the parametric study, it is necessary to establish the base conditions of the cyclic loading tests, as shown in Table 6.1. These parameters are defined based on previous studies and experience acquired at the University of Coimbra (Cajada, 2018; Goulart, 2020; Anunciação, 2020; Venda Oliveira, 2018) and on equipment limitations (described in Chapter 4).

According to Table 6.1, the number of cycles defines the number of loading cycles that the cyclic stage will have, the frequency defines the speed of the cyclic load applied (number of times that the load repeats per second, measured in Hertz), the stress/load level is defined as the ratio of the cyclic stress/load applied and the strength evaluated by the UCS or STS tests ($q_{u\ cyc}/q_{u\ max}$ or F_{cyc}/F_{max} for UCS and STS tests, respectively), and the amplitude is defined as the variation (±) of the cyclic stress/load regarding to the stress/load level applied ($\Delta q_{u\ applied}/q_{u\ max}$ or $\Delta F_{applied}/F_{max}$ for UCS and STS tests, respectively).

Table 6.1: Base conditions for cyclic loading tests (REF_{cyc})

Number of Loading Cycles (NLC)	5000
Frequency (Hz)	0.5
Stress level/Load (%)	50
Amplitude (%)	±10

6.2.1 Cyclic test procedure

After the 28 days of cure have elapsed, and after obtaining the results of $q_{u\ max}$ from the UCS test and F_{max} in the case of STS tests (reference values) described in Chapter 5, the samples are extracted from the PVC moulds, cut to have an height/diameter ratio of 2 (for UCS and STS tests) and both bases are rectified to be flat and normal to the sample axis. After weighting the sample, it is then subjected to the cyclic test (UCS_{cyc} or STS_{cyc}), carried out in the ELDYN triaxial apparatus (Figure 6.1) with a load cell capacity of 10 kN with an accuracy of 5 N, whose maximum working frequency is 5 Hz. Further details of this equipment are given in Chapter 4. The cyclic test is composed of three stages (Figure 6.2): first the sample is loaded monotonically up to a specified stress/load level (defined as a percentage of the compressive or tensile strength evaluated previously in UCS or STS tests, Chapter 5) - pre-cyclic stage; immediately after the cyclic stage begins, carried out for specific conditions (parameters) of the cyclic loading (frequency, number of cycles, stress level and amplitude) - cyclic stage; when the cyclic stage ends, the sample is monotonically discharged and then monotonically charged to failure/rupture (UCS post-cyclic, UCS_{pc} or STS post-cyclic, STS_{pc}) - post-cyclic stage. In all stages, the load and the vertical displacement are automatically recorded.

a) b)

Figure 6.1: Pictures of the equipment ELDYN

The cyclic loading test parameters, i.e., cyclic load amplitude, cyclic load frequency, number of loading cycles and stress level, are introduced directly in the GDSLAB software, allowing the cyclic test (the three stages) to be performed automatically. The cyclic loading test is a load/stress-controlled test, therefore it is of upmost importance to ensure that the applied load/stress during

the cyclic stage corresponds to the specified values, i.e., the accuracy of the ELDYN equipment must be checked. As it may be seen in Figure 6.3, the ELDYN equipment can apply with high accuracy the cyclic load specified (load/stress level) with a constant amplitude over time. Indeed, the cyclic load/stress level is applied in a sinusoidal manner, reaching major and minor peaks characterised by the amplitude of the cyclic loading. That is, the ELDYN equipment (sensors and software) has a high accuracy and a high rate reading acquisition, allowing not only the load acquisition but also the vertical displacement acquisition that will be used to analyse the vertical strain accumulated during the cyclic loading stage as illustrated in Figure 6.4.

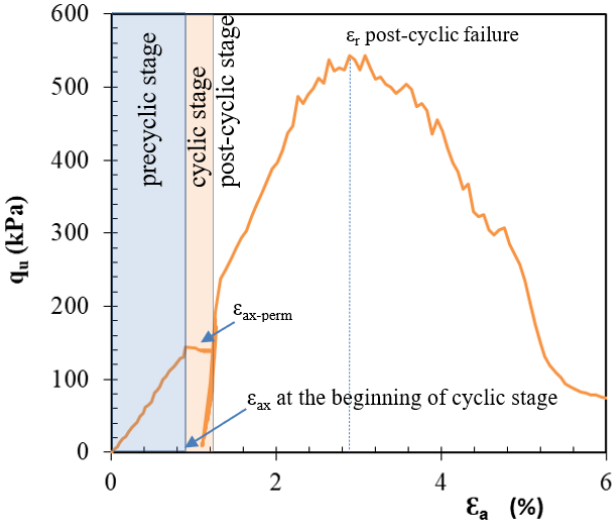

Figure 6.2: Example of the stages in an UCS cyclic loading test

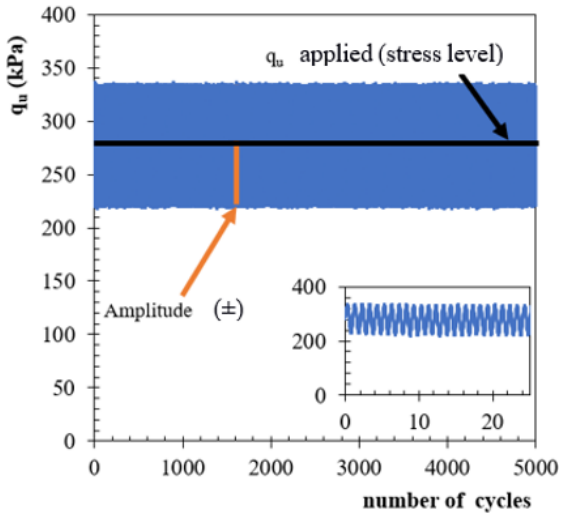

Figure 6.3: Example of the evolution of the cyclic loading during the cyclic stage in an UCS cyclic test

In order to simplify the reading and interpretation of the cyclic loading results, a representative line of the average mean load/stress and/or vertical displacement/strain measured during the cyclic stage will be used in this Chapter.

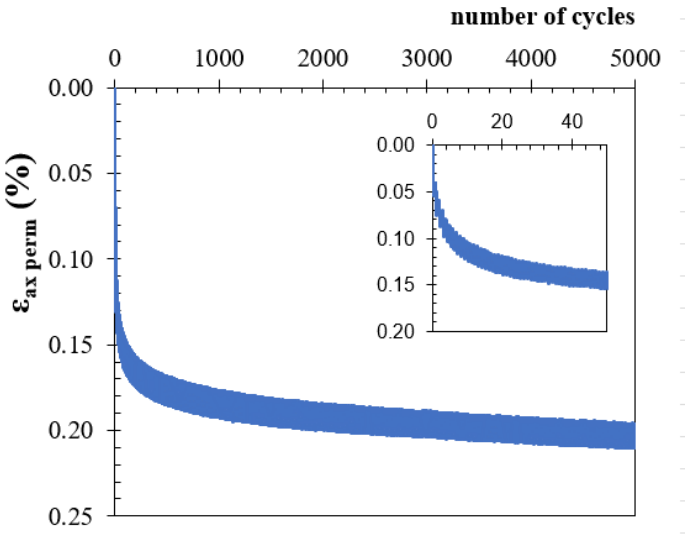

Figure 6.4: Example of the evolution of the permanent axial strain during the cyclic stage in an UCS cyclic test

6.2.2 UCS cyclic reference tests

The present section aims to study the behavior in compression of the stabilised soil unreinforced and fibre-reinforced under cyclic loading, for the reference cyclic loading parameters (Table 6.1), i.e., for a number of loading cycles of 5.000, a frequency of 0.5 Hz, a stress level of 50% of $q_{u\ max}$ (147.8 and 147.63 kPa for unreinforced and fibre-reinforced, respectively, as described in Chapter 5), and an amplitude of ± 10% of $q_{u\ max}$ (± 29.6 and ± 29.5 kPa for unreinforced and fibre-reinforced, respectively, as described in Chapter 5). Figure 6.5 show the results of the UCS cyclic reference tests for unreinforced and fibre-reinforced samples, with a zoom on the transition region between the UCS cyclic stages.

Table 6.2 and Figure 6.6 summarise the results of the reference UCS tests for both conditions, without cyclic loading (UCS tests presented in Chapter 5) and after the cyclic loading (post-cyclic UCS tests, $UCS_{pc.}$ The results clearly show that the application of loading cycles increases the strength of the composite material in comparison with the reference monotonic tests on stabilised samples unreinforced and reinforced with fibres.

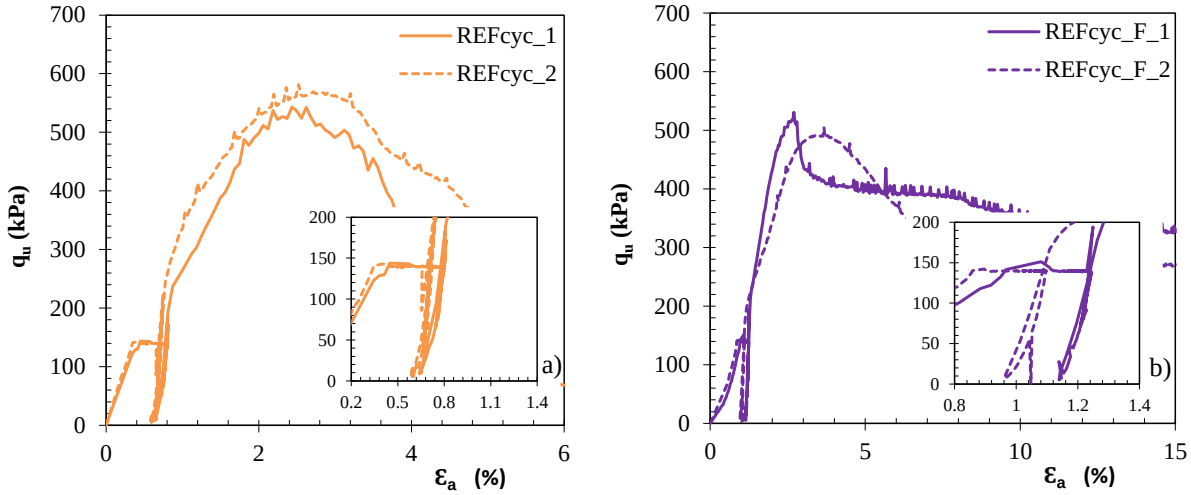

Figure 6.5: Stress-strain curve for UCS cyclic reference tests for samples: a) without fibres b) reinforced with fibres (CI42.5 R; binder quantity = 250 kg/m^3; curing time = 28 days; curing conditions: vertical stress = 0 kPa, room)

Table 6.2: Results of the UCS and UCS$_{pc}$ reference tests performed on stabilised samples unreinforced and reinforced with fibres under monotonic and cyclic loading (CI42.5 R; binder quantity = 250 kg/m^3; curing time = 28 days; curing conditions: vertical stress = 0 kPa, room)

ID	test	$q_{u\ max}$ (kPa)	ε_r (%)	E_{u50} (MPa)	w_f (%)
REF_UCS_1	UCS	302.36	1.45	33.29	71.56
REF_UCS_2	UCS	288.80	1.25	33.92	71.86
REF_UCS_1_F	UCS	293.87	4.55	14.32	70.62
REF_UCS_2_F	UCS	296.65	4.03	16.10	70.56
REF_UCSpc_1	UCSpc	543.17	1.73	91.28	69.1
REF_UCSpc_2	UCSpc	581.26	1.88	139.15	69.57
REF_UCSpc_1_F	UCSpc	531.01	1.59	79.89	72.76
REF_UCSpc_2_F	UCSpc	504.69	2.70	54.37	70.48

In Figure 6.6a it is clearly seen that the reference UCS tests and post-cyclic UCS tests, while in Figure 6.6b, there is a clear relationship of increased initial stiffness also as can be seen from the values in the table presented above.

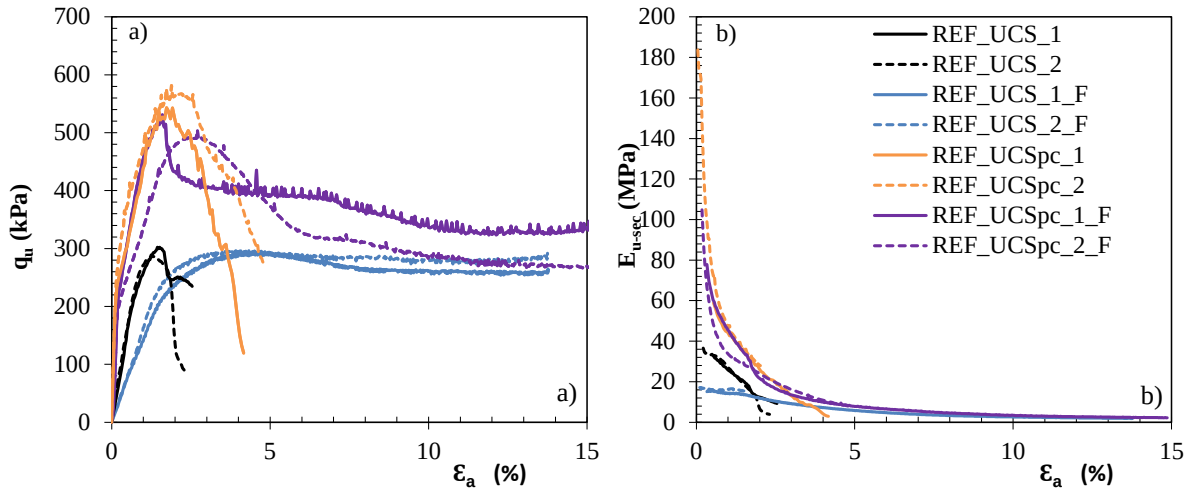

Figure 6.6: Results of the UCS and UCS$_{pc}$ reference tests performed on stabilised samples unreinforced and reinforced with fibres: a) stress-strain plot; b) $E_{u\text{-}sec}$ vs axial strain (CI42.5 R; binder quantity = 250 kg/m3; curing time = 28 days; curing conditions: vertical stress = 0 kPa, room)

The water contents measured after the end of the UCS_{pc} tests reveal a decrease as the post-cyclic occurs, which may be explained by the time elapsed during the cyclic stage (5.000 cycles = 2.78h) during which the samples dried. This fact can induce some suction effects that contribute to increasing the composite material's strength. Figure 6.7 shows the results for the maximum unconfined strength and for E_{u50}.

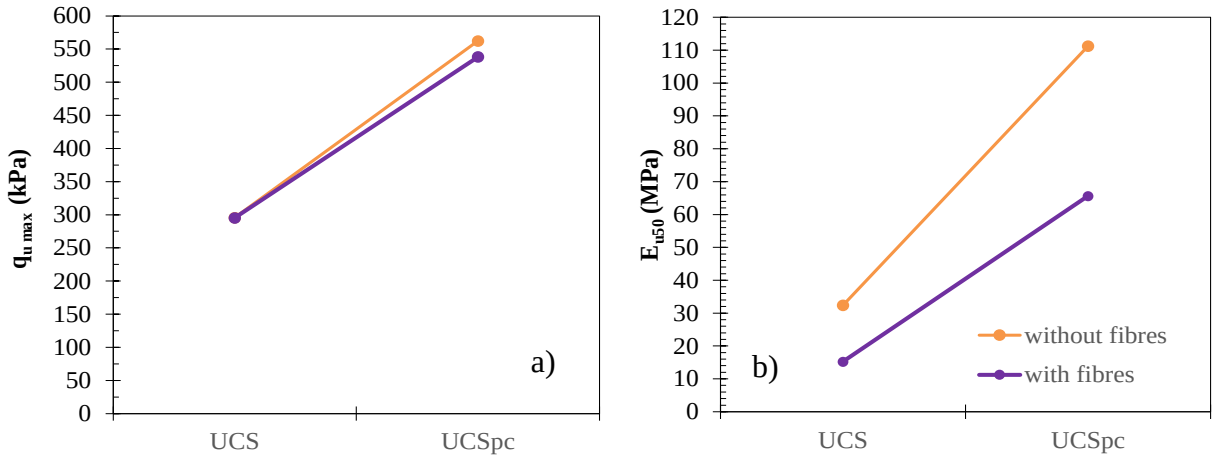

Figure 6.7: Results of the UCS and UCS_{pc} reference tests performed on stabilised samples unreinforced and reinforced with fibres - impact of the cyclic loading stage on the: a) strength; b) E_{u50} (CI42.5 R; binder quantity = 250 kg/m^3; curing time = 28 days; curing conditions: vertical stress = 0 kPa, room)

The evolution of the permanent axial strain on stabilised samples unreinforced and reinforced with fibres (Figure 6.8) is characterised by a quick increase in the first 500 load cycles followed by a slight increase for a higher number of load cycles.

Regarding the unreinforced samples, the fact that the solid skeleton of the composite material is quite hard and stiff the beginning of the cyclic stage is characterised by a quick increase in the permanent (plastic) strain due to some local breakage of the cementitious bonds, evolving gradually as the cycles increase. As expected, the degradation of the solid matrix contributes to the plastic deformation as well. In Figure 6.8 is possible to observe a progressive decrease of plastic deformations, with the increase of the loading cycle numbers, which can be interpreted as a more “elastic” phase of the material, where only a reduce number of cementitious bonds are broken at each new cycle.

In the case of the reinforced with fibres samples, the fibres are able to absorb and redistribute part of the stress induced by the cyclic loading, which results in a much lower permanent axial strain, avoiding the breakage of some cementitious bonds and the consequent deterioration of the solid

skeleton. It is understood that the fibres help to decrease the accumulated axial deformation, and this is consistent with other studies (Cajada, 2018; Goulart, 2020; Venda Oliveira, 2017).

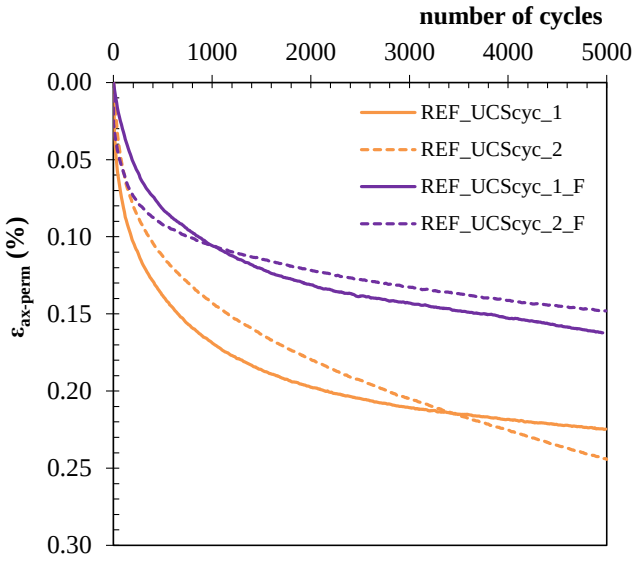

Figure 6.8: Evolution of the permanent axial strain during the cyclic stage of UCS reference tests (frequency = 0.5 Hz; number of cycles = 5.000; amplitude = 10%*$q_{u\ max}$; stress level = 50%*$q_{u\ max}$)

Table 6.3: Measurement of the axial strain during all the stages of the UCS cyclic reference tests

	REFcyc_1	REFcyc_2	REFcyc_1_F	REFcyc_2_F
ε_a (50%-$q_{u\ max}$) (%) (a)	1.02	0.96	1.08	0.94
$\varepsilon_{a\ perm}$ (%) (b)	0.22	0.24	0.16	0.15
ε_r poscyclic (%) (c)	1.73	2.12	2.59	2.7
ε_r final (%) (a+b+c)	2.97	3.32	3.83	3.79

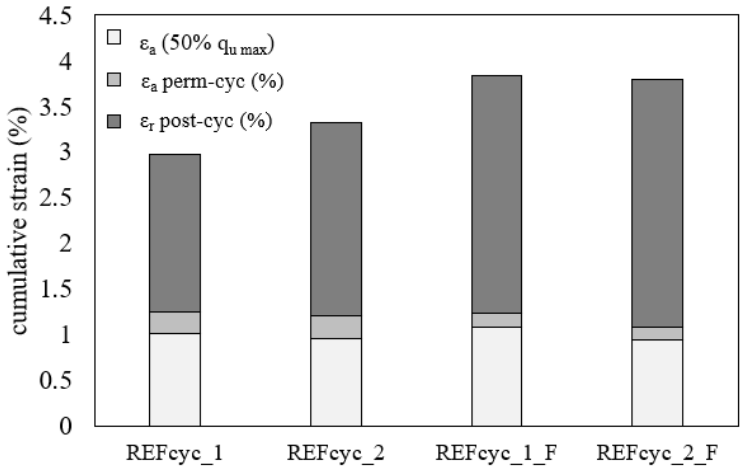

Figure 6.9: Cumulative axial strain during the UCS cyclic reference tests

Figure 6.9 depicts the cumulative strain ($\varepsilon_{ax\ final}$) with unreinforced samples and reinforced with fibres samples for the UCS, UCScyc and UCSpc tests performed. The results indicate that the increase in the $\varepsilon_{ax\ final}$ seems to be linked with the permanent deformation observed during the cyclic stage (mild gray), i.e., small deformations in the cyclic stage which allows, in the case of fibre-reinforced samples, an earlier mobilisation of the fibres which may lead to greater $\varepsilon_{ax\ final}$ in

the post-cyclic tests. That is also related with the change of behaviour from fragile to ductil given to the composite material a non negligible residual strength.

6.2.3 STS cyclic reference tests

The present section aims to study the behavior in compression of the stabilised soil unreinforced and fibre-reinforced under cyclic loading for the reference cyclic loading parameters, i.e., for a number of loading cycles of 5.000, a frequency of 0.5 Hz, a stress level of 50% of F_{max} (840 N and 750 N for unreinforced and fibre-reinforced, respectively, as described in Chapter 5), and an amplitude of ± 10% of F_{max} (±84 N and ±75 N for unreinforced and fibre-reinforced, respectively, as described in Chapter 5). Below are the plots (Figure 6.10 and 6.11) of the STS cyclic reference tests for unreinforced and fibre-reinforced samples, with a zoom on the transition region between the STS cyclic stages.

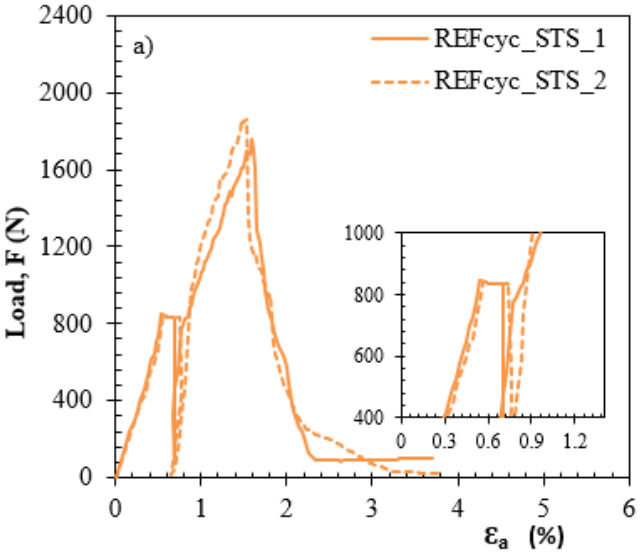

Figure 6.10: Load-displacement curves for STS cyclic reference tests for unreinforced samples (CI42.5 R; binder quantity = 250 kg/m^3; curing time = 28 days; curing conditions: vertical stress = 0 kPa; room)

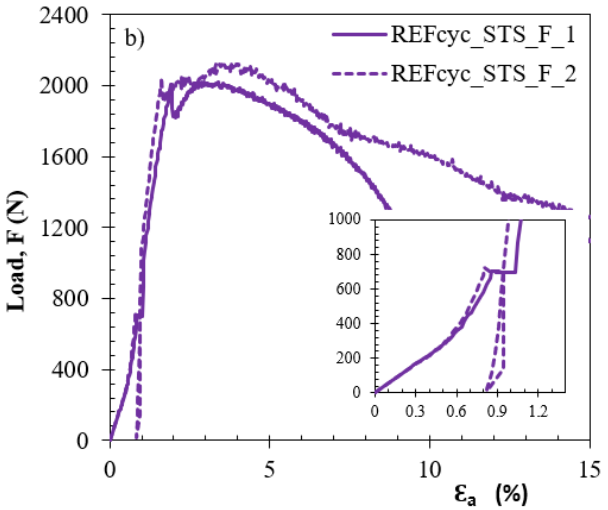

Figure 6.11: Load-displacement curves for STS cyclic reference tests for samples reinforced with fibres (CI42.5 R; binder quantity = 250 kg/m^3; fibres = 10 kg/m3; curing time = 28 days; curing conditions: vertical stress = 0 kPa; room)

Table 6.4 and Figure 6.12 summarise the results of the STS reference tests for both conditions, without cyclic loading (STS tests presented in Chapter 5) and after the cyclic loading (post-cyclic STS tests, STS_{pc}). Figure 6.13 shows the results for the maximum load.

Table 6.4: Results of the STS and STS_{pc} reference tests performed on stabilised samples unreinforced and reinforced with fibres (CI42.5 R; binder quantity = 250 kg/m^3; curing time = 28 days; curing conditions: vertical stress = 0 kPa, room)

ID	Stage	Load, F (N)	δv (mm)	w_f (%)
REF_STS_1	STS	1728	0.74	72.56
REF_STS_1	STS	1640	0.74	72.91
REF_STS_1_F	STS	1539	2.43	71.68
REF_STS_2_F	STS	1451	4.48	71.58
REF_STSpc_1	STSpc	1756.2	0.92	71.37
REF_STSpc_2	STSpc	1863.8	0.85	68.37
REF_STSpc_1_F	STSpc	2121.3	3.00	72.15
REF_STSpc_2_F	STSpc	2022.2	2.40	71.24

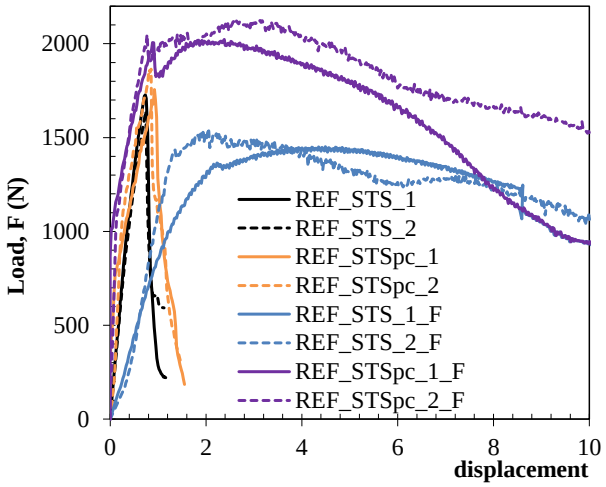

Figure 6.12: Load-displacement curves of the STS and STS_{pc} reference tests performed on stabilised samples unreinforced and reinforced with fibres (CI42.5 R; binder quantity = 250 kg/m^3; curing time = 28 days; curing conditions: vertical stress = 0 kPa, room)

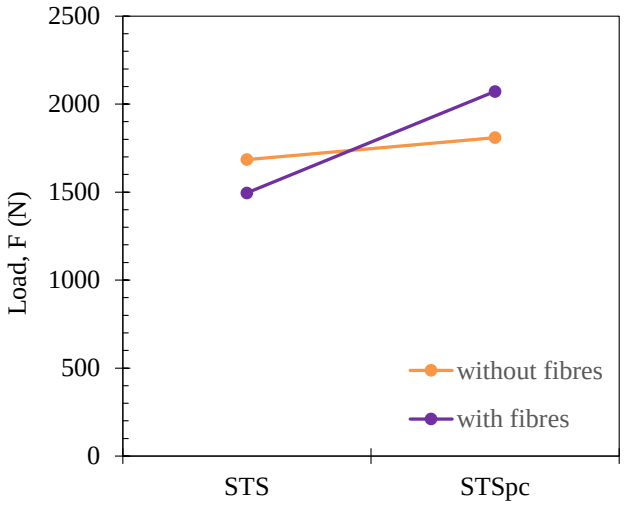

Figure 6.13: Results of the STS and STS_{pc} reference tests performed on stabilised samples unreinforced and reinforced with fibres - impact of the cyclic loading stage on the load/strength (CI42.5 R; binder quantity = 250 kg/m3; curing time = 28 days; curing conditions: vertical stress = 0 kPa; room)

The results reveal that the application of load cycles increases the strength/load of the stabilised unreinforced and reinforced with fibres in comparison with the reference monotonic tests.

The enhancement on the strength/load can be related with the load cycles performed, or better, with the permanent deformation occurred during the cycle stage. A larger deformation that occur during the cyclic stage in the fibre-reinforced samples allow an earlier mobilisation of the fibres, thus contributing to the strength/load increase. Indeed, for the STS tests, the vertical deformations concentrate on the vertical crack/failure plane which leads to a higher level of deformation with a more effective mobilisation of the fibres that cross this failure plane. Furthermore, as observed in Chapter 5 also, an earlier mobilisation of the fibres induced by the deformations occurring during the cyclic stage allows a load increase when compared to the unreinforced samples.

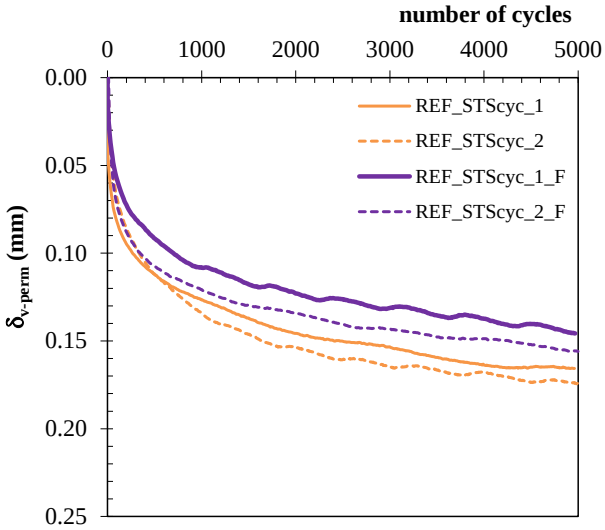

Figure 6.14: Evolution of the permanent vertical displacement during the cyclic stage of STS reference tests (frequency = 0.5 Hz; number of cycles = 5.000; amplitude = 10%*$q_{u\,max}$; stress level = 50%* $q_{u\,max}$)

Table 6.5: Measurement of the vertical displacement during all the stages of the STS cyclic reference tests

	REF_STS_1	REF_STS_2	REF_STS_1_F	REF_STS_2_F
δ_v (50% - F_{max}) (mm) (a)	0.92	0.74	1.35	1.18
δ_v perm-cyc (mm) (b)	0.16	0.16	0.14	0.15
$\delta_{v\,rupt}$ post-cyc (mm)	1.43	1.28	3.47	4.52
$\delta_{v\,rupt}$ final (mm)	2.51	2.18	4.96	5.85

Figure 6.15 depicts the cumulative vertical deformation ($\delta_{v\,rupt\,final}$) with unreinforced samples and reinforced with fibres samples for the STS, STS_{cyc} and STS_{pc} tests performed. The results suggest that the increase in the final vertical deformation to be linked with the permanent deformation observed during the cyclic stage (mild gray), i.e., higher deformations in the cyclic stage (fibre-reinforced samples) allows an earlier mobilisation of the fibres which may lead to greater $\delta_{v\,rupt\,final}$ in the post-cyclic tests.

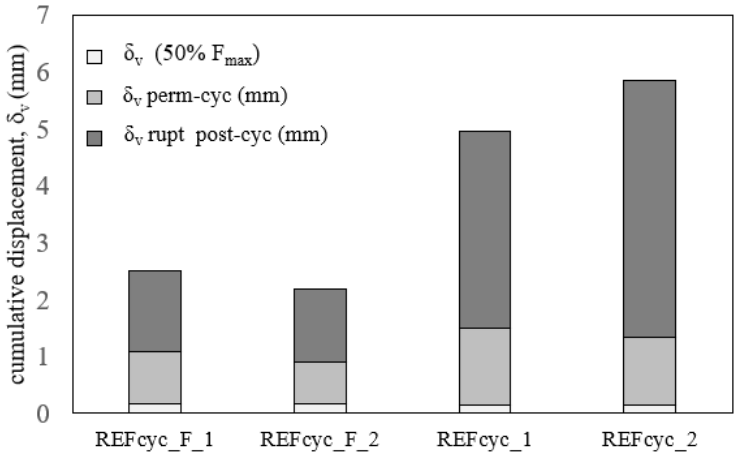

Figure 6.15: Cumulative vertical displacement during the STS cyclic reference tests

6.3 Parametric study – effect of the number of loading cycles

In order to study the effect of the loading cyclic on the mechanical behaviour of the soft soil of Baixo Mondego chemically stabilised unreinforced or reinforced with polypropylene fibres a series of UCS and STS tests under cyclic loading was designed changing the number of the loading cycles (1.000, 2.500, 5.000, 10.000, 50.000, 100.000), while it was kept constant the cyclic loading frequency (0.5 Hz), the level of stress (50% of the strength/load evaluated by the monotonic tests) and the amplitude (10% of the strength/load evaluated by the monotonic tests). For such it will be studied the evolution of the permanent axial strain (for UCS cyclic tests) and the permanent vertical displacement (for STS cyclic tests) occurred during the cyclic stage, complemented by the stress-strain curves (for UCS post-cyclic) and the load-displacement curves (for STS post-cyclic). The results from the UCS and STS cyclic tests are presented below for both materials, starting with the soft soil of Baixo Mondego chemically stabilised without fibres, followed by the case where polypropylene fibres were added as reinforcing elements.

6.3.1 Chemically stabilised unreinforced soft soil

Table 6.6 and Figures 6.16, 6.17 and 6.18 summarise the results obtained during the cyclic stage of the UCS and STS cyclic tests for different numbers of loading cycles. As it may be seen from Figures 6.16 and 6.17, the evolution of the permanent deformation (axial strain or vertical displacement for UCS and STS cyclic tests, respectively) is characterised by a quick increase in the first 500 load cycles followed by a slight increase for a higher number of load cycles. However, it was observed that after 20.000 load cycles the permanent deformation shows an increase of the deformation rate. The result of the permanent deformation follows a similar trend independently of the number of load cycles, showing that the permanent deformation increases with the number of load cycles, apart from some variability inherent to the laboratory tests. Due to the fact that the

solid skeleton of the composite material is quite hard and stiff, the increase in the permanent (or plastic) deformation is probably linked to some local breakage of the cementitious bonds, evolving gradually as the number of load cycles increases. The results suggest that the plastic deformations are intense at an early stage, which corresponds to a significant degradation of the solid matrix. Afterwards there is a progressive decrease of plastic deformations, which can be interpreted as a more "elastic" phase of the material, where only a reduced number of cementitious bonds are broken at each new cycle.

Table 6.6: Maximum permanent axial strain and permanent vertical displacement during the cyclic stage of the UCS and STS cyclic tests

ID	NLC	$\varepsilon_{ax\text{-}perm}$ (%)	$\delta_{v\text{-}perm}$ (mm)
UCScyc_1K_1	1000	0.17	-
UCScyc_2.5K_1	2500	0.21	-
REF_UCScyc_1 (5K)	5000	0.22	-
REF_UCScyc_2 (5K)	5000	0.24	-
UCScyc_10K_2	10000	0.26	-
UCScyc_50K_1	50000	1.56	-
UCScyc_100K_1	100000	1.99	-
STScyc_1K_1	1000	-	0.14
STScyc_1K_2	1000	-	0.12
STScyc_2.5K_1	2500	-	0.19
STScyc_2.5K_1	2500	-	0.22
REF_STScyc_1 (5K)	5000	-	0.20
REF_STScyc_2 (5K)	5000	-	0.22
STScyc_10K_1	10000	-	0.21

NLC: Number of loading cycles

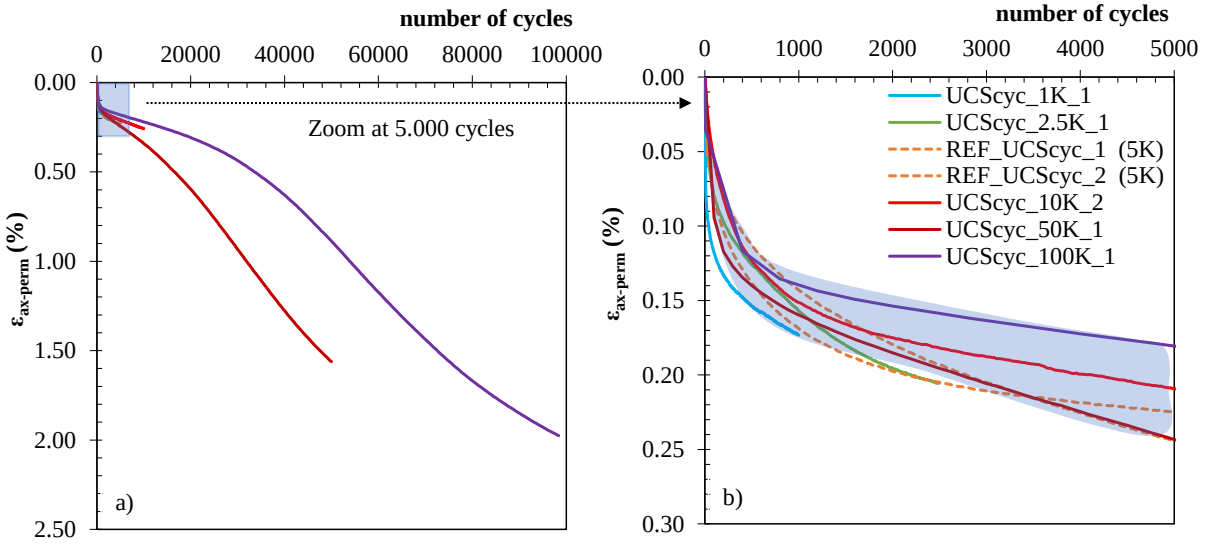

Figure 6.16: Evolution of the permanent axial strain during the cyclic stage (UCS_{cyc}) for unreinforced samples a) at 100.000 cycles; b) scaled at 5.000 cycles (frequency = 0.5 Hz; amplitude = ±10%*$q_{u\ max}$; stress level = 50%*$q_{u\ max}$)

However, with the evolution of the permanent deformation and when a certain threshold of the number of load cycles is exceeded, the plastic deformations intensify again due to the

breakage/degradation of other cementitious bonds of the composite material, evolving the composite material progressively towards failure - this type of behaviour is not seen in STS test - (although it has not been reached in any test).

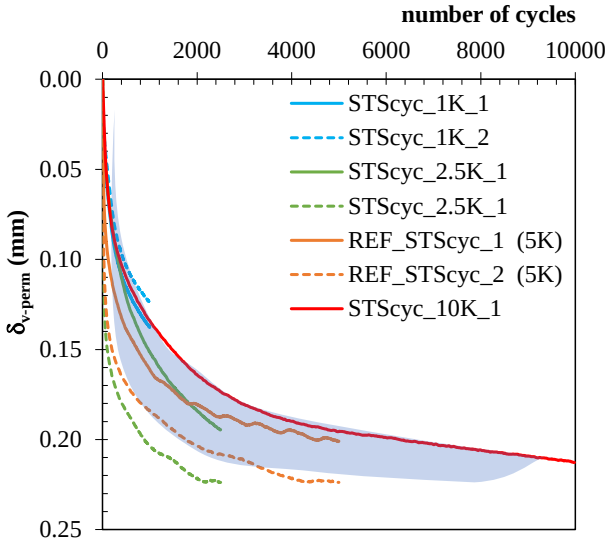

Figure 6.17: Evolution of the permanent vertical displacement during the cyclic stage in STS_{cyc} tests (frequency = 0.5 Hz; amplitude = ±10%*F_{max}; stress level = 50%*F_{max})

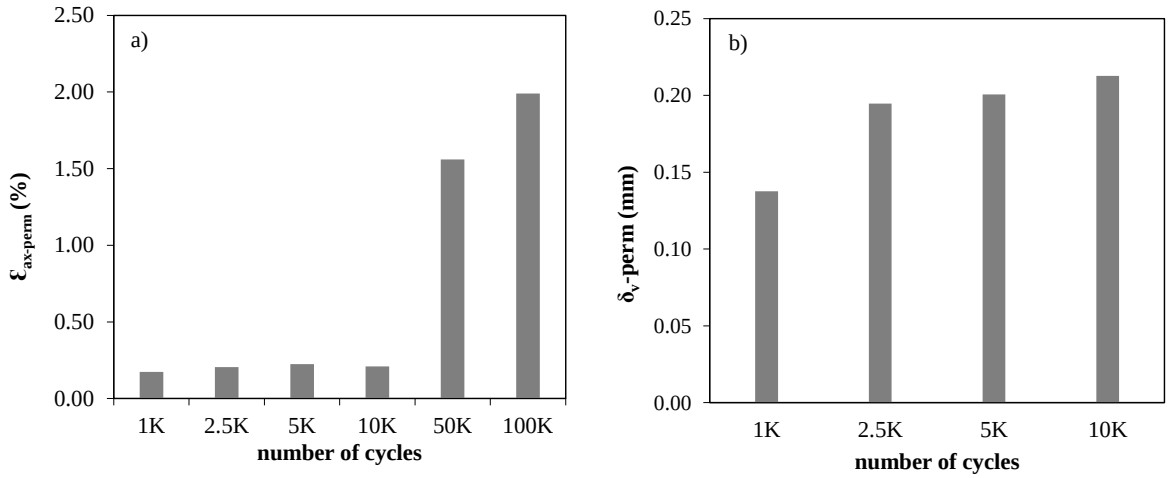

Figure 6.18: Evolution of maximum permanent axial strain/permanent vertical displacement vs the number of loading cycles for unreinforced samples a) UCS_{cyc}, b) STS_{cyc}

Tables 6.7 and 6.8 and Figures 6.19, 6.20 and 6.21 summarise the results obtained during the post-cyclic UCS and STS tests performed immediately after the cyclic stage where the number of loading cycles was changed. The results clearly show that the application of loading cycles increases the strength/load of the composite material in comparison with the reference monotonic tests. This increase appears to be related with the number of load cycles performed, with more cycles resulting in higher strength/load. However, the number of load cycles seems to have a lower impact on the post peak strength since the results exhibit a similar trend to that obtained from the monotonic tests, characterised by an almost total loss of strength. The water contents measured

after the end of the UCS_{pc} or STS_{pc} tests reveal a decrease as the number of load cycles increase, which may be explained by the time elapsed during the cyclic stage (1.000 cycles = 0.55h; 5.000 cycles = 2.78h; 100.000 cycles = 55.55h), i.e.during this stage the samples tend to dry. This fact can induce some suction effects that contribute to increasing the composite material's strength/load.

Figure 6.19 depicts the evolution of the unconfined compressive stress (q_u) and the undrained secant modulus ($E_{u\ sec}$) with the number of loading cycles for the UCS_{pc} tests performed. The results reveal that the increase in the compressive strength/stiffness with the number of loading cycles seems to be linked with the permanent deformation observed during the cyclic stage, i.e., greater deformations in the cyclic stage lead to greater strengths/stiffness in the post-cyclic tests. This trend does not reflect the expected breakage of the cementation bonds and the consequent decay of the compressive strength/stiffness which may be explained by two cumulative effects: i) suction effects due to samples dry during the cyclic stage; ii) the breakage of cementitious bonds observed in the cyclic stage can lead to a coarser apparent grain size, i.e., the permanent deformation occurred during the cyclic stage are high enough to have some well-defined rougher cracks, thus leading to a greater strength. Regarding the STS_{pc} tests (Figure 6.20 and 6.21), it was observed also that a greater deformation in the cyclic stage leads to greater load capacity in the post-cyclic tests mainly after 10.000 cycles, which once again does not explain the expected degradation of the mechanical characteristics. For this specific test, it is important to know the failure mechanism is characterised by an abrupt breakage of the cementation bonds, occurring for small vertical displacements, resulting in a vertical crack/failure plane that divides the samples into two semi-cylinder blocks. Considering the specific features of the failure mechanism of the STS test, it is expected that suction effects will prevail over coarser apparent grain size effects (or rougher vertical crack effects), thus justifying the increase of the load observed in the STS_{pc} tests.

Table 6.7: Results of the UCS and UCS_{pc} tests performed on unreinforced stabilised samples (CI42.5 R; binder quantity = 250 kg/m^3; curing time = 28 days; curing conditions: vertical stress = 0 kPa, room)

ID	NLC	$q_{u\ max\ (kPa)}$	ε_r (%)	E_{u50} (MPa)	w_f (%)
REF_UCS_1	-	302.36	1.45	33.29	71.56
REF_UCS_2	-	288.80	1.25	33.92	71.86
UCSpc_1K_1	1000	452.44	1.54	82.25	71.68
UCSpc_2.5K_1	2500	557.00	1.84	68.34	71.10
REF_UCSpc_1 (5K)	5000	543.17	1.73	91.28	69.1
REF_UCSpc_2 (5K)	5000	581.26	1.88	139.15	69.57
UCSpc_10K_1	10000	612.62	1.53	104.04	69.14
UCSpc_50K_1	50000	1707.95	1.02	291.35	61.68
UCSpc_100K_1	100000	1934.67	1.17	321.27	58.57

NLC: Number of loading cycles

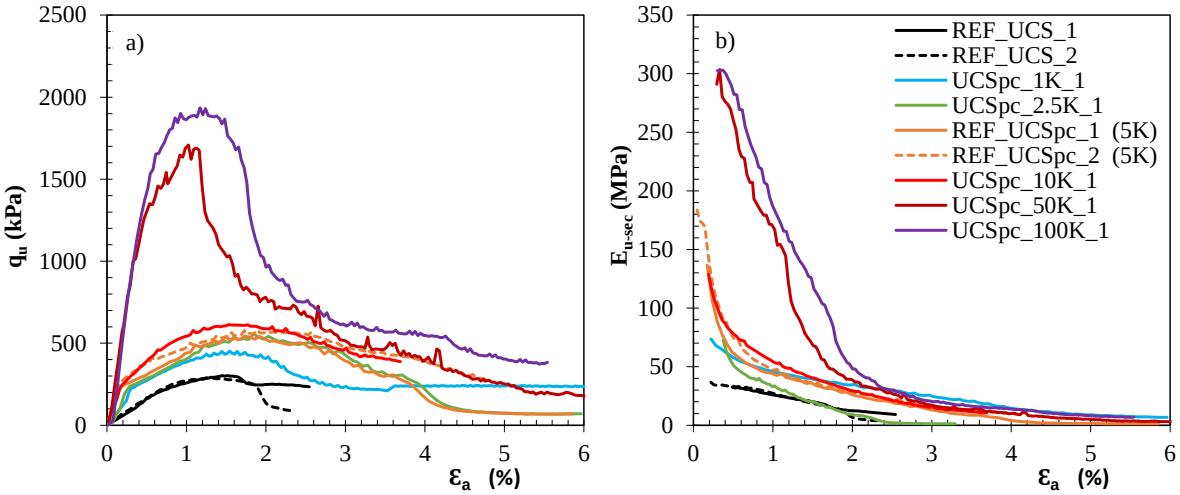

Figure 6.19: Results of the UCS and UCS_{pc} tests performed on unreinforced stabilised samples: a) stress-strain plot; b) $E_{u\text{-}sec}$ vs axial strain (CI42.5 R; binder quantity = 250 kg/m^3; curing time = 28 days; curing conditions: vertical stress = 0 kPa, room)

Table 6.8: Results of the STS and STS_{pc} tests performed on unreinforced stabilised samples (CI42.5 R; binder quantity = 250 kg/m^3; curing time = 28 days; curing conditions: vertical stress = 0 kPa, room)

ID	NLC	Load, F(N)	disp, δ_v (mm)	w_f (%)
REF_STS_1	-	1728	0.74	72.56
REF_STS_2	-	1640	0.74	72.91
STSpc_1K_1	1000	1657.30	0.74	77.64
STSpc_1K_2	1000	1892.44	0.92	78.58
STSpc_2.5K_1	2500	1799.49	0.61	73.10
STSpc_2.5K_1	2500	1755.31	1.00	73.10
REF_STSpc_1 (5K)	5000	1863.8	0.85	68.37
REF_STSpc_2 (5K)	5000	1756.2	0.92	71.37
STSpc_10K_1	10000	2219.87	1.20	72.73

NLC: Number of loading cycles

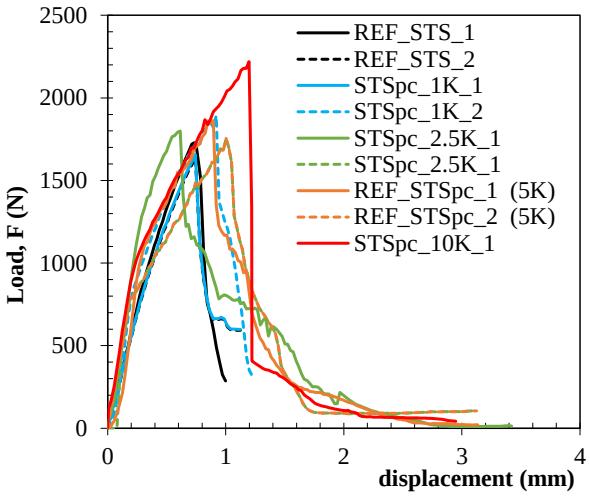

Figure 6.20: Load-displacement curves of the STS and STS_{pc} tests performed on unreinforced stabilised samples (CI42.5 R; binder quantity = 250 kg/m^3; curing time = 28 days; curing conditions: vertical stress = 0 kPa, room)

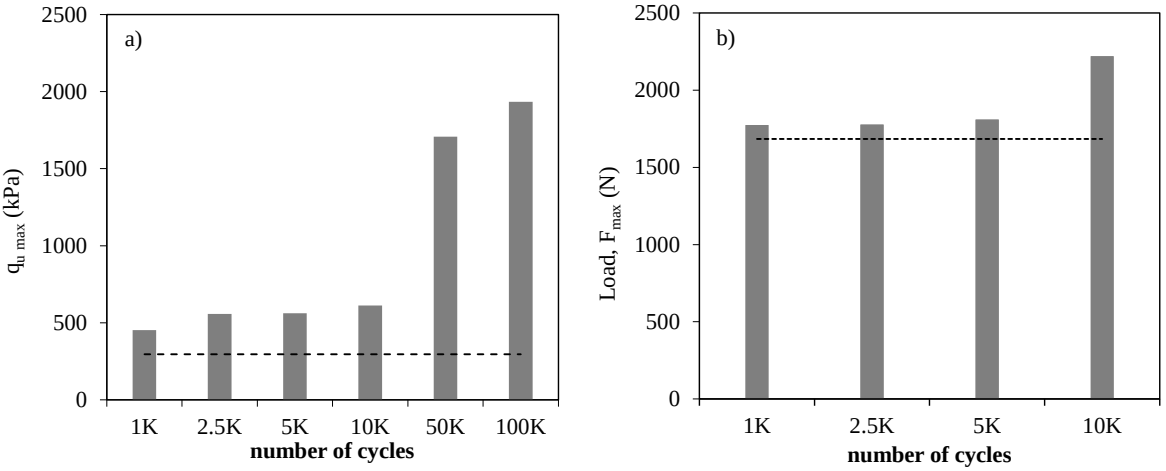

Figure 6.21: Evolution of maximum strength/load vs the number of load cycles for: a) UCS_{pc} tests; b) STS_{pc} tests

6.3.2 Chemically stabilised soft soil reinforced with polypropylene fibres

Table 6.9 and Figures 6.22 and 6.23 summarise the results obtained during the cyclic stage of the UCS and STS cyclic tests for different numbers of loading cycles for the stabilised samples reinforced with polypropylene fibres. As it may be seen from Figures 6.22 and 6.23, the evolution of the permanent deformation (axial strain or vertical displacement for UCS and STS cyclic tests, respectively) is characterised by a quick increase in the first 500 load cycles followed by a slight increase for a higher number of load cycles. With the exception of the UCS and STS cyclic test performed for 50.000 load cycles or higher and some natural experimental scattering, all other samples follow the same trend independently of the number of load cycles, with the permanent deformation evolving within a narrow band.

Due to the fact that the solid skeleton of the stabilised fibre-reinforced material is quite hard and stiff, the increase in the permanent (or plastic) deformation is probably linked to some local breakage of the cementitious bonds, evolving gradually as the number of load cycles increases. As the composite material deforms, due to the breakage of the cementitious bonds, the fibres are progressively mobilised contributing to reduce the permanent axial strain (UCS_{cyc} tests) when compared with the corresponding unreinforced sample (Figure 6.16 and Table 6.6).

Indeed, the fibres are able to absorb and redistribute part of the stresses induced by the cyclic loading, which results in a much lower permanent axial strain, avoiding the breakage of some cementitious bonds and the consequent deterioration of the solid skeleton (in agreement with Venda Oliveira et al. 2022). However, for the STS_{cyc} tests it was observed that the inclusion of the fibres promotes the increase of the permanent deformation (Figure 6.23 and Tables 6.6 and 6.9) which is in contradiction with the findings for UCS_{cyc} tests.

Table 6.9: Maximum permanent axial strain and permanent vertical displacement during the cyclic stage of the UCS and STS cyclic tests of the stabilised fibre-reinforced samples

ID	NLC	$\varepsilon_{ax\text{-}perm}$ (%)	$\delta_{v\text{-}perm}$ (mm)
UCScyc_1K_1_F	1000	0.09	
UCScyc_2.5K_1_F	2500	0.14	
REF_UCScyc_1_F (5K)	5000	0.16	
REF_UCScyc_2_F (5K)	5000	0.17	
UCScyc_10K_1_F	10000	0.17	
UCScyc_50K_1_F	50000	1.56	
STScyc_1K_1_F	1000		0.23
STScyc_2.5K_1_F	2500		0.21
REF_STScyc_1_F (5K)	5000		0.20
REF_STScyc_2_F (5K)	5000		0.22
STScyc_10K_1_F	10000		0.25
STScyc_10K_2_F	10000		0.23
STScyc_50K_1_F	50000		0.66
STScyc_100K_1_F	100000		0.77

NLC: Number of loading cycles

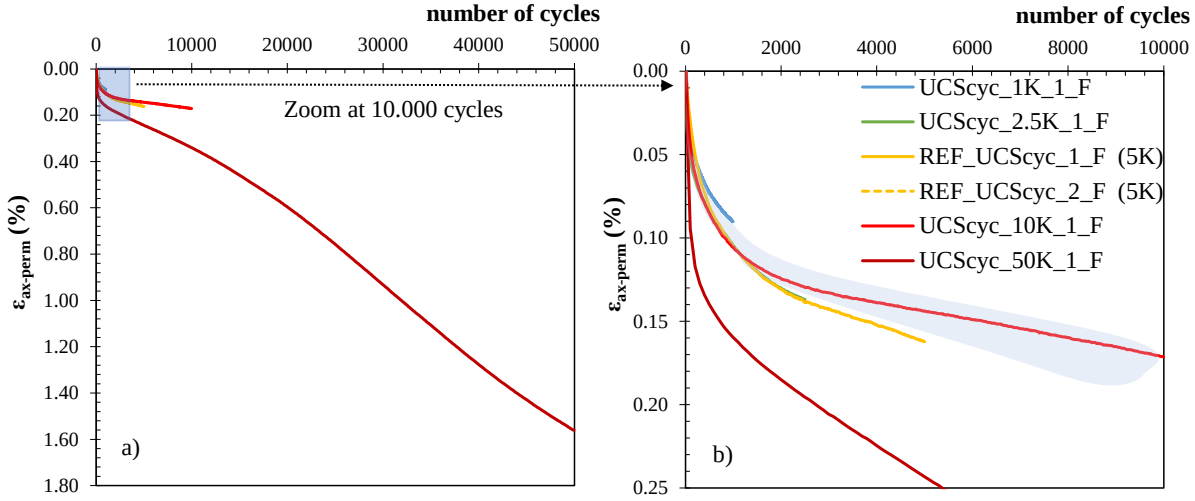

Figure 6.22: Evolution of the permanent axial strain during the cyclic stage (UCS_{cyc}) for stabilised fibre-reinforced samples: a) at 50.000 cycles; b) scaled at 10.000 cycles (frequency = 0.5 Hz; amplitude = ±10%*$q_{u\ max}$; stress level = 50%*$q_{u\ max}$)

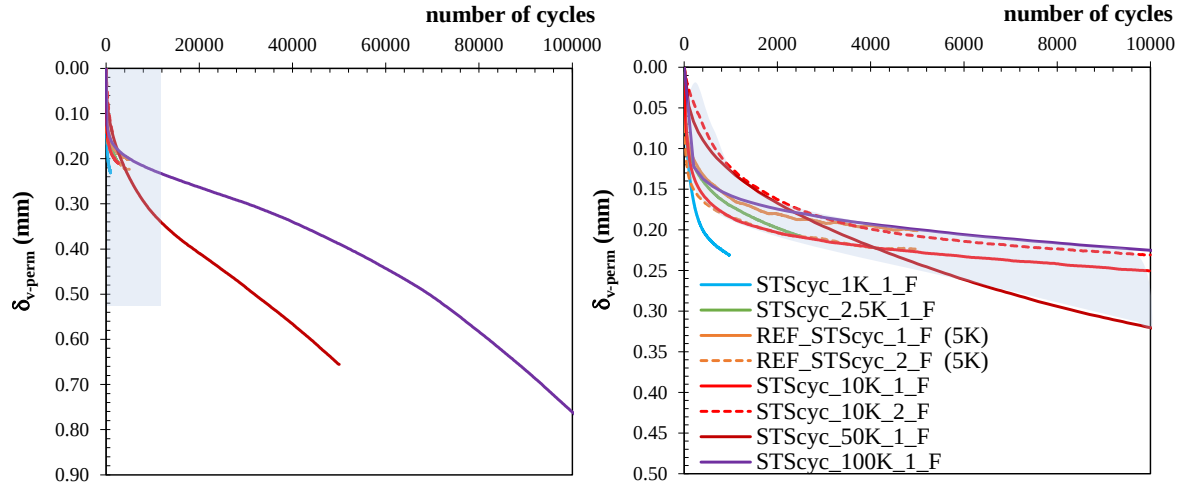

Figure 6.23: Evolution of the permanent vertical displacement during the cyclic stage (STS_{cyc}) for stabilised fibre-reinforced samples (frequency = 0.5 Hz; amplitude = ±10%*F_{max}; stress level = 50%*F_{max})

However, the analysis should consider the failure mechanism of the STS test, characterised by an abrupt breakage of the cementitious bonds, occurring for very small vertical displacements. The physical presence of the fibres prevent the development of some cementitious bonds within the composite matrix, producing a composite material with lower stiffness. Thus, the fibre-reinforced material experiences more deformations since it has lower stiffness than the unreinforced material, and the vertical displacements induced in the STS_{cyc} tests are too small for an effective fibre mobilisation.

Tables 6.10 and 6.11 and Figures 6.24 and 6.25 summarise the results obtained during the post-cyclic UCS and STS tests performed immediately after the cyclic stage where the number of loading cycles was changed for the stabilised samples reinforced with polypropylene fibres. The results suggest that the application of load cycles (> 50.000) increases the strength/load of the stabilised fibre-reinforced material in comparison with the reference monotonic tests. This increase appears to be related with the number of load cycles performed, with more cycles (or more permanent deformations during the cycle stage) resulting in higher strength/load. The larger deformations that occur during the cyclic stage in the samples with fibres allow an earlier mobilisation of the fibres, thus contributing to the strength/load increase. This effect seems to compensate the loss of unconfined compressive strength and stiffness induced by the presence of the fibres that inhibits the development of some cementitious bonds, as observed in Chapter 5. For the case of the STS tests, and as observed in Chapter 5 also, an earlier mobilisation of the fibres induced by the deformations occurring during the cyclic stage allows a load increase when compared to the unreinforced samples. Indeed, for the STS tests, the vertical deformations concentrate on the vertical crack/failure plane which leads to a higher level of deformation with a more effective mobilisation of the fibres that cross this failure plane.

The effect of the cyclic stage on the brittleness or ductility of the composite material is better demonstrated by the brittleness index, I_b which is defined in Equation 6.1, where a value equal to 0 means that the material does not lose strength after failure (ideal ductile behaviour), whereas a value of I_b equal to 1 corresponds to an ideal brittle behaviour (Table 6.10),, characterized by a complete loss of strength after peak failure.

$$I_b = 1 - \frac{q_u \; at \; (\varepsilon_{ax} \; = \; 3\%)}{q_{u-max}} \qquad \text{Equation 6.1}$$

It is clear that the addition of fibres decreases the brittleness of the stress-strain/load-displacement behaviour of the composite material, with very low I_b values. Indeed, the mobilisation of the fibres contributes to mitigate the loss of strength after the peak failure and the mobilisation of a non-

negligible residual strength. In fact, this behaviour is consistent with that observed in similar experiments (Tang et al. 2007; Consoli et al. 2009; Olgun 2013; Correia et al. 2015, Venda Oliveira et al. 2015, 2018, 2022). Despite some natural experimental scattering, it can be seen that as the axial strain/vertical displacement increases the strength/load of all the samples tends toward a very similar residual strength/load since the amount of fibres in all the samples is constant.

The water contents measured after the end of the UCS_{pc} or STS_{pc} tests reveal a decrease as the number of load cycles increases, which may be explained by the time elapsed during the cyclic stage (1.000 cycles = 0.55h; 5.000 cycles = 2.78h; 100.000 cycles = 55.55h) during which the samples dried. This fact can induce some suction effects that contribute to increasing the composite material's strength/load as explained previously. Comparing the water contents for the cases unreinforced and fibre-reinforced no clear trend is observed due to the presence of the fibres.

Figure 6.26 depicts the unconfined compressive strength ($q_{u\ max}$) and the maximum load (F_{max}) with the number of load cycles for the UCS_{pc} and STS_{pc} tests performed. The results suggest that the increase in the strength/load with the number of load cycles seems to be linked with the permanent deformation observed during the cyclic stage, i.e., greater deformations in the cyclic stage allows an earlier mobilisation of the fibres which may lead to greater strength/load in the post-cyclic tests. The suction effects and the coarser apparent grain size or rougher cracks seems to be of less importance compared to the effect of the progressive mobilisation of the fibres during the cyclic stage.

Table 6.10: Results of the UCS and UCS_{pc} tests performed on stabilised samples reinforced with fibres (CI42.5 R; binder quantity = 250 kg/m^3; curing time = 28 days; curing conditions: vertical stress = 0 kPa, room)

ID	NLC	$q_{u\ max}$ (kPa)	ε_r (%)	E_{u50} (MPa)	I_b (%)	w_f (%)
REF_UCS_1_F	-	293.87	4.55	14.32	0.06	70.62
REF_UCS_2_F	-	296.65	4.03	16.10	0.12	70.56
UCSpc_1K_1_F	1000	533.03	2.46	67.32	0.07	74.45
UCSpc_2.5K_1_F	2500	531.02	1.60	79.89	0.24	71.21
REF_UCSpc_1_F (5K)	5000	531.01	1.59	79.89	0.03	72.76
REF_UCSpc_2_F (5K)	5000	504.69	2.70	54.37	0.14	70.48
UCSpc_10K_1_F	10000	618.89	2.96	86.80	0.03	63.07
UCSpc_50K_1_F	50000	1651.11	3.44	196.29	0.01	59.19

NLC: Number of loading cycles; I_b: brittleness index = $1-[(q_{u\ at\ \varepsilon ax\ =\ 3\%})/q_{u\ max}]$

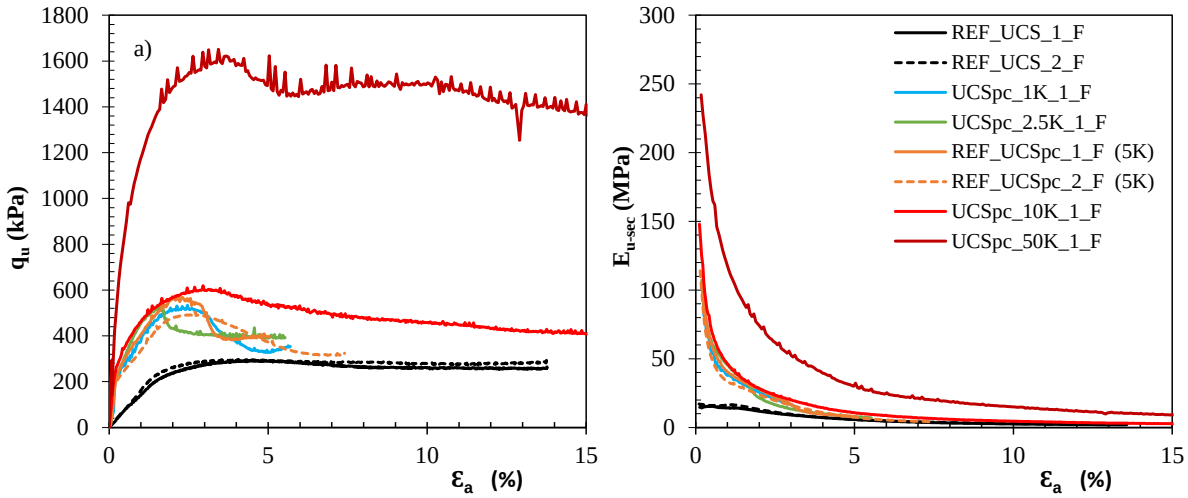

Figure 6.24: Results of the UCS and UCS_{pc} tests performed on stabilised samples reinforced with fibres: a) stress-strain plot; b) Eu-sec vs axial strain (CI42.5 R; binder quantity = 250 kg/m3; curing time = 28 days; curing conditions: vertical stress = 0 kPa, room)

Table 6.11: Results of the STS and STS_{pc} tests performed on stabilised samples reinforced with fibres (CI42.5 R; binder quantity = 250 kg/m^3; curing time = 28 days; curing conditions: vertical stress = 0 kPa, room)

ID	NLC	Load, F(N)	disp, δ_v (mm)	w_f (%)
REF_STS_1_F	-	1451.0	4.48	71.68
REF_STS_2_F	-	1539.0	2.52	71.58
STSpc_1K_1_F	1000	1943.0	3.3	73.52
STSpc_1K_2_F	1000	1913.2	2.5	73.20
STSpc_2.5K_1_F	2500	2039.4	3.1	71.50
REF_STSpc_1_F (5K)	5000	2121.3	3.0	72.15
REF_STSpc_2_F (5K)	5000	2022.2	2.4	75.24
STSpc_10K_1_F	10000	2198.3	4.2	72.62
STSpc_10K_1_F	10000	1943.0	3.3	72.15
STSpc_50K_1_F	50000	3591.2	4.2	69.30

NLC: Number of loading cycles

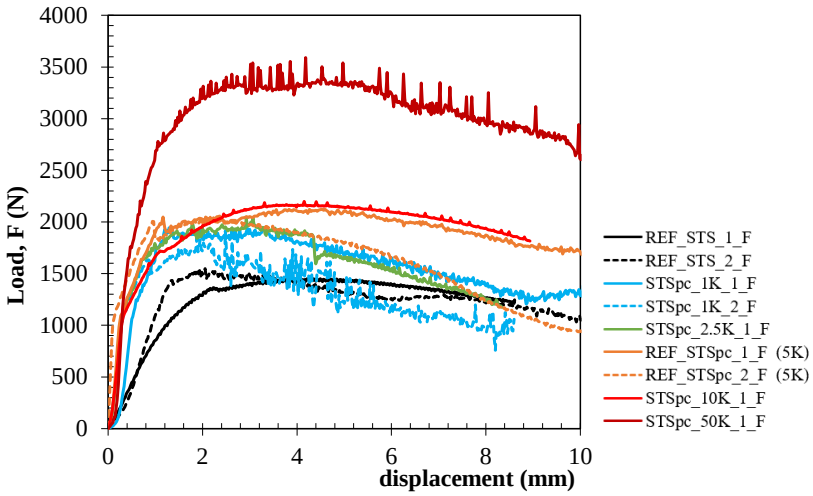

Figure 6.25: Load-displacement curves of the STS and STS_{pc} tests performed on stabilised samples reinforced with fibres (CI42.5 R; binder quantity = 250 kg/m3; curing time = 28 days; curing conditions: vertical stress = 0 kPa, room)

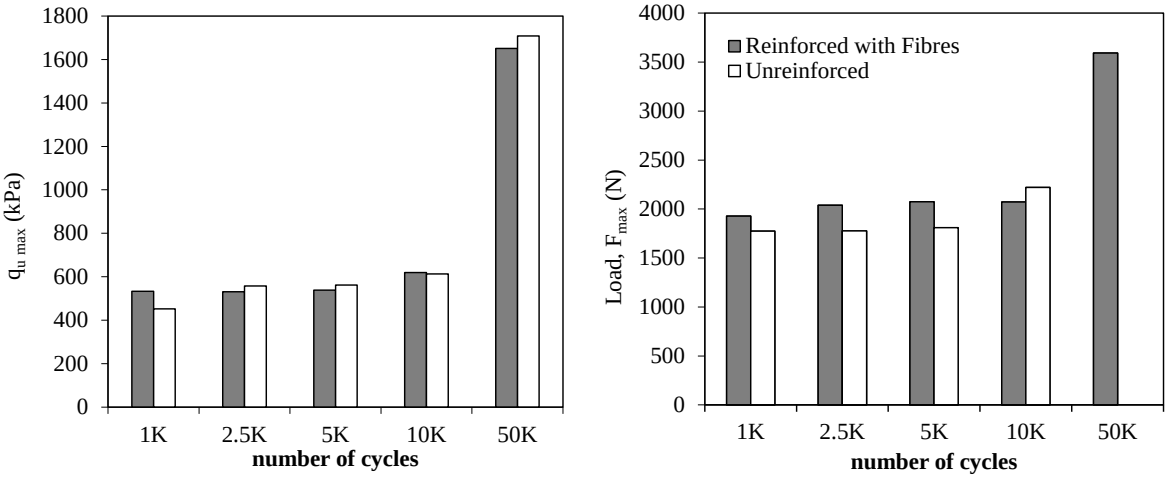

Figure 6.26: Evolution of maximum strength/load vs the number of load cycles for samples unreinforced and reinforced with fibres: a) UCS_{pc} tests; b) STS_{pc} tests

6.4 Parametric study – effect of the cyclic loading frequency

The present section studies the effect of the cyclic loading frequency on the mechanical behaviour of the soft soil chemically stabilised unreinforced or reinforced with polypropylene fibres through a series of UCS and STS tests under cyclic loading by changing the frequency (0.15, 0.25, 0.5, 1.0, 2.0, 4.0 Hz), while it was kept constant the number of loading cycles (5.000), the level of stress (50% of the strength/load evaluated by the monotonic tests) and the amplitude (±10% of the strength/load evaluated by the monotonic tests). For such it will be studied the evolution of the permanent axial strain (for UCS cyclic tests) and the permanent vertical displacement (for STS cyclic tests) occurred during the cyclic stage, complemented by the stress-strain curves (for UCS post-cyclic) and the load-displacement curves (for STS post-cyclic). The results from the UCS and STS cyclic tests are presented below for both materials, starting with the soft soil of Baixo Mondego chemically stabilised without fibres, followed by the case where polypropylene fibres were added as reinforcing elements.

6.4.1 Chemically stabilised unreinforced soft soil

Table 6.12 and Figures 6.27, 6.28 and 6.29 summarise the results obtained during the cyclic stage of the UCS and STS cyclic tests for different cyclic loading frequencies. As it may be seen from Figures 6.27 and 6.28, the evolution of the permanent deformation (axial strain or vertical displacement for UCS and STS cyclic tests, respectively) is characterised by a quick increase in the first 500 load cycles followed by a slight increase for a higher number of load cycles. The results of the permanent deformation follow a similar trend independently of the frequency,

showing that the permanent deformation decreases as the frequency increases, pointing out that higher frequency levels result in less deterioration of the stabilised matrix.

Table 6.12: Maximum permanent axial strain and the permanent vertical displacement during the cyclic stages of the UCS and STS cyclic tests

ID	Frequency (Hz)	$\varepsilon_{ax\text{-}perm}$ (%)	$\delta_{v\text{-}perm}$ (mm)
UCScyc_0.15Hz_1	0.15	0.33	-
UCScyc_0.25Hz_2	0.25	0.32	-
REF_UCScyc_1 (0.5Hz)	0.5	0.22	-
REF_UCScyc_2 (0.5Hz)	0.5	0.24	-
UCScyc_1Hz_1	1	0.17	-
UCScyc_2Hz_1	2	0.13	-
UCScyc_4Hz_2	4	0.10	-
STScyc_0.15Hz_2	0.15	-	0.27
STScyc_0.25Hz_2	0.25	-	0.20
REF_STScyc_1 (0.5Hz)	0.5	-	0.22
REF_STScyc_2 (0.5Hz)	0.5	-	0.21
STScyc_1Hz_1	1	-	0.18
STScyc_2Hz_2	2	-	0.18
STScyc_4Hz_2	4	-	0.13

These results suggest that as the frequency increases the “elastic” deformation becomes greater, i.e., there are a higher degree of reversibility in deformation due to the less occurrence of breakage of the cementation bonds; this behaviour is in agreement with the findings observed for other materials (Hernández-Olivares et al. 2002; Shao et al. 2018).

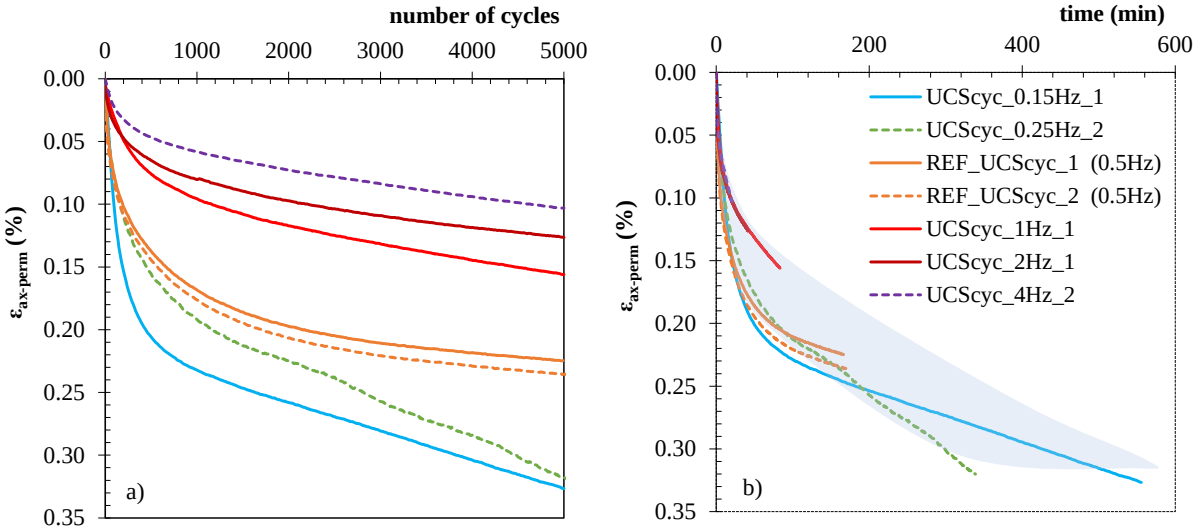

Figure 6.27: Evolution of permanent axial strain during the cyclic stage (UCS_{cyc}) for unreinforced samples: a) effect of frequency at 5.000 cycles b) effect of frequency by time (number of cycles = 5.000; level of stress = 50%*$q_{u\ max}$; amplitude = ±10%*$q_{u\ max}$)

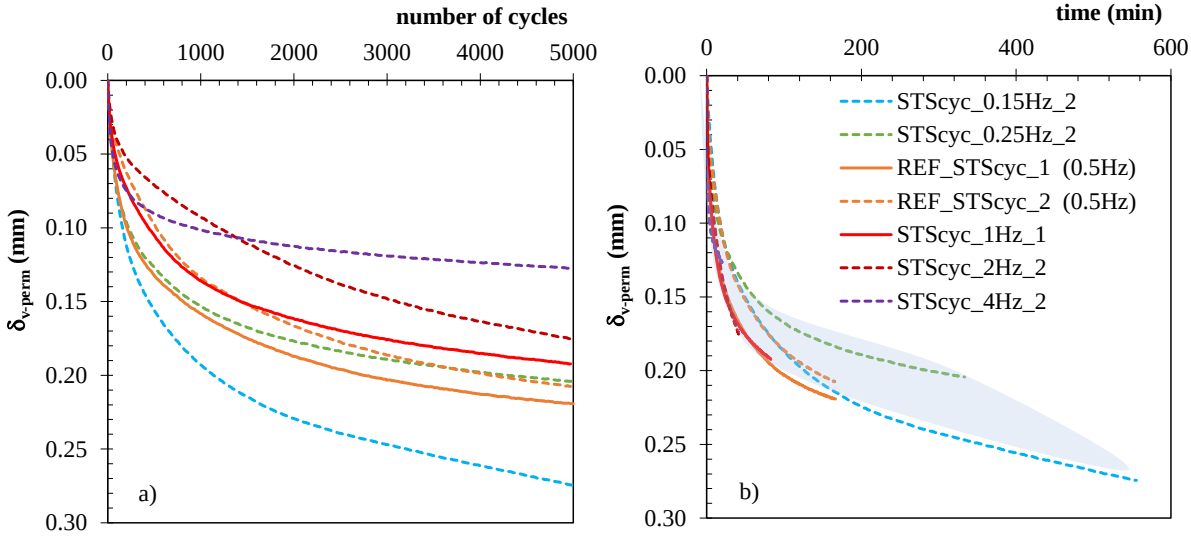

Figure 6.28: Evolution of permanent vertical displacement during the cyclic stage (STS_{cyc}) for unreinforced samples: a) effect of frequency at 5.000 cycles b) effect of frequency by time (number of cycles = 5.000; level of stress = 50%*F_{max}; amplitude = ±10%*F_{max})

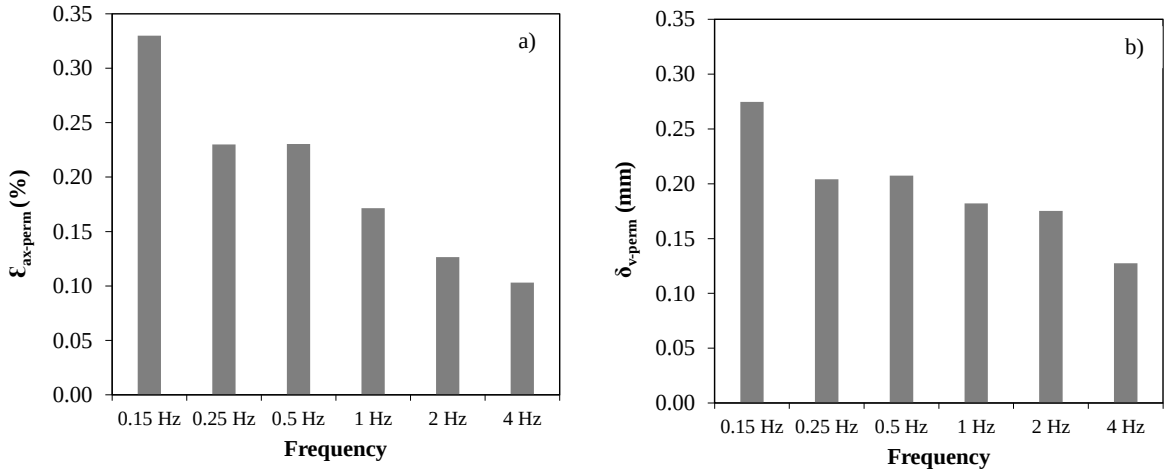

Figure 6.29: Evolution of maximum permanent axial strain/vertical displacement vs the frequency of the cyclic loading for unreinforced samples a) UCS_{cyc}, b) STS_{cyc}

Tables 6.13 and 6.14 and Figures 6.30, 6.31 and 6.32 summarise the results obtained during the post-cyclic UCS and STS tests performed immediately after the cyclic stage where the cyclic loading frequency was changed. The results show a decrease in the strength/load of the composite material when the frequency increases. The results seem to indicate the existence of a connection with the permanent deformation observed during the cyclic stage, i.e., greater deformations in the cyclic stage (associated to lower frequencies) lead to greater mechanical properties (unconfined strength, stiffness or load) in the post-cyclic tests. The water contents measured after the end of the UCS_{pc} or STS_{pc} tests reveal an increase as the cyclic loading frequency increases, which may be explained by the time elapsed during the cyclic stage (0.15 Hz = 9.26h; 0.5 Hz = 2.78h; 4.0 Hz

= 0.35h) during which the samples dried. This fact can induce some suction effects that contribute to increasing the composite material's strength/load for the lowest frequencies.

As it may be seen from Tables 6.13 and 6.14 and Figures 6.30 and 6.31, the larger deformations occurring during the cyclic stage (associated to the lower frequencies) result in larger strength/load except in cases in which the frequency is high (≥ 1Hz) where the composite material behaves "elastically" exhibiting small permanent deformations. Thus, the breakage of a smaller number of cementitious bonds in the cyclic stage does not promote a substantial change of the grain size (coarser apparent grain size as explained in the previous section), i.e., a small permanent deformation occurred during the cyclic stage (associated to higher frequencies) are not enough to roughen the shearing surfaces, thus not promoting the increase of the strength/load. Another possible explanation is related with suction effects, as presented above. For the STS_{pc} tests, they follow, in general, this trend with some specificities due to the different failure mode, as explained in the study of the effect of the number of loading cycles.

Table 6.13: Results of the UCS and UCS_{pc} tests performed on unreinforced stabilised samples (CI42.5 R; binder quantity = 250 kg/m^3; curing time = 28 days; curing conditions: vertical stress = 0 kPa, room)

ID	Freq (Hz)	$q_{u\ max}$ (kPa)	ε_r (%)	E_{u50} (MPa)	w_f (%)
REF_UCS_1	-	302.36	1.45	33.29	71.56
REF_UCS_2	-	288.80	1.25	33.92	71.86
UCSpc_0.15Hz_1	0.15	493.53	2.38	72.37	62.51
UCSpc_0.25Hz_1	0.25	476.91	3.47	26.47	64.01
REF_UCSpc_1 (0.5Hz)	0.5	543.17	1.73	91.28	69.1
REF_UCSpc_2 (0.5Hz)	0.5	581.26	1.88	139.15	69.57
UCSpc_1Hz_1	1	418.01	1.59	111.57	69.11
UCSpc_2Hz_1	2	404.92	1.11	62.13	73.12
UCSpc_4Hz_2	4	276.21	0.72	183.63	75.23

Freq: frequency

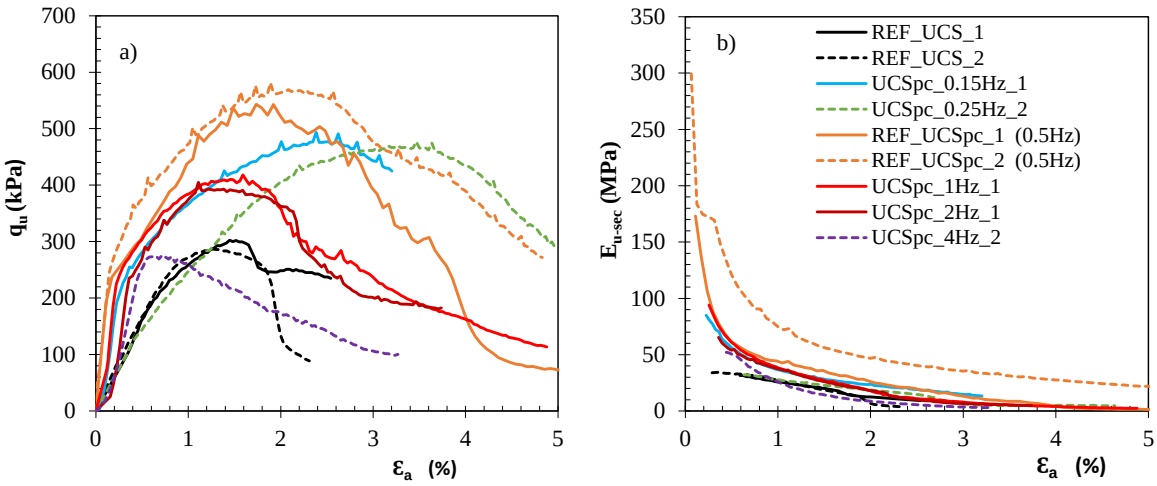

Figure 6.30: Results of the UCS and UCS_{pc} tests performed on unreinforced stabilised samples: a) stress-strain plot; b) $E_{u\text{-}sec}$ vs axial strain (CI42.5 R; binder quantity = 250 kg/m^3; curing time = 28 days; curing conditions: vertical stress = 0 kPa, room)

Table 6.14: Results of the STS and STS_{pc} tests performed on unreinforced stabilised samples (CI42.5 R; binder quantity = 250 kg/m^3; curing time = 28 days; curing conditions: vertical stress = 0 kPa, room)

ID	Freq (Hz)	F_{max} (N)	disp, δ_v (mm)	w_f (%)
REF_STS_1	-	1728	0.74	72.56
REF_STS_2	-	1640	0.74	72.91
STSpc_0.15Hz_2	0.15	2183.49	0.70	62.71
STSpc_0.25Hz_2	0.25	1620.98	0.84	65.09
REF_STSpc_1 (0.5Hz)	0.5	1863.8	0.85	68.37
REF_STSpc_2 (0.5Hz)	0.5	1756.2	0.92	71.37
STSpc_1Hz_2	1	1220.58	0.67	71.98
STSpc_2Hz_2	2	1120.43	0.46	73.4
STSpc_4Hz_2	4	1535.82	0.73	76.2

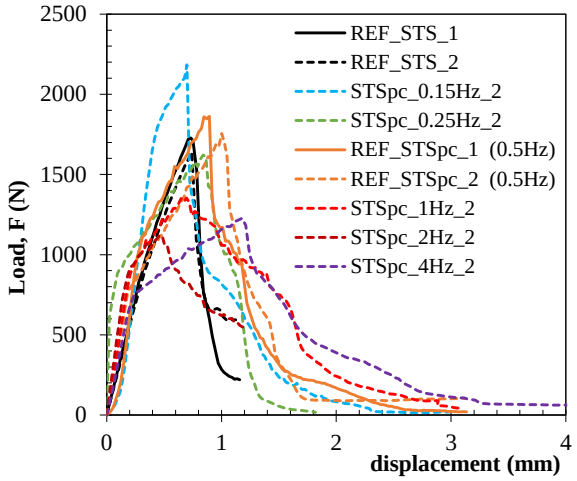

Figure 6.31: Load-displacement of the STS and STS_{pc} tests performed on unreinforced stabilised samples (CI42.5 R; binder quantity = 250 kg/m3; curing time = 28 days; curing conditions: vertical stress = 0 kPa, room)

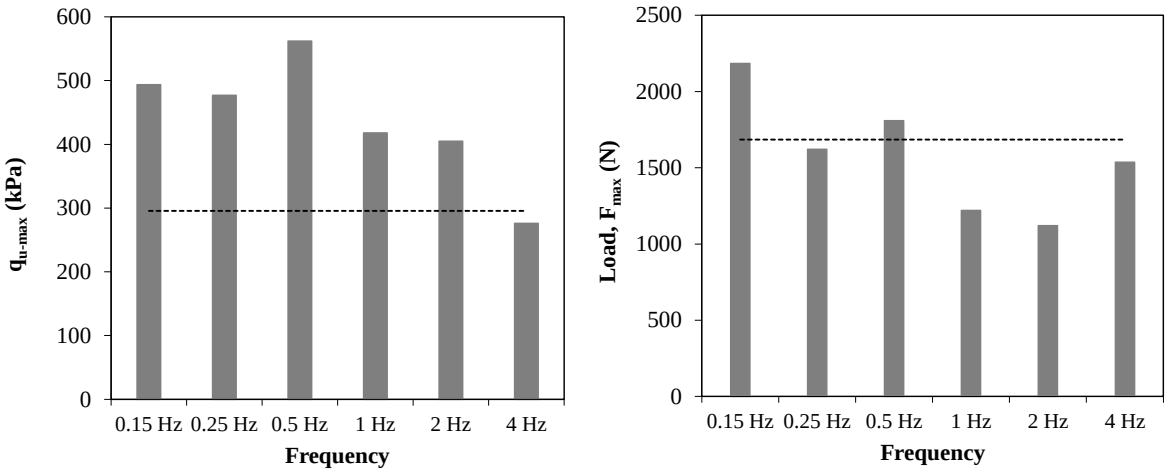

Figure 6.32: Evolution of maximum strength/load vs the frequency of the cyclic loading for unreinforced stabilised samples: a) UCS_{pc} tests; b) STS_{pc} tests

6.4.2 Chemically stabilised soft soil reinforced with polypropylene fibres

Table 6.15 and Figures 6.33, 6.34 and 6.35 summarise the results obtained during the cyclic stage of the UCS and STS cyclic tests for different cyclic loading frequencies for the stabilised samples reinforced with polypropylene fibres. As it may be seen from Figures 6.33 and 6.34, the evolution of the permanent deformation (axial strain or vertical displacement for UCS and STS cyclic tests, respectively) is characterised by a quick increase in the first 400 load cycles followed by a slight increase for a higher number of load cycles. As for the unreinforced samples, also here it is observed the permanent deformation occurring during the cyclic stage decreases as the frequency increases, with the permanent deformation evolving within a narrow band when the analysis is performed with time. This lower deformation observed for the higher frequencies means less degradation of the solid matrix (breakage of fewer cementitious bonds), suggesting that the composite material behaves more "elastically".

The addition of the fibres to the stabilised soil promotes a slight increase of the permanent deformations during the cyclic stage when compared to the unreinforced samples (Tables 6.12 and 6.15, Figure 6.35), increase that is smaller for the higher frequencies explained by the more "elastic" behaviour of the material.

Table 6.15: Maximum permanent axial strain and permanent vertical displacement during the cyclic stage of the UCS and STS cyclic tests of the stabilised fibre-reinforced samples

ID	Frequency (Hz)	$\varepsilon_{ax\text{-}perm}$ (%)	$\delta_{v\text{-}perm}$ (mm)
UCScyc_0.15Hz_2_F	0.15	0.43	-
UCScyc_0.25Hz_1_F	0.25	0.24	-
REF_UCScyc_1_F (0.5Hz)	0.5	0.16	-
REF_UCScyc_2_F (0.5Hz)	0.5	0.17	-
UCScyc_1Hz_1_F	1	0.16	-
UCScyc_1Hz_2_F	1	0.17	-
UCScyc_2Hz_1_F	2	0.12	-
UCScyc_4Hz_2_F	4	0.10	-
STScyc_0.15Hz_1_F	0.15	-	0.26
STScyc_0.15Hz_2_F	0.15	-	0.25
STScyc_0.25Hz_1_F	0.25	-	0.23
REF_STScyc_1 _F (0.5Hz)	0.5	-	0.20
REF_STScyc_2_F (0.5Hz)	0.5	-	0.22
STScyc_1Hz_2_F	1	-	0.21
STScyc_2Hz_2_F	2	-	0.20
STScyc_4Hz_1_F	4	-	0.18

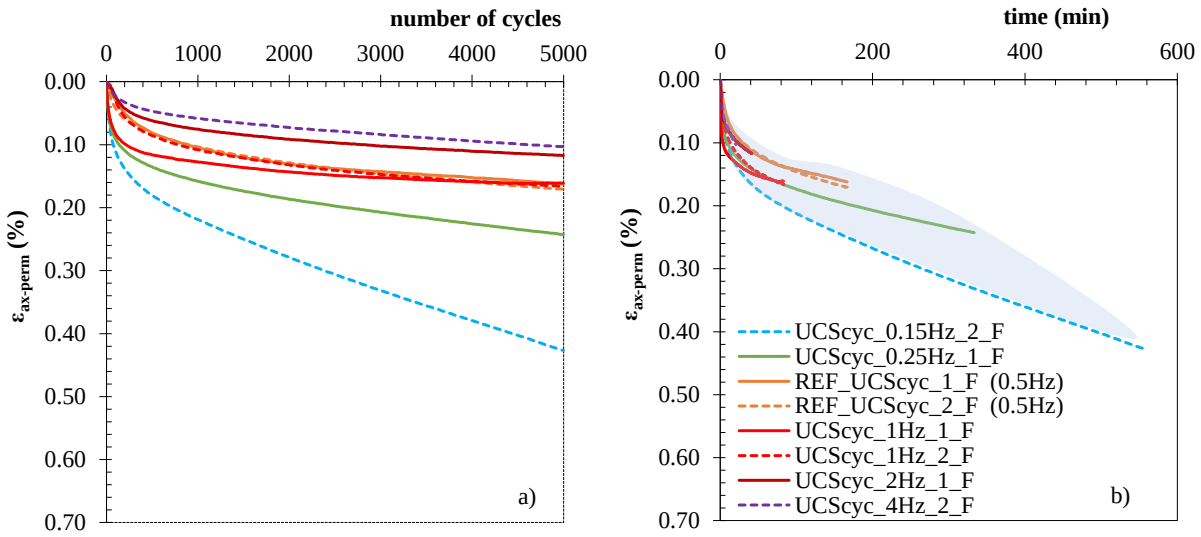

Figure 6.33: Evolution of permanent axial strain during the cyclic stage (UCS_{cyc}) for stabilised fibre-reinforced samples: a) effect of frequency at 5.000 cycles b) effect of frequency by time (number of cycles = 5.000; level of stress = 50%*$q_{u\ max}$; amplitude = ±10%*$q_{u\ max}$)

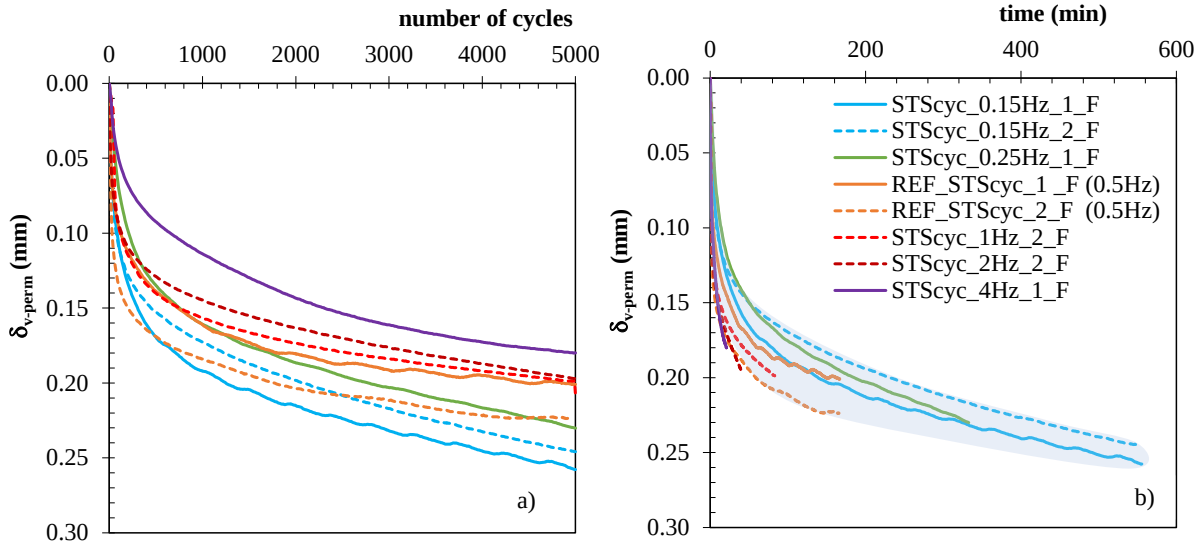

Figure 6.34: Evolution of permanent vertical displacement during the cyclic stage (STS_{cyc}) for stabilised fibre-reinforce samples: a) effect of frequency at 5.000 cycles b) effect of frequency by time (number of cycles = 5.000; level of stress = 50%*F_{max}; amplitude = ±10%*F_{max})

This slight increase due to the presence of the fibres may be explained by two combined effects: i) the physical presence of the fibres will prevent the development of some cementitious bonds within the composite matrix, producing a composite material will lower strength/stiffness; ii) the level of deformation experienced by the samples during the cyclic stage is very small not ensuring an effective mobilisation of the fibres, thus, not balancing the previous effect. This is more evident for the STS_{cyc} tests due to the fact that the deformations are concentrated along the vertical crack/failure plane.

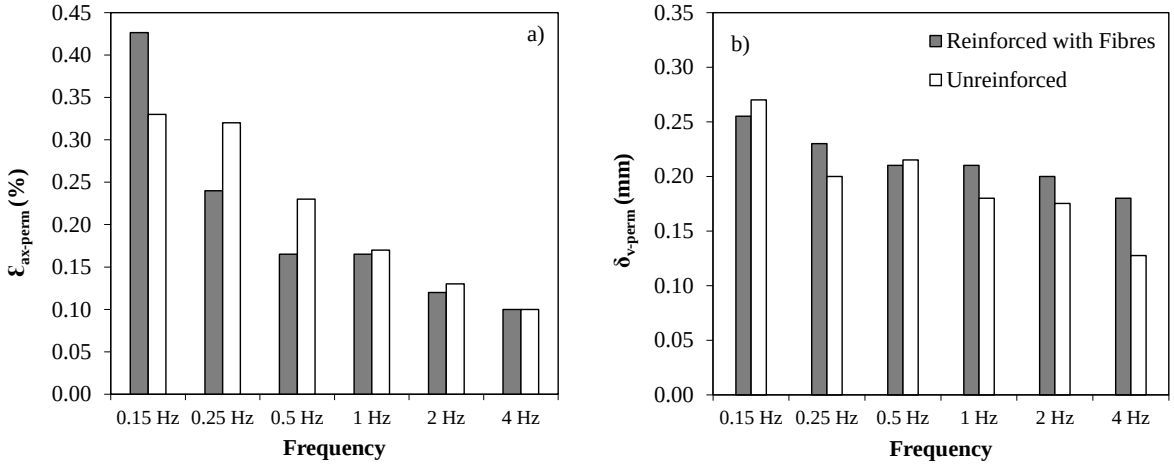

Figure 6.35: Evolution of maximum permanent axial strain/vertical displacement vs the frequency of the cyclic loading for stabilised fibre-reinforce samples: a) UCS_{cyc}, b) STS_{cyc}

Tables 6.16 and 6.17 and Figures 6.36, 6.37 and 6.38 summarise the results obtained during the post-cyclic UCS and STS tests performed immediately after the cyclic stage where the cyclic loading frequency was changed for the stabilised samples reinforced with polypropylene fibres. The results show that the application of cyclic loading increases the strength/load of the stabilised fibre-reinforced material in comparison with the reference monotonic tests (Figures 6.36 and 6.37) as well as when compared to the respective unreinforced samples (Figure 6.38). This strength/load increment decreases as the frequency increases meaning that there is a link with the deformations that occur during the cyclic stage, i.e., for the lower frequencies levels the deformations during the cyclic stage in the samples with fibres are larger which allow an earlier mobilisation of the fibres, thus contributing to the strength/load increase. When the cyclic stage was analysed, it was written that the deformation was not enough for an effective mobilisation of the fibres, which seems to be in contradiction with what is now stated. However, analysing the accumulated deformation experienced by the samples from the beginning of the cyclic test until the failure (pre-cyclic stage + cyclic stage + post-cyclic test), it is possible to see that the deformations of the samples with fibres are much larger, thus ensuring a more effective contribution of the fibres in the post-cyclic tests. It may be concluded that the effect of fibre-mobilisation seems to compensate the loss of strength/load induced by the presence of the fibres that inhibits the development of some cementitious bonds, as observed in Chapter 5. The same arguments justify the stiffness evolution.

As presented before, the brittleness index, I_b (Table 6.16) is a parameter that evaluates the brittleness or ductility of the composite material. It is clear that the addition of fibres decreases the brittleness of the stress-strain/load-displacement behaviour of the composite material, with very low I_b values. Indeed, the mobilisation of the fibres contributes to mitigate the loss of strength

after the peak failure and the mobilisation of a non-negligible residual strength. In fact, this behaviour is consistent with that observed in similar experiments (Tang et al. 2007; Consoli et al. 2009; Olgun 2013; Correia et al. 2015, Venda Oliveira et al. 2015, 2018, 2022). Despite some natural experimental scattering, it can be seen that as the axial strain/vertical displacement increases the strength/load of all the samples tends toward a very similar residual strength/load since the number of fibres in all the samples is constant.

The water contents measured after the end of the UCS_{pc} or STS_{pc} tests reveal an increase as the cyclic loading frequency increases, which may be explained by the time elapsed during the cyclic stage (0.15 Hz = 9.26h; 0.5 Hz = 2.78h; 4.0 Hz = 0.35h) during which the samples dried. This fact can induce some suction effects that contribute to increasing the composite material's strength/load for lower frequencies. Comparing the water contents for the cases unreinforced and fibre-reinforced no clear trend is observed due to the presence of the fibres.

Figure 6.38 depicts the unconfined compressive strength ($q_{u\ max}$) and the maximum load (F_{max}) with the cyclic loading frequency for the UCS_{pc} and STS_{pc} tests performed. The results reveal that the decrease in the strength/load as the frequency increases is linked with the permanent deformation observed during the cyclic stage, i.e., the greater deformations in the cyclic stage observed in lower frequencies allows an earlier mobilisation of the fibres which may lead to greater strength/load in the post-cyclic tests. For the highest frequencies levels, the composite material behaves more “elastically” meaning that the behaviour is more similar to the monotonic test. The suction effects and the coarser apparent grain size or rougher cracks seems to be of less importance compared to the effect of the progressive mobilisation of the fibres during the cyclic stage.

Table 6.16: Results of the UCS and UCS_{pc} tests performed on stabilised samples reinforced with fibres (CI42.5 R; binder quantity = 250 kg/m^3; curing time = 28 days; curing conditions: vertical stress = 0 kPa, room)

ID	Freq (Hz)	$q_{u\ max}$ (kPa)	ε_r (%)	E_{u50} (MPa)	I_b (%)	w_f (%)
REF_UCS_1_F	-	293.87	4.55	14.32	0.06	70.62
REF_UCS_2_F	-	296.65	4.03	16.10	0.02	70.56
UCSpc_0.15Hz_2_F	0.15	675.81	3.29	79.63	0.01	55.61
UCSpc_0.25Hz_1_F	0.25	571.84	2.83	63.79	0.05	61.65
REF_UCSpc_1_F (0.5Hz)	0.5	531.01	1.59	79.89	0.03	72.76
REF_UCSpc_2_F (0.5Hz)	0.5	504.69	2.70	54.37	0.14	70.48
UCSpc_1Hz_1_F	1	432.22	6.07	54.57	0.23	64.5
UCSpc_1Hz_2_F	1	641.35	1.93	102.00	0.21	64.77
UCSpc_2Hz_2_F	2	433.23	4.38	28.88	0.07	73.86
UCSpc_4Hz_1_F	4	425.07	2.20	45.77	0.11	74.61

Freq: frequency; I_b: brittleness index = $1-[(q_{u\ at\ \varepsilon ax\ =\ 3\%})/q_{u\ max}]$

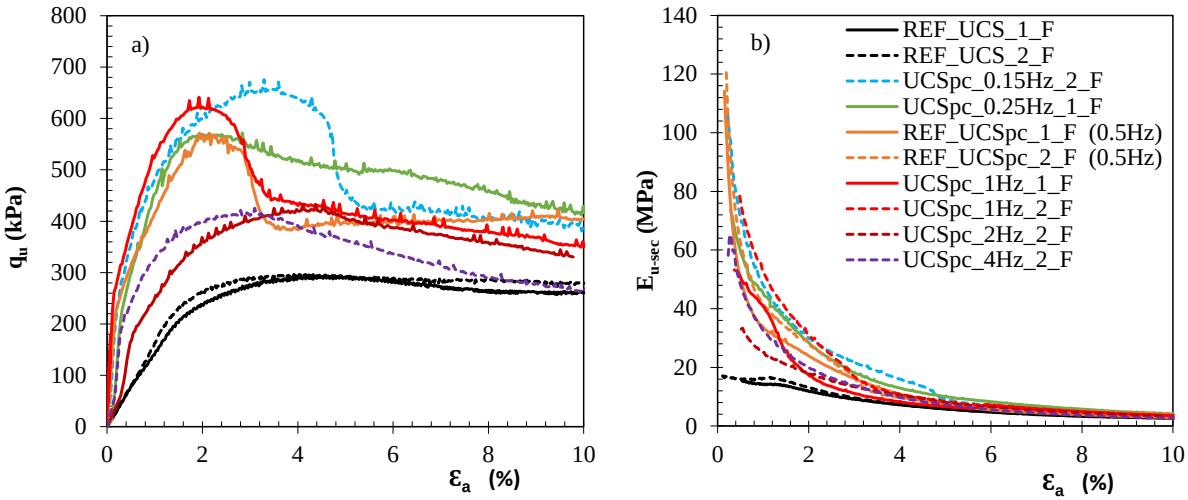

Figure 6.36: Results of the UCS and UCS_{pc} tests performed on stabilised samples reinforced with fibres: a) stress-strain plot; b) $E_{u\text{-}sec}$ vs axial strain (CI42.5 R; binder quantity = 250 kg/m^3; curing time = 28 days; curing conditions: vertical stress = 0 kPa, room)

Table 6.17: Results of the STS and STS_{pc} tests performed on stabilised samples reinforced with fibres (CI42.5 R; binder quantity = 250 kg/m^3; curing time = 28 days; curing conditions: vertical stress = 0 kPa, room)

ID	Freq (Hz)	F_{max} (N)	disp, δ_v (mm)	w_f (%)
REF_STS_1_F	-	1451.0	4.48	71.58
REF_STS_2_F	-	1539.0	2.52	71.68
STSpc_0.15Hz_1_F	0.15	2030.8	3.9	65.87
STSpc_0.15Hz_2_F	0.15	2093.9	2.8	66.11
STSpc_0.25Hz_1_F	0.25	2061.0	4.5	68.07
REF_STSpc_1 _F (0.5Hz)	0.5	2121.3	3.0	72.15
REF_STSpc_2_F (0.5Hz)	0.5	2022.2	2.4	75.24
STSpc_1Hz_2_F	1	1786.9	2.5	74.12
STSpc_2Hz_2_F	2	1766.7	2.6	76.68
STSpc_4Hz_1_F	4	1707.9	3.1	77.17

Freq: frequency

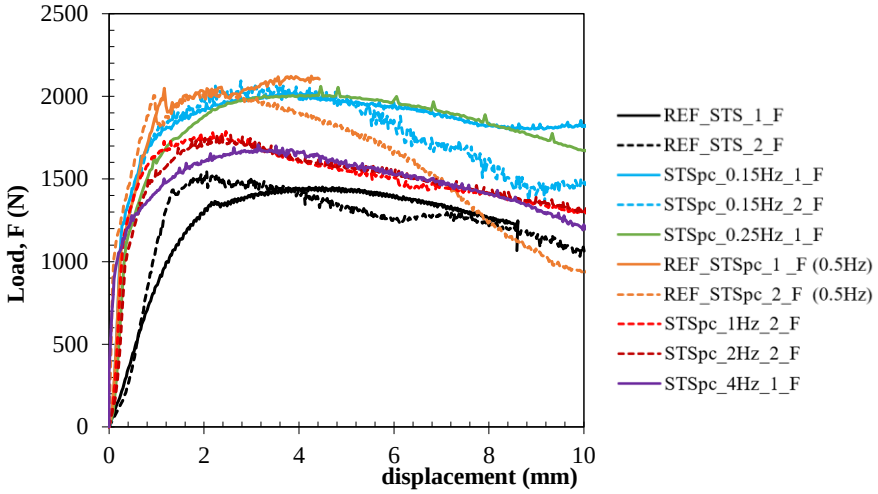

Figure 6.37: Load-displacement of the STS and STS_{pc} tests performed on stabilised samples reinforced with fibres (CI42.5 R; binder quantity = 250 kg/m^3; curing time = 28 days; curing conditions: vertical stress = 0 kPa, room)

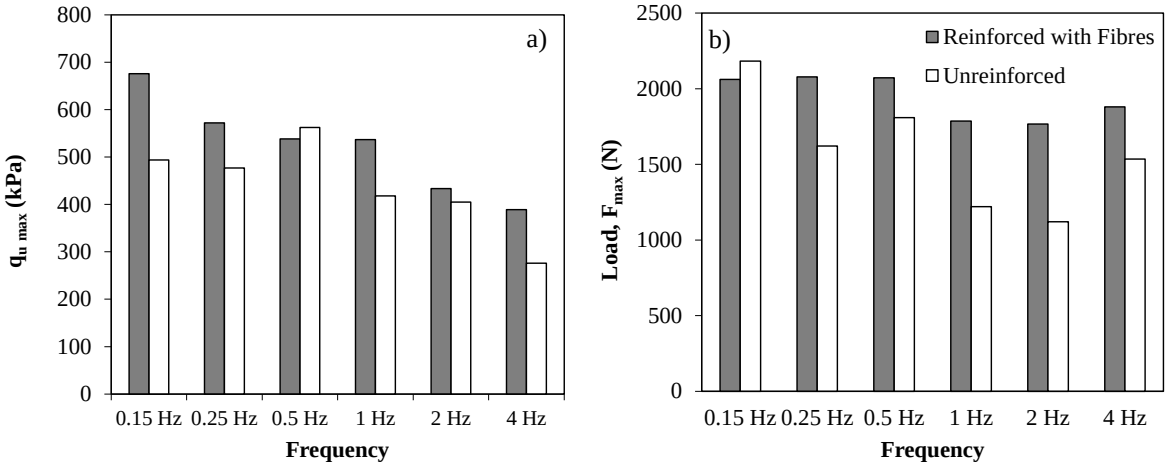

Figure 6.38: Evolution of the maximum strength/load vs the frequency of the cyclic loading for samples unreinforced and reinforced with fibres: a) UCS_{pc} tests; b) STS_{pc} tests

6.5 Parametric study – effect of the stress level

In order to study the effect of the stress level on the mechanical behaviour of soft soil of Baixo Mondego, chemically stabilised unreinforced or reinforced with polypropylene fibres. A series of UCS and STS tests under cyclic loading were carried out, varying the stress level of the cyclic loading (10, 50 and 75% of the strength/load evaluated by the monotonic tests). At the same time, it was kept constant the number of loading cycles (5.000), the cyclic loading frequency (0.5 Hz) and the amplitude (±10% of the strength/load evaluated by the monotonic tests).

For such, it will be studied the evolution of the permanent axial strain (for UCS cyclic tests), and the permanent vertical displacement (for STS cyclic tests) occurred during the cyclic stage, complemented by the stress-strain curves (for UCS post-cyclic) and the load-displacement curves (for STS post-cyclic). The results from the UCS and STS cyclic tests are presented below for both materials, starting with the soft soil of Baixo Mondego chemically stabilised without fibres, followed by the case where polypropylene fibres were added as reinforcing elements.

6.5.1 Chemically stabilised unreinforced soft soil

In Table 6.18 and Figures 6.39 and 6.40, the results obtained during the cyclic stage of the UCS and STS cyclic tests for a different level of stresses of the cyclic loading are summarised.

As shown in Figure 6.39, the evolution of the permanent deformation (axial strain or vertical displacement for UCS and STS cyclic tests, respectively) is defined by a quick rise at the start of cyclic loading, followed by a gradual increase of the deformation with the increase of the stress level.

The result of the permanent deformation follows a different trend regarding the stress level, showing that the permanent deformation rate increases when a higher stress level is applied.

As previously stated, the cyclic loading tends to damage the cementitious matrix inducing an increase in permanent deformation as the number of cycles increases. The results indicate that when the stress level is higher than 50% the plastic deformations accelerates significantly due to an intensification of the breakage/degradation of the cementitious bonds of the composite material, evolving the composite material progressively towards failure (even if it has not been reached in any test).

It is seen that the permanent deformation increases with the stress level also applied for STS tests (Figure 6.39b).

Table 6.18: Maximum permanent axial strain and permanent vertical displacement during the cyclic stage of the UCS and STS cyclic tests

ID	ls	$\varepsilon_{ax\text{-}perm}$ (%)	$\delta_{v\text{-}perm}$ (mm)
UCScyc_10ls_2	10%	0.09	-
REF_UCScyc_1 (50ls)	50%	0.16	-
REF_UCScyc_2 (50ls)	50%	0.17	-
UCScyc_75ls_2	75%	0.55	-
STScyc_10ls_1	10%	-	0.14
REF_STScyc_1 (50ls)	50%	-	0.20
REF_STScyc_2 (50ls)	50%	-	0.22
STScyc_75ls_1	75%	-	0.23

ls: level of stress

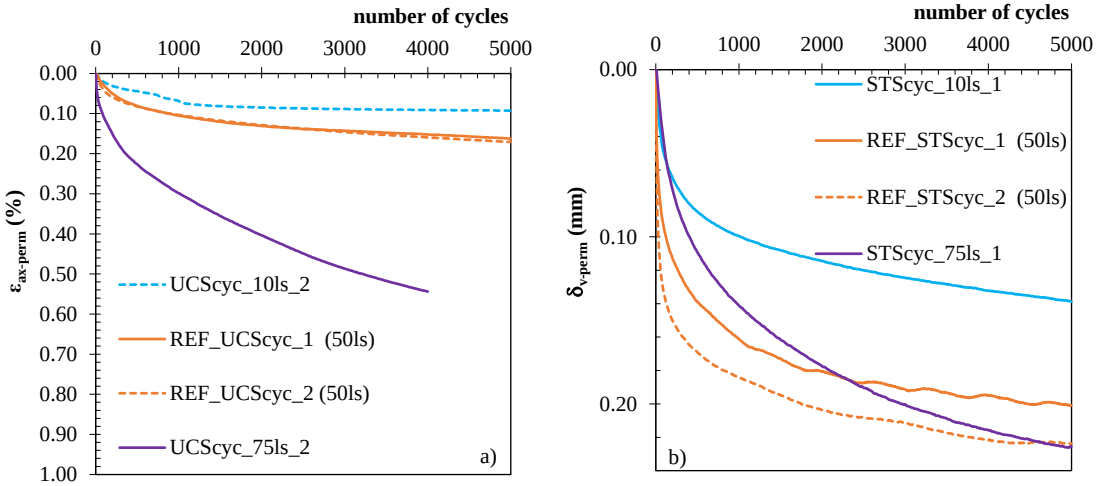

Figure 6.39: Evolution of the permanent axial strain/permanent vertical displacement during the cyclic stage for unreinforced stabilised samples: a) UCS_{cyc}; b) STS_{cyc} (frequency = 0.5 Hz; number of cycles = 5.000; amplitude = ±10%*$q_{u\ max}$ or ±10%*F_{max})

Tables 6.19 and 6.20 and Figures 6.41, 6.42 summarise the results obtained during the post-cyclic UCS and STS tests performed immediately after the cyclic stage for different stress levels. For the

stress levels of 10% and 50%, the results show that, as in the other effects studied, the application of the cyclic stage induces an higher strength/load to the composite material.

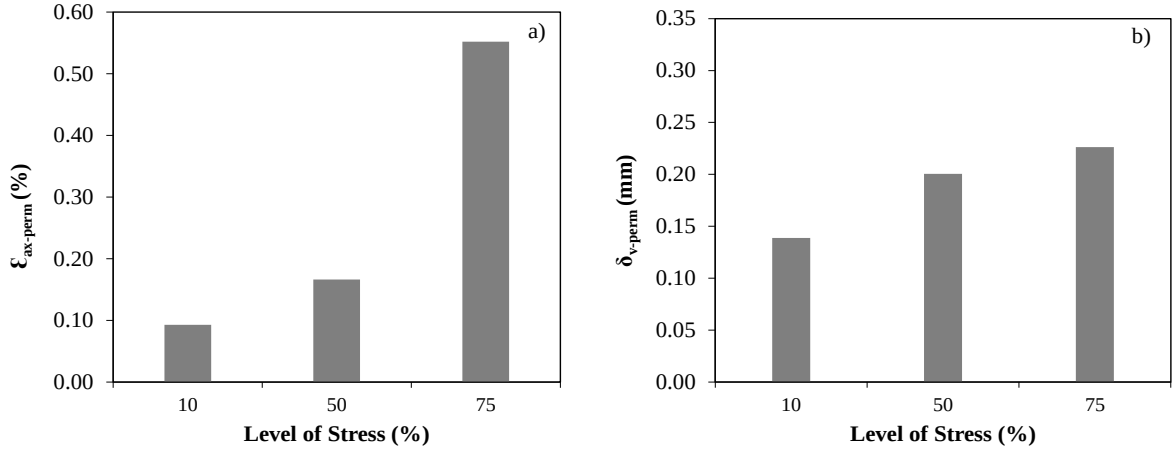

Figure 6.40: Evolution of the maximum permanent axial strain/permanent vertical displacement vs the level of stress for unreinforced stabilised samples: a) UCS_{cyc}, b) STS_{cyc}

However, the application of a stress level of 75% during the cyclic stage had a detrimental effect on the post-cyclic strength in relation to the monotonic tests; this behaviour seems to be a consequence of the significant damage the of the composite material during the cyclic stage, due to the significant accumulated permanent deformations. The water contents measured after the UCS_{pc} or STS_{pc} tests reveal negligible changes, since all the tests were carried out under 5.000 cycles and 0.5 Hz.

Table 6.19: Results of the UCS and UCS_{pc} tests performed on unreinforced stabilised samples (CI42.5 R; binder quantity = 250 kg/m^3; curing time = 28 days; curing conditions: vertical stress = 0 kPa, room)

ID	ls	$q_{u\text{-}max}$ (kPa)	ε_r (%)	E_{u50} (MPa)	w_f (%)
REF_UCS_1	-	302.36	1.45	33.29	71.56
REF_UCS_2	-	288.80	1.25	33.92	71.86
UCSpc_10ls_2	10%	506.57	1.36	81.09	71.42
REF_UCSpc_1 (50ls)	50%	543.17	1.73	91.28	69.10
REF_UCSpc_2 (50ls)	50%	581.26	1.88	139.15	69.57
UCSpc_75ls_2	75%	237.98	1.42	43.51	69.72

ls: level of stress defined ($q_{u\ cyc}/q_{u\ max}$)

Figure 6.41 depicts the evolution of the unconfined compressive stress (q_u) and the undrained secant modulus ($E_{u\ sec}$) with the stress level for the UCS_{pc} tests performed.

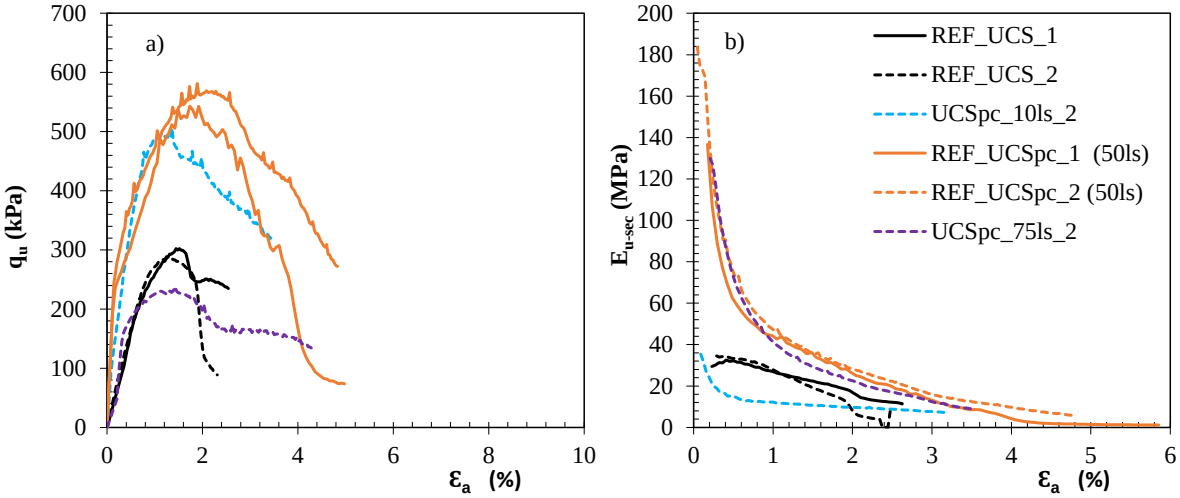

Figure 6.41: Results of the UCS and UCS_{pc} tests performed on unreinforced stabilised samples: a) stress-strain plot; b) $E_{u\text{-}sec}$ vs axial strain (CI42.5 R; binder quantity = 250 kg/m^3; curing time = 28 days; curing conditions: vertical stress = 0 kPa, room)

Those results reveal that the increase in the compressive strength/stiffness with the stress level is not linked with the permanent deformation observed during the cyclic stage. In fact, significant deformations in the cyclic stage led to greater strengths/stiffness in the post-cyclic tests, provided that the stress level does not exceed of 50%*$q_{u\,max}$. For stress levels higher than 50% the breakage of the cementation bonds is more intense and there is a decay of the compressive strength/stiffness. This may be explained by the significant breakage of cementitious bonds in the cyclic stage.

Regarding the STS_{pc} tests (Figure 6.42 and 6.43), It was observed that larger deformation in the cyclic stage results in a lower load in the post-cyclic tests, which is coherent with the expected degradation of the mechanical characteristics during the cyclic stage, namely when a higher stress level is applied.

Table 6.20: Results of the STS and STS_{pc} tests performed on unreinforced stabilised samples (CI42.5 R; binder quantity = 250 kg/m^3; curing time = 28 days; curing conditions: vertical stress = 0 kPa, room)

ID	ls	Load, F(N)	disp, δ_v (mm)	w_f (%)
REF_STS_1	-	1728	0.74	72.56
REF_STS_2	-	1640	0.74	72.91
STSpc_10ls_1	10%	1877.9	0.76	71.81
REF_STSpc_1 (50ls)	50%	1863.8	0.85	68.37
REF_STSpc_2 (50ls)	50%	1756.2	0.92	71.37
STSpc_75ls_1	75%	1400.5	0.59	71.87

ls: level of stress defined by (F_{cyc}/F_{max})

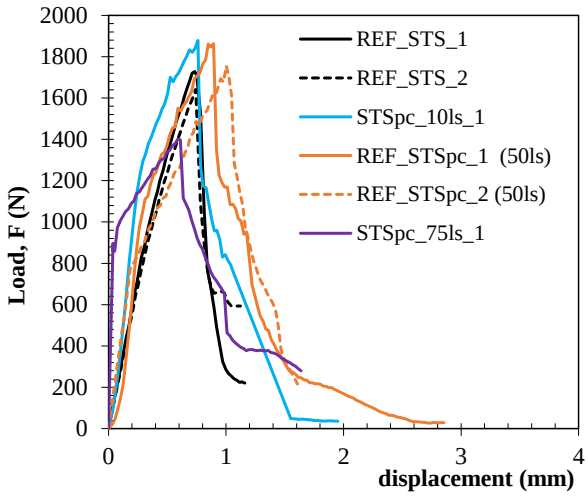

Figure 6.42: Load-displacement curves of the STS and STS_{pc} tests performed on unreinforced stabilised samples (CI42.5 R; binder quantity = 250 kg/m^3; curing time = 28 days; curing conditions: vertical stress = 0 kPa, room)

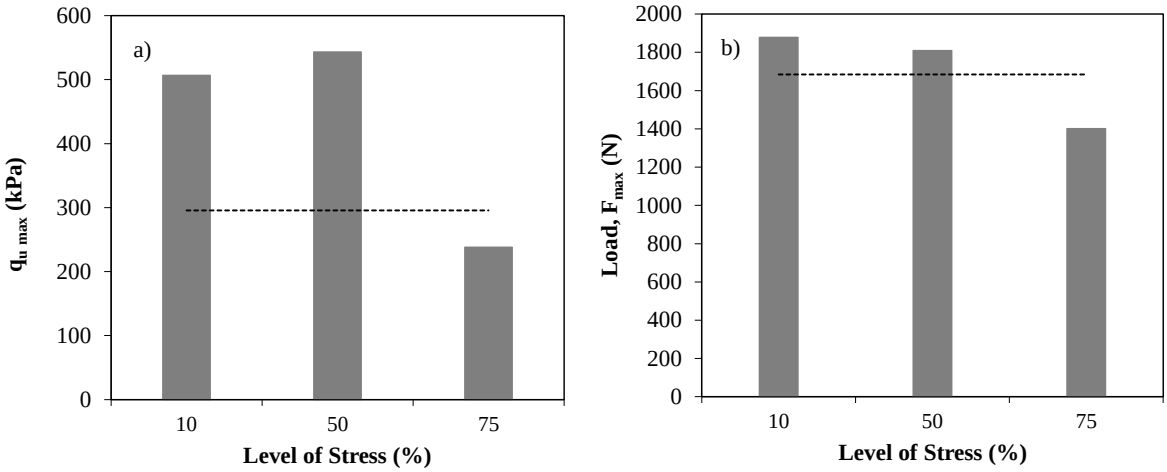

Figure 6.43: Evolution of maximum strength/load vs the level of stress of the cyclic loading for: a) UCS_{pc}, b) STS_{pc} tests

6.5.2 Chemically stabilised soft soil reinforced with polypropylene fibres

Table 6.21 and Figures 6.44 and 6.45 review the results obtained during the cyclic stage of the UCS and STS cyclic tests for a different stress levels for the stabilised samples reinforced with polypropylene fibres. As it may be seen from Figures 6.44 and 6.45, the evolution of the permanent deformation (axial strain or vertical displacement for UCS and STS cyclic tests, respectively) is characterised by a quick increase in the first 500 load cycles followed by a slight increase has as the cycles increase. As the composite material deforms due to the breakage of the cementitious bonds, the fibres are progressively mobilised, contributing to reducing the permanent axial strain (UCS_{cyc} tests) compared with the corresponding unreinforced sample (Figure 6.39 and Table 6.18). Indeed, the fibres can absorb and redistribute part of the stresses induced by the cyclic loading, which results in a lower permanent axial strain, avoiding the breakage of some

cementitious bonds and the consequent deterioration of the solid skeleton (in agreement with Venda Oliveira et al. 2022). The analysis should consider the failure mechanism of the STS test, characterised by an abrupt breakage of the cementitious bonds, occurring for minimal vertical displacements. The physical presence of the fibres will prevent the development of some cementitious bonds within the composite matrix. Producing a composite material will lower stiffness. Thus, the fibre-reinforced material will experience more deformations since it has lower stiffness than the unreinforced material. The vertical displacements induced in the STS_{cyc} tests are too small for an effective fibre mobilisation.

Table 6.21: Maximum permanent axial strain and permanent vertical displacement during the cyclic stage of the UCS and STS cyclic tests

ID	ls	$\varepsilon_{ax\text{-}perm}$ (%)	$\delta_{v\text{-}perm}$ (mm)
UCScyc_10ls_1_F	10%	0.16	-
REF_UCScyc_1_F (50ls)	50%	0.16	-
REF_UCScyc_2_F (50ls)	50%	0.17	-
UCScyc_75ls_1_F	75%	1.01	-
STScyc_10ls_1_F	10%	-	0.07
REF_STScyc_1_F (50ls)	50%	-	0.20
REF_STScyc_2_F (50ls)	50%	-	0.22
STScyc_75ls_1_F	75%	-	0.75

ls: level of stress

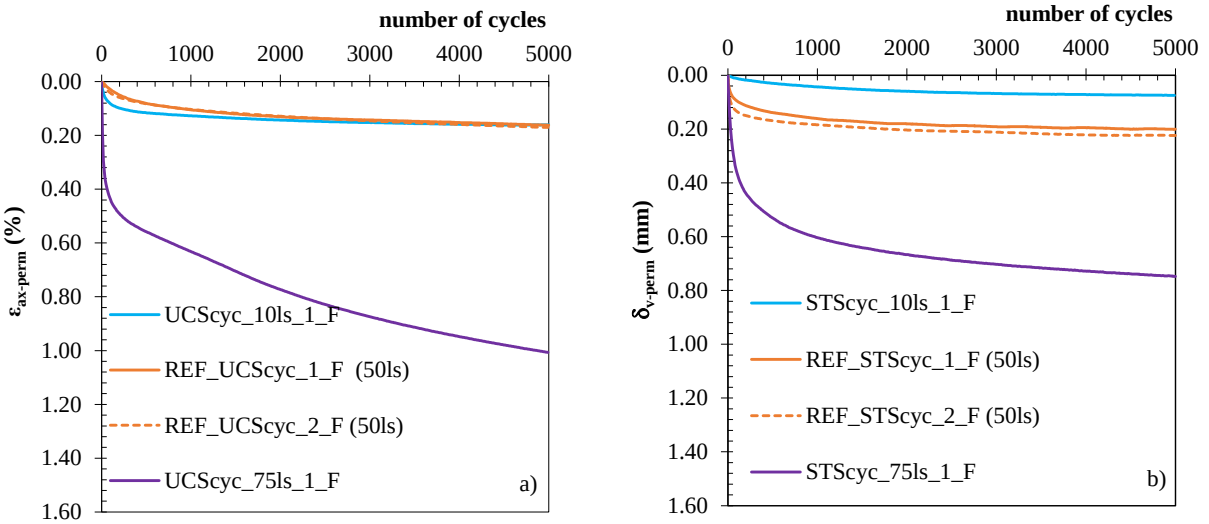

Figure 6.44: Evolution of the permanent axial strain/permanent vertical displacement during the cyclic stage for stabilised fibre-reinforced samples: a) UCS_{cyc}; b) STS_{cyc} (frequency = 0.5 Hz; number of cycles = 5.000; amplitude = ±10%*$q_{u\ max}$ or ±10%*F_{max})

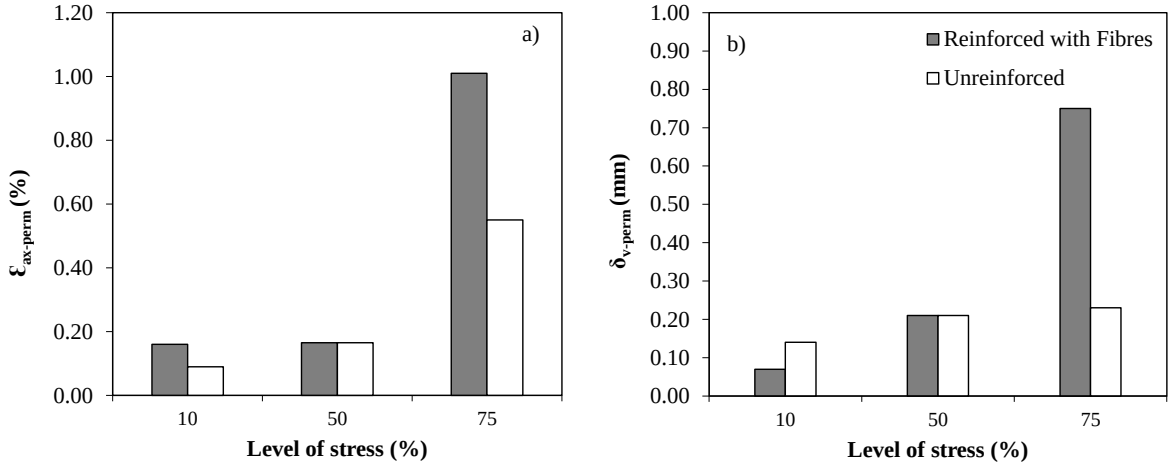

Figure 6.45: Evolution of the maximum permanent axial strain/vertical displacement vs the level of stress for stabilised fibre-reinforced samples: a) UCS_{cyc}; b) STS_{cyc} (frequency = 0.5 Hz; number of cycles = 5.000; amplitude = 10%*$q_{u\ max}$ or ±10%*F_{max})

Tables 6.22 and 6.23 and Figures 6.46, 6.47 and 6.48 summarise the results obtained during the post-cyclic UCS and STS tests performed immediately after the cyclic stage where the stress level was changed for the stabilised samples reinforced with polypropylene fibres.

The results indicate that the application of different stress levels implies an increase in the strength/load of the stabilised fibre-reinforced material compared to the reference monotonic tests. However the results also show a decrease of the strength/load for higher stress levels.

These results seem to indicate that the mobilisation of the tensile strength of the fibres during the cyclic stage was not sufficient to compensate for the degradation of the cementitious matrix induced by the cyclic stage and the loss of unconfined compressive strength and stiffness induced by the presence of the fibres that inhibit the development of some cementitious bonds, as observed in Chapter 5.

The addition of fibres also decreases the brittleness of the stress-strain/load-displacement behaviour of the composite material, with very low I_b values (Table 6.22).

Table 6.22: Main results of the UCS and UCS_{pc} tests performed on stabilised fibre-reinforced samples (CI42.5 R; binder quantity = 250 kg/m^3; curing time = 28 days; curing conditions: vertical stress = 0 kPa, room)

ID	ls	$q_{u\text{-}max}$ (kPa)	ε_r (%)	E_{u50} (MPa)	I_b	w_f (%)
REF_UCS_1_F	-	293.87	4.55	14.32	0.19	70.62
REF_UCS_2_F	-	296.65	4.03	16.10	0.12	70.56
UCSpc_10ls_1_F	10%	571.84	2.83	62.51	0.01	70.68
REF_UCSpc_1_F (50ls)	50%	531.01	1.59	79.89	0.03	72.76
REF_UCSpc_2_F (50ls)	50%	504.69	2.70	54.37	0.14	70.48
UCSpc_75ls_1_F	75%	448.40	8.34	217.52	0.14	71.21

ls: level of stress defined by ($q_{u\ cyc}/q_{u\ max}$); I_b: brittleness index = 1-[($q_{u\ at\ \varepsilon ax\ =\ 3\%}$)/$q_{u\ max}$]

Comparing the water contents for the cases unreinforced and fibre-reinforced, negligible effect is observed due to the presence of the fibres. The water contents measured after the end of the UCS_{pc}

or STS_{pc} tests reveal any significant change, which may be explained by the same time elapsed during the cyclic stage, 5.000 cycles = 2.78h during which the samples dried.

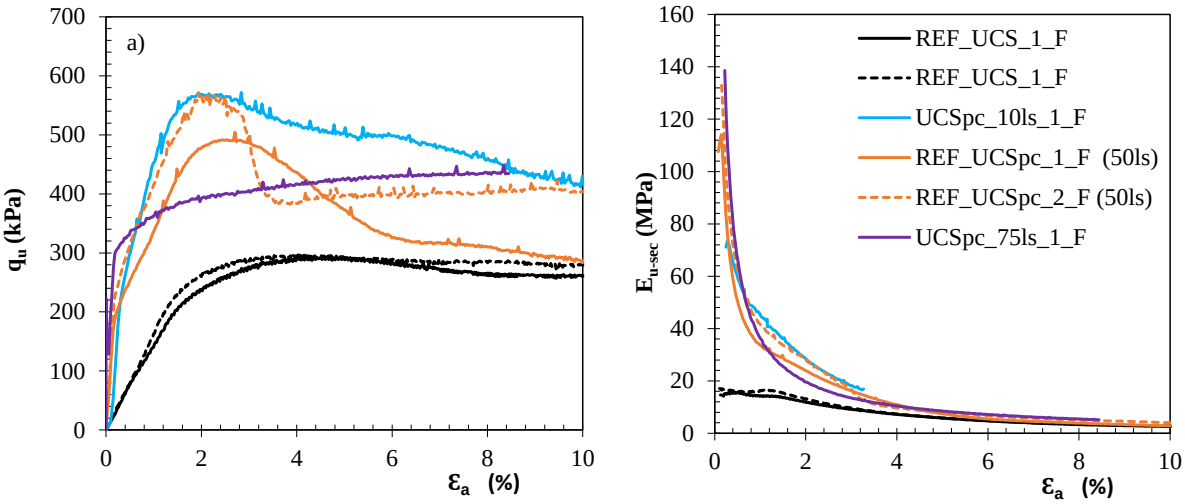

Figure 6.46: Results of the UCS and UCS_{pc} tests performed on stabilised samples reinforced with fibres: a) stress-strain plot; b) Eu-sec vs axial strain (CI42.5 R; binder quantity = 250 kg/m^3; curing time = 28 days; curing conditions: vertical stress = 0 kPa, room)

Table 6.23: Results of the STS and STS_{pc} tests performed on stabilised samples reinforced with fibres (CI42.5 R; binder quantity = 250 kg/m^3; curing time = 28 days; curing conditions: vertical stress = 0 kPa, room)

ID	ls	Load, F(N)	disp, δ_v (mm)	w_f (%)
REF_STS_1_F	-	1451.0	4.48	71.58
REF_STS_2_F	-	1539	2.43	71.68
STSpc_10ls_1_F	10%	3102.4	3.25	74.01
REF_STSpc_1_F (50ls)	50%	2121.3	3.0	72.15
REF_STSpc_2_F (50ls)	50%	2022.2	2.4	75.24
STSpc_75ls_1_F	75%	1841.7	5.33	70.71

ls: level of stress defined by (F_{cyc}/ F_{max})

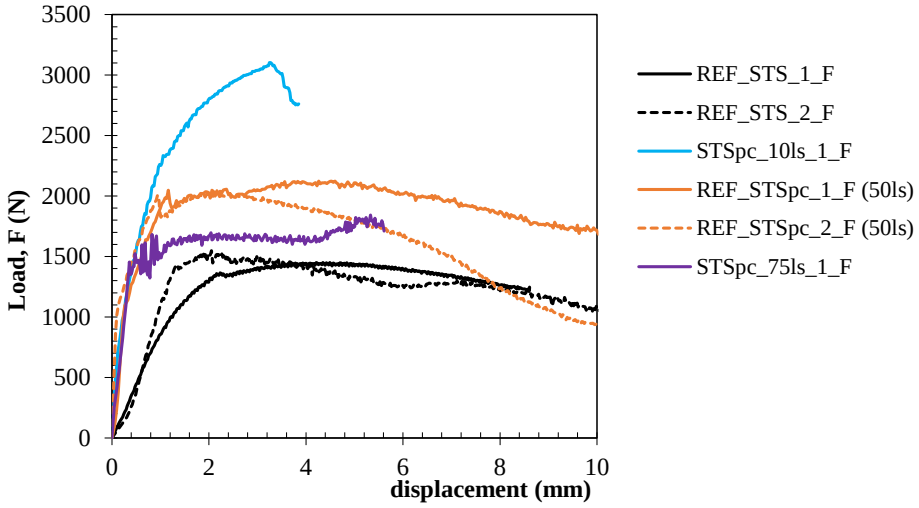

Figure 6.47: Load-displacement curves of the STS and STS_{pc} tests performed on stabilised samples reinforced with fibres (CI42.5 R; binder quantity = 250 kg/m^3; curing time = 28 days; curing conditions: vertical stress = 0 kPa, room)

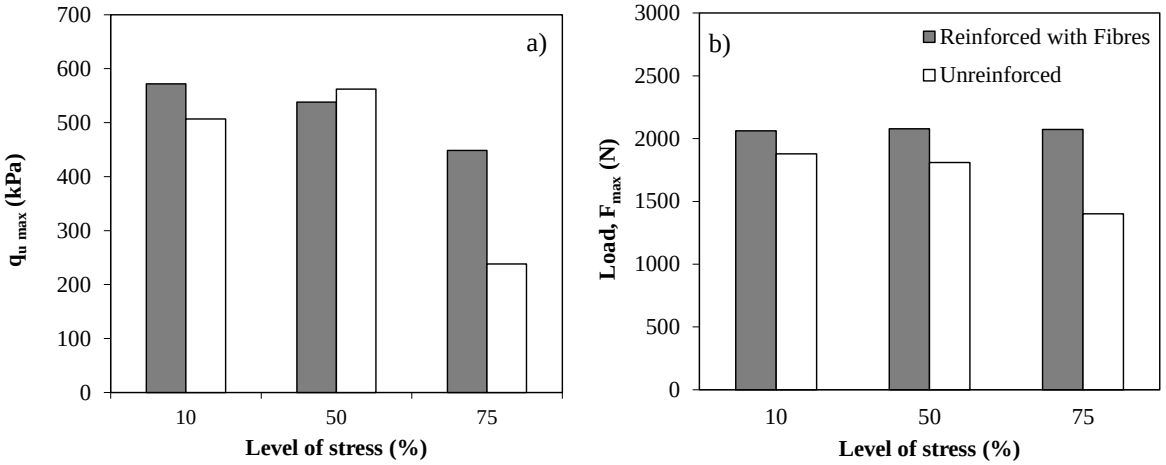

Figure 6.48: Evolution of the maximum strength/load vs the level of stress for samples unreinforced and reinforced with fibres: a) UCS_{pc}, b) STS_{pc} tests

6.6 Parametric study – effect of the amplitude of the loading cyclic

In order to study the effect of the amplitude of the cyclic loading on the mechanical behaviour of the soft soil of Baixo Mondego chemically stabilised unreinforced or reinforced with polypropylene fibres, a series of UCS and STS tests under cyclic loading were carried out. During the cyclic stage, various values of the amplitude of the cyclic loading were studied (5%, 10%, 20% of the strength/load evaluated by the monotonic tests). At the same time, it was kept constant the number of loading cycles (5.000), the cyclic loading frequency (0.5 Hz) and the stress level of the cyclic loading (50% of the strength/load evaluated by the monotonic tests). It will be examined the evolution of the permanent axial strain (for UCS cyclic tests) and the permanent vertical displacement (for STS cyclic tests) that happens during the cyclic stage, complemented by the stress-strain plots (for UCS post-cyclic tests) and the load-displacement plots (for STS post-cyclic tests). The results of the UCS and STS cyclic tests are presented in the following sections for both chemically stabilised materials, soft soil of Baixo Mondego unreinforced and reinforced with polypropylene fibres.

6.6.1 Chemically stabilised unreinforced soft soil

In Table 6.24 and Figures 6.49 and 6.50, the results obtained during the cyclic stage of the UCS and STS cyclic tests for the different amplitude of the cyclic loading are summarised.

Figure 6.49 shows the evolution of the permanent deformation (axial strain or vertical displacement for UCS and STS cyclic tests, respectively). As observed in the stress level analysis, at the beginning there is an intense deformation up to 500 cycles, followed by a progressive decrease of the deformation rate.

For both tests, it is seen that the permanent deformation increases when the amplitude applied increases (Figure 6.49), indicating a progressive damage of the solid skeleton with the increase of the amplitude of cyclic loading.

Table 6.24: Maximum permanent axial strain and permanent vertical displacement during the cyclic stage of the UCS and STS cyclic tests

	amp	$\varepsilon_{ax\text{-}perm}$ (%)	$\delta_{v\text{-}perm}$ (mm)
UCScyc_5amp_2	5%	0.08	
REF_UCScyc_1 (10amp)	10%	0.16	
REF_UCScyc_2 (10amp)	10%	0.17	
UCScyc_20amp_1	20%	0.30	
STScyc_5amp_2	5%		0.21
REF_STScyc_1 (10amp)	10%		0.20
REF_STScyc_2 (10amp)	10%		0.22
STScyc_20amp_1	20%		0.37

amp: amplitude

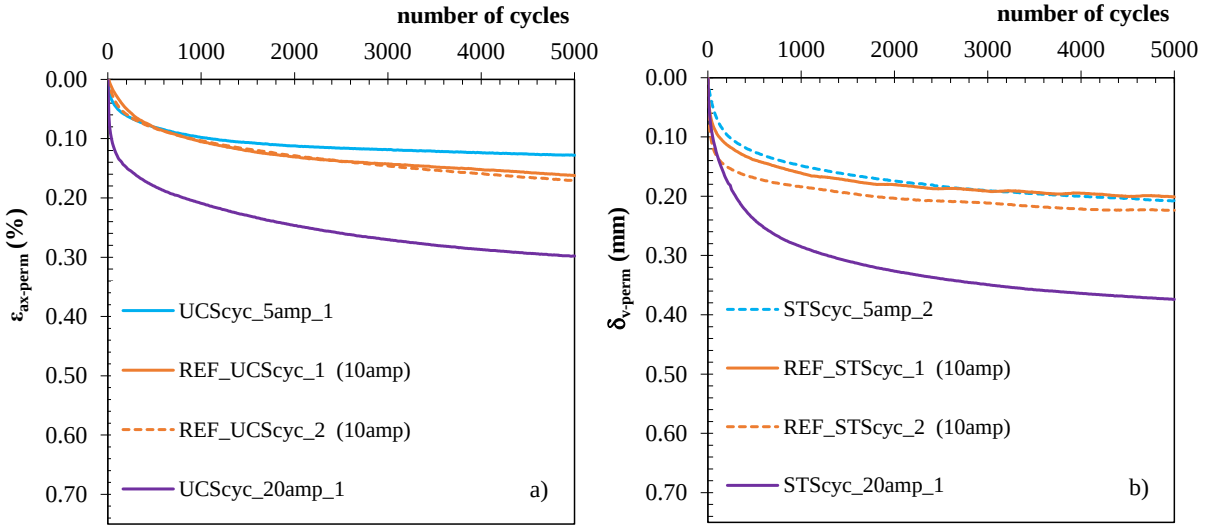

Figure 6.49: Evolution of the permanent axial strain/permanent vertical displacement during the cyclic stage for unreinforced stabilised samples a) UCS_{cyc}, b) STS_{cyc} (frequency = 0.5 Hz; number of cycles = 5.000; stress level = 50%*$q_{u\ max}$ or 50%*F_{max})

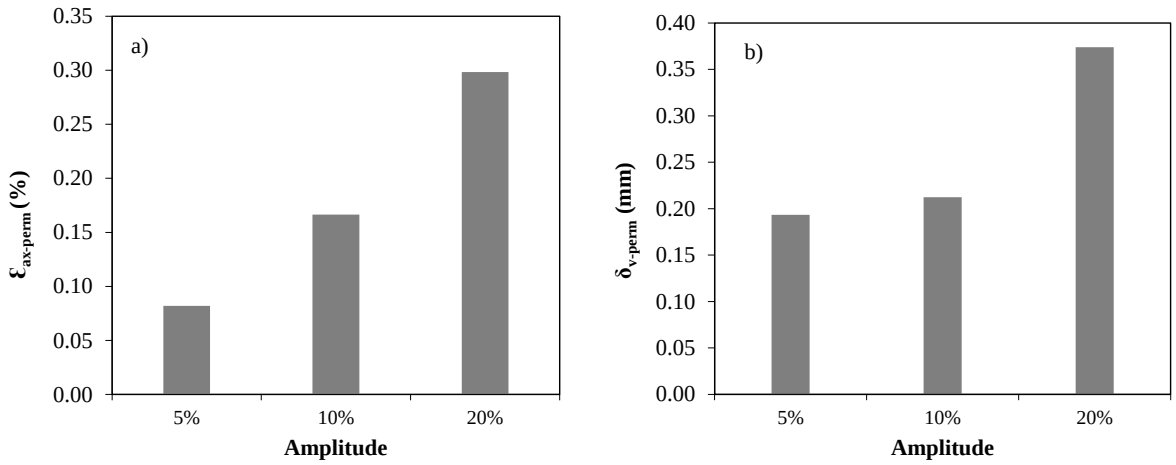

Figure 6.50: Evolution of the maximum permanent axial strain/permanent vertical displacement vs the amplitude of the cyclic loading for unreinforced stabilised samples: a) UCS_{cyc}, b) STS_{cyc}

Tables 6.25 and 6.26 and Figures 6.51, 6.52 and 6.53 summarise the results obtained during the post-cyclic UCS and STS tests performed immediately after the cyclic stage where the amplitude was changed. The results clearly show that if the amplitude is in the range of 5 – 10%, the strength/load of the composite material is higher than those of the reference monotonic tests. The breakage of cementitious bonds observed in the cyclic stage may induce a coarser apparent grain size, resulting in greater strength during the cyclic stage.

The results also reveal that an increase of the amplitude induces a decrease of the strength/load which is coherent to the progressive damage of the composite material during the cyclic stage, characterized by higher permanent deformations.

The water contents measured after the UCSpc or STSpc tests reveal negligible changes because all post cyclic tests were carried out under 5.000 cycles and a frequency of 0.5 Hz = 2.78h.

Table 6.25: Results of the UCS and UCS_{pc} tests performed on unreinforced stabilised samples (CI42.5 R; binder quantity = 250 kg/m^3; curing time = 28 days; curing conditions: vertical stress = 0 kPa, room)

ID	amp	$q_{u\ max}$ (kPa)	ε_r (%)	E_{u50} (MPa)	w_f (%)
REF_UCS_1	-	302.36	1.45	33.29	71.56
REF_UCS_2	-	288.80	1.25	33.92	71.86
UCSpc_5amp_2	5%	608.57	1.77	148.87	69.97
REF_UCSpc_1 (10amp)	10%	543.17	1.73	91.28	69.1
REF_UCSpc_2 (10amp)	10%	581.26	1.88	139.15	69.57
UCSpc_20amp_1	20%	321.78	1.21	80.46	71.97

amp: amplitude defined by the variation (±) of the cyclic stress/load regarding to the stress level applied ($\Delta q_u/q_{u\ max}$)

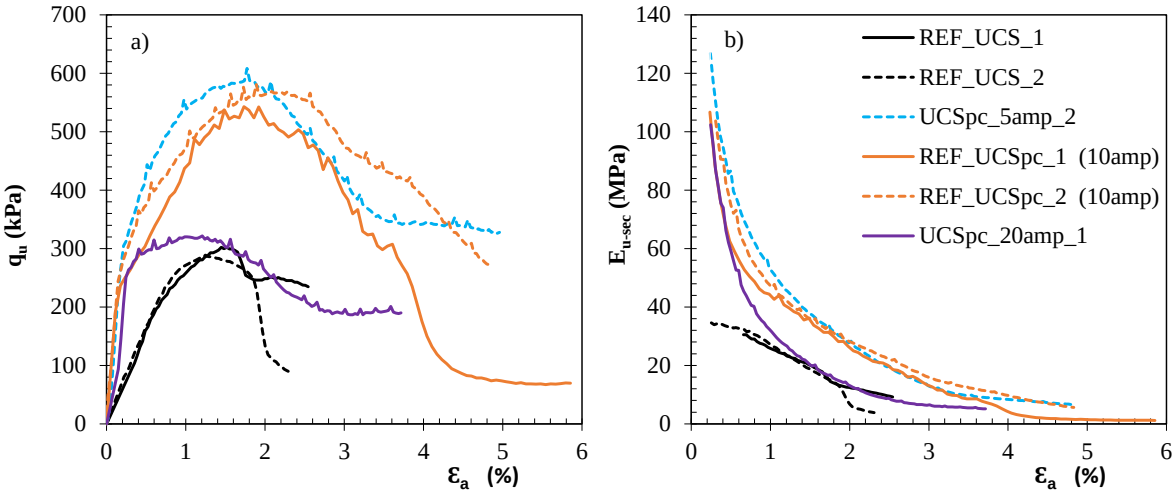

Figure 6.51: Results of the UCS and UCS_{pc} tests performed on unreinforced stabilised samples: a) stress-strain plot; b) $E_{u\text{-}sec}$ vs axial strain (CI42.5 R; binder quantity = 250 kg/m^3; curing time = 28 days; curing conditions: vertical stress = 0 kPa, room)

Table 6.26: Results of the STS and STS_{pc} tests performed on unreinforced stabilised samples (CI42.5 R; binder quantity = 250 kg/m^3; curing time = 28 days; curing conditions: vertical stress = 0 kPa, room)

ID	Amplitude	Load, F (N)	δ_v (mm)	w_f (%)
REF_STS_1	-	1728	0.74	72.56
REF_STS_2	-	1640	0.74	72.91
STSpc_5amp_2	5%	2422.57	1.45	71.12
REF_STSpc_1 (10amp)	10%	1863.8	0.85	68.37
REF_STSpc_2 (10amp)	10%	1756.2	0.92	71.37
STSpc_20amp_1	20%	1052.87	0.60	70.37

amp: amplitude defined by the variation (±) of the cyclic load regarding to the load level applied ($\Delta F/F_{max}$)

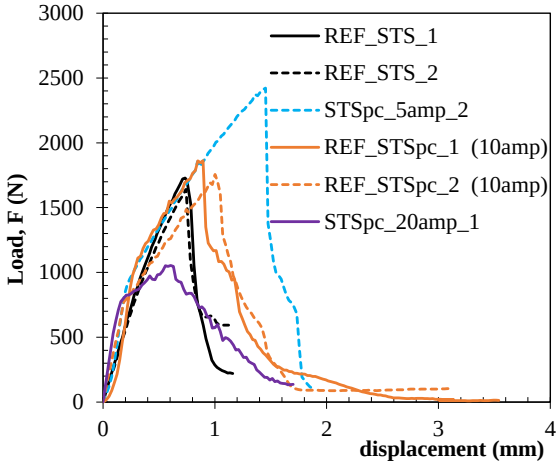

Figure 6.52: Load-displacement curves of the STS and STS_{pc} tests performed on unreinforced stabilised samples (CI42.5 R; binder quantity = 250 kg/m^3; curing time = 28 days; curing conditions: vertical stress = 0 kPa, room)

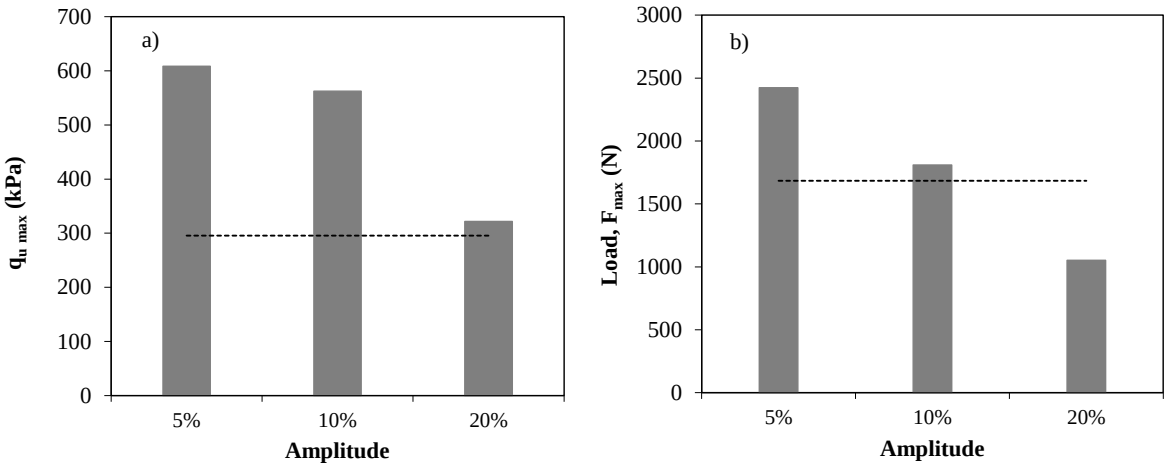

Figure 6.53: Evolution of the maximum strength/load vs the amplitude of the cyclic loading for unreinforced stabilised samples: a) UCS_{pc}, b) STS_{pc} tests

6.6.2 Chemically stabilised soft soil reinforced with polypropylene fibres

Table 6.27 and Figures 6.54 and 6.55 summarise the results obtained during the cyclic stage of the UCS and STS cyclic tests for different amplitude for the stabilised samples reinforced with polypropylene fibres.

From Figures 6.54 and 6.55, the evolution of the permanent deformation (axial strain or vertical displacement for UCS and STS cyclic tests, respectively) is characterised by a quick increase in the first 500 load cycles followed by a slight increase for a higher number of load cycles.

The comparison between unreinforced and reinforced samples show that the permanent deformation are similar in both cases for amplitudes in the range of 5-10%, For an amplitude of 20% the reinforced samples submitted to UCS tests show lower permanent deformation. In fact, when a material has a higher deformation, the fibres are progressively mobilised, contributing to reducing the permanent axial strain (UCS_{cyc} tests) compared with the corresponding unreinforced sample (Figure 6.49 and Table 6.24).

Table 6.27: Maximum permanent axial strain and permanent vertical displacement during the cyclic stage of the UCS and STS cyclic tests

ID	amp	$\varepsilon_{ax\text{-}perm}$ (%)	$\delta_{v\text{-}perm}$ (mm)
UCScyc_5amp_1_F	5%	0.15	-
REF_UCScyc_1_F (10amp)	10%	0.16	-
REF_UCScyc_2_F (10amp)	10%	0.17	-
UCScyc_20amp_1_F	20%	0.24	-
STScyc_5amp_2_F	5%		0.19
REF_STScyc_1_F (10amp)	10%		0.20
REF_STScyc_2_F (10amp)	10%		0.22
STScyc_20amp_1_F	20%		0.38

amp: amplitude

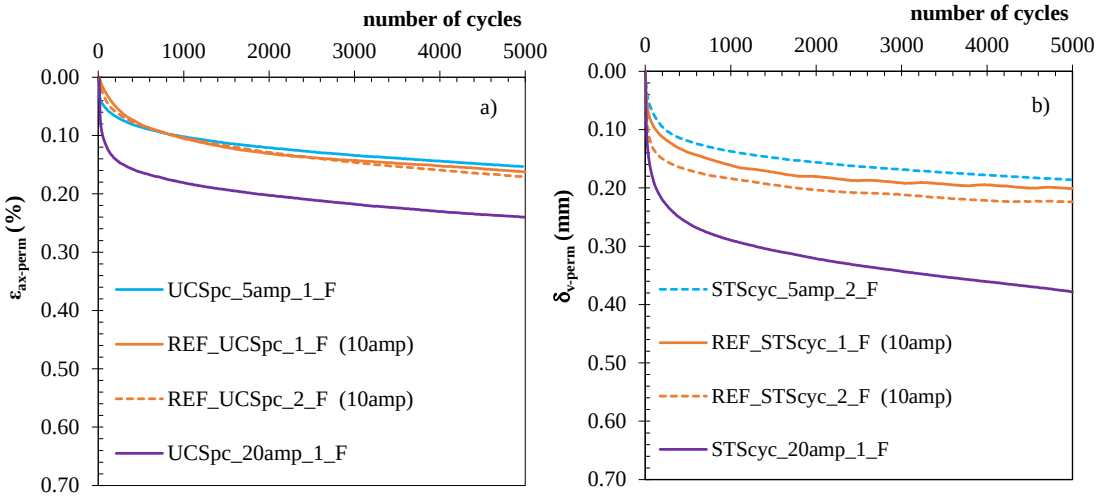

Figure 6.54: Evolution of the permanent axial strain/vertical displacement during the cyclic stage for stabilised fibre-reinforced samples: a) UCS_{cyc}, b) STS_{cyc} (frequency = 0.5 Hz; number of cycles = 5.000; stress level = 50%*$q_{u\ max}$ or 50%*F_{max})

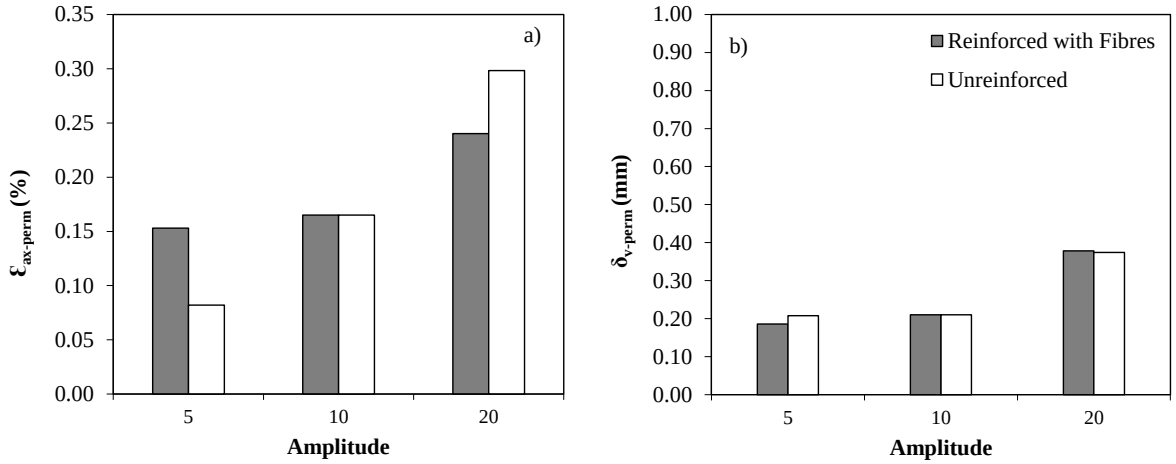

Figure 6.55: Evolution of the maximum permanent axial strain/vertical displacement during the cyclic stage for unreinforced and fibre-reinforced stabilised samples: a) UCS_{cyc}; b) STS_{cyc} (frequency = 0.5 Hz; number of cycles = 5.000; stress level = 50%*$q_{u\ max}$ or 50%*F_{max})

Tables 6.28 and 6.29 and Figures 6.56, 6.57 and 6.58 summarise the results obtained during the post-cyclic UCS and STS tests performed immediately after the cyclic stage where the amplitude was changed for the stabilised samples reinforced with polypropylene fibres.

The results indicate an increase in the strength/load of the stabilised fibre-reinforced material compared to the reference monotonic tests, although there is a reduction with the increase of the amplitude which is related to a greater degradation of the cementitious matrix during the cyclic stage

The results also show that the addition of fibres decreases the brittleness of the stress-strain/load-displacement behaviour of the composite material, with very low I_b values. Indeed, the mobilisation of the fibres contributes to mitigating the loss of strength after the peak failure and the mobilisation of a non-negligible residual strength.

The water contents measured after the end of the UCS_{pc} or STS_{pc} tests reveal negligible changes, which may be as explained by the constant time of the cyclic stage, 5.000 cycles = 2.78h.

Table 6.28: Results of the UCS and UCS_{pc} tests performed on stabilised samples reinforced with fibres (CI42.5 R; binder quantity = 250 kg/m^3; curing time = 28 days; curing conditions: vertical stress = 0 kPa, room)

ID	amp	$q_{u\ max}$ (kPa)	ε_r (%)	E_{u50} (MPa)	I_b (%)	w_f (%)
REF_UCS_1_F	-	293.87	4.55	14.32	0.19	70.62
REF_UCS_2_F	-	296.65	4.03	16.10	0.12	70.56
UCSpc_5amp_1_F	5%	631.71	3.10	38.98	0.21	69.97
REF_UCSpc_1_F (10amp)	10%	531.01	1.59	79.89	0.03	71.76
REF_UCSpc_2_F (10amp)	10%	504.69	2.70	54.37	0.14	70.48
UCSpc_20amp_1_F	20%	371.06	1.62	82.68	0.05	71.30

amp: amplitude defined by the variation (±) of the cyclic stress/load regarding to the stress level applied ($\Delta q_u/q_{u\ max}$; I_b: brittleness index = 1-[($q_{u\ at\ \varepsilon ax\ =\ 3\%}$)/$q_{u\ max}$]

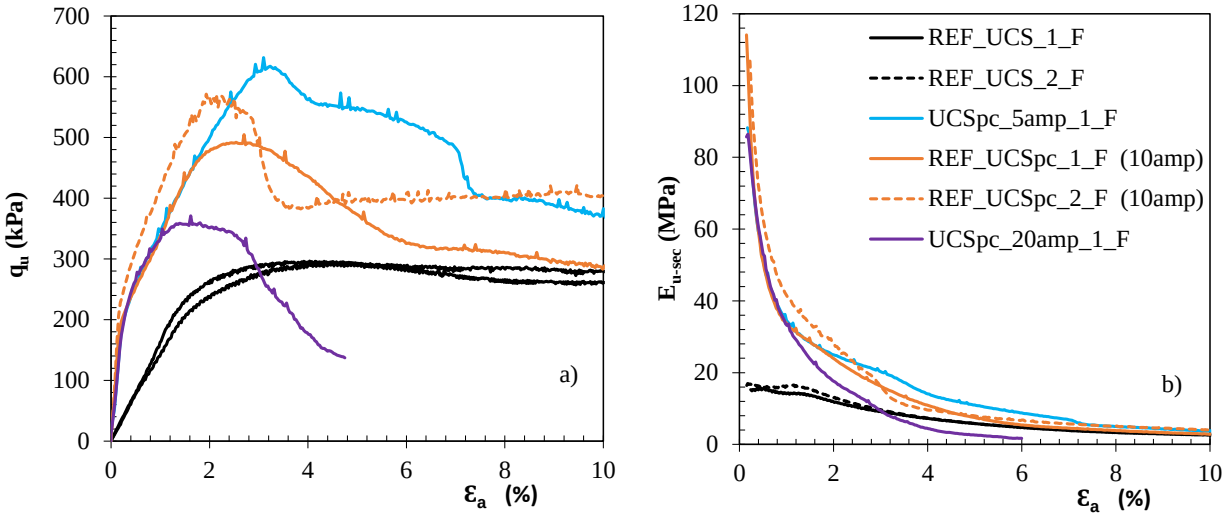

Figure 6.56: Results of the UCS and UCS_{pc} tests performed on stabilised samples reinforced with fibres: a) stress-strain plot; b) $E_{u\text{-}sec}$ vs axial strain (CI42.5 R; binder quantity = 250 kg/m^3; curing time = 28 days; curing conditions: vertical stress = 0 kPa, room)

Table 6.29: Results of the STS and STS_{pc} tests performed on stabilised samples reinforced with fibres (CI42.5 R; binder quantity = 250 kg/m^3; curing time = 28 days; curing conditions: vertical stress = 0 kPa, room)

ID	amp	Load, F (N)	δ_v (mm)	w_f (%)
REF_STS_1_F	-	1451	4.48	71.58
REF_STS_2_F	-	1539	2.43	71.68
STSpc_5amp_2_F	5%	2082	2.5	70.67
REF_STSpc_1_F (10amp)	10%	2121.3	3.0	72.15
REF_STSpc_2_F (10amp)	10%	2022.2	2.4	75.24
STSpc_20amp_1_F	20%	1816.9	2.4	75.24

amp: amplitude defined by the variation (±) of the cyclic load regarding to the stress level applied (ΔF / F_{max})

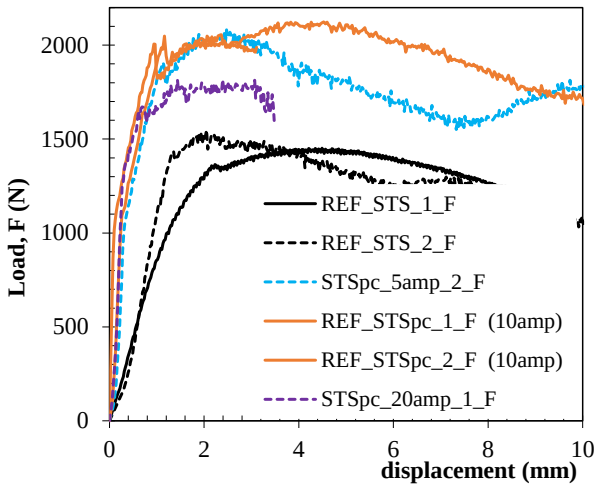

Figure 6.56: Load-displacement curves of the STS and STS_{pc} tests performed on stabilised samples reinforced with fibres (CI42.5 R; binder quantity = 250 kg/m^3; curing time = 28 days; curing conditions: vertical stress = 0 kPa, room)

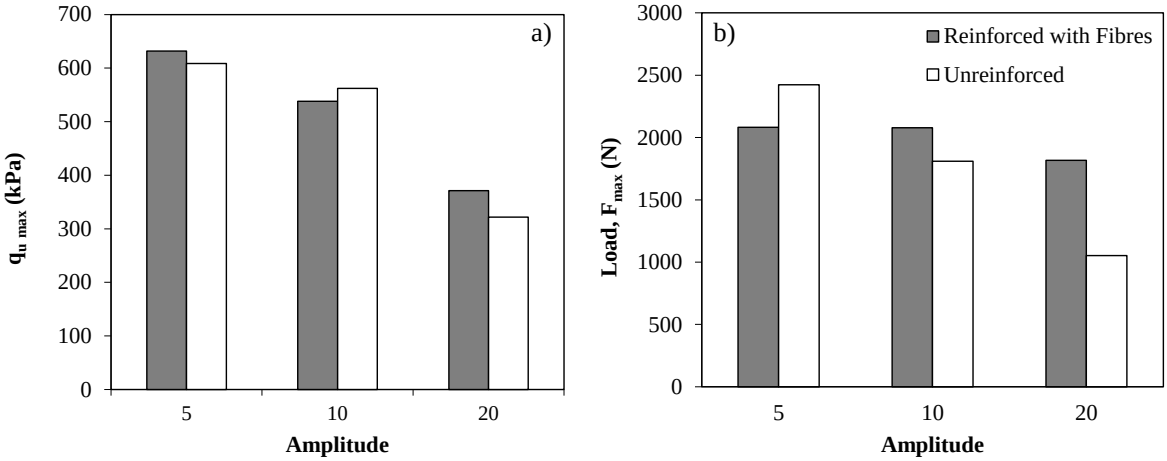

Figure 6.58: Evolution of the maximum strength/load vs the amplitude of the cyclic loading for unreinforced and fibre-reinforced stabilised samples: a) UCS_{pc}, b) STS_{pc} tests

CHAPTER 7 – COMPRESSIBILITY UNDER CYCLIC LOADING

7.1 Introduction

The knowledge acquired regarding the mechanical behaviour of the soft soil of the Baixo Mondego has shown that it has a high deformability and low mechanical strength, requiring not only the characterisation of the stress-strain-shear strength behaviour but also the compressibility and permeability characterisation. As it was presented in Chapter 2, it can be said that, in general, the mechanical behaviour of the Baixo Mondego soft soil is relatively well characterized. Regarding the mechanical behaviour of the Baixo Mondego soft soils chemically stabilized, the knowledge is still scarce mainly under cyclic loading, despite the works developed over the last years.

The present Chapter aims to contribute to the characterization of the Baixo Mondego soft soil chemically stabilised (unreinforced and reinforced with polypropylene fibres) under static and cyclic loading, focusing on aspects related to compressibility. The experimental works developed at the University of Coimbra by Correia (2011) and Costa (2018) focused on the study of the compressibility of this stabilised soil but for the unreinforced case and without any cyclic loading (Chapter 3). Nevertheless, the knowledge acquired, it is important to complement such previous studies because there is a lack of information on the compressibility behaviour when the stabilised soil is reinforced with fibres and when subjected to cyclic loading. This is the main motivation of this Chapter.

It is known that in chemically stabilised soils there are cementitious bonds between the solid particles (induced by the binder), responsible for increasing the strength and stiffness of the solid matrix and reducing the compressibility (Nagaraj et al., 1998; Kamruzzaman, 2002; Horpibulsuk et al., 2004; Lorenzo and Bergado, 2004 and 2006; Correia, 2011; Costa, 2018). It was observed that under a static monotonic loading the recompressibility index (C_r) decreases compared to the natural soil due to the fact that stabilisation induces a stiffer solid skeleton. However, the chemical

stabilisation promotes an increase of the yield stress compared to the pre-consolidation stress of the natural soil; this increase is due to the higher strength of the solid skeleton resulting from the cementitious bonds. The impact of the fibre addition and the cyclic loading will be studied in the present Chapter through oedometer tests and UCS tests subjected to a prior cyclic stage.

All samples involved in the compressibility study were prepared based on the same laboratory procedure, as shown in Chapter 5, with some modifications. That is, samples were stabilised with Portland cement applied in a quantity of 250 kg/m^3, mixed with polypropylene fibres in a quantity of 10 kg/m^3, and cured for 28 days without applying any vertical stress to the samples. During the curing period the samples were not stored in a room with temperature and humidity control (usual procedure), rather they were stored in a water tank with temperature (20±2ºC) control (immerse condition). This new curing procedure is required because for the oedometer tests it must be guaranteed that the pore pressure is almost null, i.e., the effective stress is equal to the total stress applied. For such, the oedometer samples must be in a submerged condition. In order to allow a direct comparison between oedometer and UCS tests, new UCS samples must be prepared following this new procedure (immerse curing condition), implying the definition of new reference UCS tests.

For the oedometer and UCS tests with a prior cyclic stage, the cyclic loading parameters are equal to the reference values presented in Chapter 6, i.e., the number of loading cycles is equal to 5.000, frequency is 0.5 Hz, the stress level applied is 50% and the amplitude is ± 10% of strength (yield stress or $q_{u\,max}$ for oedometer or UCS tests, respectively) measured in tests without cyclic loading stage (reference tests).

Along the next sections the compressibility results will be presented, beginning with the description of the new reference tests, followed by the compressibility results of UCS and oedometer tests without and with a prior cyclic stage.

7.2 New reference UCS tests

As stated in the previous section, the UCS reference tests presented in Chapter 5 (cured in a room, i.e., under emerged condition) are not valid here because it is required that the samples are stored, during the curing period of 28 days, in a submerged condition (inside a water tank) in order to allow a comparison with oedometer tests.

Table 7.1 and Figures 7.1 and 7.2 summarizes the results of the reference UCS tests performed on stabilised samples without and with fibres for both curing conditions, in a room (emerged, Chapter

5) and submerged in a water tank (tests identified by the first letter of the word 'submerged' at the test ID).

Table 7.1: Results of the UCS reference tests performed on stabilized samples unreinforced and reinforced with fibres for different curing conditions (CI42.5 R; binder quantity = 250 kg/m^3; curing time = 28 days; vertical stress = 0 kPa)

ID	Fibres	Curing Conditions	$q_{u\ max}$ (kPa)	ε_r (%)	E_{u50} (kPa)	w_f (%)
REF_UCS_1	No	room	302.36	1.45	31.13	77.56
REF_UCS_2	No	room	288.80	1.25	33.62	77.56
REF_UCS_1_F	Yes	room	293.87	4.55	14.32	70.62
REF_UCS_2_F	Yes	room	296.65	4.03	16.10	70.56
S_REF_UCS_1	No	tank	510.33	1.10	84.52	75.45
S_REF_UCS_2	No	tank	477.10	1.04	59.75	77.95
S_REF_UCS_1_F	Yes	tank	672.72	2.04	41.76	78.04
S_REF_UCS_2_F	Yes	tank	683.88	2.33	51.45	77.62

As it may be seen, the samples cured in a submerged condition (inside water tank) exhibit better mechanical properties (higher $q_{u\ max}$ and $E_{u50\%}$) than the samples cured in a room, which seems to be in contradiction with the findings presented in section 5.2.1. However, the results are for different curing times, 7 days in section 5.2.1 while now the samples are cured for 28 days. This means that for a longer curing time the "free access" to water allows the development of more cementitious reactions, which results in a stronger and stiffer solid skeleton, i.e., in a better mechanical behaviour. The presence of the fibres gives to the composite material a ductile behaviour characterised by a smaller loss of strength after peak failure, exhibiting a substantial residual strength. This behaviour is due to the progressive mobilisation of the fibres strength as the strain/deformation evolves. The results also show that when the samples are cured in a submerged condition (immerse in a water tank) the fibres addition has a positive impact in terms of unconfined compressive strength but a negative impact on stiffness.

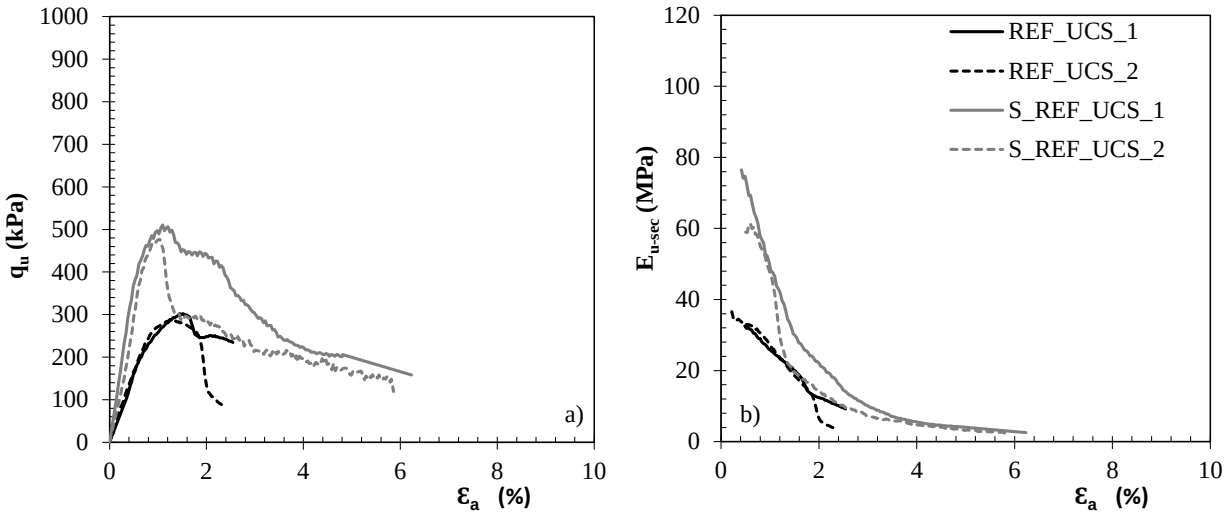

Figure 7.1: Results of the UCS reference tests performed on unreinforced stabilised samples: a) stress-strain plot; b) $E_{u\text{-}sec}$ vs axial strain (CI42.5 R; binder quantity = 250 kg/m^3; curing time = 28 days; curing conditions: vertical stress = 0 kPa, room and in tank)

Such behaviour is explained by the fact that the physical presence of the fibres may prevent the development of some cementitious bonds within the composite matrix, producing a composite material will lower stiffness. Thus, the fibre-reinforced material will experience more deformations at failure (as expressed by the higher strain at failure), allowing a "more effective" mobilisation of the fibres, contributing to the strength improvement.

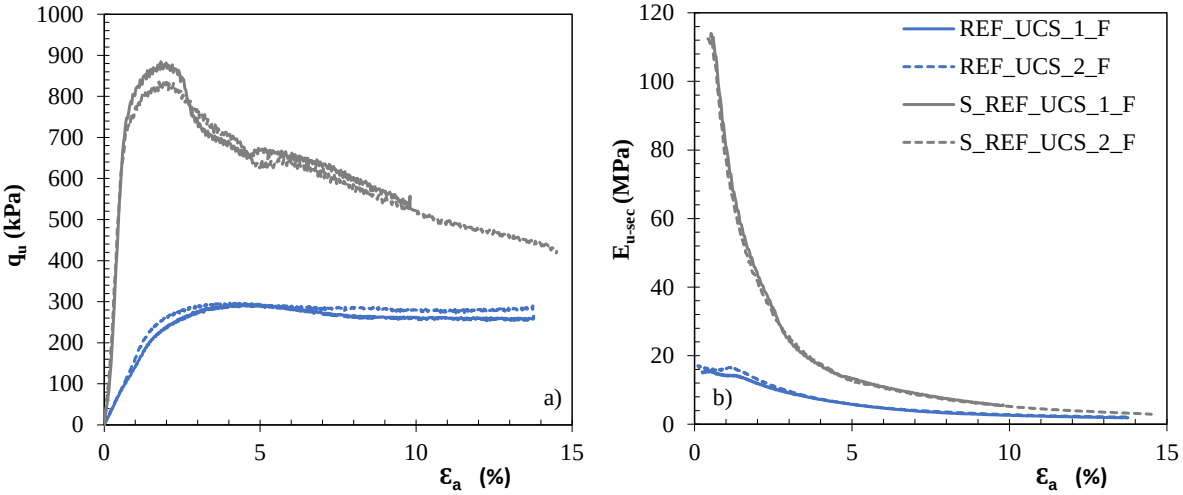

Figure 7.2: Results of the UCS reference tests performed on stabilised samples reinforced with fibres: a) stress-strain plot; b) $E_{u\text{-}sec}$ vs axial strain (CI42.5 R; binder quantity = 250 kg/m^3; curing time = 28 days; curing conditions: vertical stress = 0 kPa, room and in tank)

It is also important to analyse the impact that the cyclic loading has on the evolution of the permanent axial strain and on the post-cyclic UCS tests for stabilised samples without and with fibres for the new curing condition, immersion in water tank. For such, new samples were produced and submitted to cyclic UCS tests following the procedure described in Chapter 6. Table 7.2 and Figures 7.3 and 7.4 summarize the results obtained for both curing conditions, in a room (emerged, Chapter 6) and submerged in a water tank (tests identified by the first letter of the word 'submerged' at the test ID).

Table 7.2: Results of the cyclic UCS tests performed on stabilized samples unreinforced and reinforced with fibres for different curing conditions (CI42.5 R; binder quantity = 250 kg/m^3; curing time = 28 days; vertical stress = 0 kPa)

ID	$\varepsilon_{ax\ perm}$ (%)	Fibres	Curing Conditions	ID	$q_{u\text{-}max}$ (kPa)	ε_r (%)	E_{u50} (MPa)	w_f (%)
REF_UCScyc_1	0.22	No	room	REF_UCSpc_1	543.17	1.73	91.28	69.1
REF_UCScyc_2	0.24	No	room	REF_UCSpc_2	581.26	1.88	139.15	69.57
REF_UCScyc_1_F	0.16	Yes	room	REF_UCSpc_1_F	531.01	1.59	79.89	72.76
REF_UCScyc_2_F	0.15	Yes	room	REF_UCSpc_2_F	504.69	2.70	54.37	70.48
S_UCScyc_1	0.24	No	tank	S_UCSpc_1	721.52	1.49	100.02	74.65
S_UCScyc_2	0.22	No	tank	S_UCSpc_2	691.09	1.28	124.14	73.80
S_UCScyc_1_F	0.33	Yes	tank	S_UCSpc_1_F	884.48	1.82	102.98	72.09
S_UCScyc_2_F	0.32	Yes	tank	S_UCSpc_2_F	835.09	1.76	104.68	71.27

Figure 7.3 exhibits the same trend as observed for other cyclic tests, characterised by a quick increase of the permanent axial strain in the first 500 load cycles followed by a slight increase as the number of load cycles increases. In general, and independently of the presence of the fibres, the submerged samples present a maximum permanent axial strain of the same order or higher than the corresponding samples cured in an emerged condition (in a room). For the submerged cured condition, it is expected to have negligible suction effects, allowing larger axial strains during the cyclic stage, which are even larger for the fibre-reinforced case due that the physical presence of the fibres may prevent the development of some cementitious bonds within the composite matrix, producing a composite material will lower stiffness, i.e., with larger deformations.

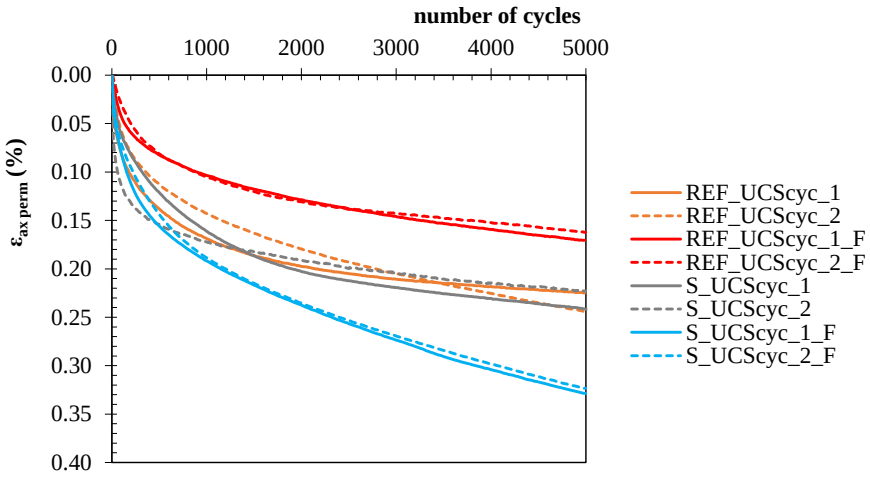

Figure 7.3: Evolution of permanent axial strain during the UCS cyclic tests (cyclic stage) performed on stabilised samples unreinforced and fibre reinforced (CI42.5 R; binder quantity = 250 kg/m^3; curing time = 28 days; curing conditions: vertical stress = 0 kPa, room and in tank)

In terms of mechanical properties (stress-strain and $E_{u\text{-}sec}$ curves) evaluated post-cyclic stage, Figure 7.4 summarize the results obtained. As it may be seen, the samples cured in a submerged condition (inside water tank) exhibit better mechanical properties than the corresponding samples cured in a room, explained by the fact that the "free access" to water allows the development of more cementitious reactions, which results in a stronger and stiffer solid skeleton, i.e., in a better mechanical behaviour. The addition of fibres to the submerged samples promotes the increase of the unconfined compressive strength and a slightly decrease of the stiffness, i.e., the largest deformations occurred during the cyclic stage (associated to the physical presence of the fibres that may prevent the development of some cementitious bonds resulting in a stiffness decrease) for the fibre-reinforced samples allow a "more effective" mobilisation of the fibres, contributing to the strength improvement.

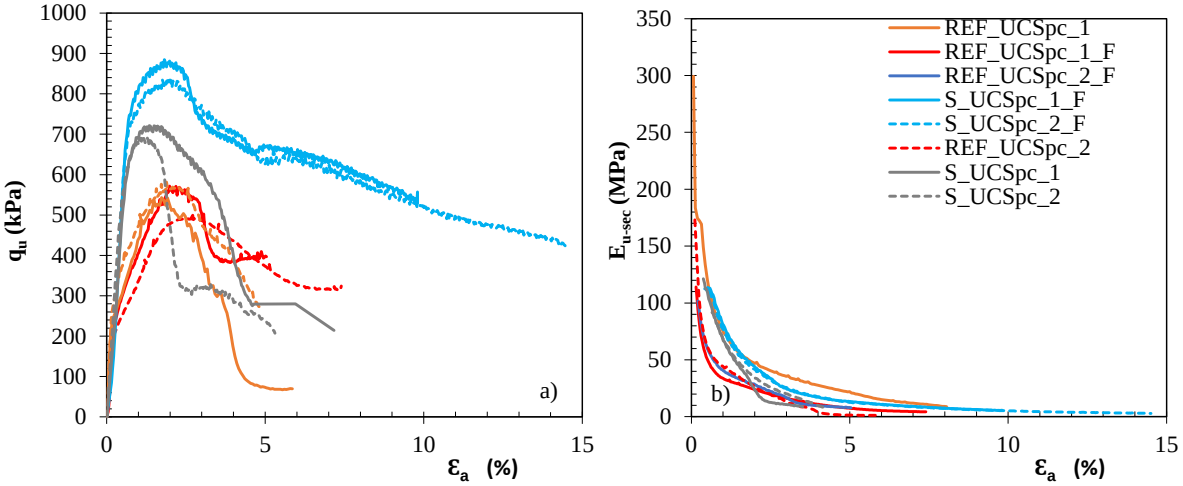

Figure 7.4: Results of the post-cyclic UCS tests performed on stabilised samples unreinforced and fibre-reinforced: a) stress-strain plot; b) $E_{u\text{-}sec}$ vs axial strain (CI42.5 R; binder quantity = 250 kg/m^3; curing time = 28 days; curing conditions: vertical stress = 0 kPa, room and in tank)

7.3 Post-cyclic UCS test in a confined condition

As stated before, the main goal of the present Chapter is to study the compressibility of samples of Baixo Mondego soft soil chemically stabilised unreinforced and fibre-reinforced, under cyclic loading. For such, oedometer tests will be performed in which the samples are radially confined, i.e. no radial deformation is allowed. In order to better understand the deformations to be developed during the cyclic loading in oedometer tests, it was considered relevant to perform some cyclic UCS tests in a confined condition, i.e., the cyclic stage is performed in a confined condition (zero radial deformation). For this it was necessary to build a metallic cylindrical tube (cut vertically in two pieces, Figure 7.5) with an internal diameter equal to the samples to be tested, thus ensuring that there will be no radial deformation during cyclic loading.

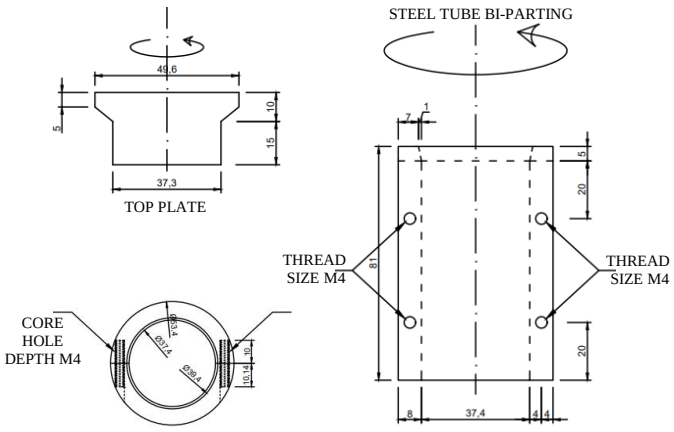

Figure 7.5: Metallic cylindrical tube and the top plate for confined cyclic test (all dimensions in mm)

To ensure that cyclic loading is applied centrally, this metal cylindrical tube has an extra conical height that guides the load application top plate, Figure 7.5. Once the sample is placed in the

ELDYN GDS equipment, it is encased by the two halves of the metallic cylindrical tube, which are tightly fixed with screws, and then the cyclic stage/test can be started.

Figure 7.6 shows the metallic cylindrical tube and the top plate in operational mode, immediately before the start of the cyclic stage, where a bubble level is seen on the top plate to ensure that the load is applied centrally and with no eccentricity.

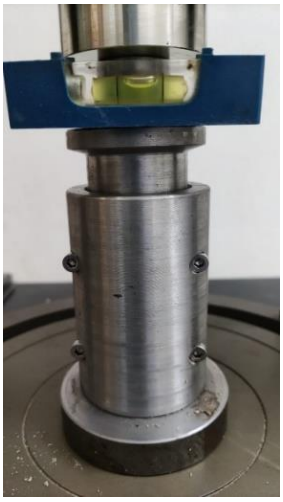

Figure 7.6: View of a confined cyclic test in operational mode

7.3.1 Chemically stabilised unreinforced soft soil

Table 7.3 and Figure 7.7 summarise the results obtained during the cyclic stage of the UCS cyclic tests performed on unreinforced stabilised samples for different confining conditions: the unconfined cyclic loading tests (section 7.2) and the radially confined cyclic loading tests (tests identified by the letters ‘conf’ at the test ID indicating the sample was tested in a radially confined condition).

As it may be seen from Figure 7.7, the evolution of the permanent axial strain is characterised by a quick increase in the first 500 to 1000 load cycles followed by a slight increase as the number of load cycles increases. It is clear that for the confined condition the initial quick increase of the permanent axial strain ends earlier (around 300 load cycles) than for the unconfined condition, and the subsequent evolution of the permanent axial strain evolves at a slower rate for the samples tested in a confined condition. That is, for the samples tested in a confined condition the permanent axial strain is smaller due to the radial deformation restriction, so, it is expected a smaller degradation of the stabilised matrix for the samples tested in a confined condition. These results suggest that the confined condition induces a greater “elastic” deformation, i.e., there are a higher degree of reversibility in deformation due to the less occurrence of breakage of the cementation bonds.

Table 7.3: Maximum permanent axial strain during the cyclic stage of the UCS cyclic and UCS cyclic confined tests for stabilised unreinforced samples

ID	$\varepsilon_{ax\text{-}perm}$ (%)
S_UCScyc_1	0.24
S_UCScyc_2	0.22
S_UCScyc_conf_1	0.14
S_UCScyc_conf_2	0.15

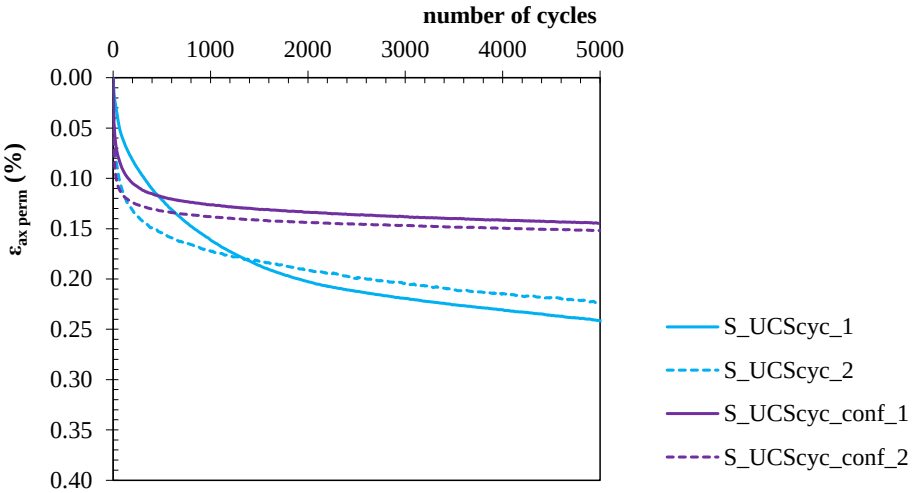

Figure 7.7: Evolution of permanent axial strain during the cyclic stage of the UCS cyclic and UCS cyclic confined tests for unreinforced stabilised samples

Table 7.4 and Figure 7.8 summarize the main characteristics observed during the UCS tests performed immediately after the cyclic stage for unreinforced stabilised samples cured for 28 days in a submerged condition. For a better interpretation of the test results, the values obtained with the UCS reference tests and with the post-cyclic UCS tests performed in unconfined condition (presented in section 7.2) were added to the table and figure.

As it was shown previously (section 7.2), the results show that the cyclic stage has a positive impact on strength development, which may be explained by the fact that suction effects overcome the degradation of the cementitious matrix induced by cyclic stage deformations. It is interesting to observe that when the samples are tested in a confined condition (S_UCS$_{pc}$_conf), the mechanical properties ($q_{u\ max}$ and E_{u50}) are characterised by smaller values compared to samples tested in unconfined condition (S_UCS$_{pc}$), which seems to be explained by suction effects: for the samples tested in confined condition during the cyclic stage (which lasts 2.78 h) the loss of water content is smaller due to the fact that the samples are surrounded by the metallic cylindrical tube, not being in direct contact with the ambient air. For a higher water content (w_f) the matric suction will be lower, so does the mechanical properties.

Table 7.4: Results of the UCS and UCS_{pc} tests performed on stabilized samples unreinforced for different cyclic confining conditions

ID	$q_{u\text{-}max}$ (kPa)	ε_r (%)	E_{u50} (MPa)	w_f (%)
S_REF_UCS_1	510.33	1.10	84.52	75.45
S_REF_UCS_2	477.10	1.04	59.75	77.95
S_UCSpc_1	721.52	1.49	100.02	74.65
S_UCSpc_2	691.09	1.28	124.14	73.80
S_UCSpc_Conf_1	628.89	1.81	54.81	76.88
S_UCSpc_Conf_2	673.72	1.54	69.48	76.15

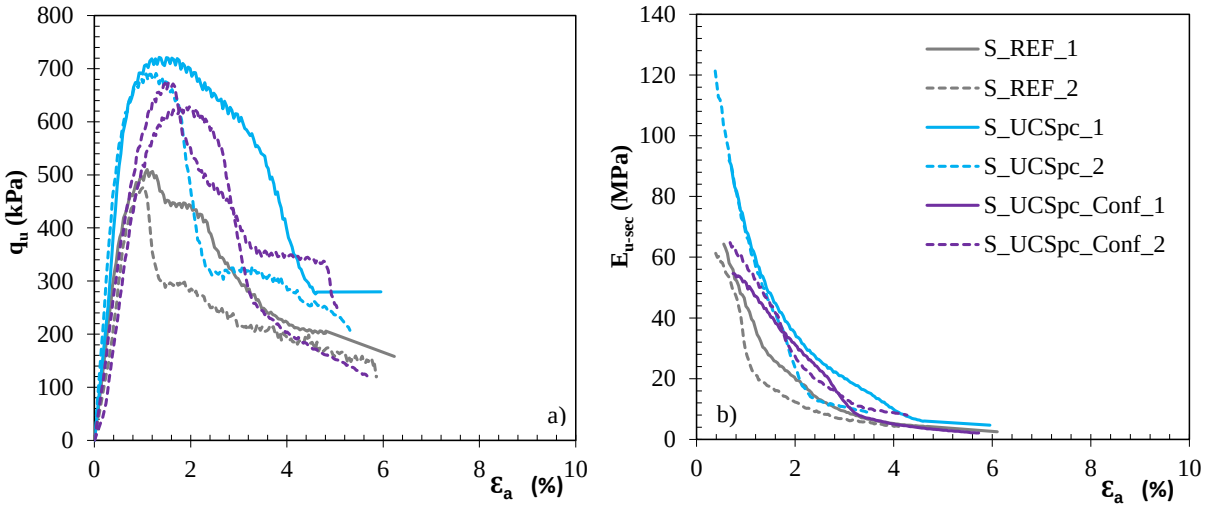

Figure 7.8: Results of the UCS and UCS_{pc} tests performed on stabilized samples unreinforced for different cyclic confining conditions: a) stress-strain plot; b) $E_{u\text{-}sec}$ vs axial strain (CI42.5 R; binder quantity = 250 kg/m^3; curing time = 28 days; curing conditions: vertical stress = 0 kPa, tank)

7.3.2 Chemically stabilised soft soil reinforced with polypropylene fibres

Table 7.5 and Figure 7.9 summarise the results obtained during the cyclic stage of the UCS cyclic tests for the stabilised samples reinforced with polypropylene fibres for different confining conditions: the unconfined cyclic loading tests (section 7.2) and the radially confined cyclic loading tests (tests identified by the letters 'conf' at the test ID indicating the sample was tested in a radially confined condition).

As it was observed for the unreinforced case, here also it is observed the evolution of the permanent axial strain (Figure 7.9) is characterised by a quick increase in the first 500 load cycles followed by a slight increase for a higher number of load cycles (in agreement with results in Chapters 5 and 6). It is also observed that for the confined condition the initial quick increase of the permanent axial strain ends earlier (around 300 load cycles) than for the unconfined condition, and the subsequent evolution of the permanent axial strain evolves at a slower rate for the samples tested in a confined condition. Such behaviour is justified by the same effects as presented for the

unreinforced case, i.e., when the radial deformation is prevented (confined condition) there is less degradation of the stabilised matrix leading to less permanent axial strain during the cyclic stage.

Table 7.5: Maximum permanent axial strain and permanent during the cyclic stage of the UCS cyclic and UCS cyclic confined tests for stabilised fibre-reinforced samples

ID	$\varepsilon_{ax\text{-}perm}$ (%)
S_UCScyc_1_F	0.33
S_UCScyc_2_F	0.32
S_UCScyc_conf_1_F	0.14
S_UCScyc_conf_2_F	0.14

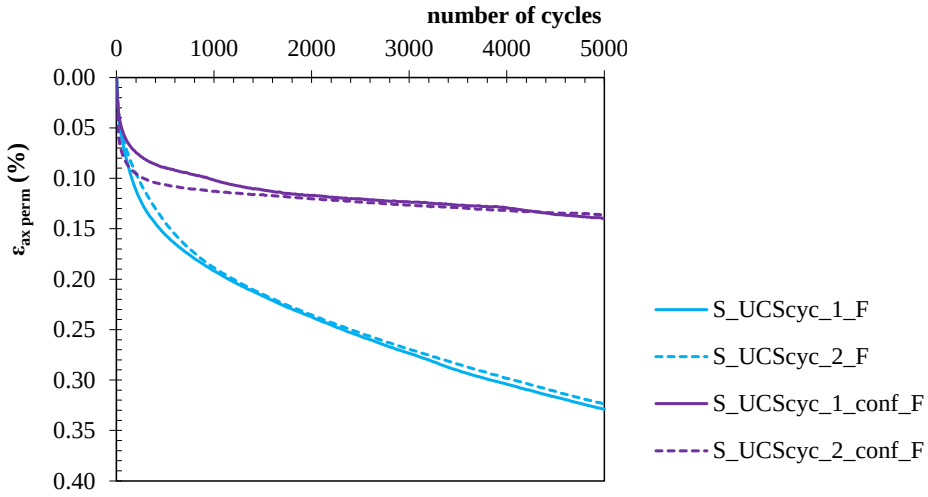

Figure 7.9: Evolution of the permanent axial strain during the cyclic stage of the UCS cyclic and UCS cyclic confined tests for reinforced samples

In Table 7.6 and Figure 7.10 it may be seen a summary of the results obtained in the UCS tests performed immediately after the cyclic stage, for the stabilised samples reinforced with polypropylene fibres for different confining conditions: the unconfined cyclic loading tests (section 7.2) and the radially confined cyclic loading tests (tests identified by the letters 'conf' at the test ID indicating the sample was tested in a radially confined condition). As it was observed previously, after a cyclic stage the unconfined compressive strength increase (qu max of UCSpc tests) due to two cumulative effects: i) the deformations happened during the cyclic loading stage allows a "more effective" mobilisation of the fibres strength; ii) suction effects are more expressive for the samples subjected to cyclic loading stage. It is clear that these two effects overcome the degradation of the cementitious matrix induced by cyclic stage deformations. The results also show that the samples tested in confined condition ($S\_UCS_{pc}\_conf$) exhibit lower mechanical properties ($q_{u\ max}$ and E_{u50}) than the ones tested in unconfined condition (S_UCS_{pc}). Such behaviour may be justified by a partial loss of the suction effect for the samples tested in

confined condition: due to a smaller loss of water content since the samples are surrounded by the cylindrical metallic tube, not being in direct contact with the ambient air.

Table 7.6: Results of the UCS and UCS_{pc} tests performed on stabilized fibre-reinforced samples for different cyclic confining conditions

ID	$q_{u\text{-}max}$ (kPa)	ε_r (%)	E_{u50} (MPa)	w_f (%)
S_REF_UCS_1_F	672.72	2.04	41.76	78.04
S_REF_UCS_2_F	683.88	2.33	51.45	77.62
S_UCSpc_1_F	884.48	1.82	102.98	72.09
S_UCSpc_2_F	835.09	1.76	104.68	71.27
S_UCSpc_Conf_1_F	766.35	2.69	66.38	75.59
S_UCSpc_Conf_2_F	774.01	2.60	84.62	74.83

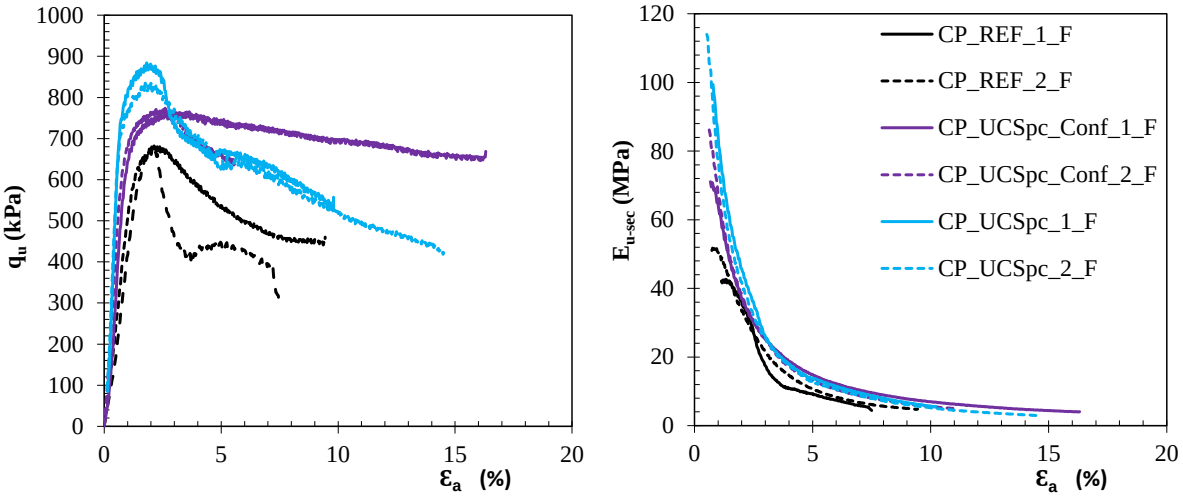

Figure 7.10: Results of the UCS and UCS_{pc} tests performed on stabilized samples reinforced with fibres for different cyclic confining conditions: a) stress-strain plot; b) $E_{u\text{-}sec}$ vs axial strain (CI42.5 R; binder quantity = 250 kg/m^3; curing time = 28 days; curing conditions: vertical stress = 0 kPa, tank)

Figures 7.11 and 7.12 allow the study of the fibres addition to the stabilised samples loaded cyclic in a confined condition. As it may be seen, the introduction of the fibres originates less permanent axial strains in the cyclic loading stage due to a progressive mobilisation of the fibres that absorb and redistribute part of the stresses within the stabilised matrix contributing to a lesser degradation of the stabilised matrix. In terms of unconfined compressive strength measured after the cyclic stage (Figure 7.12), the fibres addition allows the mobilisation of the fibres strength leading to higher strength.

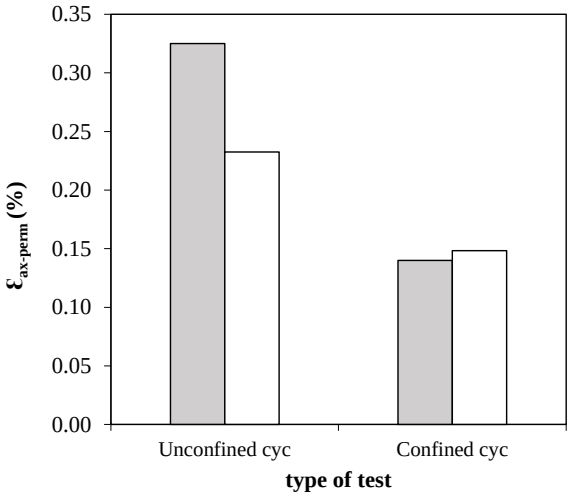

Figure 7.11: Maximum permanent axial strain for unreinforced and fibre-reinforced stabilised samples cyclic loaded under unconfined and confined conditions

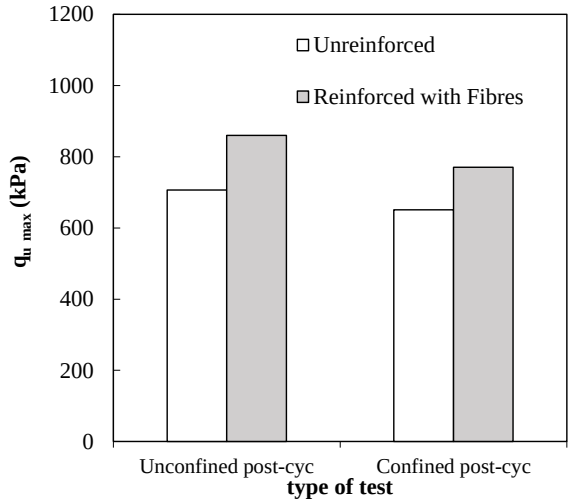

Figure 7.12: Post-cyclic unconfined compressive strength for unreinforced and fibre-reinforced stabilised samples cyclic loaded under unconfined and confined conditions

7.4 Oedometer tests without and with a cyclic stage

This section is focused on study the compressibility behaviour of the Baixo Mondego soft soil chemically stabilised unreinforced and reinforced with fibres and when subjected to a prior cyclic loading stage. For such it was designed a laboratory testing program based on oedometer tests, more precisely, 4 classical and 2 cyclic oedometer tests, half for unreinforced stabilised samples (2 classical + 1 cyclic), half for fibre-reinforced stabilised samples (2 classical + 1 cyclic). The stabilised samples for oedometer tests were prepared following the procedure described in Chapter 4 (section 4.4.3) with the modifications described at the beginning of this Chapter: during the curing period (28 days) the oedometer samples were submerged in water inside the oedometer cell, and stored in a room with temperature (20±2ºC) and humidity (95±5%) control. As explained, this procedure aims to guarantee null suction, i.e., the effective stress is equal to the total stress

applied. Due to the fact that the stabilised soil may exhibit high yield stress, it was decided to use the 50mm diameter oedometer ring in order to achieve higher stress levels during the oedometer tests.

The oedometer tests (identified by the first three letters, OED) were performed according to the British Standard BS 1377-5 (1990), as described in section 4.4.5. At the end of the oedometer test the sample was weighted and the final water content was measured, allowing the evaluation of the final void ratio (e_f). Based on the compression curve (*e-log* σ'_v) it is possible to evaluate the compressibility parameters of the composite material, namely, the recompressibility index (C_r), the compressibility index (C_c) and the yield stress (σ'_y).

For the cyclic oedometer tests (identified as OED_{cyc}), i.e., for the oedometer tests with a prior cyclic stage it was adopted the procedure as described below. The cyclic oedometer test is composed of three stages: first, at the end of the curing period, the oedometer cell is placed in the ELDYN GDS apparatus (Figure 6.1, details of this equipment are given in Chapters 4 and 6) and the sample is loaded monotonically up to a specified stress level (defined as 50% of the yield stress evaluated in a classical oedometer test) - pre-cyclic stage; immediately after the cyclic stage begins, carried out for the reference loading cyclic parameters (frequency of 0.5 Hz, number of cycles equal to 5.000, stress level and amplitude equal to 50% and ±10% of the yield stress evaluated in a classical oedometer test, respectively) - cyclic stage; when the cyclic stage ends, the sample is placed in the oedometer apparatus and the oedometer test begins following the procedure described above. In all stages, the vertical displacement is automatically recorded as a function of the vertical stress level applied.

In order to allow the cyclic oedometer stage to be performed on the ELDYN GDS apparatus, it was necessary to build an auxiliary part to centrally fix the oedometer cell (Figures 7.13 and 7.14).

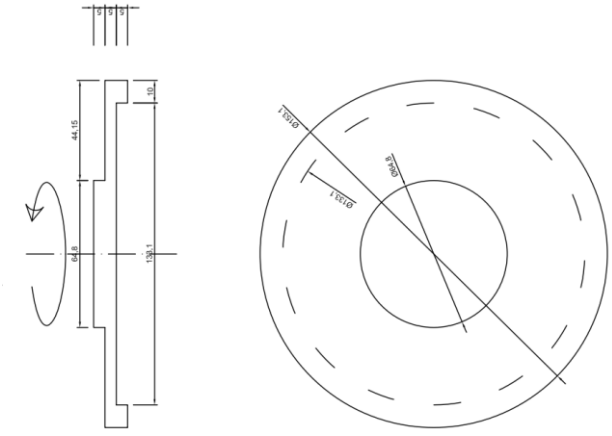

Figure 7.13: Auxiliary part for oedometer tests

It must be mentioned that for the evaluation of the yield stress (σ'_y), preference was given to the method of Butterfield (1979) instead of the usual evaluation by the Casagrande method, due to the limitations of the second method (difficulty in defining the point of greatest radius of curvature of the compression curve; nonlinearity of the "virgin" or normal consolidation line for some soils) and because the first method allows a less unambiguous definition of the yield stress in the bi-logarithmic plane (Correia, 2011).

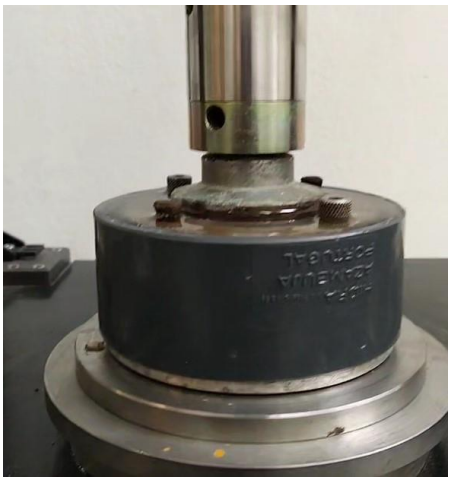

Figure 7.14: Oedometer test under cyclic loading on the ELDYN GDS apparatus

In the following two sections it is presented and discussed the results of the oedometer tests performed for unreinforced stabilised samples and for fibre-reinforced stabilised samples. The results are compared with the UCS tests performed on confined conditions, comparing the permanent axial strains developed during the cyclic stage, and trying to define a relationship between the yield stress from the oedometer tests and the unconfined compressive strength from UCS tests.

7.4.1 Chemically stabilised unreinforced soft soil

Table 7.7 and Figure 7.15 summarise the results obtained during the cyclic stage of the oedometer cyclic test performed on unreinforced stabilised samples, which are compared to UCS cyclic tests performed in unconfined and confined conditions.

Table 7.7: Maximum permanent axial strain during the cyclic stage of the oedometer cyclic test and UCS cyclic unconfined and confined tests – unreinforced stabilized samples

ID	$\varepsilon_{ax\text{-}perm}$ (%)
S_UCScyc_1	0.24
S_UCScyc_2	0.22
S_UCScyc_conf_1	0.14
S_UCScyc_conf_2	0.15
OEDcyc_1	0.16

As it may be seen from Figure 7.15, the evolution of the permanent axial strain is characterised by a quick increase in the first 1000 load cycles followed by a slight increase as the number of load cycles increase, in agreement with previous results. It should be highlighted the good agreement between the results of the oedometer and UCS confined tests, indicating that these tests are equivalent. It is interesting to note that in the first part of the permanent axial strain curves the vertical strain increases more sharply for the UCS confined tests which is most likely due to the fact that the initial confinement is not as perfect as for the oedometer samples (in the UCS there is a very small gap between the sample and the metallic cylindrical tube). However, the final permanent axial strain value in both tests is very similar.

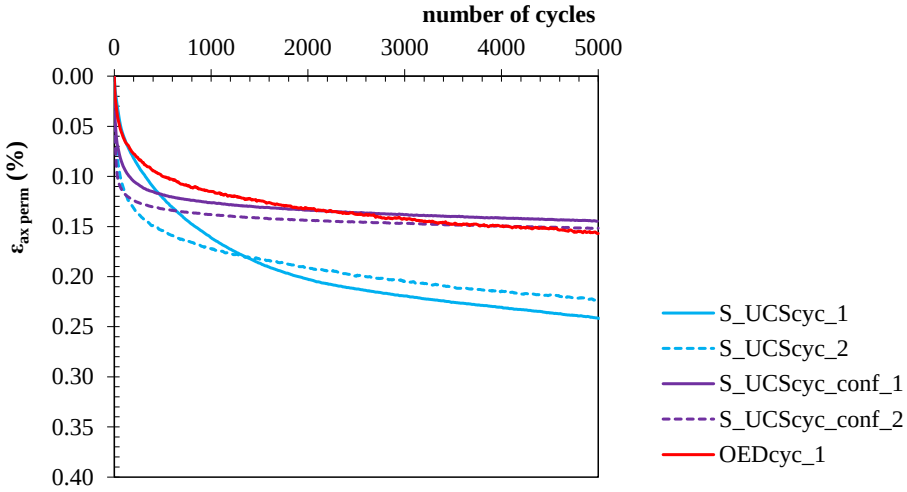

Figure 7.15: Evolution of permanent axial strain during the cyclic stage (UCS and oedometer tests) for unreinforced stabilised samples

Figure 7.16 presents the evolution of the void ratio with vertical effective stress (compression curve) applied during the oedometer tests performed on unreinforced stabilised samples, without and with a prior cyclic stage. From the compression curves it is possible to evaluate some compressibility parameters, summarised in Table 7.8, yield stress (σ'_y), recompression (C_r) and compression (C_r) indices, as well as to define a relationship between the yield stress and the unconfined compressive strength of the UCS test.

From the compression curves it is possible to observe that the stabilised material is characterised by a high yield stress and a low compressibility up to the yield stress. Such pre-yield behaviour is a direct consequence of the cementitious bonds established between the solid particles, conferring to the stabilised material a high strength and stiffness, i.e., a reduced compressibility. Although it was not possible to define the “virgin” line well, it is clear that after the yield stress (post-yield behaviour), the behaviour is characterised by high compressibility due to the abrupt breakage of cementitious bonds (destructuring). Note that this high post-yield compressibility occurs only for

high effective stresses (higher than $q_{u\,max}$), in general, higher than the service stresses imposed by geotechnical works (Correia, 2011). For the cyclic oedometer test it was observed compressibility indices of the same order, but the yield stress is now higher. This increase in yield stress is not related with suction effects (samples were cured and tested in a submerged condition), rather it seems to be related to the deformations that occurred in the cyclic stage, which induced a lower initial void ratio in the sample.

Table 7.8 also presents a relationship between the unconfined compressive strength and the yield stress (0.51 – 0.70) measured in UCS and oedometer tests, respectively, which may be helpful since it allows to estimate the yield stress of the stabilized soil by just performing UCS tests.

Table 7.8: Characterisation of the compressibility of unreinforced stabilised samples through classic oedometer and cyclic oedometer tests

ID	e_0	e_f	C_r	C_c	σ'_y (kPa)	$q_{u\,max}$ (kPa) [1]	Observations[2]	$q_{u\,max}$ / σ'_y (-)
OED_1	2.13	1.58	0.04	0.60	723.71	493.72	S_REF_UCS	0.68
OED_2	2.03	1.53	0.04	0.57	703.19			0.70
OEDcyc_1	1.88	1.61	0.03	0.41	1272.19	651.31	S_UCSpc_Conf	0.51

[1] average of $q_{u\,max}$ of the corresponding UCS tests
[2] UCS test ID

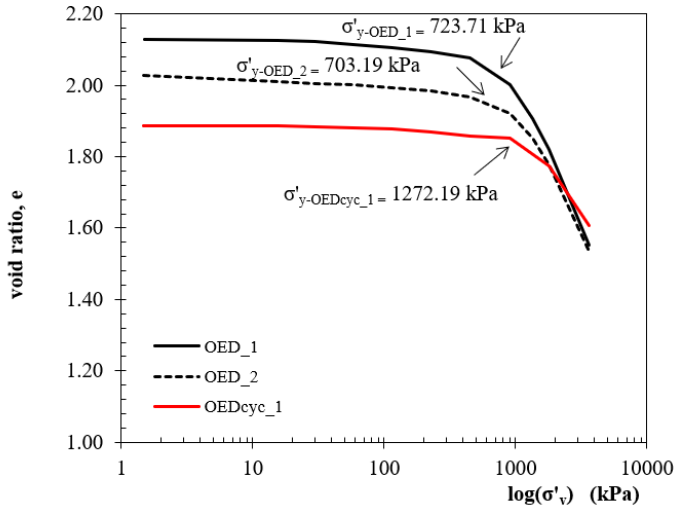

Figure 7.16: Compression curves from classical oedometer and cyclic oedometer tests carried out on unreinforced stabilised samples

7.4.2 Chemically stabilised soft soil reinforced with polypropylene fibres

Table 7.9 and Figure 7.17 summarise the results obtained during the cyclic stage of the oedometer cyclic test performed on fibre-reinforced stabilised samples, which are compared to UCS cyclic tests performed in unconfined and confined conditions.

Table 7.9: Maximum permanent axial strain during the cyclic stage of the oedometer cyclic test and UCS cyclic unconfined and confined tests – fibre-reinforced stabilised samples

ID	$\varepsilon_{ax\text{-}perm}$ (%)
S_UCScyc_1_F	0.33
S_UCScyc_2_F	0.32
S_UCScyc_conf_1_F	0.14
S_UCScyc_conf_2_F	0.14
OEDcyc_1_F	0.15

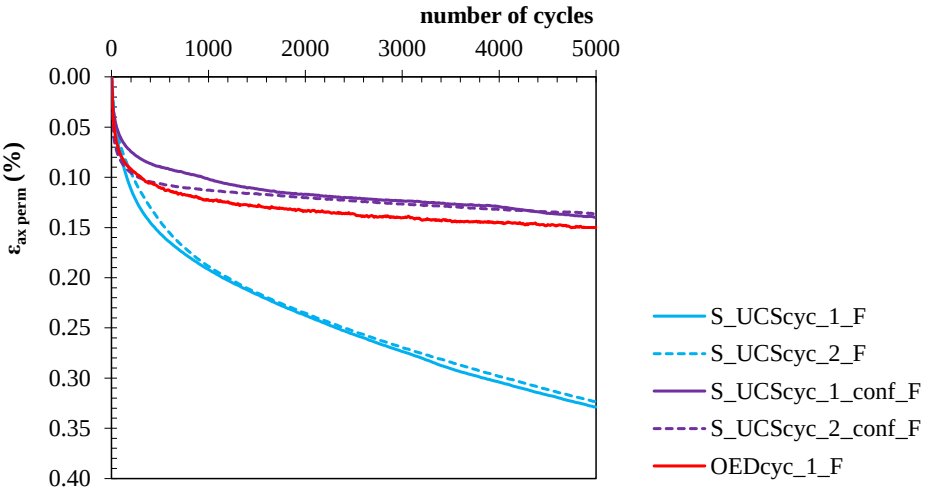

Figure 7.17: Evolution of permanent axial strain during the cyclic stage (UCS_{cyc} and OED_{cyc}) for samples reinforced with fibres (number of cycles = 5.000; frequency = 0.5 Hz; level of stress = 50%*$q_{u\ max}$; amplitude = ±10%*$q_{u\ max}$)

In general, the behaviour follows very closely the one that was previously observed for the unreinforced case, with a good agreement between the cyclic oedometer test and cyclic UCS tests performed in confined condition. Comparing the unreinforced with fibre-reinforced stabilised samples (Tables 7.7 and 7.9), it may be observed the addition of fibres induces similar permanent axial strains during the cyclic stage, which is unexpected because the physical presence of the fibres may prevent the development of some cementitious bonds within the composite matrix, producing a composite material with lower stiffness, i.e., with higher deformations. Moreover, the polypropylene fibres are characterised by a lower surface roughness (as presented in Chapter 4) promoting a reduction of the frictional strength component, which also evolved lead to more deformation. More oedometer tests are required to further investigate this issue.

Table 7.10 and Figure 7.18 summarise the results of the oedometer tests performed on fibre-reinforced stabilised samples, from which the compressibility characteristics are evaluated. Table 7.10 presents also the relationship between the yield stress and the unconfined compressive strength of the UCS test. As it was observed for the unreinforced case, the compression curves of the fibre-reinforced stabilised samples are characterised by a high yield stress and a low compressibility up to the yield stress, reflecting the high strength and stiffness of the stabilised matrix induced by the cementitious bonds established between the solid particles. As it may be

seen from the compression curve of the OED_1_F test, which has reached a vertical stress of 7.205 kPa allowing a clear definition of the compressibility index, the post-yield compressibility is characterised by a high compressibility index (higher than that of natural soil, $Cc \approx 0.5$ as presented in Chapter 2), reflecting the collapsible behaviour of the stabilized material with the abrupt breakage of cementitious bonds (destructuring), i.e., the stabilised material "wants to evolve" to the isotropic compression line of the natural soil (Horpibulsuk and Miura, 2001; Lorenzo and Bergado, 2004 and 2006; Correia, 2011). Once again it must be stated that this high post-yield compressibility occurs only for high effective stresses (higher than $q_{u\ max}$), in general, higher than the service stresses imposed by geotechnical works (Correia, 2011). As observed for the unreinforced samples, for the fibre-reinforced samples the cyclic oedometer test exhibit compressibility indices of the same order of the classic oedometer tests but with an higher yield stress. This increase in yield stress is not related with suction effects (samples were cured and tested in a submerged condition), rather it seems to be related to the deformations that occurred during the cyclic loading stage which induces a smaller initial void ratio. It may be discussed why the initial void ratio of the cyclic test is not lower than that of the oedometer classical test, as observed in the unreinforced samples: on one hand the deformation occurred in the cyclic stage induces lower initial void ratio, however on the other hand the addition of fibres contributes to the increase of the void ratio, so the final result is not obvious. In general, the results indicate that the addition of fibres promotes a slight increase of the initial void ratio.

Table 7.10: Characterisation of the compressibility of the stabilised soil reinforced with fibres through classic monotonic oedometer and cyclic oedometer tests

ID	e_0	e_f	C_r	C_c	σ'_y (kPa)	$q_{u\ max}$ (kPa) [2]	Observations[3]	$q_{u\ max}$ / σ'_y (-)
OED_1_F	2.09	1.16	0.09	0.98	723.77	678.3	S_REF_UCS_F	0.94
OED_2_F	2.05	1.54	0.07	0.73	829.76			0.82
OEDcyc_1_F	2.09	1.71	0.04	0.62	914.58	770.18	S_UCSpc_Conf_F	0.84

[1] at ending of curing time; [2] average of maximum strength ($q_{u\ max}$) from reference test in section 7.2; [3] Identification of $q_{u\ max}$

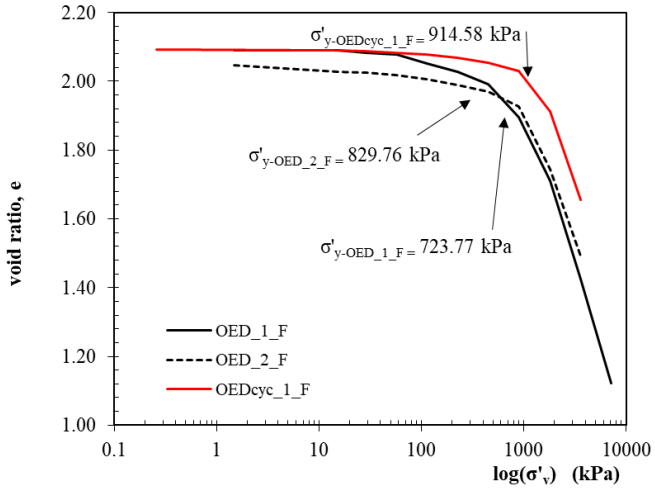

Figure 7.18: Results of the classical oedometer and cyclic oedometer tests carried out on stabilised samples reinforced with fibres

In Figure 7.19 represents in a bar plot the results of axial permanent strain comparing the three different tests UCScyc, UCScyc confined and Oedcyc and Figure 7.20 shows another bar plot that shows the effect of the yield stress against the maximum strength from the reference tests.

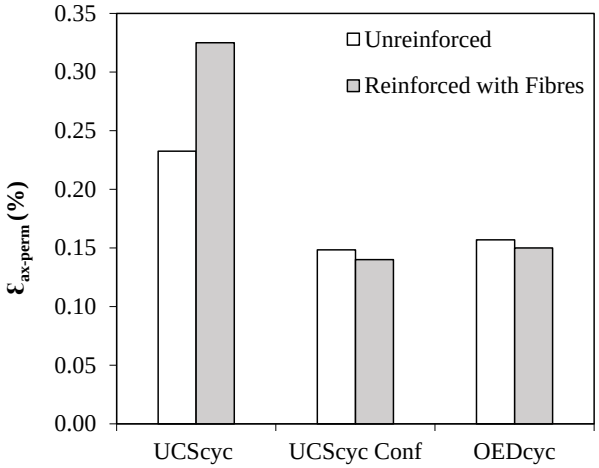

Figure 7.19: Maximum permanent axial strain comparison of confined cyclic loading tests

Comparing the unreinforced with fibre-reinforced stabilised samples, it may be observed the addition of fibres induces compressibility indices of the same order or slightly higher and a slightly smaller yield stress. It may be explained by the fact that the physical presence of the fibres prevents the development of some cementitious bonds within the composite matrix, producing a composite material will lower strength and stiffness, i.e., with higher compressibility. Moreover, it is known that the compressibility of a stabilised material depends only on the frictional strength component, which is only mobilised due to the volume change occurred in the oedometer test (Nagaraj et al., 1998; Correia, 2011). Thus, the presence of the polypropylene fibres promotes a reduction of the

frictional strength component (the fibres are made of a synthetic material with a lower surface roughness as presented in Chapter 4), which justifies the higher compressibility characteristics observed when compared with the unreinforced stabilised oedometer samples. This behaviour justifies the fact that the addition of fibres has the opposite effect to that observed in the UCS tests, i.e., the presence of the fibres induces a reduction of the yield stress measured in the oedometer test (the fibres are not mobilised, and the behaviour is only depend on the frictional strength) while the opposite was observed for the $q_{u\,max}$ (the UCS failure mechanism allows fibres mobilisation).

Figure 7.20 summarizes the evolution of the ratio between the unconfined compressive strength (evaluated in UCS confined tests) and the yield stress (measured in oedometer tests) for both stabilised samples, unreinforced and fibre-reinforced. As it was shown above, the fibres addition promotes the decrease of the yield stress and the increase of the unconfined compressive strength, so, as expected the ratio $q_{u\,max}/\sigma'_y$ increases.

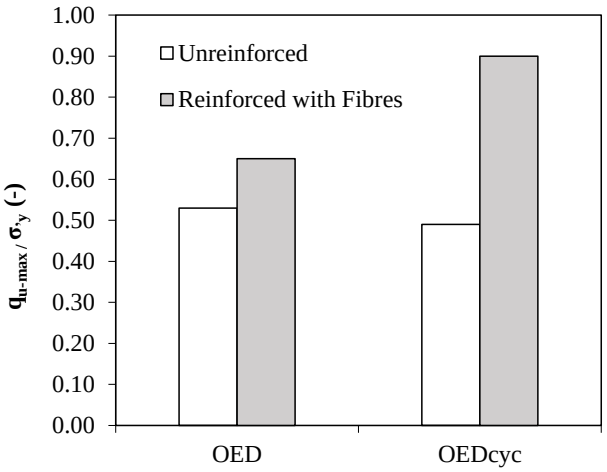

Figure 7.20: Ratio from yield stress versus maximum strength on unconfined and confined test under oedometer monotonic/classics and cyclic

CHAPTER 8 – STRESS-STRAIN-SHEAR STRENGTH BEHAVIOUR

8.1 Introduction

As it was shown in Chapters 2 and 3 the stress-strain-shear strength behaviour of the Baixo Mondego soft soil is relatively well characterised, but the same is not true when this soft soil is chemically stabilised, in particular when reinforced with fibres and under cyclic loading. The present Chapter aims to contribute to the characterisation of the Baixo Mondego soft soil chemically stabilised (unreinforced and reinforced with polypropylene fibres) under static and cyclic loading, focusing on aspects related to the stress-strain-shear strength behaviour and on the yield surface of the composite material. The characterisation of the yield surface is of upmost importance since it allows to distinguish between elastic and plastic behaviour, i.e., it defines where destructuration of the stabilised material begins. This knowledge is essential to develop more realistic constitutive models that can predict the behaviour of cement-based stabilised soils especially when reinforced with fibres and under cyclic loading conditions.

The experimental works developed at the University of Coimbra by Correia (2011), Silveira et al. (2012), Correia et al. (2015) and Santos et al. (2021) focused on the study of the stress-strain-shear strength behaviour of the Baixo Mondego stabilised soil but for the unreinforced case and without any cyclic loading, identifying the yield locus for same tests but without defining the yield surface. Nevertheless the knowledge acquired, it is important to complement such previous studies because there is a lack of information on the stress-strain-shear strength behaviour and on the yield surface when the stabilised soil is reinforced with fibres and when subjected to cyclic loading. This is the main motivation of this Chapter.

It is known that in chemically stabilised soils there are cementitious bonds between the solid particles (induced by the binder), responsible for the enhancement of the mechanical behaviour (Horpibulsuk 2001; Åhnberg 2006; Lorenzo and Bergado, 2006; Correia, 2011). It was observed that for confining pressures below the yield stress of the stabilised soil, the material under drained

or undrained shear conditions begins to exhibit a very rigid behaviour due to the of cementitious bonds. However, when the confining pressure exceeds the strength of the cementitious bonds, the structure of the stabilised soil changes due to the progressive breakage of cementitious bonds and its behaviour tends to be identical to that of the unstabilised (original) soil since its strength becomes dependent only on the frictional component (Coop and Atkinson, 1993; Uddin et al, 1997; Malandraki et al. 1997; Cuccovillo and Coop, 1999; Horpibulsuk 2001; Åhnberg 2006; Correia 2011). Regarding the yield locus, and as shown in Chapter 7, the chemical stabilisation promotes an increase of the yield stress compared to the pre-consolidation stress of the unstabilised (original) soil due to the higher strength of the solid skeleton resulting from the cementitious bonds. Nevertheless, the knowledge acquired, the addition of fibres to the stabilised soil and the cyclic loading will certainly promote changes in the stress-strain-shear strength behaviour and on the yield surface that should be characterised. For such, a series of triaxial tests, complemented by pulse velocity tests, will be performed, some of them subjected to a prior cyclic stage.

All samples involved in the stress-strain-shear strength behaviour and on the yield surface study were prepared based on the laboratory procedure described in Chapter 7. That is, samples were stabilised with Portland cement applied in a quantity of 250 kg/m^3, mixed with polypropylene fibres in a quantity of 10 kg/m^3 for the fibre-reinforced samples, and cured for 28 days without applying any vertical stress to the samples. During the curing period the samples were stored in a water tank with temperature (20±2ºC) control (submerged condition) in order to help in the initial saturation phase of the samples.

Table 8.1 summarises the number of triaxial and pulse velocity tests performed for each different condition, i.e., unreinforced and fibre-reinforced stabilised samples under monotonic or subjected to a prior cyclic stage. In order to guarantee the reliability of the study, for each mixture, 2 or 3 stabilised samples were prepared, one of which was used in UCS control test to be compared with the corresponding reference test, monotonic or post-cyclic (presented in Chapter 7). The other samples of each mixture were used in the triaxial tests. In order to evaluate the elastic parameters (Young's modulus of elasticity, E; shear modulus, G; and Poisson's ratio, ν) of the composite materials, pulse velocity tests were carried out in all samples prior the UCS control tests, before and immediately after the cyclic stage and before any triaxial test. The pulse velocity tests are as well a supplementary measure to ensure the quality of the samples and the good reproducibility of the sample preparation procedure since, initially, there are only 2 sets of samples, unreinforced and fibre-reinforced.

The UCS control tests, as well as triaxial and pulse velocity tests were performed following the procedures described in Chapter 4. For the triaxial tests, different stress paths were followed aiming to characterise the stress-strain-shear strength behaviour and to identify the locus of the yield surface. The triaxial tests performed were: i) isotropic compression test (CIC); ii) consolidated isotropically undrained compression test (CIU) for an effective consolidation stress of 50 kPa; iii) consolidated isotropically drained compression tests (CID) for effective consolidation stresses of 50, 200 and 350 kPa. In order to evaluate the impact of the cyclic loading, some triaxial tests are performed after a prior cyclic stage, i.e., before starting the triaxial test the sample is loaded monotonically up to a stress level equals to 50% of the unconfined compressive strength previously evaluated in UCS tests (new reference tests, Chapter 7) - pre-cyclic stage; immediately after the cyclic stage starts, carried out for the reference cyclic loading conditions (frequency of 0.5 Hz, number of cycles equal to 5.000, stress level and amplitude equals to 50% and ±10% of the $q_{u\ max}$) - cyclic stage; when the cyclic stage ends, the sample is monotonically discharged, pulse velocity test is performed and immediately after the sample is placed in the stress-path cell apparatus for triaxial test. In some cases, immediately after the end of the cyclic stage and after carrying out the pulse velocity test, the sample is monotonically loaded up to failure/rupture as a control test (UCS post-cyclic, UCS_{pc}) to be compared with new reference post cyclic test (Chapter 7).

Table 8.1: Summary of the triaxial and pulse velocity testing programme – number of tests

Test	Unreinforced		Fibre-Reinforced	
	Monotonic	Cyclic	Monotonic	Cyclic
UCS Control	5	$3^a + 5^b + 5^c$	3	$3^a + 3^b$
Pulse Velocity	10	$6^a + 2^c$	9	$6^a + 4^c$
CIC	2	1	2	2
CIU 50	1	1	1	1
CID 50	1	1	1	2
CID 200	1	1	2	2
CID 350	1	1	1	1

a) before cyclic stage; b) cyclic stage; c) post-cyclic stage

Along the next sections the stress-strain-shear strength behaviour and the yield surface of the Baixo Mondego soft soil chemically stabilised will be studied, starting by presenting and discuss the results of the unreinforced samples without and with a prior cyclic stage, followed by the results of the fibre-reinforced samples without and with a prior cyclic stage.

8.2 Stress-strain-shear strength behaviour of unreinforced stabilised soft soil

In this section it will be presented and discussed the results of several tests performed with the final goal to characterise the stress-strain-shear strength behaviour of the Baixo Mondego soft soil

chemically stabilised and without fibre addition (unreinforced case). In this study the effect of different loading conditions will be analysed, namely the static/monotonic versus cyclic. The tests performed for such studies were: isotropic compression, undrained and drained triaxial tests, complemented by UCS control/reference tests in order to guarantee the good quality and reproducibility of the stabilised samples. The experimental programme includes also pulse velocity tests in order to evaluate the elastic parameters of the composite material, performed before and after the cyclic stage. Moreover, for the cyclic loading case, UCS cyclic tests were also carried out in order to characterize the evolution of the permanent axial strain during the cyclic stage.

The triaxial tests will be characterised by the appropriated plots in order to extract the most valuable information regarding the characterisation of the stress-strain-shear strength behaviour and yield locus of the composite material. Examples of the plots considered are: compression curves, stress-strain plots, excess of pore pressure versus axial strain, evolution of the secant and tangent undrained stiffness modulus versus axial strain, volumetric strain vs mean effective stress, axial strain vs p' and strain ratio vs stress ratio. The results from the tests performed are presented below for both loading conditions, starting with the soft soil of Baixo Mondego chemically stabilised without fibres under static/monotonic loading condition, followed by the case where a cyclic loading was previously applied to the unreinforced stabilised samples.

8.2.1 Behaviour under static/monotonic loading condition

8.2.1.1 Pulse velocity and reference/control tests

Table 8.2 summarises the results obtained in the pulse velocity tests, presenting the density values of the composite samples, and the primary (V_p) and shear wave (V_s) velocities. As explained in Chapter 4, with this information it is possible to determine the elastic parameters of the composite material E, G and ν with equations 4.13, 4.14 and 4.15, assuming that the composite material is isotropic. From the results, it may be concluded that unreinforced stabilised samples exhibit very low variability in terms of density, V_p, V_s, ensuring the homogeneity of the samples which reflects a good reproducibility of the experimental laboratory samples preparation procedure. As expected, the primary wave velocity values (V_p) are higher than the shear wave (V_s) due to the fact the primary wave is a compression wave propagated directly through the solid skeleton of the sample, corresponding to the first transmitted arrival. In order to determine the shear wave arrival time more accurately shear-transducer elements were used minimising by this way reflections of the compression wave and vibrations due to the ringing of the transducers (ASTM D2845-05).

The Young's modulus or elasticity modulus (E) evaluated from the pulse velocity tests are as expected higher than the values evaluated from UCS reference tests (E_{u50}), presented in Chapter 7, because they were evaluated in different strain conditions: at very small strains or for an axial strain equal to the 50% of $q_{u\text{-}max}$, respectively for the pulse velocity and UCS tests. It is believed that the Young's modulus evaluated by the pulse velocity test reproduces more accurately the real elastic stiffness of the composite material. Based on the elasticity theory the shear modulus, G, is approximately 1/3 of the Young's modulus (Atkinson and Bransby, 1978). Regarding the Poisson's ratio (ν), the values are very close to 0.5 suggesting that the material has an almost undrained elastic behaviour.

Table 8.2: Pulse Velocity Test results and elastic parameters for unreinforced stabilised samples

Mix No.	ρ (kg/m^3)	Vp (m/s)	Vs (m/s)	E (MPa)	G (MPa)	ν
1	1528.49 (± 0.3%)	1705.67 (± 0.4%)	470.33 (± 2.7%)	986.91 (± 5.3%)	338.28 (± 5.4%)	0.46 (± 0.6%)
2	1522.84 (± 0.5%)	1705.67 (± 1.5%)	474.67 (± 0.9%)	1000.56 (± 2.0%)	343.12 (± 1.9%)	0.46 (± 0.1%)
3	1535.71 (± 0.2%)	1705.67 (± 0.4%)	483.67 (± 0.3%)	1046.38 (± 0.8%)	359.26 (± 0.7%)	0.46 (± 0.0%)
4	1527.07 (± 0.6%)	1712.00 (± 0%)	479.67 (± 3.8%)	1025.00 (± 8.1%)	351.70 (± 8.3%)	0.46 (± 0.6%)
5	1529.97 (± 0.2%)	1683.50 (± 0.6%)	474.00 (± 2.1%)	1001.88 (± 3.8%)	343.86 (± 3.9%)	0.46 (± 0.6%)
8	1521.80 (± 0.4%)	1693.00 (± 1.1%)	482.33 (± 3.0%)	1031.14 (± 5.6%)	354.17 (± 5.9%)	0.46 (± 0.5%)
9	1533.36 (± 0.1%)	1686.67 (± 0.4%)	486.33 (± 0.6%)	1055.13 (± 1.0%)	362.67 (± 1.0%)	0.45 (± 0.1%)
10	1528.48 (± 0.4%)	1674.33 (± 1.1%)	475.00 (± 2.3%)	1004.74 (± 4.9%)	345.00 (± 5.1%)	0.46 (± 0.4%)
11	1513.55 (± 0.2%)	1668.33 (± 1.5%)	452.00 (± 1.9%)	903.46 (± 4.0%)	309.33 (± 4.1%)	0.46 (± 0.3%)
12	1516.02 (± 0.1%)	1693.00 (± 1.1%)	455.33 (± 1.7%)	918.60 (± 3.4%)	314.38 (± 3.5%)	0.46 (± 0.2%)

Table 8.3 and Figure 8.1 summarise the results of the UCS control tests compared with reference UCS test (presented in Chapter 7). The UCS test are characterised by the unconfined compressive strength ($q_{u\text{-}max}$), the axial strain at rupture (ε_r), the undrained stiffness evaluated at 50% of $q_{u\text{-}max}$ (E_{u50}) and the final water content (w_f). All the results are characterised by a lower dispersion compared to the reference tests (S_REF_1 and S_REF_2), suggesting once more the homogeneity of the samples and the good reproducibility of the experimental laboratory samples preparation procedure.

Table 8.3: Results of the UCS control tests performed on unreinforced stabilised samples

Mix No.	ID	$q_{u\ max}$ (kPa)	ε_r (%)	E_{u50} (MPa)	w_f (%)
	S_REF _1	510.30	1.10	84.52	75.45
	S_REF _2	477.10	1.04	59.75	77.95
1	C_MIX_1	476.40	1.14	57.62	74.10
2	C_MIX_2	539.80	1.66	44.77	74.60
4	C_MIX_4	570.90	1.41	57.66	75.18
8	C_MIX_8	389.50	0.97	89.51	74.19
11	C_MIX_11	450.20	1.34	47.42	73.28

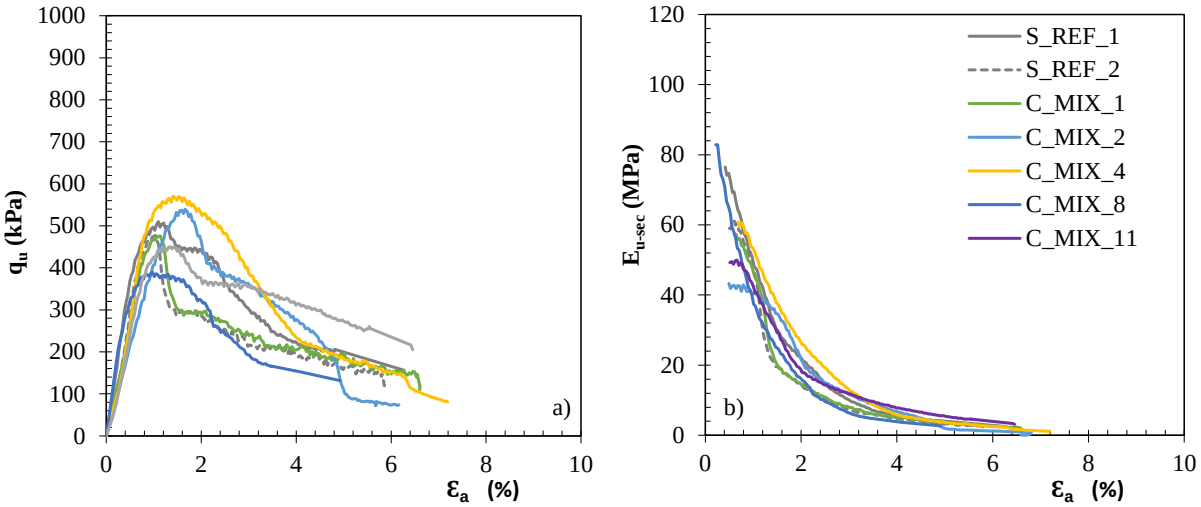

Figure 8.1: Results of the UCS control tests performed on unreinforced stabilised samples: a) stress-strain plot; b) $E_{u\text{-}sec}$ vs axial strain

8.2.1.2 Isotropic Compression triaxial test (CIC)

The analysis of the results of the isotropic compression test for the monotonic loading condition of the unreinforced samples is described in this section.

Table 8.2 summarises the results obtained, and Figure 8.2 shows the evolution of the volumetric strain with the logarithm of the mean effective stress (ε_{vol}-log p'). As it may be seen the evolution of the volumetric strain is characterised by a low compressibility up to the yield stress (pre-σ'_y), reflecting the effect of the chemical stabilisation effect (Correia, 2011; Lorenzo and Bergado, 2006).

The yield of the stabilised material is characterised by a sudden and abrupt breakage of cementitious bonds, inducing a high volumetric strain. The behaviour after the yield stress (post-σ'_y) is characterised by high compressibility (higher than of the natural soil) due to an abrupt breakage of the cementitious bonds (destructuration), evolving gradually to the behaviour of the natural soil.

The probable yield locus is defined by the intersection of these two linear trends, pre-σ'_y and post-σ'_y, represented by a square in Figure 8.2. As presented in Chapter 3, this methodology is similar to the Casagrande method used to evaluate the preconsolidation pressure of unstabilised soils (Jamiolkowski et al. 1985).

Table 8.4: Isotropic compression triaxial tests (CIC) results and yield locus for unreinforced stabilised samples

Mix No.	ID	$p'_y = \sigma'_y$ (kPa)
1	CIC_1	**535.9**
4	CIC_2	**574.8**

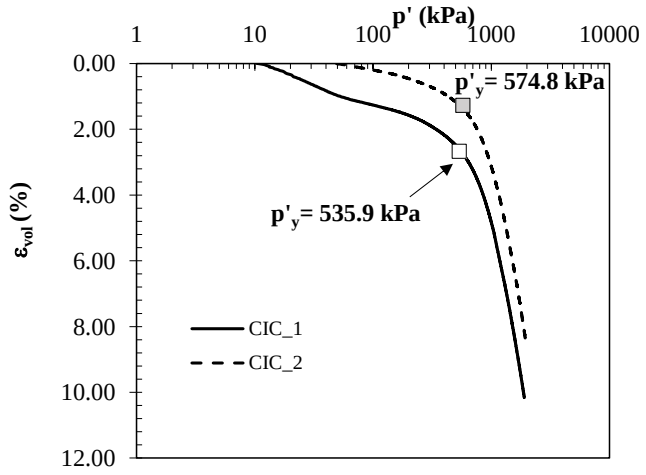

Figure 8.2: Compression curve from CIC tests performed on unreinforced stabilised samples and yield locus

8.2.1.3 Isotropically consolidated undrained triaxial test (CIU)

Figure 8.3 and Table 8.5 summarise the main results of the CIU triaxial test performed with the unreinforced stabilised sample, following the procedures described in Chapter 4. The evolution of the deviatoric stress (q), the excess pore pressure (Δu) and the secant undrained stiffness modulus ($E_{u\text{-}sec}$) with axial strain (ε_a) is presented in Figure 8.3. In terms of the evolution of the excess pore pressure, it can be seen that, unlike the deviator stress, it is dependent on the confining pressure. Figure 8.3b shows that the initial generation of Δu is such that it tends to null the applied confining pressure, i.e., the failure/rupture occurs in a condition very close to unconfined, hence the deviatoric stress value measured in CIU triaxial tests corresponding to the first noticeable breakage of cementitious bonds ($q \approx 475$ kPa in Figure 8.3a), is very close to the values of the unconfined compressive strength ($q_{u\,max}$) values measured in the reference and control tests (Table 8.3). The undrained strength (q_{max}) is characterised by a higher deviatoric stress due to some local particularities in the failure plane potentiated by the fact that the stabilise material exhibit an apparent coarser grain size. Regarding the undrained stiffness modulus, the values presented in Figure 8.3c) are of the same magnitude as the UCS reference and control tests, showing once again that a sample tested in an undrained triaxial condition is equivalent to an unconfined test. As presented in the Chapter 3, the structural yield point can be interpreted as the beginning of the breakage of cementitious bonds (Vaughan 1993; Malandraki and Toll, 1996 and 2000). According to the model, the destructuration (yield) point corresponds to a discontinuity in the mechanical behaviour of the composite material which can be identify by plotting the evolution of tangent

undrained stiffness modulus ($E_{u\,tan}$) versus axial strain (ε_a) bi-log plot, Figure 8.4 (the yield point is identified by a red square).

Table 8.5: Isotropically consolidated undrained (CIU) test results and yield stress for unreinforced stabilised samples

Mix No	ID	q_{max} (kPa)	ε_r (%)	Yield Criteria for Undrained Tests			
				$E_{u\,tan}$ (MPa)	ε_a (%)	q (kPa)	p' (kPa)
3	CIU_3_50	641.62	5.50	**66.91**	0.54	406.8	137.5

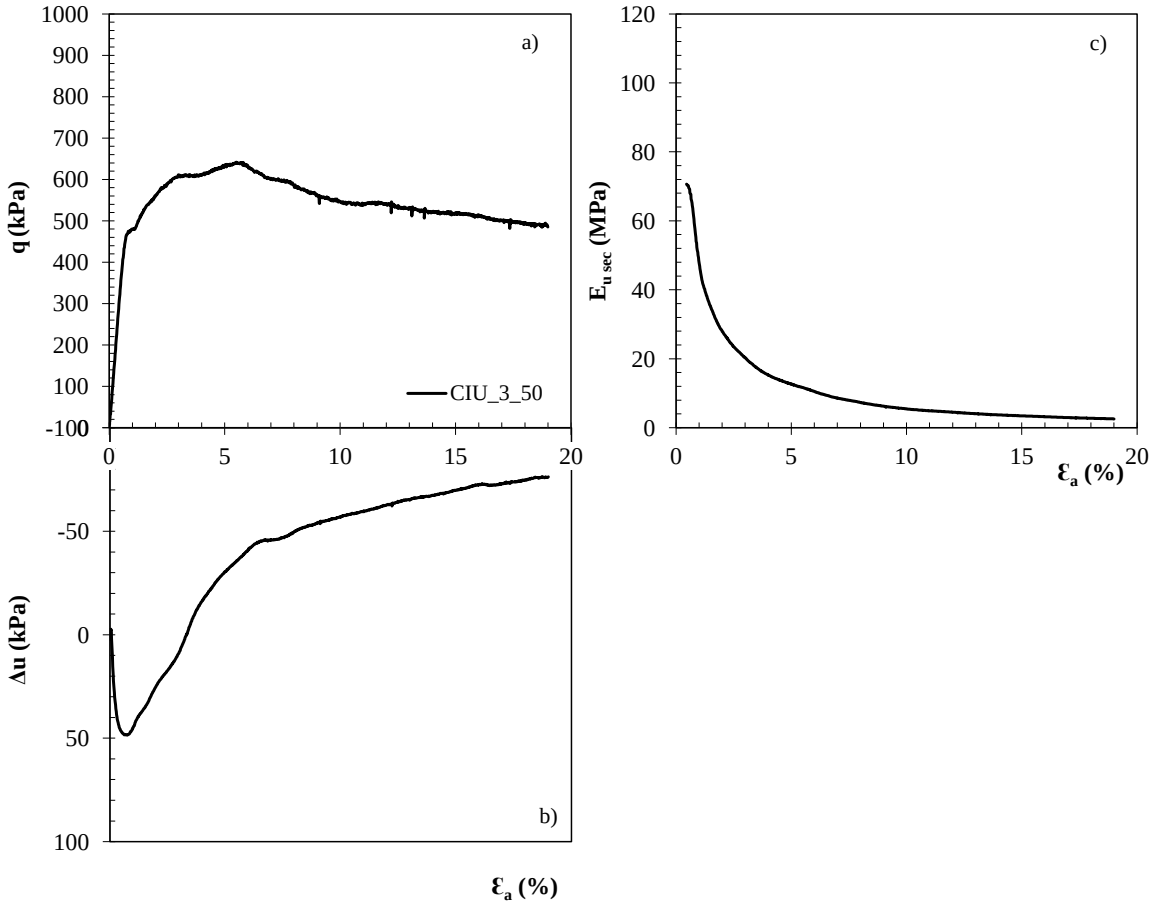

Figure 8.3: Results of the CIU test for unreinforced stabilised samples: a) stress-strain plot; b) excess of pore pressure vs axial strain; c) $E_{u\text{-}sec}$ vs axial strain

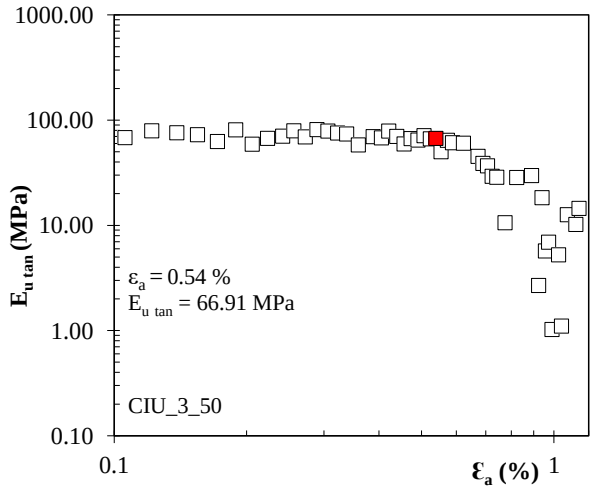

Figure 8.4: Evolution of $E_{u\text{-}tan}$ vs axial strain for CIU test for unreinforced stabilised samples and yield locus

8.2.1.4 Isotropically consolidated drained triaxial tests (CID)

Table 8.6 summarises the main results of the CID triaxial tests performed with unreinforced stabilised samples under three different effective confining stresses (50, 200 and 350 kPa), following the procedures described in Chapter 4. The evolution of the deviatoric stress (q), the axial (ε_a) and volumetric strains (ε_{vol}) with the mean effective stress (p') and finally the stress ratio (q/p') versus strain ratio ($\delta\varepsilon_{vol}/\delta\varepsilon_s$) for all CID triaxial tests are presented in Figure 8.5.

For the sample with the smallest effective confining stress (50 kPa) the behaviour is typically of an overconsolidated soil (σ'_c = 50 kPa is much lower than the yield evaluated in CIC triaxial test), characterised by a peak strength, after which the value of the deviatoric stress (q) decreases as the axial strain increases (ε_a), Figure 8.5a. In terms of volumetric strain (Figure 8.5b) the sample initially decrease in volume (contracts) but after it expands substantially as the test proceeds. Regarding the evolution of axial strain (ε_a) with the mean effective stress (p') Figure 8.5c) the behaviour is characterised by an initial linear path up to a maximum value of the mean effective stress (p') decreasing after towards a constant value of p' ("critical state"). Finally, the analysis of the curve of the stress ratio (q/p') versus strain ratio ($\delta\varepsilon_{vol}/\delta\varepsilon_s$) Figure 8.5d) is characterised by an initial path approximately vertical, reflecting the elastic behaviour of the composite material. After that the path proceeds almost horizontally to the left until the maximum deviatoric stress (failure/rupture) is achieved, and subsequently the stress ratio (q/p') decreases evolving gradually to the "critical state", where $\delta\varepsilon_{vol}/\delta\varepsilon_s = 0$.

For the samples with effective confining stresses of 200 and 350 kPa the behaviour is typically of a lightly overconsolidated soil characterised by a gradual increase of the deviatoric stress as the axial strain increases, Figure 8.5a. In terms of volumetric strain (Figure 8.5b) a gradual decrease

(contracts) of the volumetric strain is observed. Near the end of the test the volumetric strain tends to be constant suggesting that the samples are at the "critical state". Regarding the evolution of axial strain (ε_a) with the mean effective stress (p'), Figure 8.5c, the behaviour is characterised by an initial linear path evolving gradually to the maximum and constant value of the mean effective stress ("critical state"). Finally, the analysis of the curve (q/p' - $\delta\varepsilon_{vol}/\delta\varepsilon_s$) is characterised by an initial path approximately vertical, reflecting the elastic behaviour of the composite material, immediately followed by an almost horizontally path to the left until the maximum deviatoric stress (failure/rupture) is achieved. After that the stress ratio (q/p') decreases evolving gradually to the "critical state", where $\delta\varepsilon_{vol}/\delta\varepsilon_s = 0$.

As presented in Chapter 3, the yield of the stabilised material is characterised by an abrupt breakage of the cementitious bonds (destructuration), which may be evaluated by different yield criteria (p' - ε_a), (p' - ε_{vol}) and ($\delta\varepsilon_{vol}/\delta\varepsilon_s$ - q/p'). For the two first yield criteria the yield loci is defined as the end of the first linear trend in such plots (Mouratidis and Magnan, 1983; Venda Oliveira and Lemos, 2014). Regarding the third yield criterion ($\delta\varepsilon_{vol}/\delta\varepsilon_s$ - q/p') the yield is identified as the end of the initial approximately vertical path (Coop and Wilson, 1993; Cruz, 2008). In Figure 8.5 the yield loci are represented by a circle (p' - ε_a), triangle (p' – ε_{vol}), and diamond ($\delta\varepsilon_{vol}/\delta\varepsilon_s$ - q/p'), which values are presented in Table 8.6.

Table 8.6: Isotropically consolidated drained (CID) test results and yield criteria for unreinforced stabilised samples

Mix. No	ID	q_{max} (kPa)	ε_r (%)	Yield criteria	Yield Criteria for Drained Tests					
					q (kPa)	**p' (kPa)**	ε_a (%)	ε_{vol} (%)	$\delta\varepsilon_{vol}/\delta\varepsilon_s$ (-)	q/p' (-)
10	CID_4_50	754.76	2.09	**(p' - ε_a)**	560.41	**237.01**	**1.02**	-	-	-
				(p' - ε_{vol})	563.71	**237.90**	-	**0.66**	-	-
				($\delta\varepsilon_{vol}/\delta\varepsilon_s$) - (q/p')	560.40	237.10	-	-	**0.74**	**2.36**
8	CID_5_200	1201.66	6.98	**(p' - ε_a)**	659.00	**419.01**	**0.94**	-	-	-
				(p' - ε_{vol})	620.61	**406.26**	-	**0.56**	-	-
				($\delta\varepsilon_{vol}/\delta\varepsilon_s$) - (q/p')	645.78	415.13	-	-	**1.03**	**1.56**
9	CID_6_350	1505.46	10.47	**(p' - ε_a)**	464.00	**505.00**	**0.51**	-	-	-
				(p' - ε_{vol})	452.00	**500.81**	-	**0.31**	-	-
				($\delta\varepsilon_{vol}/\delta\varepsilon_s$) - (q/p')	397.40	482.85	-	-	**1.29**	**1.02**

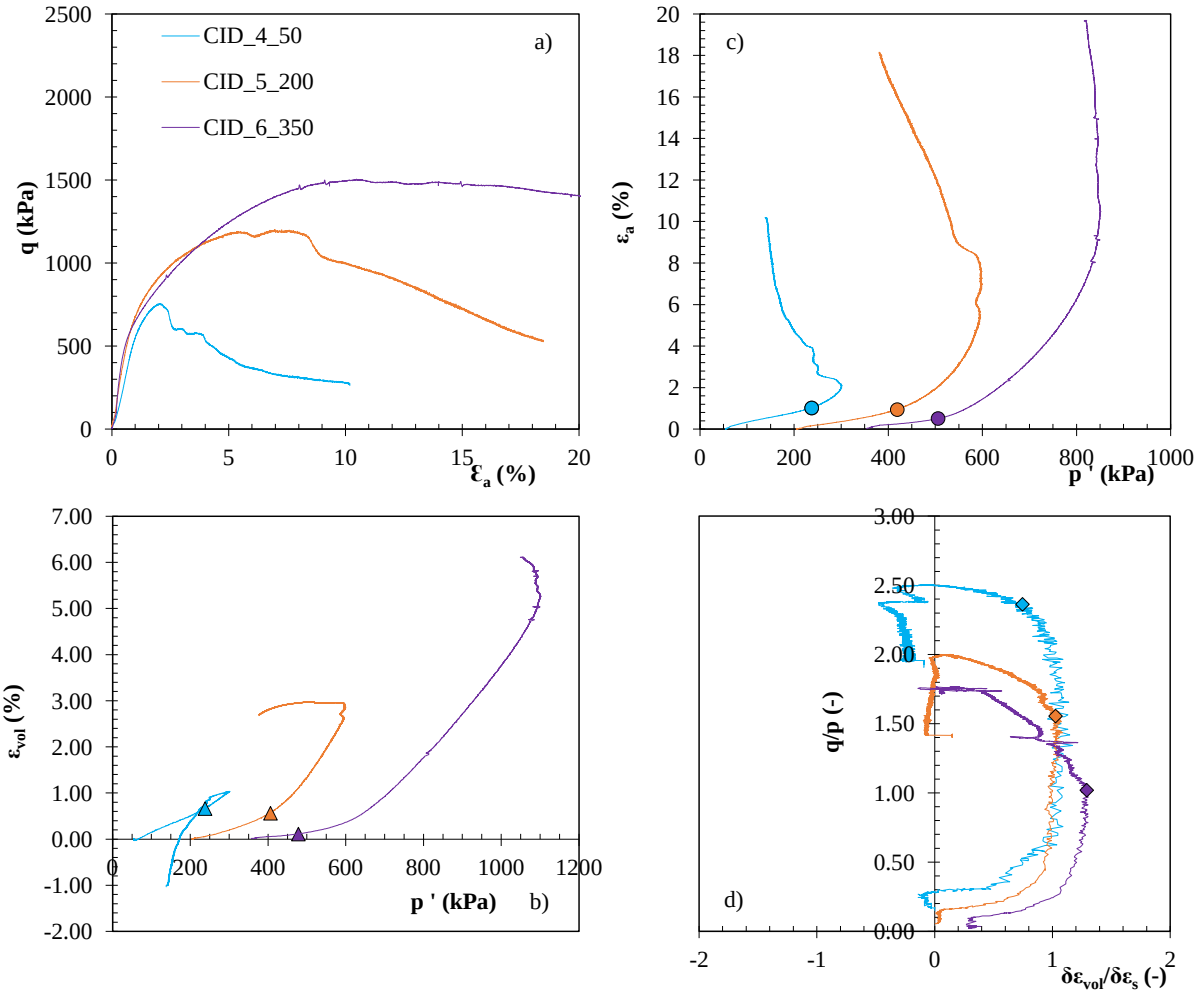

Figure 8.5: Results of the CID tests for stabilised samples: a) stress-strain plot; b) volumetric strain vs mean effective stress, p'; c) axial strain vs p'; d) strain ratio vs stress ratio

8.2.1.5 Yield surface of the unreinforced stabilised soft soil under static/monotonic loading condition

Figure 8.6 presents the stress path of all triaxial tests performed with the corresponding yield points, defined by the criteria showed previously, allowing the definition of the most probable yield surface. As it may be seen from the figure, there is a good correlation among the different yield criteria. The yield surface is a well-defined curved line that will be used as the reference to be compared with the yield surface of the other composite materials and loading conditions.

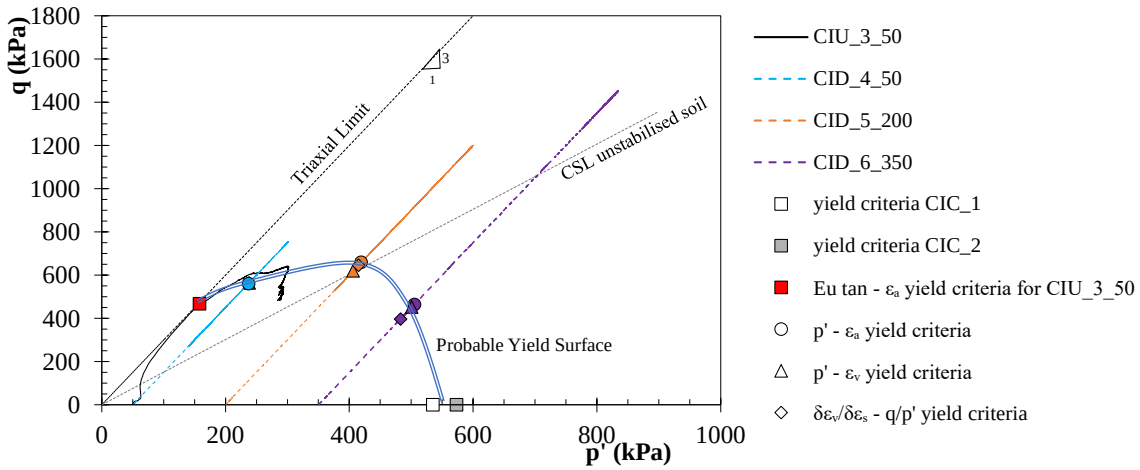

Figure 8.6: Effective stress path and yield loci of triaxial tests performed on unreinforced stabilised samples and possible yield surface

8.2.2 Behaviour under cyclic loading condition

The results of tests performed to characterise the stress-strain-shear strength behaviour of the Baixo Mondego soft soil chemically stabilised and without fibre addition (unreinforced case) but subjected to a prior cyclic loading will be presented and discussed in this section. A similar testing programme was developed, involving UCS control tests, cyclic loading tests to study the evolution of the permanent axial strain throughout the cyclic stage, post-cyclic CIC/CIU/CID triaxial tests, complemented by pulse velocity tests done before and after the cyclic loading stage aiming to evaluate the impact of the cyclic loading on the elastic properties of the composite material.

As it was shown in section 8.2.1, the triaxial tests will be characterised by appropriated plots to extract the information that allows to characterise the stress-strain-shear strength behaviour and yield locus of the composite material after a prior cyclic loading stage. The results from the tests performed are presented below.

8.2.2.1 Pulse velocity and reference/control tests

Table 8.7 summarises the results obtained in the pulse velocity tests as well as the elastic parameters (E, G, ν) for two different conditions, before an immediately after the cyclic loading stage. Analysing the results performed before the cyclic loading stage, it may be concluded that unreinforced stabilised samples exhibit very low variability in terms of density, V_p, V_s, ensuring the homogeneity of the samples which reflects a good reproducibility of the experimental

laboratory samples preparation procedure as mentioned in section 8.2.1.1. It is interesting to analyse the values related with the post-cyclic Pulse velocity tests (identified in Table 8.7 by the letters 'pc' added to the mixture number). As expected, the density of the post-cyclic tests is of the same order of the ones performed before the cyclic stage because during the cyclic stage there is no loss of mass of the samples. However, the V_p and V_s values of the post-cyclic tests are lower than the pre-cyclic tests which is explained by the breakage of cementitious bonds of the composite material (matrix degradation) occurred during the cyclic loading stage, leading to permanent (plastic) deformations. This matrix degradation has a major impact on the primary wave velocity (V_p) because it is a compression wave propagated directly through the matrix and if the matrix contains discontinuities (breakage of cementitious bonds) the compression wave arrival time increases and the V_p decreases. These post-cyclic lower velocity values are associated to lower elastic parameters (E, G, ν) indicating that there has been a degradation of the elastic properties of the composite material due to cyclic loading.

Table 8.7: Pulse Velocity Test results and elastic parameters for unreinforced stabilised samples tested before and after cyclic loading

Mix No.	ρ (kg/m^3)	Vp (m/s)	Vs (m/s)	E (MPa)	G (MPa)	ν
13	1524.92 (± 0.6%)	1693.00 (± 1.1%)	484.67 (± 1.9%)	1042.90 (± 3.6%)	358.31 (± 3.7%)	0.46 (± 0.42%)
14	1513.27 (± 0.3%)	1693.00 (± 0%)	459.33 (± 0.2%)	932.47 (± 0.6%)	319.28 (± 0.59%)	0.46 (± 0.01%)
15	1523.22 (± 0.2%)	1636.33 (± 3.5%)	449.67 (± 6.8%)	906.02 (± 12.9%)	310.58 (± 13.1%)	0.46 (± 1.11%)
16	1521.93 (± 0.6%)	1687.00 (± 0.4%)	489.00 (± 0.2%)	1058.39 (± 0.4%)	363.92 (± 0.4%)	0.45 (± 0.12%)
17	1518.07 (± 0.2%)	1699.33 (± 0.8%)	481.33 (± 0.4%)	1024.46 (± 0.8%)	351.72 (± 0.9%)	0.46 (± 0.3%)
18	1514.06 (± 0.2%)	1705.67 (± 0.4%)	477.67 (± 2.8%)	1007.33 (± 5.6%)	345.60 (± 5.7%)	0.46 (± 0.35%)
13pc	1533.40 (± 0%)	976.00 (± 0%)	438.00 (± 0%)	808.31 (± 0%)	294.16 (± 0%)	0.37 (± 0%)
14pc	1517.80 (± 0%)	1064.00 (± 0%)	475.00 (± 0%)	942.15 (± 0%)	342.46 (± 0%)	0.38 (± 0%)

Table 8.8 and Figure 8.7 summarise the results of the UCS control tests performed on some unreinforced stabilised samples in order to ensure good reproducibility of the experimental laboratory samples preparation procedure. Analysing the results, it is clear once again that all results are characterised by a lower dispersion compared to the reference tests (S_REF_1 and S_REF_2), certifying that the samples are homogeneous/similar to each other.

Table 8.8: Results of the UCS control tests performed before the cyclic stage on unreinforced stabilised samples

Mix No.	ID	$q_{u\ max}$ (kPa)	ε_r (%)	E_{u50} (MPa)	w_f (%)
	S_REF 1	510.3	1.10	84.52	75.45
	S_REF_2	477.1	1.04	59.75	77.95
14	C_MIX_14	527.7	1.70	39.41	75.92
16	C_MIX_16	510.3	1.20	64.91	76.18
17	C_MIX_17	567.4	2.10	35.00	76.21

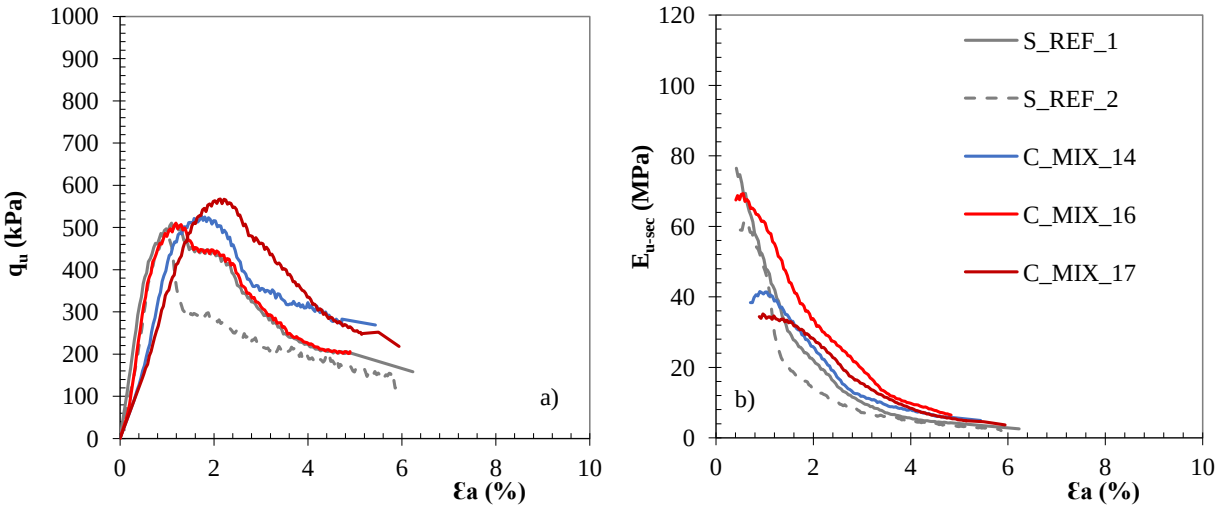

Figure 8.7: Results of the UCS control tests performed on stabilised samples unreinforced: a) stress-strain plot; b) $E_{u\text{-}sec}$ vs axial strain

8.2.2.2 Cyclic loading stage

Table 8.9 and Figures 8.8 and 8.9 summarise the results of the UCS cyclic loading tests and the UCS tests performed immediately after the end of the cyclic loading test (UCS_{pc}), as well as the corresponding reference values (Chapter 7).

As it may be seen from Figure 8.8, the evolution of the permanent axial strain is characterised by a quick increase in the first 500 load cycles followed by a slight increase as the number of load cycles increase, in accordance with reference results shown in Chapter 7 (S_REF_1cyc, S_REF_2cyc). Analysing the results of the UCS_{pc} tests (Table 8.9 and Figure 8.9) it can be seen that there is a reasonable agreement between the values now obtained and the values of the reference tests (S_REF_1pc, S_REF_2pc). These results confirm once more the reliability of the experimental laboratory samples preparation procedure.

Table 8.9: Results of the cyclic stage and post-cyclic UCS control tests performed on unreinforced stabilised samples

ID	$\varepsilon_{ax\ perm}$ (%)	ID	$q_{u\ max}$ (kPa)	ε_r (%)	E_{u50} (MPa)	w_f (%)
S_REF_1cyc	0.24	S_REF_1pc	721.52	1.49	100.02	74.71
S_REF_2cyc	0.22	S_REF_2pc	691.09	1.28	124.14	73.81
C_MIX_14cyc	0.28	C_MIX_14pc	675.57	2.13	48.80	72.80
C_MIX_15cyc	0.25	C_MIX_15pc	552.26	1.60	59.32	72.50
C_MIX_16cyc	0.25	C_MIX_16pc	848.11	1.76	106.89	73.60
C_MIX_17cyc	0.24	C_MIX_17pc	854.21	2.21	78.20	73.80
C_MIX_18cyc	0.25	C_MIX_18pc	625.19	1.38	66.26	72.60

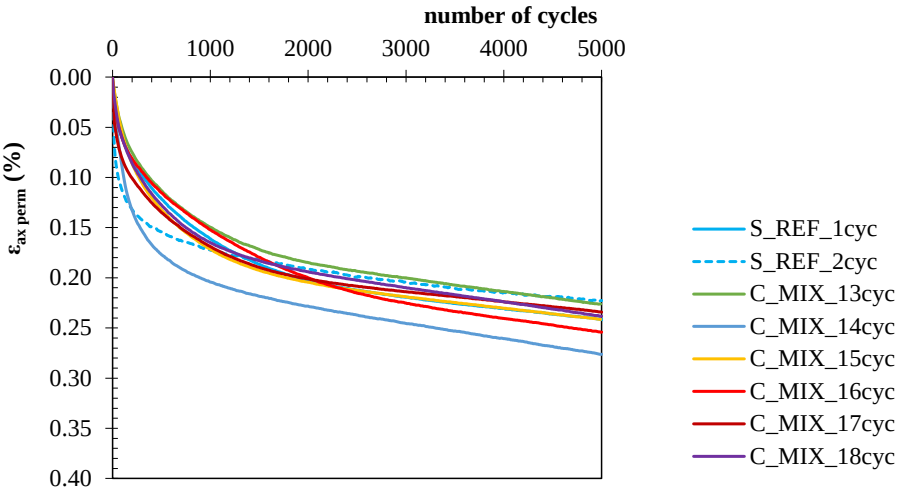

Figure 8.8: Evolution of permanent axial strain during the cyclic stage of the UCS cyclic control tests for unreinforced stabilised samples

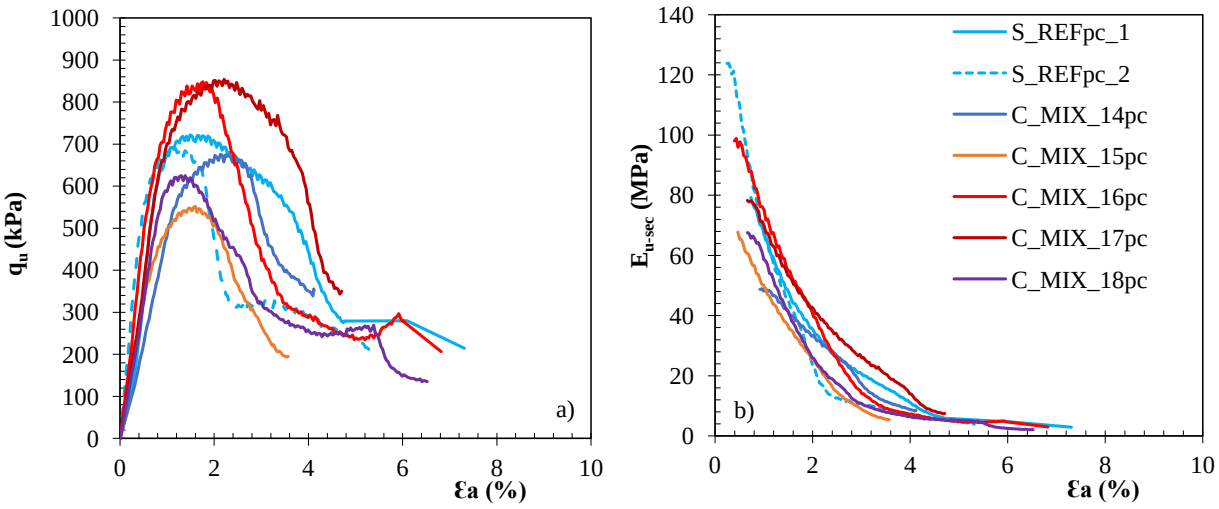

Figure 8.9: Results of the UCS_{pc} control tests performed on unreinforced stabilised samples: a) stress-strain plot; b) $E_{u\text{-}sec}$ vs axial strain

8.2.2.3 Post-cyclic Isotropic Compression triaxial test (CIC_{pc})

Table 8.10 and Figure 8.10 summarise of results from the CIC test performed on a sample previously submitted to a cyclic loading test. As it may be seen, the evolution of the volumetric strain with the logarithm of the mean effective stress (ε_{vol}-log p') follows a very similar trend as it was observed in section 8.2.1.2, characterised by a low compressibility up to yield stress (pre-σ'_y) and once the yield stress is exceeded (post-σ'_y) the behaviour changes being characterised by high compressibility or high volumetric strain. The transition point between the two behaviours is the yield stress (σ'_y or p'_y), corresponding to the moment from which the breakage of cementitious bonds intensifies (start of destructuration). The probable yield locus can be defined

by the intersection of these two linear trends, pre and post-σ'_y, represented by a square in Figure 8.10.

Comparing the yield stress of both loading conditions, monotonic (Table 8.4 and Figure 8.2, $\sigma'_y \approx 550$ kPa) with the post-cyclic loading ($\sigma'_y = 481$ kPa), it may be seen that the cyclic loading induced an earlier yield explained by the breakage of cementitious bonds happened during the cyclic loading stage, which lead to a deterioration of the mechanical properties of the composite material, i.e., the yield happened for lower stresses. The effect of the cyclic loading on the yield stress is the opposite of that observed in the edometric tests (Figure 7.16) which reflects the effect of the different confinement conditions.

Table 8.10: Post-cyclic isotropic compression triaxial tests (CIC_{pc}) results and yield locus for unreinforced stabilised samples

Mix No.	ID	$p'_y = \sigma'_y$ (kPa)
13	CICpc_1	**481**

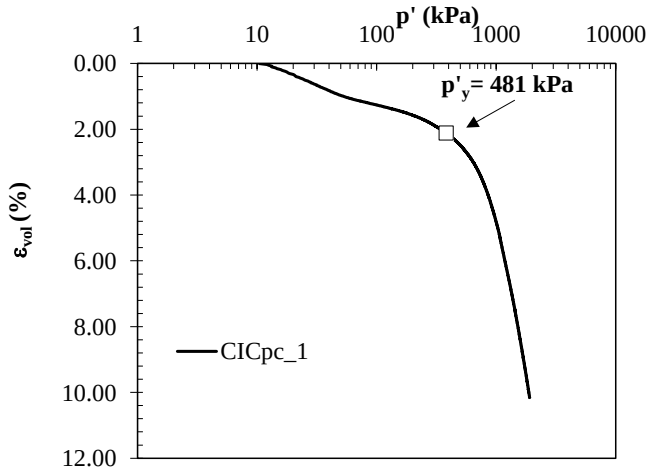

Figure 8.10: Compression curve from CIC_{pc} test performed on unreinforced stabilised samples and yield locus

8.2.2.4 Post-cyclic Isotropically consolidated undrained triaxial test (CIU_{pc})

Figure 8.11 and Table 8.11 summarise the main results of the isotropically consolidated undrained triaxial tests performed on unreinforced stabilised samples previously submitted to a cyclic loading test. The evolution of the deviatoric stress (q), the excess pore pressure (Δu) and the secant undrained stiffness modulus ($E_{u\text{-}sec}$) with axial strain (ε_a) is presented Figure 8.11.

In general, the results of the CIU_{pc} triaxial tests follow a similar trend as described in section 8.2.1.3, with some particularities that must be highlighted:

i) when comparing with the results of the samples without a prior cyclic loading stage, it may be seen that now the yielding occurs for lower stresses, or happened earlier, because the

matrix of the composite material is weakened due to the breakage of cementitious bonds that occurred during the prior cyclic loading stage;

ii) the maximum deviatoric stress (failure/rupture, q_{max}) is higher than in the monotonic case (Table 8.5), similarly to what occurs between the UCS and UCS_{pc} tests, partly explained by the fact that the breakage of the cementitious bonds happened during the cyclic loading may induce an apparent coarser grain size along the failure plane, resulting in the mobilisation of an higher frictional strength at failure/rupture.

Table 8.11: Post-cyclic isotropically consolidated undrained (CIU_{pc}) test results and yield stress for unreinforced stabilised samples

Mix No	ID	q_{max} (kPa)	ε_r (%)	Yield Criteria for Undrained Tests			
				$E_{u\ tan}$ (MPa)	**ε_a (%)**	q (kPa)	p' (kPa)
15	CIUpc_2_50	552.44	2.58	**73.5**	**0.53**	360.78	123.4

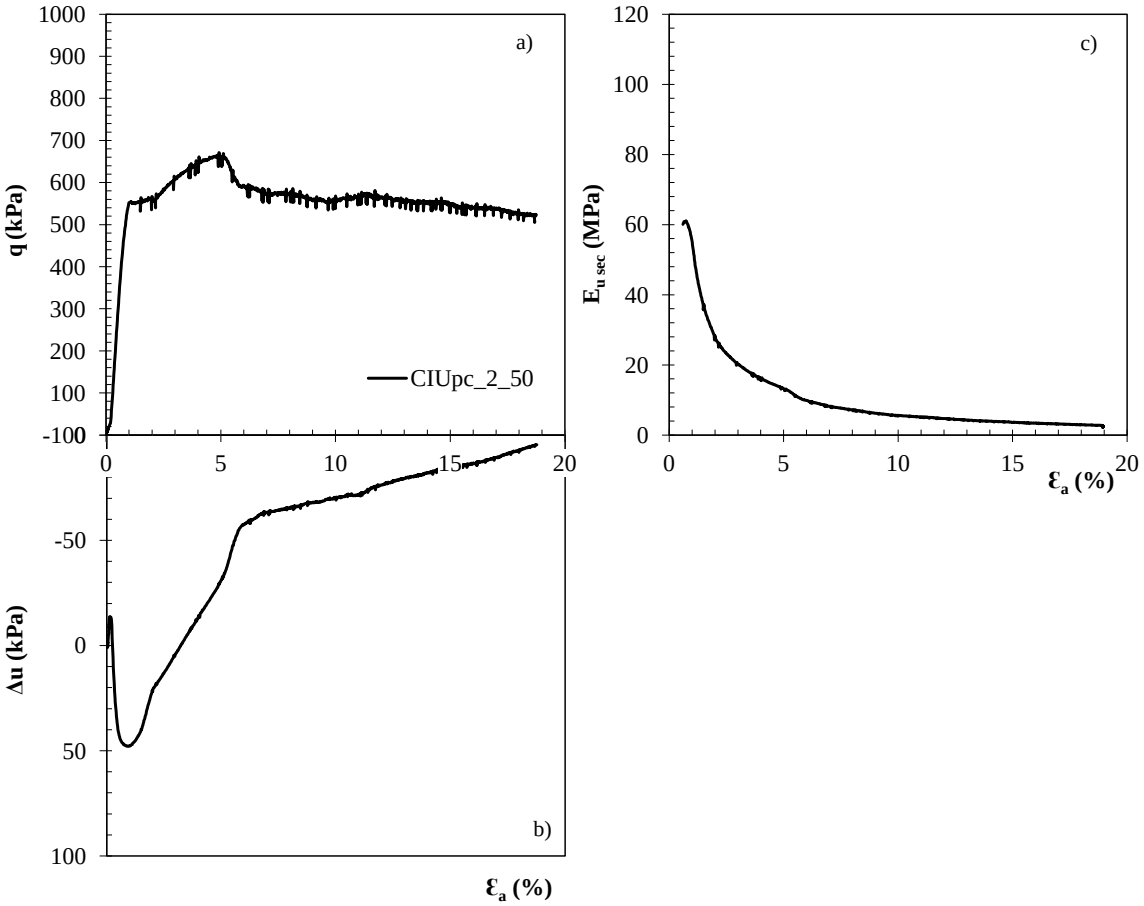

Figure 8.11: Results of CIU_{pc} test for unreinforced stabilised samples: a) Stress-strain plot; b) excess of pore pressure vs axial strain; c) $E_{u\text{-}sec}$ vs axial strain

The yield locus (destructuration) corresponds to a discontinuity in the mechanical behaviour of the composite material which can be identified in the tangent undrained stiffness modulus ($E_{u\,tan}$) versus axial strain (ε_a) bi-log plot, Figure 8.12, where the yield point is identified by a red square.

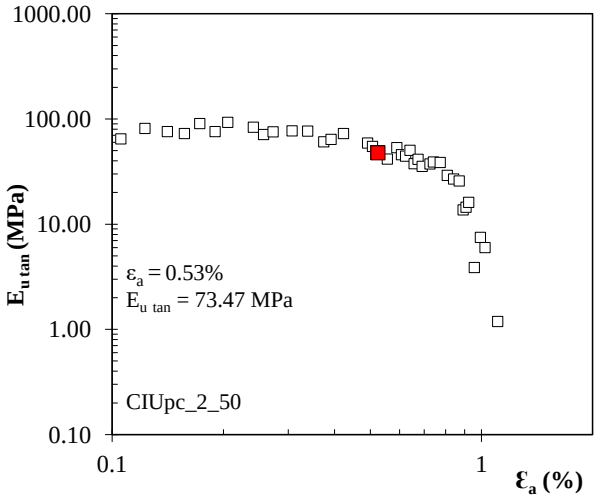

Figure 8.12: Evolution of $E_{u\text{-}tan}$ vs axial strain for CIUpc test performed on unreinforced stabilised samples and yield locus

8.2.2.5 Post-cyclic Isotropically consolidated drained triaxial tests (CID_{pc})

Table 8.12 presents the main results of the isotropically consolidated drained triaxial tests performed with unreinforced stabilised samples previously submitted to a cyclic loading test, under three different effective confining stresses (50, 200 and 350 kPa). The evolution of the deviatoric stress (q), the axial (ε_a) and volumetric strains (ε_{vol}) with the mean effective stress (p') and finally the stress ratio (q/p') versus strain ratio ($\delta\varepsilon_{vol}/\delta\varepsilon_s$) for all CID_{pc} triaxial tests are presented in Figure 8.13. As it was observed for the CIU_{pc} triaxial tests, also in the case of the CID_{pc} triaxial tests the results follow very closely the trend described in section 8.2.1.4, with some particularities that must be highlighted:

i) independently of the effective confining pressure, the maximum deviatoric stress (failure/rupture, q_{max}) tends to be slightly higher than the one observed in the corresponding monotonic tests (Table 8.6), similarly to what occurs between the UCS and UCS_{pc} tests, once again explained in part by the fact that the breakage of the cementitious bonds happened during the prior cyclic loading may induce an apparent coarser grain size along the failure plane, resulting in the mobilisation of higher frictional strength at failure/rupture. However, this observation is not valid for the CID_{pc} triaxial test with the lowest effective confining pressure (50 kPa) which may be related with the fact that the samples from the mixture n.º 14 exhibited the lowest density and elastic properties among all the samples (Table 8.7), even though the deviation from the average value is small;

ii) the breakage of cementitious bonds that happened during the prior cyclic loading stage induced a somehow weaker stabilised matrix, leading to an earlier yielding, i.e., the yield occurs for lower stresses, when compared to the yield of the samples without a prior cyclic loading stage.

As stated before, the yield of the stabilised material is characterised by an abrupt breakage of the cementitious bonds (destructuration), which may be evaluated by different yield criteria (p' - ε_a), (p' - ε_{vol}) and ($\delta\varepsilon_{vol}/\delta\varepsilon_s$ - q/p'). For the two first yield criteria the yield locus is defined as the end of the first linear trend of such plots, while for the third yield criterion the yield is identified as the end of the initial approximately vertical path. These yield loci are identified in Figure 8.13 by a circle (p' - ε_a), triangle (p' – ε_{vol}), and diamond ($\delta\varepsilon_{vol}/\delta\varepsilon_s$ - q/p'), corresponding to the values that are presented in Table 8.12.

Table 8.12: Post-cyclic isotropically consolidated drained (CID_{pc}) test results and yield criteria for unreinforced stabilised samples

Mix No	ID	q_{max} (kPa)	ε_r (%)	Yield criteria	Yield Criteria for Undrained Tests					
					q (kPa)	p' (kPa)	ε_a (%)	ε_{vol} (%)	$\delta\varepsilon_{vol}/\delta\varepsilon_s$ (-)	q/p' (-)
14	CIDpc_4_50	717.60	2.48	**(p' - ε_a)**	527.40	**225.50**	**1.24**	-	-	-
				(p' - ε_{vol})	556.30	**235.40**	-	**0.53**	-	-
				($\delta\varepsilon_{vol}/\delta\varepsilon_s$) - (q/p')	482.00	210.12	-	-	**0.74**	**2.18**
15	CIDpc_5_200	1252.4	6.62	**(p' - ε_a)**	621.60	**407.40**	**0.78**	-	-	-
				(p' - ε_{vol})	598.10	**398.90**	-	**0.51**	-	-
				($\delta\varepsilon_{vol}/\delta\varepsilon_s$) - (q/p')	645.80	415.10	-	-	**1.39**	**1.52**
16	CIDpc_6_350	1566.8	7.74	**(p' - ε_a)**	398.60	**483.20**	**0.56**	-	-	-
				(p' - ε_{vol})	418.00	**489.00**	-	**0.26**	-	-
				($\delta\varepsilon_{vol}/\delta\varepsilon_s$) - (q/p')	411.0	487.00	-	-	**1.39**	**0.84**

8.2.2.6 Yield surface of the unreinforced stabilised soft soil under cyclic loading condition

Figure 8.14 presents the stress path of all post-cyclic triaxial tests performed with the corresponding yield points, defined by the criteria showed previously, allowing the definition of the most probable yield surface of the unreinforced stabilised material when submitted to a prior cyclic loading. As it may be seen from the figure, there is a good correlation among the different yield criteria, allowing the definition of the new probable yield surface (a well-defined curved line). Comparing the two yielding surfaces for stabilised unreinforced materials it can be seen that both surfaces are homothetic, with the yielding surface of cyclic loading lying inside that of monotonic loading, reflecting the fact that the yield occurs earlier if there is submitted to a previous cyclic loading. As it was shown along the section, the cyclic loading induces the degradation of the cementitious matrix due the breakage of the cementitious bonds, as such, the yield occurs earlier than the yield for the static/monotonic case.

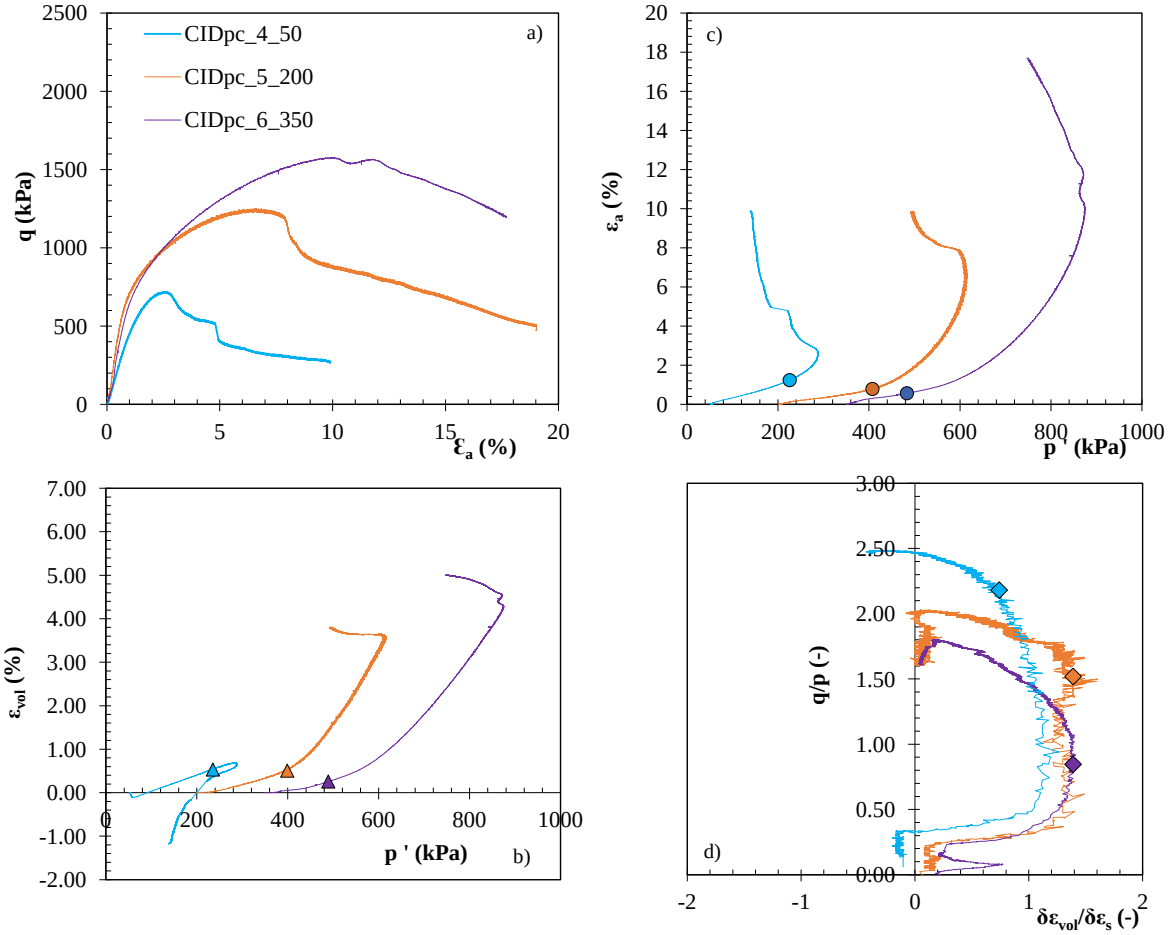

Figure 8.13: Results of the CID_{pc} tests performed on unreinforced stabilised samples: a) stress-strain plot; b) volumetric strain vs p'; c) axial strain vs mean effective stress, p'; d) strain ratio vs stress ratio

Another interesting feature that may be seen from Figure 8.14 is that the effective stress paths seem to evolve to the critical state line of the unstabilised soil at large deformations level, independently of the loading condition (cyclic or static/monotonic).

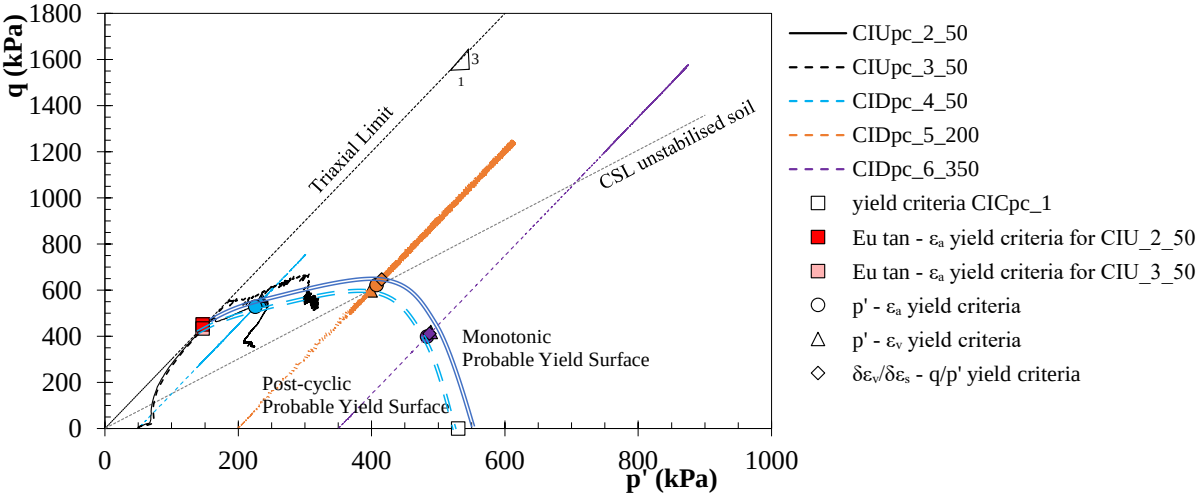

Figure 8.14: Effective stress path and yield loci of post-cyclic triaxial tests performed on unreinforced stabilised samples and possible yield surface

8.3 Stress-strain-shear strength behaviour of reinforced stabilised soft soil

As stated in the last two sections, the effect of differents loading conditions were analysed, static/monotonic versus cyclic loading for stabilised samples. Now, in this section it will be presented and discussed the results of several tests performed aiming to characterise the stress-strain-shear-strength behaviour of the Baixo Mondego soft soil fibre-reinforced chemically stabilised.

It was designed a similar experimental programme comprising isotropic compression, undrained and drained triaxial tests, complemented by UCS control/reference tests in order to guarantee the good quality and reproducibility of the stabilised samples, and by pulse velocity tests in order to evaluate the elastic parameters of the composite material, performed before and after the cyclic stage. Moreover, for the cyclic loading case, UCS cyclic tests were also carried out in order to characterize the evolution of the permanent axial strain during the cyclic stage.

The results will be presented in appropriated plots in order to extract to most valuable information regarding the characterisation of the stress-strain-shear strength behaviour and yield locus of the fibre-reinforced stabilised.

The results from the tests performed are presented below for both loading conditions, starting with the soft soil of Baixo Mondego chemically stabilised and reinforced with fibres under static/monotonic loading condition, followed by the case where a cyclic loading was previously applied to the fibre-reinforced stabilised samples.

8.3.1 Behaviour under static/monotonic loading condition

8.3.1.1 Pulse velocity and reference/control tests

Table 8.13 presents the results obtained in the pulse velocity tests for the fibre-reinforced samples, namely the density values, the primary (V_p) and shear wave (V_s) velocities, as well as the elastic parameters (E, G, ν, evaluated by the equations presented in Chapter 4), assuming that the composite materials behaves elastically. As it was shown for the unreinforced material, it is observed here that the fibre-reinforced samples exhibit very low variability in terms of density, V_p, V_s, ensuring the homogeneity of the samples which reflects a good reproducibility of the experimental laboratory samples preparation procedure. The evolution of the primary wave and shear wave velocities follow a very similar trend as described in section 8.2.1.1 for the unreinforced stabilised samples, characterised by very small variabilities, explained by the natural experimental variability of the study. Comparing both materials (unreinforced, Table 8.2, and

fibre-reinforced, Table 8.13) it is seen that the addition of fibres to the stabilised material induces a small decrease of the primary wave velocity (V_p), in agreement with the findings of Cristelo et al. (2015) and Miturski et al. (2021) who have reported that an addition of fibres induces a decrease of the primary wave velocity. The decrease of the primary wave velocity is explained by the fact that a material with lower density has a lower compression wave propagation velocity (Mooney, 2015; Miturski et al., 2021), and this is true when fibres are added to the stabilised material since the polypropylene fibres have lower density than the Portland cement and soil's particles, also lower than the water. When the analysis is focused on the shear wave velocity of both materials (unreinforced, Table 8.2, and fibre-reinforced, Table 8.13), the results also show a small decrease, sometimes marginal, of the shear wave velocity (V_s) for the material reinforced with polypropylene fibres. Similar results were reported by Fatahi et al. (2013). This small reduction can be explained by the density reduction promoted by the fibres which creates a softer region along the wave travel path, constantly reducing the energy of the shear wave (Cristelo et al., 2015; Miturski et al., 2021).

The elastic parameters (E, G, ν) of the fibre-reinforced stabilised material (Table 8.13) are lightly small than those evaluated for the unreinforced stabilised material (Table 8.2), reflecting the decrease in density when fibres were added to the stabilised material.

Table 8.13: Pulse Velocity Test results and elastic parameters for fibre-reinforced stabilised samples

Mix No.	ρ (kg/m^3)	Vp (m/s)	Vs (m/s)	E (MPa)	G (MPa)	ν
19	1516.91 (± 0.2%)	1693.00 (± 0%)	463.50 (± 1.0%)	951.35 (± 2.1%)	325.92 (± 2.1%)	0.46 (± 0.2%)
20	1505.94 (± 0.1%)	1683.51 (± 0.6%)	453.50 (± 0.3%)	904.91 (± 0.5%)	309.72 (± 0.5%)	0.46 (± 0.2%)
21	1512.87 (± 0.1%)	1680.33 (± 0.8%)	454.33 (± 0.2%)	912.22 (± 0.5%)	312.29 (± 0.4%)	0.46 (± 0.1%)
22	1518.54 (± 0.5%)	1680.33 (± 0.8%)	466.33 (± 0.8%)	963.18 (± 1.2%)	330.25 (± 1.2%)	0.46 (± 0.2%)
23	1508.69 (± 1.1%)	1724.67 (± 0.4%)	452.00 (± 0.4%)	901.95 (± 1.2%)	308.23 (± 1.2%)	0.46 (± 0.1%)
24	1498.86 (± 1.7%)	1699.33 (± 1.9%)	465.00 (± 1.5%)	946.31 (± 4.6%)	324.21 (± 4.8%)	0.46 (± 0.5%)
25	1506.92 (± 0.2%)	1668.00 (± 0.4%)	456.33 (± 0.2%)	916.02 (± 0.4%)	313.8 (± 0.4%)	0.46 (± 0.1%)
26	1507.98 (± 0.3%)	1668.00 (± 0.4%)	453.33 (± 2.1%)	905.25 (± 4.5%)	310.00 (± 4.6%)	0.46 (± 0.4%)
27	1511.87 (± 0.5%)	1674.00 (± 0%)	451.67 (± 2.5%)	901.41 (± 5.4%)	308.56 (± 5.6%)	0.46 (± 0.4%)

Table 8.14 and Figure 8.15 summarise the results of the UCS control tests performed on some fibre-reinforced stabilised samples as well as the results of the reference UCS tests (presented in Chapter 7). The comparison of the results shows a very low dispersion, explained by the natural experimental variability, ensuring the good reproducibility of the experimental laboratory samples preparation procedure.

Table 8.14: Results of the UCS control tests performed on fibre-reinforced stabilised samples

Mix No.	ID	$q_{u\ max}$ (kPa)	ε_r (%)	E_{u50} (MPa)	w_f (%)
	S_REF_1_F	672.72	2.04	41.76	75.45
	S_REF_2_F	683.88	2.33	51.45	77.95
20	C_MIX_20_F	728.24	4.29	27.96	74.10
25	C_MIX_25_F	732.39	3.91	55.72	76.20
26	C_MIX_26_F	699.58	4.39	51.37	75.80

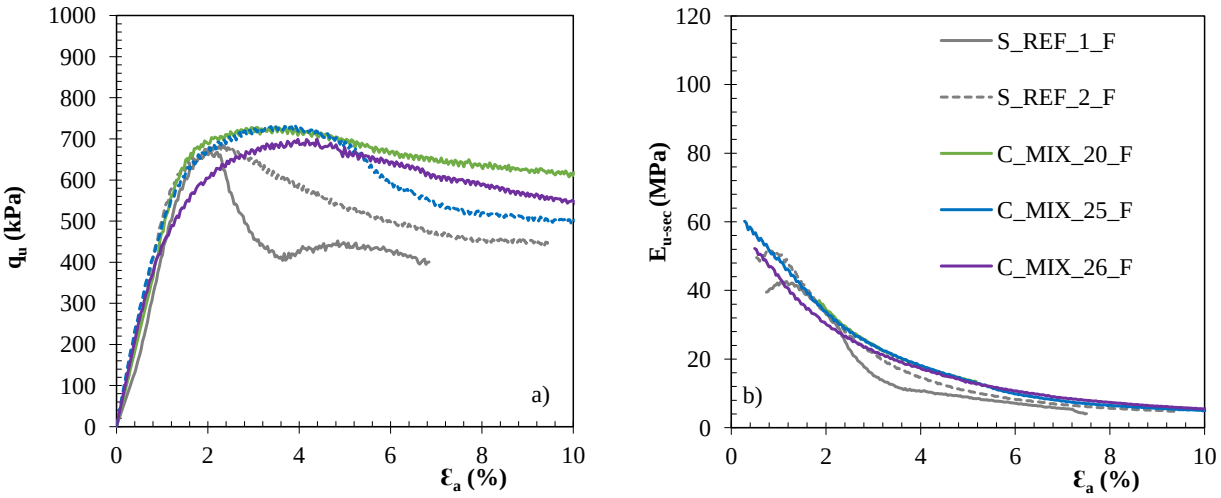

Figure 8.15: Results of the UCS control tests performed on fibre-reinforced stabilised samples: a) stress-strain plot; b) $E_{u\text{-}sec}$ vs axial strain

8.3.1.2 Isotropic Compression triaxial tests (CIC)

Table 8.15 summarises the results of the CIC triaxial tests for monotonic loading conditions of fibre-reinforced samples. Figure 8.16 depicts the evolution of the volumetric strain with the logarithm of the mean effective stress (ε_{vol}-log p') showing a similar trend as it was observed in section 8.2.1.2, characterised by an initial low compressibility up to yield stress (pre-σ'_y) followed by a high compressibility once the yield stress is exceeded (post-σ'_y). The changing point between the two behaviours is the yield stress (σ'_y or p'_y, represented by a square in Figure 8.10), related to the instant from which the breakage of cementitious bonds intensifies (start of destructuration).

Table 8.15: Isotropic compression triaxial tests (CIC) results and yield locus for fibre-reinforced stabilised samples

Mix No.	ID	$\mathbf{p'_y = \sigma'_y}$ **(kPa)**
20	CIC_1_F	**519.69**
26	CIC_2_F	**497.20**

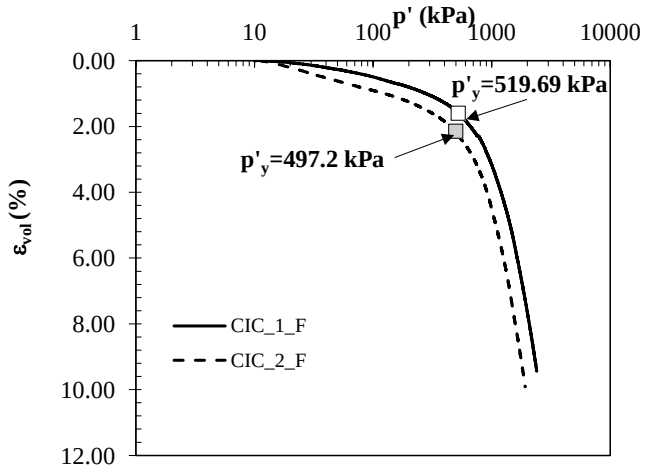

Figure 8.16: Compression curve from CIC tests performed on fibre-reinforced stabilised samples and yield locus

Comparing the yield stress of both stabilised materials, unreinforced (Table 8.4 and Figure 8.2, $\sigma'_y \approx 550$ kPa) with the fibre-reinforced samples ($\sigma'_y \approx 510$ kPa), it may be seen that the addition of fibres generates an earlier yield, i.e., the yielding occurs at lower stresses which may be explained by the fact that the physical presence of the fibres tends to hinder the development of some cementitious bonds, and/or introducing at the same time some discontinuities in the cementitious matrix, resulting in a reduction in the stiffness of the fibre-reinforced stabilised material, in well agreement with the elastic parameters evaluated by pulse velocity tests (Table 8.13).

8.3.1.3 Isotropically consolidated undrained triaxial test (CIU)

Figure 8.17 and Table 8.16 summarise the main results of the CIU triaxial test performed on fibre-reinforced stabilised samples. As it was done for the previous sections dealing with CIU tests, the evolution of the deviatoric stress (q), the excess pore pressure (Δu) and the secant undrained stiffness modulus ($E_{u\text{-}sec}$) with axial strain (ε_a) is presented Figure 8.17. In general, the results of the CIU triaxial test follow a similar trend as described in section 8.2.1.3, with some features that should be pointed out. First, when comparing the yield stress of both composite materials, unreinforced (section 8.2.1.3) and fibre-reinforced, it can be seen that for the fibre-reinforced stabilised material the yielding occurs at lower stresses as a result of the cementitious matrix being weakened by the presence of the fibres that prevents some cementitious bonds within the composite matrix, inducing a less stiff and stronger matrix. Secondly, the fibre-reinforced stabilised material is characterised by an higher strength at failure/rupture ($q_{max} \approx 760$ kPa) when compared with the unreinforced stabilised samples ($q_{max} \approx 640$ kPa, Table 8.5), because as the

CIU test evolves (increase of axial strains) there is a progressive mobilisation of the tensile strength of the fibres, thus, contributing to the increase of the strength at failure/rupture.

Table 8.16: Isotropically consolidated undrained (CIU) test results and yield stress for fibre-reinforced stabilised samples

Mix No	ID	q_{max} (kPa)	ε_r (%)	Yield Criteria for Undrained Tests			
				$E_{u\ tan}$ (MPa)	**ε_a (%)**	q (kPa)	p' (kPa)
24	CIU_4_50_F	759.96	9.59	**64.3**	**0.58**	349.0	120.9

The most probable yield locus may be identified in the tangent undrained stiffness modulus ($E_{u\ tan}$) versus axial strain (ε_a) bi-log plot (Figure 8.18), corresponding to a discontinuity in the mechanical behaviour of the composite material, which indicates the beginning of the destructuration (the yield point is identified by a red square in Figure 8.18).

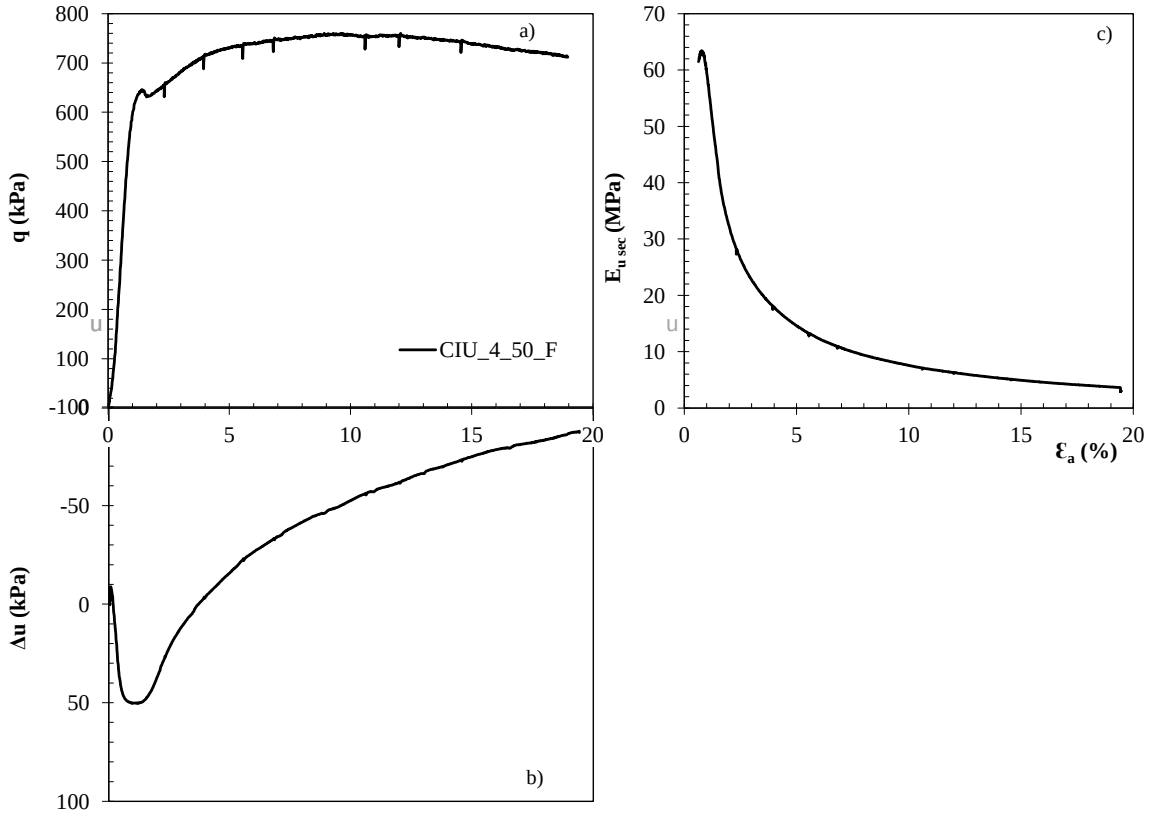

Figure 8.17: Results of CIU test for fibre-reinforced stabilised samples: a) stress-strain plot; b) excess of pore pressure vs axial strain; c) $E_{u\text{-}sec}$ vs axial strain

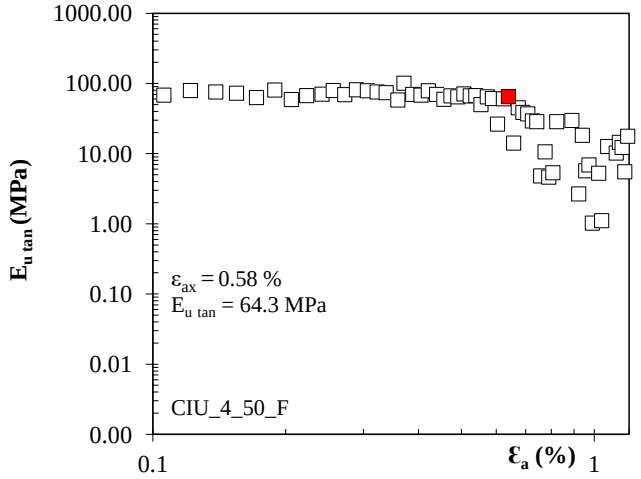

Figure 8.18: Evolution of $E_{u\text{-}tan}$ vs axial strain for CIU test for fibre-reinforced stabilised samples and yield locus

8.3.1.4 Isotropically consolidated drained triaxial tests (CID)

Table 8.17 summarises the main results of the CID triaxial tests performed with fibre-reinforced stabilised samples under three different effective confining stresses (50, 200 and 350 kPa). Figure 8.19 depicts the evolution of the deviatoric stress (q), the axial (ε_a) and volumetric strains (ε_{vol}) with the mean effective stress (p'), and finally the stress ratio (q/p') versus strain ratio ($\delta\varepsilon_{vol}/\delta\varepsilon_s$) for all CID triaxial tests.

In general, the triaxial CID tests performed with fibre-reinforced stabilised samples show a very similar trend to those described for the unreinforced stabilised samples (section 8.2.1.4). The samples with the smallest effective confining pressure (50 kPa) exhibit a stress-strain behaviour typically of an overconsolidated soil (the confining stress is much lower than the yield stress evaluated in CIC triaxial test), while for the samples with effective confining stresses of 200 and 350 kPa the behaviour is typically of a lightly overconsolidated soil (the confining stresses are slightly lower than the yield stress evaluated in CIC triaxial test). Despite the similarities with the behaviour described in section 8.2.1.4, there are some different features that are highlighted below.

As it was shown previously, the addition of fibres seems to prevent the development of some cementitious bonds, introducing some discontinuities in the cementitious matrix, resulting in a reduction in the stiffness of the fibre-reinforced stabilised material. This effect induces an earlier yielding of the composite material, i.e., the yield occurs for lower stresses than those observed for the unreinforced material. However, the addition of fibres promotes an increase of the strength of the composite material which seems to be in contradiction with the stiffness decrease. It must be

highlighted that yielding is associated to low level of strains (beginning of destructuration) while the failure/rupture of a stabilised material reinforced with fibres happens for a much higher level of strains, compatible with the mobilisation of the tensile strength of the fibres. This fibre mobilisation is responsible for the strength increase observed for all confining stresses. Moreover, and as it was shown in Chapters 5 to 7, the fibres addition confers to the composite material a more ductile behaviour, clearly displayed in the evolution of the deviatoric stress (q) with the axial strain (ε_a), Figure 8.19a).

Table 8.17: Isotropically consolidated drained (CID) test results and yield locus for fibre-reinforced stabilised samples

Mix No	**ID**	q_{max} (kPa)	ε_r (%)	**Yield criteria**	Yield Criteria for Drained Tests					
					q (kPa)	p' (kPa)	ε_a (%)	ε_{vol} (%)	$\delta\varepsilon_{vol}/\delta\varepsilon_s$ (-)	q/p' (-)
19	CID_5_50_F	781.38	4.11	**(p' - ε_a)**	504.00	**216.10**	**0.88**	-	-	-
				(p' - ε_{vol})	545.20	**231.60**	-	**0.66**	-	-
				($\delta\varepsilon_{vol}/\delta\varepsilon_s$) - (q/p')	421.00	190.00	-	-	**0.7**	**2.22**
23	CID_6_200_F	1207.61	5.01	**(p' - ε_a)**	678.80	**426.20**	**1.05**	-	-	-
				(p' - ε_{vol})	662.10	**420.50**	-	**0.87**	-	-
				($\delta\varepsilon_{vol}/\delta\varepsilon_s$) - (q/p')	559.00	386.00	-	-	**1.11**	**1.57**
25	CID_7_200_F	1045.62	6.67	**(p' - ε_a)**	652.00	**427.40**	**1.55**	-	-	-
				(p' - ε_{vol})	665.00	**421.00**	-	**1.29**	-	-
				($\delta\varepsilon_{vol}/\delta\varepsilon_s$) - (q/p')	666.75	421.61	-	-	**1.08**	**1.58**
22	CID_8_350_F	1530.80	12.2	**(p' - ε_a)**	366.39	**472.30**	**0.53**	-	-	-
				(p' - ε_{vol})	369.72	**474.80**	-	**0.39**	-	-
				($\delta\varepsilon_{vol}/\delta\varepsilon_s$) - (q/p')	376.14	475.60	-	-	**1.28**	**0.7**

As stated before, three different yield criteria [(p' - ε_a), (p' - ε_{vol}) and ($\delta\varepsilon_{vol}/\delta\varepsilon_s$ - q/p')] may be used to evaluate the yield stress locus in CID triaxial tests. For all yield criteria, the yield locus corresponds to a discontinuity in the respective plots, highlighting a change in the stress-strain behaviour (beginning of destructuring). These yield loci are identified in Figure 8.19 by a circle (p' - ε_a), triangle (p' – ε_{vol}), and diamond ($\delta\varepsilon_{vol}/\delta\varepsilon_s$ - q/p'), corresponding to the values that are presented in Table 8.17.

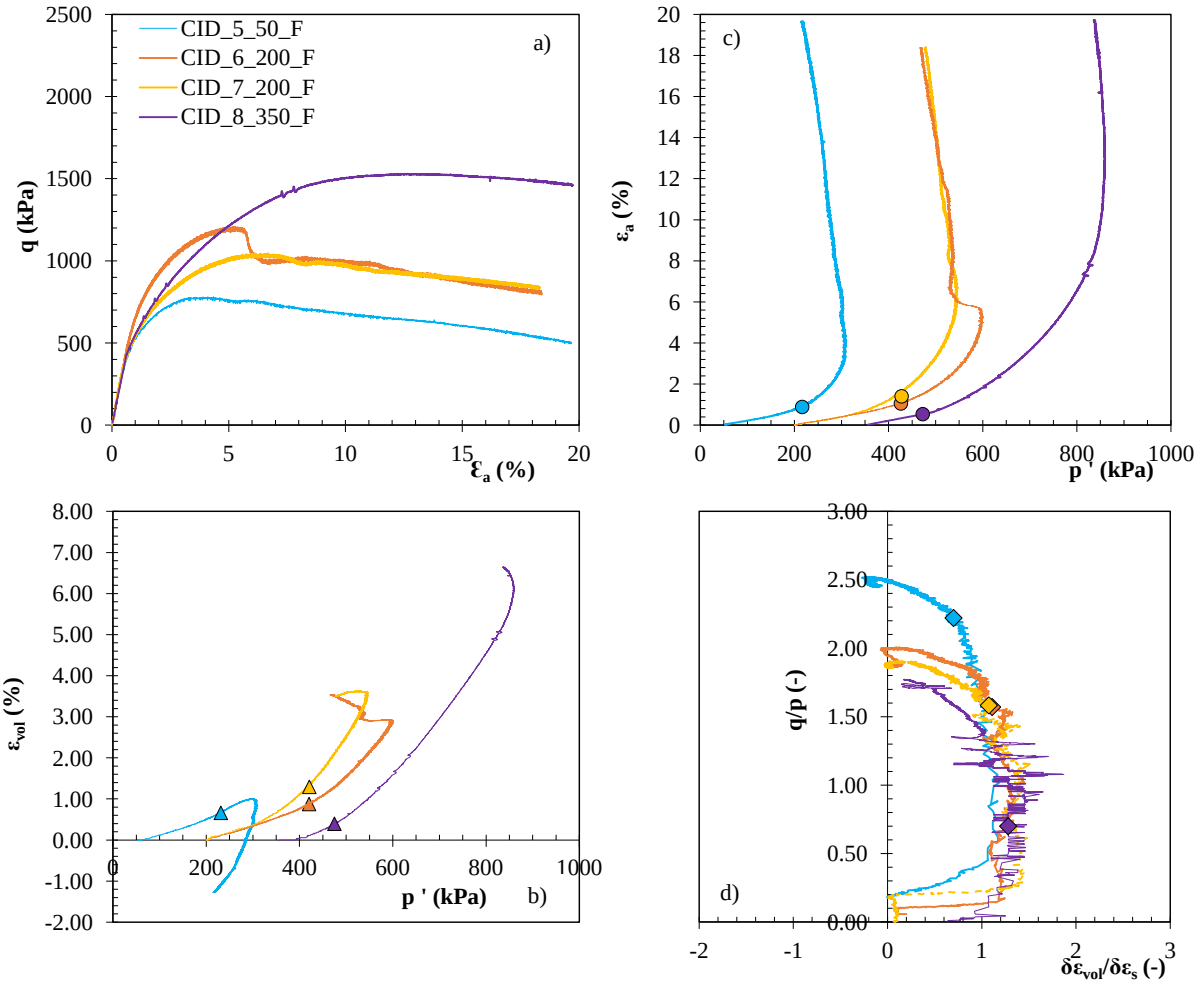

Figure 8.19: Results of the CID tests performed on fibre-reinforced stabilised samples: a) stress-strain plot; b) volumetric strain vs p'; c) axial strain vs mean effective stress, p'; d) strain ratio vs stress ratio

8.3.1.5 Yield surface of the stabilised soft soil reinforced with fibres under static/monotonic loading condition

Figure 8.20 presents the stress path of all triaxial tests performed with fibre-reinforced stabilised samples as well as the respective yield loci, defined by the yield criteria studied previously. As it may be seen from the figure, there is a good correlation among the different yield criteria, allowing the definition of the new probable yield surface (a well-defined curved line).

For comparison purposes, the yield surface of the unreinforced stabilised material (section 8.2.1.5) is also presented in Figure 8.20. The analysis of the two yielding surfaces (fibre-reinforced and unreinforced) shows that they are homothetic. The fibre-reinforced stabilised material is characterised by a smaller (or inner) yield surface than the one defined for the unreinforced material. As previously pointed out, the addition of fibres weakens the cementitious matrix of the composite material, resulting in an earlier yielding.

It is interesting to observe that the effective stress paths of the triaxial tests at large strains level do not achieve the critical state line (CSL) of the unstabilised soil, evolving into a line that is slightly above this one (CSL). Such behaviour seems to be due to the mobilization of fibres tensile strength, responsible for a residual strength higher than that of the unreinforced material. That is, the fibre-reinforced stabilised material seems to evolve to a new CSL corresponding to the fibre-reinforced unstabilised material (unfortunately this new CSL was not yet defined for the Baixo Mondego soft soil).

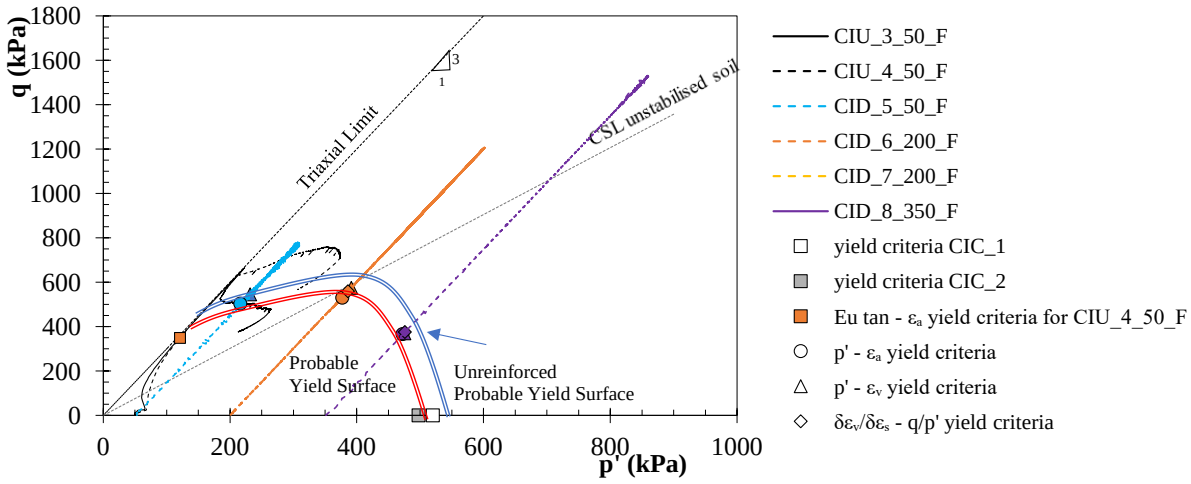

Figure 8.20: Effective stress path and yield loci of triaxial tests performed on fibre-reinforced stabilised samples and possible yield surface

8.3.2 Behaviour under cyclic loading condition

This section aims to characterise the stress-strain-shear-strength behaviour and the yield surface of the Baixo Mondego soft soil chemically stabilised and reinforced with polypropylene fibres subjected to a prior cycle loading stage. For such it was designed an experimental testing programme comprising pulse velocity and UCS control tests in order to verify the quality and homogeneity of the samples, cyclic loading tests to study the evolution of the permanent axial strain during the cyclic stage, complemented by pulse velocity tests carried out immediately after the cyclic loading stage aiming to examine the effect of the cyclic loading on the composite material's elastic properties, and finally, post-cyclic CIC/CIU/CID triaxial tests. The results of these tests will be analysed and discussed using appropriate plots. The results from the tests carried out are presented below.

8.3.2.1 Pulse velocity and reference/control tests

Table 8.18 summarises the results obtained in the pulse velocity tests and the respective elastic parameters (E, G, ν) for two different conditions, before an immediately after (tests identified by the letters 'pc', of post-cyclic, added to the mixture number) the cyclic loading stage of fibre-reinforced stabilised samples. Once again, the results present a very low variability in terms of density, V_p and V_s, ensuring homogeneity and good quality of the samples which reflects a good reproducibility of the experimental laboratory samples procedure.

Analysing the pulse velocity results of the tests performed before the cyclic loading stage it may be seen that are in well agreement with the values observed in section 8.3.1.1 as expected, since the samples are "equal". When the analysis is focused on the results from the post-cyclic loading tests, it is evident that the density remains almost unchanged because during the cyclic loading stage there is no loss of mass of the samples. However, it may be seen that V_p and V_s values of the post-cyclic tests are lower than the pre-cyclic tests which, one more time, may be explained by the breakage of cementitious bonds of the composite material happened during the cyclic loading stage. A major impact is observed for V_p than for V_s because the primary wave velocity is a compression wave propagated directly through the matrix and if the matrix contains discontinuities (induced by the breakage of cementitious bonds) the compression wave arrival time increases and the V_p decreases. As expected, lower values of the post-cyclic wave velocities are associated to lower elastic parameters (E, G, ν) indicating that there has been a degradation of the elastic properties of the composite material due to cyclic loading.

Moreover, when comparing the wave velocities and the elastic parameters of both stabilised materials (fibre-reinforced, Table 8.18, and unreinforced, Table 8.7), it may be seen that, in general, the fibre addition promotes a slight reduction of wave velocities explained, as previously presented, by the fact that the polypropylene fibres have lower density than the Portland cement and soil's particles, also lower than the water. These changes will produce a slight decrease of the elastic parameters.

Table 8.18: Pulse Velocity Test results and elastic parameters for fibre-reinforced stabilised samples

Mix No.	ρ (kg/m^3)	Vp (m/s)	Vs (m/s)	E (MPa)	G (MPa)	ν
28	1504.72 (± 0.5%)	1680.33 (± 0.8%)	472 (± 0.1%)	978.30 (± 0.4%)	335.70 (± 0.4%)	0.46 (± 0.2%)
29	1508.7 (± 0.5%)	1680.33 (± 0.8%)	465 (± 1.5%)	951.77 (± 3.4%)	326.28 (± 3.5%)	0.46 (± 0.1%)
30	1504.72 (± 0.5%)	1686.67 (± 1.5%)	468 (± 0.6%)	961.28 (± 1.8%)	329.59 (± 1.8%)	0.46 (± 0.2%)
31	1515.72 (± 0.4%)	1680.67 (± 0.7%)	466 (± 1.1%)	960.03 (± 1.5%)	329.15 (± 1.5%)	0.46 (± 0.1%)
34	1533.30 (± 0.2%)	1705.67 (± 0.4%)	466 (± 0.6%)	972.05 (± 1.0%)	332.97 (± 1.0%)	0.46 (± 0.1%)
36	1528.77 (± 0.3%)	1680.67 (± 0.7%)	469 (± 0.6%)	981.80 (± 1.0%)	336.77 (± 1.1%)	0.46 (± 0.3%)
28pc	1501.00 (± 0%)	1074 (± 0%)	457 (± 0%)	871.14 (± 0%)	313.48 (± 0%)	0.39 (± 0%)
29pc	1502.61 (± 0%)	1080 (± 0%)	455 (± 0%)	866.10 (± 0%)	311.08 (± 0%)	0.39 (± 0%)
37pc	1501.34 (± 0%)	1044 (± 2.1%)	455.5 (± 0.1%)	861.07 (± 0.2%)	311.50 (± 0.2%)	0.38 (± 1.7%)
38pc	1502.14 (± 0%)	1049 (± 2.6%)	456 (± 0.2%)	864.09 (± 0.9%)	312.35 (± 0.4%)	0.38 (± 1.8%)

Table 8.19 and Figure 8.21 present the results of the UCS control tests of some fibre-reinforced stabilised samples carried out before the cyclic loading stage, as well as the UCS reference tests (S_REF_1_F and S_REF_2_F) described in Chapter 7. From the analysis of the results it may be concluded that there is good agreement between all the results, ensuring once more that the samples are homogeneous to each other, reflecting the good reproducibility of the experimental laboratory samples procedure.

Table 8.19: Results of the UCS control tests performed before the cyclic stage on fibre-reinforced stabilised samples

Mix No.	ID	$q_{u\ max}$ (kPa)	ε_r (%)	E_{u50} (MPa)	w_f (%)
	S_REF_1_F	672.72	2.04	41.76	75.45
	S_REF_2_F	683.88	2.33	51.45	77.95
28	C_MIX_28_F	654.70	2.10	57.40	72.81
31	C_MIX_31_F	527.70	1.70	39.41	76.12
36	C_MIX_36_F	679.80	1.40	70.41	75.81

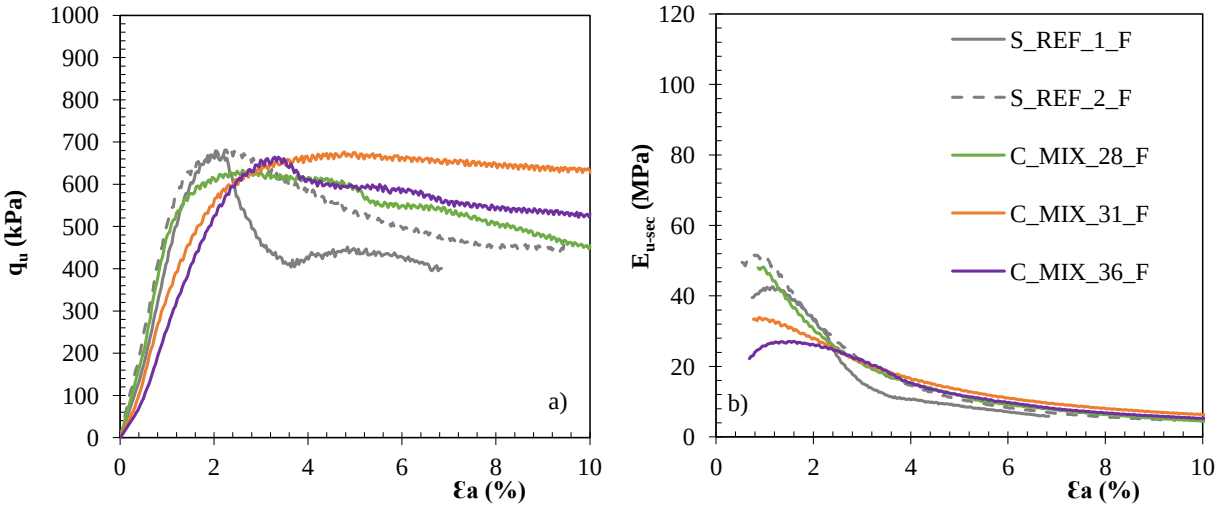

Figure 8.21: Results of the UCS control tests performed on fibre-reinforced stabilised samples: a) stress-strain plot; b) $E_{u\text{-}sec}$ vs axial strain

8.3.2.2 Cyclic loading stage

Table 8.20 and Figure 8.22 summarise the results of the cyclic loading tests performed with the fibre-reinforced stabilised samples, as well as the corresponding reference values (S_REF_cyc_1_F, S_REF_cyc_2_F, presented in Chapter 7).

As it may be seen from Figure 8.22, the evolution of the permanent axial strain of the new cyclic loading tests fits relatively well with the reference results. These results confirm again the reliability of the experimental laboratory samples preparation procedure.

Table 8.20: Results of the cyclic loading tests performed on fibre-reinforced stabilised samples

ID	$\varepsilon_{ax\text{-}perm}$ (%)
S_REF_cyc_1_F	0.33
S_REF_cyc_2_F	0.32
C_MIX_31cyc_F	0.28
C_MIX_37cyc_F	0.33
C_MIX_38cyc_F	0.31

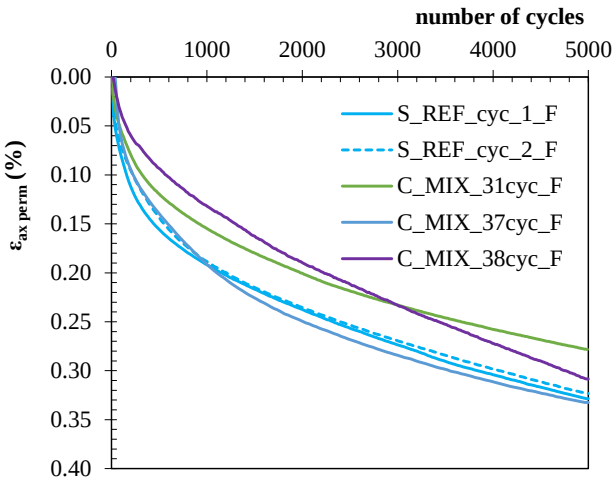

Figure 8.22: Evolution of permanent axial strain during the cyclic stage of the UCS cyclic control tests for fibre-reinforced stabilised samples

8.3.2.3 Post-cyclic Isotropic Compression triaxial tests (CIC_{pc})

The analysis of the results of the isotropic compression tests of fibre-reinforced stabilised samples carried out immediately after the cyclic loading is described in this section. Table 8.21 summarises the results obtained, and Figure 8.23 shows the evolution of the volumetric strain with the logarithm of the mean effective stress (ε_{vol}-log p'). As it may be seen, the evolution of the volumetric strain is characterised by a low compressibility up to the yield stress (pre-σ'_y), followed by high compressibility once the yield stress is exceeded (post- σ'_y), behaviour that is in agreement with the observations made for the previous CIC tests (e.g., section 8.2.2.3). The point of transition between the two behaviours is defined as the yield stress (σ'_y or p'_y, represented by a square in Figure 8.23), corresponding to the moment from which the breakage of cementitious bonds intensifies (start of destructuration).

Analysing the yield stress of both loading conditions for fibre-reinforced stabilised samples, monotonic (Table 8.15 and Figure 8.16, $\sigma'_y \approx 505$ kPa) with the post-cyclic loading ($\sigma'_y \approx 594$ kPa), it is observed that the cyclic loading induces the increase of the yield stress of the fibre-reinforced stabilised samples. This effect may be explained by the fact that the breakage of cementitious bonds happened during the cyclic loading stage allows an earlier mobilisation of the

fibres as the CIC_{pc} tests evolve, i.e., the fibres may absorb and redistribute part of the stresses within the cementitious matrix, contributing to the increase of the yield stress of the composite material. This is in contradiction with the observations made for the unreinforced stabilised material (section 8.2.2.3), pointing out the relative importance of the fibres under cyclic loading condition.

Table 8.21: Post-cyclic isotropic compression triaxial tests (CIC_{pc}) results and yield locus for reinforced stabilised samples

Mix No.	ID	$p'_y = \sigma'_y$ (kPa)
31	CICpc_1_F	**589.5**
38	CICpc_2_F	**598**

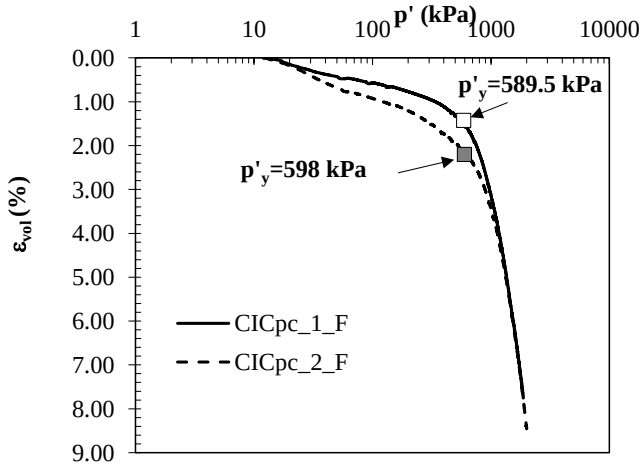

Figure 8.23: Compression curves from CIC_{pc} tests performed on reinforced stabilised samples and yield locus

8.3.2.4 Post-cyclic Isotropically consolidated undrained triaxial test (CIU_{pc})

Figure 8.24 and Table 8.22 summarise the main results of CIU_{pc} triaxial test performed on the fibre-reinforced stabilised sample submitted to a prior cyclic loading test. Figure 8.24 depicts the evolution of the deviatoric stress (q), the excess pore pressure (Δu) and the secant undrained stiffness modulus ($E_{u\text{-}sec}$) with axial strain (ε_a).

The results of the CIU_{pc} triaxial test follow a similar trend as described in section 8.3.1.3, with a few new features that must be stressed out.

Regarding the yield stress, it may be seen that the yielding of the fibre-reinforced stabilised samples submitted to a prior cyclic loading occurs for higher stresses than those observed for the samples not submitted to a prior cyclic loading (Table 8.16, section 8.3.1.3). Although the cementitious matrix of the composite material may be weakened by the physical presence of the

fibres that tends to hinder/prevent the development of some cementitious bonds (as described in section 8.3.1.3), such effect becomes less important when there is a previous cyclic loading stage. Indeed, the breakage of cementitious bonds that occurred during the cyclic loading stage allows as earlier mobilisation of the fibres as the CIU_{pc} test evolves, i.e., the fibres contribute to increase the yield stress of the composite material submitted to a prior cyclic loading. This observation is in contradiction with the results for the unreinforced stabilised material (section 8.2.2.4) where it was observed a negative impact of the cyclic loading on the mechanical behaviour, highlighting the relative importance of the fibres under cyclic loading condition.

The beginning of destructuration, or yield locus, corresponds to a discontinuity in the stress-strain behaviour of the composite material which can be identified in the tangent undrained stiffness modulus ($E_{u\,tan}$) versus axial strain (ε_a) bi-log plot, Figure 8.25, where the yield point is identified by a red square.

In terms of the maximum deviatoric stress (failure/rupture, q_{max}), it may be seen that the failure/rupture for the fibre-reinforced sample submitted to a prior cyclic loading occurs for higher values than in the monotonic case (Table 8.11). This behaviour is explained by two contradictory effects: by one hand the physical presence of the fibres tends to hinder/prevent the development of some cementitious bonds inducing a less stiff and resistant composite material. On the other hand, as the CIU_{pc} tests evolves (increase of axial strains) there is a gradual mobilisation of the tensile strength of the fibres, effect that is potentiated by the fact that the breakage of cementitious bonds that occurred during the cyclic loading stage allows as earlier mobilisation of the fibres, contributing to the increase of the strength of the composite material. The analysis of the results of the fibre-reinforced stabilised materials shows that the effect of the physical presence of the fibres is less important than the effect of the progressive mobilisation of the fibres with the evolution of the deformation.

Table 8.22: Post-cyclic isotropically consolidated undrained (CIU_{pc}) test results and yield locus for fibre-reinforced stabilised samples

Mix No	**ID**	q_{max} (kPa)	ε_r (%)	Yield Criteria for Undrained Tests			
				$E_{u\,tan}$ (MPa)	ε_a (%)	q (kPa)	p' (kPa)
38	CIUpc_4_50_F	857.93	9.13	**75.8**	**0.59**	547.7	182.80

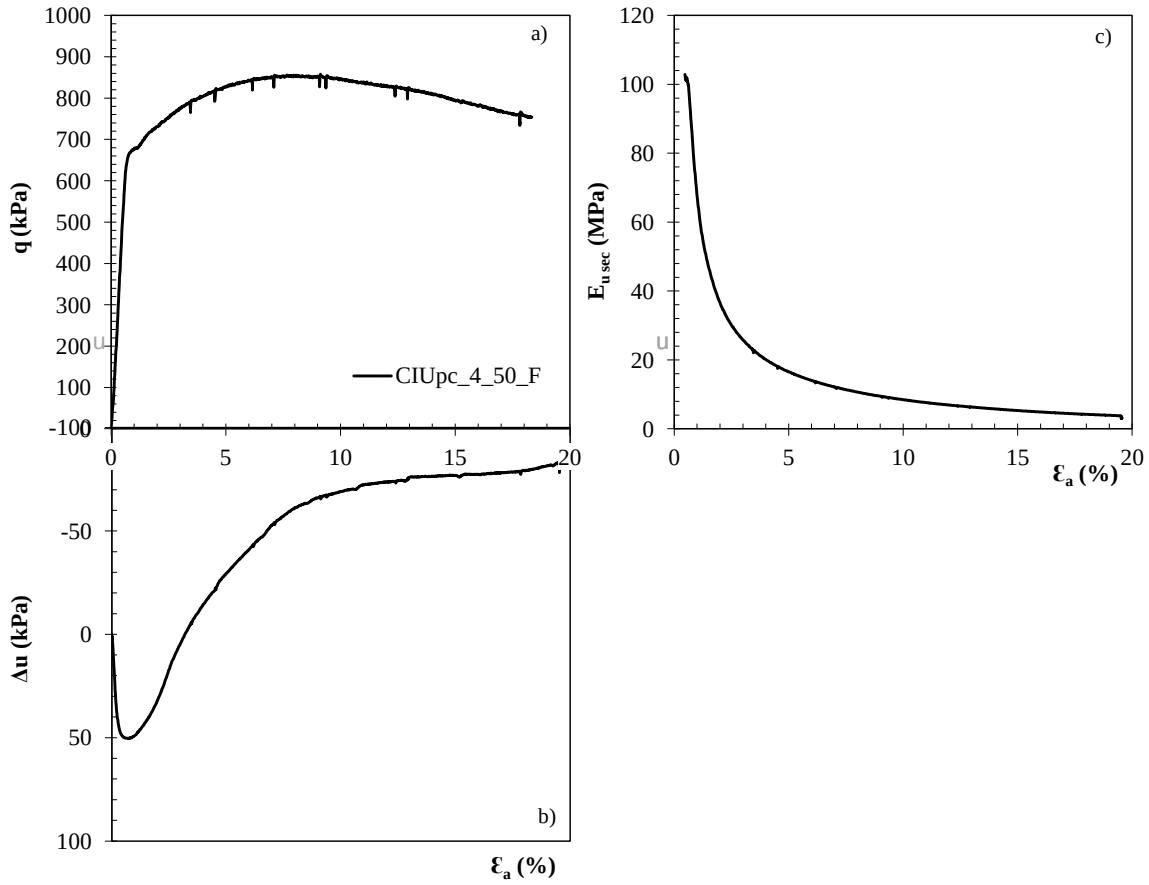

Figure 8.24: Results of CIU_{pc} test for fibre-reinforced stabilised samples: a) stress-strain plot; b) excess of pore pressure vs axial strain; c) $E_{u\text{-}sec}$ vs axial strain

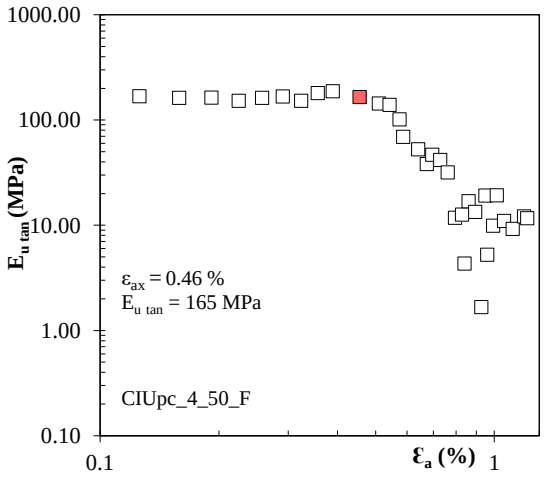

Figure 8.25: Evolution of $E_{u\text{-}tan}$ vs axial strain for CIU_{pc} tests for fibre-reinforced stabilised samples and yield locus

8.3.2.5 Post-cyclic Isotropically consolidated drained triaxial tests (CID_{pc})

Table 8.23 and Figure 8.26 presents the main results of the CID_{pc} triaxial tests performed with fibre-reinforced stabilised samples previously submitted to a cyclic loading test, under three different effective confining stresses (50, 200 and 350 kPa). The evolution of the deviatoric stress (q), the axial (ε_a) and volumetric strains (ε_{vol}) with the mean effective stress (p'), and finally the stress ratio (q/p') versus strain ratio ($\delta\varepsilon_{vol}/\delta\varepsilon_s$) for all CID_{pc} triaxial tests are presented in Figure 8.26.

In a similar way as it was observed for the CIU_{pc} triaxial tests, also in the case of CID_{pc} triaxial tests the results follow the same pattern as described for the monotonic loading condition (section 8.3.1.4) with a few features that must be highlighted:

i) in general, the maximum deviatoric stress (failure/rupture, q_{max}) is higher than the one observed for the corresponding monotonic tests (Table 8.17), independently of the effective confining stress. As stated before, this effect is due to the breakage of some cementitious bonds occurred during the cyclic loading stage, which allows an earlier and progressive mobilisation of the tensile strength of the fibres. The fibres have the ability to absorb and redistribute part of the stresses induced by the external load, mobilising other regions of the cementitious matrix and, therefore, contributing to the strength increase. Moreover, the failure/rupture occurs at a strain level compatible with an effective mobilisation of the fibres. Finally, the progressive mobilisation of the fibres is also responsible for a more ductile behaviour exhibit by the samples (Figure 8.26a).

ii) the yielding of the fibre-reinforced stabilised samples submitted to a prior cyclic loading occurs for higher stresses than those observed for the samples submitted to monotonic loading (Table 8.17, section 8.3.1.4). As it was stated for the CIU_{pc} test, for the post-cyclic CID triaxial tests it is observed that the effect of the physical presence of the fibres assumes a relative lower importance when compared with the effect of fibres mobilisation, i.e., the breakage of cementitious bonds that occurred during the cyclic loading stage allows as earlier mobilisation of the fibres as the CID_{pc} tests evolve, i.e., the fibres contribute to increase the yield stress of the composite material submitted to a prior cyclic loading. This observation is in contradiction with the results for the unreinforced stabilised material (section 8.2.2.5) where a negative impact of the cyclic loading on the mechanical behaviour of the unreinforced stabilised material was observed, highlighting the relative importance of the fibres under cyclic loading condition.

As stated before, the yield of the stabilised material is characterised by an abrupt breakage or discontinuity of the cementitious bonds (destructuration), which may be evaluated by three different yield criteria (p' - ε_a), (p' - ε_{vol}) and ($\delta\varepsilon_{vol}/\delta\varepsilon_s$ - q/p'). The yield loci of these three yield

criteria are identified in Figure 8.26 by a circle (p' - ε_a), triangle (p' – ε_{vol}), and diamond ($\delta\varepsilon_{vol}/\delta\varepsilon_s$ - q/p'), corresponding to values are presented in Table 8.23.

Table 8.23: Post-cyclic isotropically consolidated drained (CID_{pc}) test results and yield locus for fibre-reinforced stabilised samples

Mix No	ID	q_{max} (kPa)	ε_r (%)	Yield criteria	Yield Criteria for Drained Tests					
					q (kPa)	p' (kPa)	ε_a (%)	ε_{vol} (%)	$\delta\varepsilon_{vol}/\delta\varepsilon_s$ (-)	q/p' (-)
34	CIDpc_5_50_F	873.27	2.64	**(p' - ε_a)**	557.95	**235.86**	**0.75**	-	-	-
				(p' - ε_{vol})	592.20	**247.50**	-	**0.53**	-	-
				($\delta\varepsilon_{vol}/\delta\varepsilon_s$) - (q/p')	588.36	246.00	-	-	**0.57**	**2.39**
38c	CIDpc_6_50_F	869.40	1.67	**(p' - ε_a)**	593.30	**247.00**	**0.62**	-	-	-
				(p' - ε_{vol})	588.30	**246.10**	-	**0.41**	-	-
				($\delta\varepsilon_{vol}/\delta\varepsilon_s$) - (q/p')	508.00	219.00	-	-	**0.76**	**2.32**
37a	CIDpc_7_200_F	1262.69	7.4	**(p' - ε_a)**	638.5	**412.78**	**0.87**	-	-	-
				(p' - ε_{vol})	652.4	**417.5**	-	**0.69**	-	-
				($\delta\varepsilon_{vol}/\delta\varepsilon_s$) - (q/p')	654.6	418.45	-	-	**0.93**	**1.56**
31	CIDpc_8_200_F	1182.60	8.14	**(p' - ε_a)**	640.6	**413.5**	**1.15**	-	-	-
				(p' - ε_{vol})	651.9	**416.91**	-	**0.7**	-	-
				($\delta\varepsilon_{vol}/\delta\varepsilon_s$) - (q/p')	654.8	417.98	-	-	**0.87**	**1.56**
37b	CIDpc_9_350_F	1427.02	12.89	**(p' - ε_a)**	535.59	**529.03**	**0.39**	-	-	-
				(p' - ε_{vol})	553.69	**534.55**	-	**0.36**	-	-
				($\delta\varepsilon_{vol}/\delta\varepsilon_s$) - (q/p')	559.73	536.82	-	-	**1.16**	**1.04**

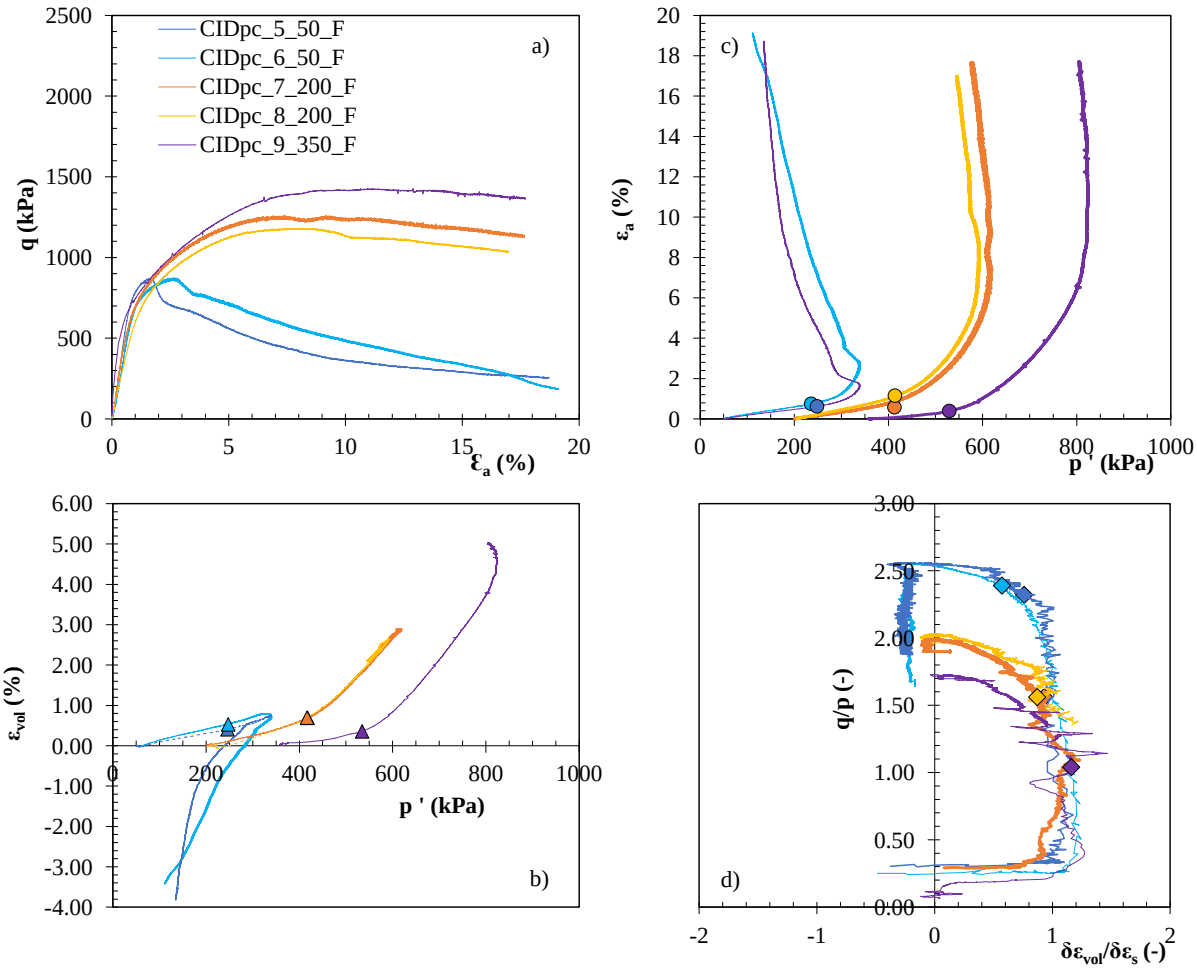

Figure 8.26: Results of the CID_{pc} tests performed on fibre-reinforced stabilised samples: a) stress-strain plot; b) volumetric strain vs p'; c) axial strain vs mean effective stress, p'; d) strain ratio vs stress ratio

8.3.2.6 Yield surface of the stabilised soft soil reinforced with fibres under cyclic loading condition

Figure 8.27 presents the stress path of all post-cyclic triaxial tests performed as well as the corresponding yield points, defined by the criteria showed previously, allowing the definition of the most probable yield surface of the fibre-reinforced stabilised material when submitted to a prior cyclic loading stage. It is possible to see from the figure that there is a good correlation among the different yield criteria. In order to allow a better comparison, the two yield surfaces for stabilised fibre-reinforced materials are compared (monotonic and cyclic loading). From the analysis of the figure it is possible to see that they are homothetic, with the yield surface of the cyclic loading lying outside that of monotonic loading. Although the fibres can reduce the development of cementitious bonds, it is confirmed that the presence of fibres in samples subjected to a prior cyclic loading plays a less relevant role. Indeed, the effect of the progressive mobilisation of the fibres with the evolution of the deformation contributes to increase the yield stress of the composite material submitted to a prior cyclic loading.

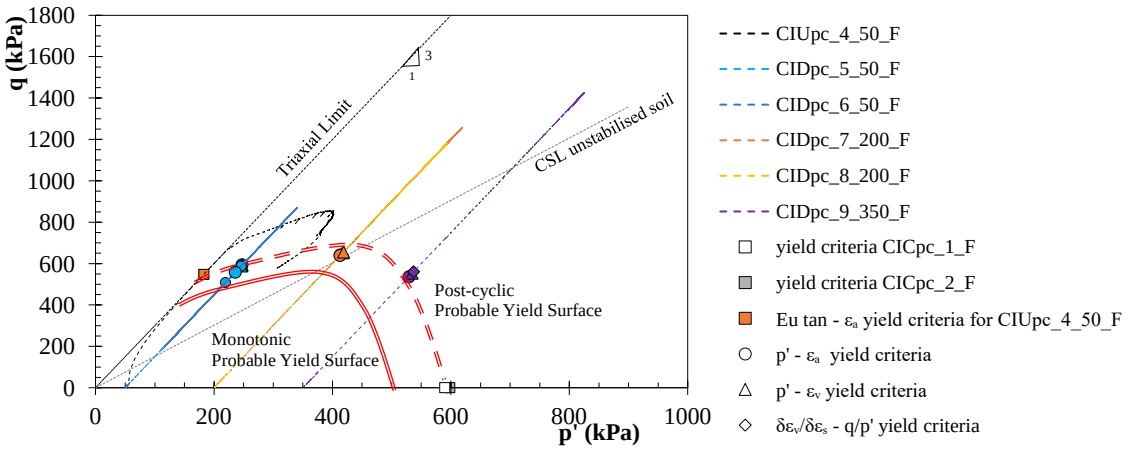

Figure 8.27: Effective stress path and yield loci of triaxial tests performed on fibre-reinforced stabilised samples and possible yield surface

Another observation is that as stated in the section 8.3.1.5 the effective stress paths of the triaxial tests at large strains level do not achieve the critical state line (CSL) of the unstabilised soil, evolving into a line that is slightly above this one (CSL). Once again, this behaviour may be caused by the mobilisation of the fibres as the strains evolve, which makes the material stronger than it would be without being reinforced. That is, the fibre-reinforced stabilised material seems to evolve to a new CSL corresponding to the fibre-reinforced unstabilised material (unfortunately this new CSL was not yet defined for the Baixo Mondego soft soil).

8.4 Global analysis of the yield surfaces

Figure 8.28 presents the most probable yield surfaces for all stabilised materials (unreinforced and fibre-reinforced) and loading conditions studied (monotonic/static and cyclic).

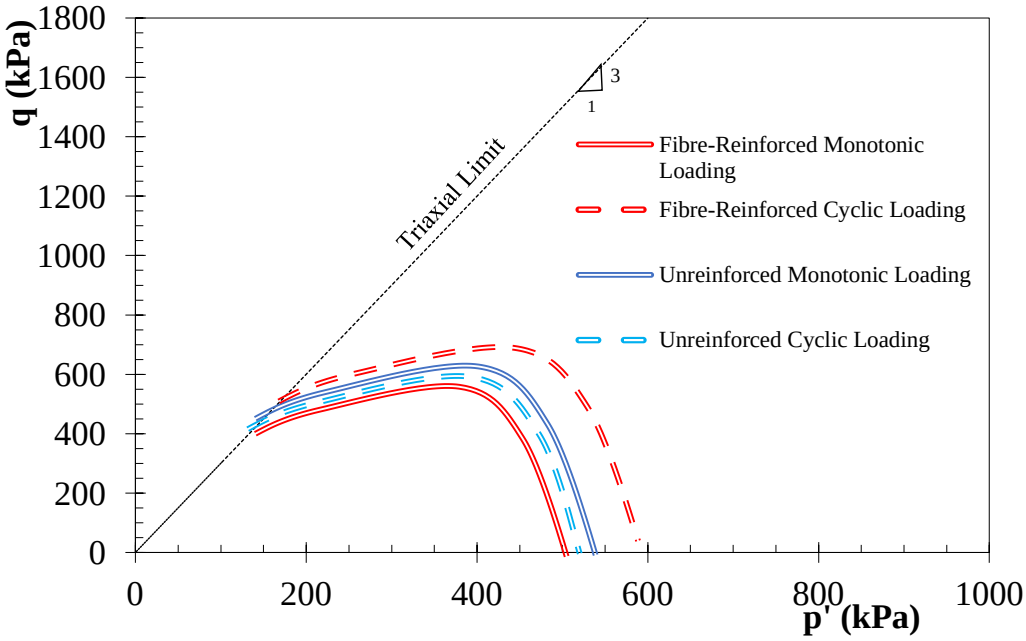

Figure 8.28: Possible yield surfaces for all stabilised materials unreinforced and fibre-reinforced stabilised samples under monotonic and cyclic loading conditions

In general, the yield surfaces exhibit a homothetic shape, varying only in size. For the unreinforced stabilized the cyclic loading induces a degradation of the stabilized matrix (generating a lower stiff material) and as a result the yielding occurs earlier or for lower stresses. For the fibre-reinforced stabilised material, on one hand, the physical presence of the fibres prevents some cementations bonds of the composite matrix of the material, with an earlier yielding. However, after cyclic loading the fibres seem to be mobilised earlier, allowing a redistribution of stresses within the material which is reflected in a later yielding (or occurring for higher stresses).

Finally, the yield surfaces now defined can be introduced in constitutive models of stabilised soils to improve the analysis of geotechnical structures involving these composite materials.

CHAPTER 9 – CONCLUDING REMARKS AND FUTURE WORKS

9.1 Main Conclusions

As stated at the beginning of the thesis, the main motivation of this work was to improve the understanding of the mechanical behaviour of chemically stabilised soft soils, that are reinforced or not with polypropylene fibres, under monotonic and cyclic loading. Through an extensive laboratory test programme, it was possible to achieve most of the objectives initially defined. The main conclusions of the work can be summarised as followed:

- An analysis of the state-of-the-art literature confirms that knowledge relating to the mechanical behaviour of stabilised soft soils reinforced with fibres under cyclic loading is still scarce and sometimes the results published are contradictory, justifying the present scientific research.
- The stress-strain behaviour of the chemically stabilised Baixo Mondego soft soil depends on the curing conditions, namely the curing time, the vertical effective stress applied to the samples and whether the curing occurred under water or not. It was observed that increases in curing time and in the vertical effective stress promote the improvement of the mechanical characteristics of the stabilised material. It was also noted that for shorter curing times (7 days) the curing of the samples under water (submerged condition) is detrimental while for longer curing times (28 days) the opposite was observed. This beneficial effect for longer curing times is independent of the presence of the fibres, and seems to be related to the "free access" to water (submerged condition) that allows the development of more cementitious reactions, producing a stronger and stiffer solid skeleton.
- It was verified that there are sustainable alternatives to reduce the use of Portland cement for the chemical stabilisation of the soft soil. The results showed that the partial substitution of Portland cement by eggshell powder is beneficial in terms of mechanical behaviour, while contributing to a reduction in the environmental footprint associated with

Portland cement. However, eggshell does not exist in powder form, requiring energy and mechanical actions (ball mill) to obtain it, which may compromise its environmental role. Thus, it was concluded that more studies are needed before it can be claimed that eggshell corresponds to an effective sustainable solution.

- In terms of tensile behaviour, it was noted that the tensile strength depends on the type of failure mechanism imposed by each test. It was observed that for the unreinforced stabilised samples, the tensile behaviour is strongly linked with the cementitious bonds. However, when fibres are added to the stabilised soft soil the tensile behaviour depends on the type of failure mechanism imposed by each test. For example, during the DTS test, there is a mobilisation of the tensile strength of the fibres that cross the "horizontal" failure plane at the beginning of the test. A similar effect occurs for the STS test, characterised by a vertical crack/failure plane, allowing a more effective mobilisation of the tensile strength of the fibres that cross this failure plane. However, for the FS test the fact that only half of the fibres present in the vertical cross-section at mid-span are mobilised (the fibres on the tensioned side), leads to a decrease of the flexural/bending load-bearing capacity. It seems that the mobilisation of half the fibres in the FS test does not compensate for the fact that the physical presence of the fibres prevents the development of some cementitious bonds within the composite matrix, producing a composite material with lower strength and stiffness.

- In terms of the addition of fibres, it was found that the presence of the fibres in a stabilised matrix modifies the mechanical behaviour from brittle to ductile, reduces the peak-strength loss and confers a non-negligible residual strength. Such detrimental effects seem to be explained by the fact that the physical presence of the fibres prevents the development of some cementitious bonds within the composite matrix, producing a composite material with lower strength and stiffness. However, as the strain evolves the fibres are progressively mobilised minimising the post-peak strength loss and thus producing the ductile behaviour of the composite material. The value of the residual strength depends on the fibres' characteristics (tensile strength, surface roughness, length), the quantity of fibres and failure mechanism imposed.

- The results also showed that the addition of fibres promotes two contradictory effects: the yield occurs earlier due to the fact that the physical presence of the fibres prevents the development of some cementitious bonds, resulting in a less stiff and weaker stabilised matrix; however, as the deformation evolves there is a gradual and progressive

mobilisation of the fibres' tensile strength allowing an improvement in the peak strength, as was demonstrated by the results of the triaxial tests.

- In order to improve knowledge about the effects of cyclic loading, several parameters of the cyclic loading were studied. Independently of the number of loading cycles, frequency, level of stress and amplitude, it was observed that the permanent deformations show a sharp increase at the beginning of the cyclic stage followed by a decrease in the strain rate for unreinforced and fibre-reinforced samples. While the addition of fibres promotes a reduction in the permanent axial strains for the UCS cyclic tests, the opposite effect was observed for the STS cyclic tests, explained by the different failure mechanisms associated with each test.

- Regarding the post-cyclic mechanical behaviour, it was observed that: i) the increase in the number of loading cycles originates an increase in the permanent deformations, leading to greater strengths/stiffness in the post-cyclic tests; ii) as the frequency decreases the composite material becomes stronger and stiffer than the reference values, i.e., it exhibits greater permanent deformations and higher strength; iii) for levels of stress and amplitudes of up to 50% of the maximum strength/load, the samples exhibit lower permanent deformations but become stronger and stiffer than the reference values (monotonic tests). These observations are valid for both stabilised materials (unreinforced and fibre-reinforced). Such behaviours may be explained by three possible effects: suction effects due to the samples drying during the cyclic stage that may induce higher strength/load; the permanent deformation occurring during the cyclic stage is high enough to have some well-defined rougher cracks, which may induce an apparent coarser grain size thus leading to a greater strength/load; the effect of the progressive mobilisation of the fibres during the cyclic stage that may result in a greater strength/load.

- In terms of the compressibility of both stabilised materials, unreinforced and fibre-reinforced, under static/monotonic and cyclic loading conditions, it was observed that the behaviour is characterised by a high yield stress and a low compressibility up to the yield stress as a direct consequence of the cementitious bonds established between the solid particles, giving the stabilised material a high strength and stiffness, i.e., a reduced compressibility. After the yield stress (post-yield behaviour), the behaviour is characterised by high compressibility due to the abrupt breakage of cementitious bonds (destructuring). The cyclic loading did not change the compressibility indices, but the yield stress was now higher, explained by the deformations that occurred during the cyclic stage, which induced a lower initial void ratio in the sample.

- For the unreinforced stabilised material, it was observed that the application of a cyclic load caused an earlier yielding because the deformations occurring during the cyclic loading promote a degradation of the cementitious matrix. It was also observed that the post-cyclic maximum strength increases, which may be partly explained by the fact that the breakage of the cementitious bonds, occurring during the cyclic loading, may induce an apparent coarser grain size along the failure plane, resulting in the mobilisation of a higher frictional strength at rupture/failure. On the other hand, when the stabilised material is reinforced with polypropylene fibres, it was observed that the yielding occurs earlier because the physical presence of the fibres prevents the development of cementitious bonds, resulting in a less rigid cementitious matrix. However, the deformations that occur during the cyclic loading stage allow an earlier mobilisation of the fibres, which induces that later yielding. With the evolution of the deformations, the fibres are gradually mobilised which contributes to the increase in the peak strength.
- For both stabilised materials (unreinforced and fibre-reinforced) and for both loading conditions studied (monotonic/static and cyclic), it was observed that the yield surfaces exhibit a homothetic shape, varying only in size. Thus, the yield surface of a specific stabilised soil, reinforced or not with fibres, under monotonic or cyclic loads, can be defined by carrying out triaxial tests and later introduced in constitutive models to improve the analysis of any geotechnical structures involving these composite materials.

Despite, the natural differences between the Baixo Mondego and the Magallanes soft soils, as described in Chapter 2, there are sufficient similarities between them that allow to the author of the present Thesis to say that the main conclusions obtained from his experimental study, developed with the Baixo Mondego soft soil, can be extrapolated, with caution, to the Magallanes soft soils.

9.2 Prospects for future research work

Notwithstanding, the results and conclusions presented, some questions about the behaviour of the composite material under analysis still need to be studied. In order to complete this research, some future studies are proposed to broaden the knowledge about the subject under analysis, such as:

- To chemically stabilise different soils making use of sustainable binders (e.g., eggshell powder, fly ashes).

- To study the effect of different fibres, varying in nature, length, roughness and tensile characteristics, such as, as coir, cotton, wool sheep, among others. The effect of the fibre content should also be investigated.
- To quantify the suction of the samples and to assess its effect on the stress-strain-shear strength behaviour of the composite materials.
- To study the practical feasibility of the chemical stabilisation technique with the addition of polypropylene fibres in the field and to compare the results with those obtained in the laboratory.
- Concerning the stress-strain-shear strength behaviour, it is necessary to go deeper in terms of the laboratory testing by using internal measurement to allow a better definition of the yield locus. Also using bender elements to compare the elastic parameters with the Pulse velocity results.
- To study the microstructure of the stabilised material, unreinforced and fibre-reinforced, by Scanning Electron Microscopy (SEM) and Energy Dispersive X-ray Spectroscopy EDS tests.

REFERENCES

Anunciação, G. (2020). *Análise do comportamento mecânico de um solo arenoso estabilizado e reforçado com fibras sob influência de carregamentos monotónicos e cíclico*. MSc. Dissertation, Universidade de Coimbra.

Abtahi, M., Okhovat, N., Pourhosseini, R. and Hejazi, M. (2010). *Improvement of soil strength by natural fibers*. From res to des Europ prac, Bratislava, Slovak Republic.

Abuel-Naga, H., Bergado, D. and Chaiprakaikeow, S. (2006). *Innovative thermal technique for enhancing the performance of prefabricated vertical drain during the preloading process.* Geotextiles and Geomembranes, **24** (6), pp. 359-370.

Agboola, O., Sadiku, E. R., Popoola, P., Fayomi, O. S. I., Ayeni, A. O., Dick, D. T., Adegbola, A. T., Moropeng, L. & Ramakhokhovhu, M. (2021). Surface roughness of ternary blends: Polypropylene/chitosan/sisal fiber membranes. Materials Today: Proceedings, **38** pp. 2342-2346.

Aguiar, A. (1992). *Caracterização geotécnica de solos moles de Portugal: uma contribuição*. Universidade Nova de Lisboa, Lisboa.

Ahmed, A. and Naggar, M. H. (2018). *Effect of cyclic loading on the compressive strength of soil stabilized with bassanite–tire mixture.* Journal of Material Cycles and Waste Management, **20** (1), pp. 525-532.

Åhnberg, H. (2006). *Strength of stabilised soil-A laboratory study on clays and organic soils stabilised with different types of binder*. Ph.D. Thesis, Lund University.

Åhnberg, H., Johansson, S., Retelius, A., Ljungkrantz, C., Holmqvist, L. and Holm, G. (1995). *Cement and lime for deep stabilisation of soil.* Stabilization of Organic Soils by Cement and Puzzolanic Reactions, 48th Report of Swedish Geotechnical Institute.

Åhnberg, H., Johansson, S.-E., Pihl, H. and Carlsson, T. (2003). *Stabilising effects of different binders in some Swedish soils.* Proceedings of the Institution of Civil Engineers-Ground Improvement, **7** (1), pp. 9-23.

Al-Akhras, N., Attom, M., Al-Akhras, K. and Malkawi, A. (2008). *Influence of fibers on swelling properties of clayey soil.* Geosynthetics International, **15** (4), pp. 304-309.

Ali, F. H., Adnan, A. and Choy, C. K. (1992). *Geotechnical properties of a chemically stabilized soil from Malaysia with rice husk ash as an additive.* Geotechnical and Geological Engineering, **10** (2), pp. 117-134.

Ang, E. C. and Loehr, J. E. (2003). *Specimen size effects for fiber-reinforced silty clay in unconfined compression.* Geotechnical Testing Journal, **26** (2), pp. 191-200.

ASTM-2435-02 (2003). *One-Dimensional Consolidation Properties of Soils.* American Society for Testing and Materials.

ASTM-2845-05 (2000). *Standard Test Method for Laboratory Determination of Pulse Velocities and Ultrasonic Elastic Constants of Rock.* American Society for Testing and Materials.

ASTM-C168 (1997). *Standard Terminology Relating to Thermal Insulating Materials*. American Society for Testing and Materials.

ASTM-CRD-C-164 (1992). *Standard Test Method for Direct Tensile Strength of Cylindrical Concrete or Mortar Specimens.* American Society for Testing and Materials.

ASTM-D2166 (2000). *Method for Unconfined Compressive Strength of Cohesive Soil.* American Society for Testing and Materials.

ASTM-D2487 (2017). *Standard Practice for Classification of Soils for Engineering.* American Society for Testing and Materials.

Atkinson, J., Richardson, D. and Stallebrass, S. (1990). *Effect of recent stress history on the stiffness of overconsolidated soil.* Géotechnique, **40** (4), pp. 531-540.

AustroUmag (2018). *Estudios de Mecánica de Suelos de Diversos Sitios de Punta Arenas.* Laboratory report. Universidad de Magallanes.

Axelsson, K., Johansson, S.-E. and Andersson, R. (2002). *Stabilization of organic soils by cement and Puzzolanic reactions–feasibility study.* Swedish Deep Stabilization Research Centre, Report, 3 pp. 1-51.

Babasaki, R. (1997). *Japanese Geotechnical Society technical committee report-Factors influencing the strength of improved soil.* Proceedings of the Proc. 2nd Int. Conf. Ground Improvement Geosystems-Grouting and Deep Mixing-, 1997 Balkema.

Baracos, A., Graham, J. and Domaschuk, L. (1980). *Yielding and rupture in a lacustrine clay.* Canadian Geotechnical Journal, **17** (4), pp. 559-573.

Bishop, A. & Wesley, L. (1975). *A hydraulic triaxial apparatus for controlled stress path testing.* Geotechnique, **25** (4), pp. 657-670.

Biswas, S., Ahsan, Q., Cenna, A., Hasan, M. and Hassan, A. (2013). *Physical and mechanical properties of jute, bamboo and coir natural fiber.* Fibers and Polymers, **14** (10), pp. 1762-1767.

Bonito, F. A. B. (2008). *Reologia dos lodos e de outros sedimentos recentes da Ria de Aveiro*. Ph.D. Thesis, Departamento de Engenharia Civil - University of Aveiro.

Brenner, P., Nutalaya, P., Chilingarian, G. V. & Robertson jr, J. O. (1981) *Engineering geology of soft clay.* Developments in Geotechnical Engineering,20, pp. 157-238.

BS-1377-5 (1990). *Methods of test for soils for civil engineering purposes – part 5: compressibility, permeability and durability tests.* British Standards Institution, London.

BS-1377-7 (1990). *Methods of test for soils for civil engineering purposes – part 7: Shear strength tests (total stress).* British Standards Institution, London.

BS-1377-8 (1990). *Methods of test for soils for civil engineering purposes – part 8: shear strength tests (effective stress).* British Standards Institution, London

BS-1881-203 (1986). *Testing concrete - Recommendations for measurement of velocity of ultrasonic pulses in concrete.* British Standards Institution, London

BS-EN14679 (2006). *Execution of Special Geotechnical Works Deep Mixing.* British Standards Institution, London

Cai, Y., Shi, B., Gao, W., Chen, F.-J. and Tang, C.-S. (2006). *Experimental study on engineering properties of fibre-lime treated soils.* Chinese Journal of Geotechnical Engineering, **28** (10), pp. 1283-1287.

Cajada, J. (2017). *Chemical Stabilization of Different Soils with Addition of Polypropylene Fibers,* MSc. Dissertation, University of Coimbra.

Carlsten, P. and Ekstrom, J. (1997). *Lime and Lime Cement Columns - Guide for Project Planning, Construction and Inspection*. Swedish Geotechnical Society, Report, 4 pp. 95.

Carneiro, F. (1943). *A new method to determine the tensile strength of concrete.* In Proceedings of the Proceedings of the 5th meeting of the Brazilian Association for Technical Rules, Vol. 3, pp. 126-129.

Carrasco, R. (2014) *Proyecto: Construcción 50 Viviendas, Barranco Amarillo, Punta Arenas, Región De Magallanes Y Antártica Chilena*. Technical reports.

Carvalho, A. G. & Carvalho, G. S. (2005) *Geologia sedimentar*. Âncora Editora

Carvalho, R., Fangueiro, R. & Neves, J. (2014) Durability of Natural Fibers for Geotechnical Engineering. In: Key Engineering Materials, December 2014, **634**, pp. 447–454.

Casagrande, M. D. T. (2001). Estudo do comportamento de um solo reforçado com fibras de polipropileno visando o uso como base de fundações superficiais. MSc. Dissertation, University of Rio Grande do Sul.

Chai, K. Onitsuka, and S. Hayashi (2006) *Physical modelling of consolidation behaviour of a composite foundation consisting of a cement-mixed soil column and untreated soft marine clay.* Geotechnique, **56** (8), pp. 579-582.

Chaudhary, A. K., Gope, P. C. and Singh, V. K. (2015). *Water absorption and thickness swelling behavior of almond (Prunus amygdalus L.) shell particles and coconut (Cocos nucifera) fiber hybrid epoxy-based biocomposite.* Science Engineering of Composite Materials, **22** (4), pp. 375-382.

Chauhan, M. S., Mittal, S. and Mohanty, B. (2008). *Performance evaluation of silty sand subgrade reinforced with fly ash and fibre.* Geotextiles and Geomembranes, **26** (5), pp. 429-435.

Chew, S., Kamruzzaman, A. and Lee, F. (2004). *Physicochemical and engineering behavior of cement treated clays.* Journal of geotechnical geoenvironmental engineering, **130** (7), pp. 696-706.

Chia, A. V. (2010). *Determinación de los parámetros para el cálculo de los asentamientos del suelo fino denominado mazacote en Punta Arenas.* Bachelor Dissertation, Universidad de Magallanes, Chile.

Chile, Banco Central de (2016) *Documentos de Trabajo (Banco Central de Chile)*, (278), 1.

Coelho, P. (2000) *Caracterização geotécnica de solos moles: estudo do local experimental da Quinta do Foja (Baixo Mondego).* MSc. Dissertation. Universidade de Coimbra.

Consoli, N. C., Bassani, M. A. A., & Festugato, L. (2010). *Effect of fiber-reinforcement on the strength of cemented soils.* Geotextiles and Geomembranes, **28** (4), 344-351.

Consoli, N. C., Casagrande, M. D., Prietto, P. D. and Thomé, A. n. (2003). *Plate load test on fiber-reinforced soil.* Journal of Geotechnical and Geoenvironmental Engineering, **129** (10), pp. 951-955.

Consoli, N., Festugato, L. and Heineck, K. (2009a). *Strain-hardening behaviour of fibre-reinforced sand in view of filament geometry.* Geosynthetics International, **16** (2), pp. 109-115.

Consoli, N. C., Vendruscolo, M. A., Fonini, A. and Dalla Rosa, F. (2009b). *Fiber reinforcement effects on sand considering a wide cementation range.* Geotextiles and Geomembranes, **27** (3), pp. 196-203.

Consoli, N. C., Zortéa, F., de Souza, M. and Festugato, L. (2011). *Studies on the dosage of fiber-reinforced cemented soils.* Journal of Materials in Civil Engineering, **23** (12), pp. 1624-1632.

Coop, M. and Atkinson, J. (1993). *The mechanics of cemented carbonate sands.* Geotechnique, **43** (1), pp. 53-67.

Coop, M. R., & Willson, S. M. (2003). *Behavior of hydrocarbon reservoir sands and sandstones.* Journal of Geotechnical and Geoenvironmental Engineering, **129** (11), 1010-1019

Correia, A. A. S. (2011). *Aplicabilidade da Técnica de Deep Mixing aos Solos Moles do Baixo Mondego.* Ph.D Thesis. Universidade de Coimbra, Coimbra.

Correia, A. A. S., Venda Oliveira, P. J., Teles, J. M. N. P. C. and Pedro, A. M. G. (2017). *Strength of a stabilised soil reinforced with steel fibres.* Proceedings of the Institution of Civil Engineers - Geotechnical Engineering, **170** (4), pp. 312-321.

Correia, A. A., Oliveira, P. J. V. and Custódio, D. G. (2015). *Effect of polypropylene fibres on the compressive and tensile strength of a soft soil, artificially stabilised with binders.* Geotextiles and Geomembranes, **43** (2), pp. 97-106.

Correia, A. A., Venda Oliveira, P. J., Teles, J. M., & Pedro, A. M. (2017). *Strength of a stabilised soil reinforced with steel fibres.* Proceedings of the Institution of Civil Engineers-Geotechnical Engineering, **170** (4), 312-321.

Correia, A.A.S.; Venda Oliveira, P.J. and Lemos, L.J.L., (2015). *Stress-Strain Behavior of a Cement-Based Stabilised Soft Soil*, 6th International Symposium on Deformation Characteristics of Geomaterials, Buenos Aires, Argentina, pp. 963-969.

Coutinho (1988). *Fabrico e propriedades do betão,* Vol. 1, 2ª edição, LNEC, Lisboa, p. 401.

Cristelo, N., Cunha, V. M., Dias, M., Gomes, A. T., Miranda, T., & Araújo, N. (2015). *Influence of discrete fibre reinforcement on the uniaxial compression response and seismic wave velocity of a cement-stabilised sandy-clay.* Geotextiles and Geomembranes, **43** (1), 1-13.

Cruz, R. (2008). *Influecia de parámetros fundamentais na rigidez, resistencia e dilatancia de una areia artificialmente cimentada.* UFRGS, Porto Alegre, Brasil.

Cuccovillo, T. and Coop, M. (1999). *On the mechanics of structured sands.* Géotechnique, **49** (6), pp. 741-760.

Custódio, D. G. (2013). *Mechanical Behaviour of a Stabilized Soft Soil with Polypropylene Fibres*. MSc Dissertation, Universidade de Coimbra, Portugal.

da Fonseca, A. V., Rios, S., Amaral, M. and Panico, F. (2013). *Fatigue cyclic tests on artificially cemented soil*. Geotechnical Testing Journal, **36** (2), pp. 227-235.

Dall'Aqua, G. P., Ghataora, G. and Ling, U. (2010). *Behaviour of fibre-reinforced and stabilized clayey soils subjected to cyclic loading.* Studia Geotechnica et Mechanica, **32** pp. 3-16.

Donoso, P. (2006). *Caracterización Geotécnica y Geomecánica del Suelo Fino de Punta Arenas denominado Mazacote.* Bachelor dissertation, Universidad de Magallanes, Chile

Duong, N.T., Satomi, T., & Takahashi, H. (2021). *Potential of corn husk fiber for reinforcing cemented soil with high water content*. Construction and Building Materials, 271, 121848.

EN 14679 2005. *Execution of special geotechnical works – deep mixing.* CEN, English version, April of 2005, p. 52.

E196 (1966). *Solos – Análise granulométrica*. Especificação do LNEC, Lisboa, Portugal.

E197 (1966). *Solos – Ensaio de compactação*. Especificação do LNEC, Lisboa, Portugal.

E201 (1967). *Solos - Determinação do teor em matéria orgânica.* Especificação do LNEC, Lisboa, Portugal.

E378 (1993). *Betões. Guia para a utilização de ligantes hidráulicos.* Especificação do LNEC, Lisboa, Portugal.

Edil, T. and Staab, D. (2005). *Practitioner's guide for deep-mixed stabilization of organic soils and peat.* Final Report, The National Deep Mixing Research Program, Project Number NDM302, pp. 60.

Egeli, I. (1980). *Pore pressures and volume changes in undrained unsaturated clays*. Ph.D. Thesis. Imperial College of London, UK.

Estabragh, A., Namdar, P. and Javadi, A. (2012). *Behavior of cement-stabilized clay reinforced with nylon fiber*. Geosynthetics International, **19** (1), pp. 85-92.

Esteves, E. (2014). *Aluviões Silto-Argilosos Moles De Portugal.* Ph.D. Thesis. University of Porto, Porto. (in Portuguese).

EuroSoilStab (2002). *Development of design and construction methods to stabilise soft organic soils: Design guide soft soil stabilisation.* Industrial and Materials Technologies Programme (Brite-EuRam III), European Commission, p. 94.

Falorca, I. and Pinto, G. I. (2011). *Effect of short, randomly distributed polypropylene microfibres on shear strength behaviour of soils.* Geosynthetics International, **18** (1), pp. 2-11.

Falorca, I.. (2010). *Solos Reforçados com Micro Fibras Comportamento sob Carregamento Estático e Dinâmico.* Ph.D. Thesis. Universidade da Beira Interior, Portugal.

Festugato, L. F., A.; Consoli, N. C. (2013). *Cyclic shear response of fibre-reinforced cemented paste backfill.* Géotechnique Letters, **3**, pp. 5-12.

Feuerharmel, M. R. (2000). *Comportamento de solos reforçados com fibras de polipropileno.* Ph.D thesis, UFRGS, Brasil.

Folkes, D. J., & Crooks, J. H. A. (1985). *Effective stress paths and yielding in soft clays below embankments.* Canadian Geotechnical Journal, **22** (3), 357-374.

Foppa, D. (2005). *Analysis of key-parameters for the strength control of artificially cemented soils*. Ph.D Thesis, Universidade de Rio Grande do Sul, Brasil.

Frocht, M.M., *Photoelasticity*, Wiley, New York, 2,83 (1948).

Furtado, R. J. A. (1995). *Aterros sobre solos argilosos moles: a doca n°4 do Porto de Leixões - um caso típico.* 5° Encontro Nacional de Geotecnia, **3**, pp. 203-2019.

Gaspard, K., & Mohammad, L. (2002). *Laboratory evaluation of soil modified with cement and fibrillated polypropylene fibers.* Louisiana Transportation Research Center (No. 360). Report.

Gelder, C. and Fowmes, G. (2016). *Mixing and compaction of fibre-and lime-modified cohesive soil.* Proceedings of the Institution of Civil Engineers-Ground Improvement, **169** (2), pp. 98-108.

Gomes, C. F. (1988). Argilas-o que são e para que servem, Fund. Calouste Gulbenkian, Lisboa, Portugal.

Gomes, F. L. & Ladeira, F. L. (1991). *Resistencia ao corte não drenada em aluviões lodosas.* IV Encontro Nacional de Geotecnia, Lisboa, **2** pp. 5.

Gonzalez de Vallejo, L. (2004). *Ingeniería Geológica.* Pearson, Prentice Hall. Madrid.

Gosavi, M. and Patil, K. (2004). Improvement of properties of black cotton soil subgrade through synthetic reinforcement. Journal of the Institution of Engineers (India), Part CV, Civil Engineering Division, **84** pp. 257-262.

Goulart, D. (2019). *Influência do tipo de fibra no comportamento mecânico de um solo arenoso cimentado sob ações estáticas e dinâmicas.* MSc. Dissertation. Universidade de Coimbra.

Gowthaman, S., Nakashima, K. and Kawasaki, S. (2018). *A state-of-the-art review on soil reinforcement technology using natural plant fiber materials: Past findings, present trends, and future directions.* Materials, **11** (4), pp. 553.

Graham, A. (2009). *The Andes: a geological overview from a biological perspective.* Annals of the Missouri Botanical Garden, **96** (3), pp. 371-385.

Graham, J., Crooks, J. A., and Lau, S. K. (1988). *Yield envelopes: identification and geometric properties.* Géotechnique, **38** (1), 125-134.

Graham, J., Noonan, M. and Lew, K. (1983). *Yield states and stress–strain relationships in a natural plastic clay.* Canadian geotechnical journal, **20** (3), pp. 502-516.

Güllü, H. and A., K. (2014). *Effect of freeze-thaw cycles on unconfined compressive strength of fine-grained soil treated with jute fibre, steel fibre and lime.* Cold Regions Science and Technology, 106-107, pp. 55-65.

Head, K. H. (1985). *Manual of soil laboratory testing*. Pentech Press, London, Vol. 1, 2 & 3.

Hejazi, S. M., Sheikhzadeh, M., Abtahi, S. M. and Zadhoush, A. (2012). *A simple review of soil reinforcement by using natural and synthetic fibers.* Construction and Building Materials, **30** pp. 100-116.

Hindle, M. J. (1994). *A study of the compressibility and residual shear strength of a soft soil from Figueira da Foz, Portugal*. MSc Dissertation, School of Engineering, University of Durham.

Hong, S., Yoon, S., Kim, J., Lee, C., Kim, S. & Lee, Y. (2020). *Evaluation of condition of concrete structures using ultrasonic pulse velocity method.* Applied Sciences, **10** (2), pp. 706.

Hoover, J., Moeller, D., Pitt, J., Smith, S. and Wainaina, N. (1982). *Performance of randomly oriented fiber reinforced roadway soils.* Lowa DOT Project-HR-211, Department of Transportation, Highway Division, Lowa State University.

Horpibulsuk, S. (2001). *Analysis and assessment of engineering behavior of cement stabilized clays.* Ph.D. Thesis, Suranaree University of Technology, Thailand.

Huang, J., Chen, J., Lu, Y., Yi, S., Cheng, H., & Cui, L. (2020). *Deformation behaviors and dynamic backbone curve model of saturated soft clay under bidirectional cyclic loading*. International. Journal of Geomechanics, **20** (4), 04020016.

Indraratna, A., Balasubramanian, A. and Khan, M. (1995). *Effect of fly ash with lime and cement on the behavior of a soft clay.* Quarterly Journal of Engineering Geology and Hydrogeology, **28** (2), pp. 131-142.

INE. (2017). *Censo de Población y Vivienda, 2017*. Instituto Nacional de Estadística, Chile.

Ingles, O. G., & Metcalf, J. B. (1972). *Soil stabilization principles and practice.* Transport and Road Research Laboratory. **11**, No. Textbook.

Islam, M. S. and Iwashita, K. (2010) *Earthquake resistance of adobe reinforced by low cost traditional materials.* Journal of Natural Disaster Science, **32** (1), pp. 1-21.

ISO-13320-1 (1999) *Particle Size Analysis – Laser Diffraction Method. Part 1. General Principles.* International Standard Organization.

ISO1920-7 (2004). *Non-destructive test methods for use on hardened concrete*. International Standard Organization.

Jamiolkowski, M., Ladd, C. C., Germaine, J. T. and Lancellotta, R. (1985). *New developments in field and lab testing of soils.* 11th International Conference on Soil Mechanics and Foundation Engineering, **1**, San Francisco, p. 57-154.

Janz, M. and Johansson, S. (2002). *The function of different binding agents in deep stabilization*. 9th Report of Swedish Deep Stabilization Research Centre. Linkoping, Sweden.

JGS 0821 (2000). Practice for making and curing stabilized soil specimens without compaction. Japanese Geotechnical Society.

Jiang, H., Cai, Y. and Liu, J. (2010). *Engineering properties of soils reinforced by short discrete polypropylene fiber.* Journal of Materials in civil Engineering, **22** (12), pp. 1315-1322.

Jordan, M., Meseguer & Quiroz, M. (2008). *Prospección Geológica, Mineralogía y Ceramicidad de las Arcillas Grises de Punta Arenas.* Macla: revista de la Sociedad Española de Mineralogía, (9), 157.

K. G.Ghee (2006). *Constitutive behavior of cement treated marine clay.* Ph.D. Thesis, National University of Singapore, Singapore.

Kalkan, E. (2013). *Preparation of scrap tire rubber fiber–silica fume mixtures for modification of clayey soils.* Applied Clay Science, **80** pp. 117-125.

Kamei, T., Ahmed, A. and El Naggar, M. H. (2018). *Performance of ground improvement projects incorporating sustainable reuse of geo-composite wastes.* Transportation Geotechnics, **14** pp. 22-28.

Kaniraj, S. R. and Havanagi, V. G. (2001). *Behavior of cement-stabilized fiber-reinforced fly ash-soil mixtures.* Journal of geotechnical and geoenvironmental engineering, 1**27** (7), pp. 574-584.

Kempfert, H.-G. and Gebreselassie, B. (2006). *Excavations and foundations in soft soils.* Springer Science and Business Media.

Khattak, M. J. and Alrashidi, M. (2006*). Durability and mechanistic characteristics of fiber reinforced soil–cement mixtures.* International Journal of Pavement Engineering, **7** (1), pp. 53-62.

Kitazume, M. and Terashi, M. (2002). *The deep mixing method principle, design and construction.* Coastal Development Institute of Technology, Balkema, Japan, pp. 4-7.

Kitazume, M., & Terashi, M. (2013). *The deep mixing method* (Vol. 21). London: CRC press.

Kitazume, M., Nakamura, T., Terashi, M. and Ohishi, K. (2003). *Laboratory tests on long-term strength of cement treated soil.* Grouting and ground treatment, pp. 586-597

Kumar, P., and Singh, S. P. (2008). *Fiber-reinforced fly ash subbases in rural roads.* Journal of transportation engineering, **134** (4), 171-180.

Kumar, S. and Tabor, E. (2003). *Strength characteristics of silty clay reinforced with randomly oriented nylon fibers.* Electronic Journal of Geotechnical Engineering, **8** (2), pp. 10.

Kumar, S. S., Krishna, A. M. and Dey, A. (2013). *Parameters influencing dynamic soil properties: a review treatise.* Proceedings of the National conference on recent advances in civil engineering, pp. 1-10.

Lade, P. V. and Overton, D. D. (1989). *Cementation effects in frictional materials.* Journal of Geotechnical Engineering, **115** (10), pp. 1373-1387.

Ladeira, F. K. & Gomes, F. L. (1991). *Estudos geotécnicos na zona de Cacia (Aveiro) e sua importância para o projecto.* IV Encontro Nacional de Geotecnia, Lisboa, **2** pp. 12.

Lee, F.-H., Lee, Y., Chew, S.-H. and Yong, K.-Y. (2005). *Strength and modulus of marine clay-cement mixes.* Journal of geotechnical geoenvironmental engineering, **131** (2), pp. 178-186.

Lemos, L., Correia, A. A. and Oliveira, P. V. (2021). *Comportamento de solos estabilizados quimicamente e reforçados com fibras sob ações monotónicas e cíclicas.* Geotecnia, **(152),** pp. 509-529.

Leroueil, S. and Vaughan, P. (1990). *The general and congruent effects of structure in natural soils and weak rocks.* Géotechnique, **40** (3), pp. 467-488.

Leroueil, S., Magnan, J.-P. & Tavenas, F. (1990). *Embankments on soft clays.* Ellis Horwood, Chichester, UK.

Lindh, P. (2004). *Compaction-and strength properties of stabilised and unstabilised fine-grained tills.* Ph.D Thesis. Structural Mechanics.

Locat, J., Bérubé, M.-A. and Choquette, M. (1990). *Laboratory investigations on the lime stabilization of sensitive clays: shear strength development.* Canadian Geotechnical Journal, **27** (3), pp. 294-304.

Locat, J., Trembaly, H. and Leroueil, S. (1996). *Mechanical and hydraulic behaviour of a soft inorganic clay treated with lime.* Canadian geotechnical journal, **33** (4), pp. 654-669.

Lorenzo, G. A. and Bergado, D. T. (2004). *Fundamental parameters of cement-admixed clay—New approach.* Journal of geotechnical and geoenvironmental engineering, **130** (10), pp. 1042-1050.

Lorenzo, G. A. and Bergado, D. T. (2006). *Fundamental characteristics of cement-admixed clay in deep mixing.* Journal of materials in civil engineering, **18** (2), pp. 161-174.

Lovisa, J., Shukla, S. K. and Sivakugan, N. (2010). *Behaviour of prestressed geotextile-reinforced sand bed supporting a loaded circular footing.* Geotextiles and Geomembranes, **28** (1), pp. 23-32.

Maccarini, M. (1987). Laboratory studies for a weakly bonded artificial soil. Ph. D. Thesis, University of London.

Maher, M. and Ho, Y. (1994). *Mechanical properties of kaolinite/fiber soil composite.* Journal of Geotechnical Engineering, **120** (8), pp. 1381-1393.

Maher, M. H. and Gray, D. H. (1990). *Static response of sands reinforced with randomly distributed fibers.* Journal of Geotechnical Engineering, **116** (11), pp. 1661-1677.

Makusa, G. P. (2013). *Soil stabilization methods and materials in engineering practice: State of the art review.* Report, Luleå University of Technology,

Malandraki, V. and Toll, D. (1996). *The definition of yield for bonded materials.* Geotechnical and Geological Engineering, **14** (1), pp. 67-82.

Malandraki, V. and Toll, D. (2000). *Drained probing triaxial tests on a weakly bonded artificial soil.* Géotechnique, **50** (2), pp. 141-151.

Malandraki, V. and Toll, D. (2001). *Triaxial tests on weakly bonded soil with changes in stress path*. Journal of Geotechnical and Geoenvironmental Engineering, **127** (3), pp. 282-291.

Mamat, R. C. (2013). *Engineering properties of Batu Pahat soft clay stabilized with lime, cement and bentonite for subgrade in road construction.* MSc. Dissertation. Universiti Tun Hussein Onn Malaysia.

Marandi, S., Bagheripour, M., Rahgozar, R. and Zare, H. (2008). *Strength and ductility of randomly distributed palm fibers reinforced silty-sand soils.* American Journal of Applied Sciences, **5** (3), pp. 209-220.

Marcuson III, William F and Jr, C. (1981). *Field and laboratory determination of soil moduli.* Journal of the Geotechnical Engineering Division, **107** (10), pp. 1269-1291.

Marques, R. (1989). *A utilização do pentrómetro estático na avaliação de asssentamentos - a experiencia da consolidação do terrapleno do novo terminal de contentores de Leixões.* Encontro Nacional de Geotecnia, **3** pp. 23-32.

Marreiros, J. M. & Carneiro, J. (1995). *Caracterização geotecnica de materiais aluvionares da margem direita do rio Tejo entre Lisboa e Entroncamento.* V. Encontro Nacional de Geotecnia, Coimbra. **1**, pp. 205-216.

Matos Fernandes, M. (2006). *Mecânica dos Solos: Conceitos e Princípios Fundamentais*. Volume I, FEUP, Porto.

Mattone, R. (2005). *Sisal fibre reinforced soil with cement or cactus pulp in bahareque technique.* Cement and Concrete Composites, **27** (5), pp. 611-616.

Michalowski, R. L. and Zhao, A. (1996). *Failure of fiber-reinforced granular soils.* Journal of geotechnical engineering, **122** (3), pp. 226-234.

Miller, C. J. and Rifai, S. (2004). *Fiber reinforcement for waste containment soil liners.* Journal of Environmental Engineering, **130** (8), pp. 891-895.

Mirzababaei, M., Miraftab, M., Mohamed, M. and McMahon, P. (2013). *Impact of carpet waste fibre addition on swelling properties of compacted clays.* Geotechnical and Geological Engineering, **31** (1), pp. 173-182.

Mitchell, J. K. & Soga, K. (2005). *Fundamentals of soil behavior*. Hoboken, New Jersey, pp. 558.

Mitchell, R. J. (1970). *On the yielding and mechanical strength of Leda clays.* Canadian geotechnical journal, **7** (3), 297-312.

Miturski, M., Sas, W., Radzevičius, A., Šadzevičius, R., Skominas, R., Stelmaszczyk, M., & Głuchowski, A. (2021*). Effect of dispersed reinforcement on ultrasonic pulse velocity in stabilized soil*. Materials, **14** (22), 6951.

Miura, N., Bergado, D., Singh, N. and Panichayatum, B. (1988). *Improvement of soft Bangkok clay using vertical band drains based on full scale test.* Proceedings of the Proc. of the Intl. Conf. on Eng'g Problems of Regional Soils, pp. 379-384.

Mooney, W. D. (2010). 1.*11 crust and lithospheric structure–global crustal structure.* Seismology and Structure of the Earth: Treatise on Geophysics, **1**, 361.

Mouratidis, A. and Magnan, J. (1983). *Un modèle élastoplastique anisotrope avec écrouissage pour les argiles molles naturelles: Mélanie.* Revue Francaise de Geotechnique, (25), pp. 55-62.

NCh151 (1979) .*Cemento - Método de determinación de la consistencia normal.* Norma definitiva de Instituto de Normalización de Chile

NCh1516 (1979). *Mecanica de Suelos - Determinación de la densidad en el terreno - Método del cono de arena.* Norma definitiva de Instituto de Normalización de Chile

NCh1532 (1980) *Mecánica de suelos - Determinación de la densidad de partículas sólidas.* Norma definitiva de Instituto de Normalización de Chile

NP-143 (1969). *Solos - Determinação dos limites de consistência*. Norma Portuguesa Definitiva

NP-83 (1965). *Solos – Determinação da densidade das partículas sólidas*. Norma Portuguesa Definitiva.

NP-EN-12390-3 (2011). *Ensaios do betão endurecido.* Norma Portuguesa Definitiva.

NP-EN-197-1 (2001). *Cimento. Parte 1: Composição, especificações e critérios de conformidade para cimentos correntes*, IPQ, edição de Abril de 2001, p. 35. Norma Portuguesa.

NP-EN-206-1 (2001). *Betão. Parte 1: Especificação, desempenho, produção e conformidade*. IPQ, edição de Junho de 2007, p. 84. Norma Portuguesa.

NP-EN-450-1 (2005). *Cinzas volantes para betão. Parte 1: Definição, especificações e critérios de conformidade.* IPQ. Norma Portuguesa.

Olgun (2013). *Effects of polypropylene fiber inclusion on the strength and volume change characteristics of cement-fly ash stabilized clay soil.* Geosynthetics International **20** (4), pp. 263-275.

O'Reilly, M. P. and Brown, S. F. (1991). *Cyclic loading of soils: from theory to design.* Blackie Glasgow, UK.

Otero, R. A., Torres, T., Le Roux, J. P., Hervé, F., Fanning, C. M., Yury-Yáñez, R. E. & Rubilar-Rogers, D. (2012). *Una edad eocena tardía propuesta para la Formación Loreto (península de Brunswick, extremo sur de Chile), basada en peces cartilaginosos fósiles, paleobotánica y evidencia radiógena.* Andean Geology, **39** (1), pp. 180-200.

Park, S.-S. (2011). *Unconfined compressive strength and ductility of fiber-reinforced cemented sand.* Construction building materials, **25** (2), pp. 1134-1138.

Parry, R. H. G., & Nadarajah, V. (1973). *A volumetric yield locus for lightly overconsolidated clay.* Géotechnique, **23** (3), 450-453.

Pedro, A. (2013) Geotechnical investigation of Ivens shaft in Lisbon. PhD Thesis. Imperial College London.

Petchgate, K., Sukmongkol, W., and Voottipruex, P (2001) "Effect of height and diameter ratio on the strength of cement stabilized soft Bangkok clay." Geotech. Eng., **31** (3), pp. 227–239.

Phillipson, M. (1994). *Shear strength properties of a fine compressible soil from Coimbra.* MSc. Dissertation, University of Durham, U.K.

Porbaha, A., Shibuya, S. and Kishida, T. (2000). *State of the art in deep mixing technology. Part III: geomaterial characterization.* Proceedings of the Institution of Civil Engineers-Ground Improvement, **4** (3), pp. 91-110.

Ramesh, H., Manoj, K. and Mamatha, H. (2010). *Compaction and strength behavior of lime-coir fiber treated Black Cotton soil.* Geomechanics and Engineering, **2** (1), pp. 19-28.

Rao, G. and Balan, K. (2000). *Coir geotextiles—Emerging trends. Kerala State Coir Corporation Limite*. Alappuzha, India.

Raymond, G. P. (2002). *Reinforced ballast behaviour subjected to repeated load.* Geotextiles and Geomembranes, **20** (1), pp. 39-61.

Rocha, F. (1993) *Argilas aplicadas a estudos litoestratigráficos e paleoambientais na bacia sedimentar de Aveiro.* Ph.D Thesis. Universidade de Aveiro.

Rodrigues, C.M.G. (2003). *Caracterização geotécnica e estudo do comportamento geomecânico de um saprólito granítico da Guarda*. Ph.D Thesis. Universidade de Coimbra.

Rojas, E. & Le Roux, J. P. (2010). *Sedimentary processes on a Gilbert-type delta in Lake Llanquihue, southern Chile.* Andean Geology, **32** (1), pp. 19-32.

Roscoe, K. H., Schofield, A., & Wroth, A. P. (1958). *On the yielding of soils.* Geotechnique, **8** (1), 22-53.

Roscoe, K., Schofield, A. and Thurairajah, A. J. G. (1963). *Yielding of clays in states wetter than critical.* Geotechnique. **13** (3), pp. 211-240.

Saitoh, S., Suzuki, Y. and Shirai, K. (1985). *Hardening of soil improved by deep mixing method.* Proceedings of the Proc. of the 11th International Conference on Soil Mechanics and Foundation Engineering, Vol. 3, pp. 1745-1748.

Santos, N.C; Villarroel-Ortega, J.; Correia, A.A.S.; Venda Oliveira, P.J.; Lemos L.J.L. (2021). *An experimental study on the shape of the yield surface of a chemically stabilised soil.* International Conference on Deep Mixing 2021, Gdańsk, Poland, pp. 830-839.

Sarbaz, H., Ghiassian, H. and Heshmati, A. A. (2014). *CBR strength of reinforced soil with natural fibres and considering environmental conditions.* International Journal of Pavement Engineering, **15** (7), pp. 577-583.

Sernageomin (2013) *Anuario de la geología y minería de Chile.* Santiago, Chile

Sharma, S. S. and Fahey, M. (2003). *Degradation of Stiffness of Cemented Calcareous Soil in Cyclic Triaxial Tests.* Journal of Geotechnical and Geoenvironmental Engineering, **129** (7), pp. 619-629.

Shukla, S. K. (2017). *Fundamentals of fibre-reinforced soil engineering.* Springer.

Silva, J. A. H. (1984). *Solos compressiveis da baixa de St. André (área de Sines) - geologia e caracterização geomecânica.*. Geotecnia, pp. 63-81

Silveira, R.E.I.; Correia, A.A.S. e Venda Oliveira, P.J., (2012). *Cedência estrutural do solo mole do Baixo Mondego estabilizado quimicamente*, VI Congresso Luso-Brasileiro de Geotecnia, Lisboa, Portugal, 10 p.

Singh, V. & Arora, V. (2019). *Strength Improvement of Silt Loam Using Egg Shell Powder and Quarry Dust.* Recycled Waste Materials. Springer, pp. 59-68.

Sivakumar Babu, G., Vasudevan, A. and Sayida, M. (2008). *Use of coir fibers for improving the engineering properties of expansive soils.* Journal of Natural Fibers, **5** (1), pp. 61-75.

Soares, F. (1995). Caracterização geotécnica de solos da baixa aluvionar do Rio Mondego. Ph.D Thesis. Universidade de Coimbra.

Sobhan, K. and Krizek, R. J. (1999). *Fatigue behavior of fiber-reinforced recycled aggregate base course.* Journal of materials in civil engineering, **11** (2), pp. 124-130.

Spritzer, J., Khachan, M. and Bhatia, S. (2015). *Influence of synthetic and natural fibers on dewatering rate and shear strength of slurries in geotextile tube applications.* International Journal of Geosynthetics and Ground Engineering, **1** (3), pp. 26.

Subramaniam, P. and Banerjee, S. (2014). *Factors affecting shear modulus degradation of cement treated clay.* Soil Dynamics and Earthquake Engineering, **65** pp. 181-188.

Sukontasukkul, P., & Jamsawang, P. (2012). *Use of steel and polypropylene fibers to improve flexural performance of deep soil–cement column.* Construction and Building Materials, **29**, 201-205.

Tang, C. S., Shi, B., & Zhao, L. Z. (2010). *Interfacial shear strength of fiber reinforced soil.* Geotextiles and Geomembranes, **28** (1), 54-62.

Tang, C., Shi, B., Gao, W., Chen, F. and Cai, Y. (2007). *Strength and mechanical behaviour of short polypropylene fiber reinforced and cement stabilized clayed soil.* Geotextiles and Geomembranes, **25** pp. 194-202.

Tavenas, F., & Leroueil, S. (1980). *The behaviour of embankments on clay foundations.* Canadian geotechnical journal, **17** (2), 236-260.

Taylor, H. F. (1997). *Cement chemistry (Vol. 2, p. 459).* London: Thomas Telford.

Teles, J. M. (2013). Comportamento Mecânico do Solo Mole do Baixo Mondego Quimicamente Estabilizado Com Adição de Fibras Metálicas. MSc. Dissertation. Universidade de Coimbra.

Temuujin, J., Surenjav, E., Ruescher, C. H., & Vahlbruch, J. (2019). *Processing and uses of fly ash addressing radioactivity (critical review).* Chemosphere, **216**, 866-882.

Terashi, M. (1980). *Fundamental properties of lime and cement treated soils.* Report of PHRI, **19** (1), pp. 33-62.

Terashi, M. (1997). *Theme lecture: deep mixing method–brief state of the art.* Proceedings of the Proceedings of the 14 th International Conference on Soil Mechanics and Foundation Engineering Vol. 4, pp. 2475-2478.

Terzaghi, K., Peck, R. B. & Mesri, G. (1996). *Soil mechanics in engineering practice.* John Wiley & Sons.

Toll, D. (1990). *A framework for unsaturated soil behaviour.* Géotechnique, 40 (1), pp. 31-44.

Uddin, K. (1994). *Strength and Deformation Behavior of Cement-Treated Bangkok Clay.* Phd. Thesis. Asian Institute of Technology, Bangkok, Thailand.

Uddin, K., Balasubramaniam, A. and Bergado, D. (1997). *Engineering behavior of cement-treated Bangkok soft clay.* Geotechnical Engineering, **28** pp. 89-119.

UNE-EN-12504-4 (2006). *Testing concrete - Part 4: Determination of ultrasonic pulse velocity.*

Uribe, P. (1982). *Geología y consideraciones geotécnicas para el estudio de los suelos de fundación de la ciudad de Punta Arenas.* Bachelor Dissertation. Departamento de Geología, Universidad de Chile.

Vakili, A. H., Kaedi, M., Mokhberi, M., bin Selamat, M. R. & Salimi, M. (2018). *Treatment of highly dispersive clay by lignosulfonate addition and electroosmosis application.* Applied Clay Science, **152** pp. 1-8.

Van Eekelen, H. (1980). *Isotropic yield surfaces in three dimensions for use in soil mechanics.* International Journal for Numerical Analytical Methods in Geomechanics, **4** (1), pp. 89-101.

Vasquez, A. (2012). *Suelos De Fundación De La Ciudad De Punta Arenas, Región De Magallanes Y Antártica Chilena*. Master dissertation. University of Chile.

Vasquez, A., Foncea, C. & Roux, J. L. (2014). *Caracterización Geotécnica Y Tentativa De Zonificación De Los Suelos De Punta Arenas.* Conferencia de Mecánica de Suelos de la Sociedad Geotécnica de Chile, Concepción. pp. 1–10.

Vaughan (1985). *Mechanical and hydraulic properties of in situ residual soils-general report.* Proceedings of the 1st International Conference on Geomechanics in Tropical Lateritic and Saprolitic Soils, Brasilia, Brasilian Society for Soil Mechanics, **3**, pp. 231–63.

Vaughan;, Maccarini; and Mokhtar. (1988). *Indexing the engineering properties of residual soil.* Quarterly Journal of Engineering Geology, **21** pp. 61–84.

Venda Oliveira, P. J. (1992). *Algumas características do comportamento de um solo de baixa plasticidade.* Master dissertation, Universidade Nova de Lisboa, Portugal.

Venda Oliveira, P. J., Anunciação, G. R., and Correia, A. A. (2022*). Effect of cyclic loading frequency on the behavior of a stabilized sand reinforced with polypropylene and sisal fibres.* Journal of Materials in Civil Engineering, **34** (1), 06021008.

Venda Oliveira, P. J., Correia, A. A. S. and Cajada, J. C. A. (2018). *Effect of the type of soil on the cyclic behaviour of chemically stabilised soils unreinforced and reinforced with polypropylene fibres.* Soil Dynamics and Earthquake Engineering, **115** pp. 336-343.

Venda Oliveira, P. J., Correia, A. A. S., Teles, J. M. and Pedro, A. M. G. (2016). *Effect of cyclic loading on the behaviour of a chemically stabilised soft soil reinforced with steel fibres*. Soil Dynamics and Earthquake Engineering, **92** pp. 122-125.

Venda Oliveira, P. J., Correia, A. A. S., Teles, J. M. N. P. C., & Custódio, D. G. (2016). *Effect of fibre type on the compressive and tensile strength of a soft soil chemically stabilised.* Geosynthetics International, 23(3), 171-182.

Vermeer, P. & Neher, H. (1999). *A soft soil model that accounts for creep.* Proceedings of the Proceedings of the international symposium "Beyond 2000 in Computational Geotechnics", pp. 249-261.

Viana da Fonseca, A., Rios, S., Amaral, M. F. and Panico, F. (2013). *Fatigue Cyclic Tests on Artificially Cemented Soil*. Geotechnical testing journal, **36** (2), pp. 1-9.

Villarroel, J. & Damianovic, R. (2008). *Propuesta De Procedimiento Experimental Para Medir Las Expansiones, pérdida de capacidad portante Y Compacidad En Subbases Y Bases Sometidos A Condiciones De Tiempo Frío En La Ciudad De Punta Arenas.* Bachelor dissertation. Universidad de Magallanes, Chile

Vinod, J. S., Indraratna, B. & Mahamud (2010). *Stabilisation of an erodible soil using a chemical admixture.* Proceedings of the Institution of Civil Engineers-Ground Improvement, **163** (1), pp. 43-51.

Vivar, B. (2013). *Calibración Del Penetrometro y Veleta De Corte Aplicado a Suelos Finos De Punta Arenas y Su Correlación con el CBR.* Bachelor dissertation. Universidad Austral of Chile.

Wong, P. K. K., and Wong, P. K. K. (1975). *Yielding and plastic flow of sensitive cemented clay.* Geotechnique, **25** (4), 763-782.

Xie, Q., Li, F., Li, J., Wang, L., Li, Y., Zhang, C., Xu, J. & Chen, S. (2018). *A new biodegradable sisal fiber–starch packing composite with nest structure.* Carbohydrate Polymers, **189** pp. 56-64.

Yang, C., Cui, Y. J., Pereira, J. M. and Huang, M. S. (2008). *A constitutive model for unsaturated cemented soils under cyclic loading.* Computers and Geotechnics, **35** (6), pp. 853-859.

Yin, J.-H. and Fang, Z. (2006). *Physical modelling of consolidation behaviour of a composite foundation consisting of a cement-mixed soil column and untreated soft marine clay.* Geotechnique, **56** (1), pp. 63-68.

Yoshida, M., Kuno, G. and Kataoka, H. (1992). *Long term strength on cement treated soil by shallow mixing method.* Proceedings of the Proc. of the 27th Japan National Conference on Soil Mechanics and Foundation Engineering, pp. 2323-2326.

Young, I. & Mullins, C. (1991). *Factors affecting the strength of undisturbed cores from soils with low structural stability.* Journal of soil science, **42** (2), pp. 205-217.

Zaimoglu, A. S. and Yetimoglu, T. (2012). *Strength behavior of fine grained soil reinforced with randomly distributed polypropylene fibers.* Geotechnical and Geological Engineering, **30** (1), pp. 197-203.